Enhancement of electrochemotherapy by non-thermal plasma-treated liquids : protocol design and proof of concept

Thai-Hoa Chung

université PARIS-SACLAY

Enhancement of Electrochemotherapy by Non-Thermal Plasma-Treated Liquids: Protocol Design and Proof of Concept

Thèse de doctorat de l'université Paris-Saclay

École doctorale n° 569 : Innovation thérapeutique : du fondamental à l'appliqué (ITFA)

Spécialité de doctorat : sciences pharmacologiques

Unité de recherche : Université Paris-Saclay, CNRS, Institut Gustave Roussy, Aspects métaboliques et systémiques de l'oncogenèse pour de nouvelles approches thérapeutiques, 94805 Villejuif, France

Référent : Faculté de pharmacie

Thèse présentée et soutenue à Villejuif, le 25 janvier 2021, par

Thai-Hoa CHUNG

Composition du Jury

Emmanuel ODIC Professeur, CentraleSupélec, Génie électrique et électronique de Paris (GEEPS)	Président du jury
Anne-Laure BULTEAU Chargée de rechercher, HDR, LVMH Recherche : Parfums & Cosmétiques	Rapporteure & Examinatrice
Thierry DUFOUR Maître de conférences, HDR, Sorbonne Université	Rapporteur & Examinateur
Marie-Pierre ROLS Directrice de Recherche, CNRS, UMR 5089, IBPS, Toulouse	Examinatrice
Lluis M. MIR Directeur de recherche émérite, CNRS, UMR 9018, Institut Gustave Roussy	Directeur de thèse
Franck M. ANDRÉ Chargé de Recherche, CNRS, UMR 9018, Institut Gustave Roussy	Co-encadrant de thèse
Muriel GOLZIO Directrice de Recherche, CNRS, UMR 5089, IBPS, Toulouse	Invitée
Pierre-Marie GIRARD Chargé de Recherche, CNRS, UMR 3347, Institut Curie	Invité

Thèse de doctorat

NNT : 2021UPASQ005

A ma mère,

source d’amour qui m’a arrosée de tendresse et d’espoirs

PREFACE

Despite the panoply of anticancer therapies, many limitations remain to this day. The anticancer therapeutic strategies present specificity problems towards the tumour cells, thus causing unexpected and severe side effects. The precise targeting of tumours by local treatments is not always feasible. The development of multidrug resistance and the weak induction of immunogenic cell death (ICD) remain limiting factors. Thus, other therapeutic strategies based on new approaches are required to enhance the eradication of cancers, particularly the combination of different methods such as physical modalities that allow local treatment and are less subject to resistance in cancer cells. In the last thirty years, electrochemotherapy (**ECT**) – an established local eradication of tumour-based electroporation technology – has been widely employed in Europe in human and veterinary medicine with alleviated systemic side effects.

Meanwhile, non-thermal plasma (**NTP**) is gaining momentum for application in life science, specifically in oncology, thanks to their potential as rich sources of reactive oxygen and nitrogen species, amongst others. As a new specialised medical branch, NTP recently gave birth to plasma oncology and clinical plasma oncology as palliative care. Nevertheless, little is known about NTP anti-cancer effects, and there still are challenges to be overcome for both ECT and NTP oncology.

This thesis was dedicated to enhancing electrochemotherapy through non-thermal plasma medicine. Indeed, although ECT is an established and standardised targeted anti-cancer treatment, given its nature, it still has some inherent drawbacks, *e.g.*, causing some discomfort due to the application of intense pulsed electric fields (**PEFs**). This multidisciplinary approach, at the crossroads of physics, chemistry, biotechnologies and medicine, was supported by a consortium of three laboratories in the framework of the ANR (Agence Nationale de la Recherche) project INCa PlanCancer N°17CP087-00: my laboratory UMR 9018 METSY (Metabolic and systemic aspects of oncogenesis for new therapeutic approaches, ex-UMR 8203 Laboratoire de Vectorologie et Thérapeutiques Anticancéreuses) located at the Institute Gustave Roussy (Villejuif, France), the GREMI (Groupe de Recherche sur l'Énergétique

des Milieux Ionisés, UMR 7344, CNRS/Université d'Orléans, France) and the LPGP (Laboratoire de Physique des Gaz et des Plasmas, CNRS/Université Paris-Saclay, Orsay, France).

For the project, a novel helium NTP multijet device with a grounded and compensated circuit for stable uses has been designed and manufactured by the GREMI for *in vitro* and *in vivo* anticancer studies. By combining indirect NTP (*i.e.*, plasma-treated liquids) with µsPEFs, we **succeeded in reducing the electric pulsed amplitude *in vitro* and *in vivo* compared with that used in practical ECT for clinics** or with NTP as mono-therapy while maintaining the anti-cancer efficiency. Moreover, **the *in vivo* combined treatment with NTP and ECT improved the efficiency of ECT**. The stability, the components and the pH over different storage conditions of the plasma-treated liquids have also been studied to establish the best production and storage conditions where reproducibly prepared plasma-treated liquids were stable and reproductive for various investigations and utilisations. All those studies within the novel approach combining NTP and µsPEFs contributed to complete anti-cancer therapies panoply.

During three years, my thesis led to the publication of two scientific articles, the submission of a third article, an article in preparation, and various scientific presentations at national and international conferences and workshops listed below.

1 Publications

Stancampiano, A., Chung, T.-H., Dozias, S., Pouvesle, J.-M., Mir, L. M. and Robert, É. (**2019b**). Mimicking of human body electrical characteristic for easier translation of plasma biomedical studies to clinical applications. *IEEE Trans. Radiat. Plasma Med. Sci.* **4**, 335–342.

Chung, T.-H., Stancampiano, A., Sklias, K., Gazeli, K., André, F. M., Dozias, S., Douat, C., Pouvesle, J.-M., Santos Sousa, J., Robert, É., *et al.* (**2020**). Cell Electropermeabilisation Enhancement by Non-Thermal-Plasma-Treated PBS. *Cancers (Basel).* **12**, 219–239.

Sklias K., Chung T.-H., Stancampiano A., Gazeli K., Bauville G., André F.M., Dozias S., Douat C., Pouvesle J.-M., Robert E., *et al*. Preserving the anti-cancer efficacy of plasma-treated liquids over time: a prerequisite for their clinical application. *(In preparation - to be submitted at Scientific Reports).*

Chung, T.-H., Sklias, K., André, F. M., Polrot M., Stancampiano, A., Gazeli, K., Bauville G., Dozias, S., Douat, C., Pouvesle, J.-M., *et al. In vivo* studies of non-thermal plasma and its combination with electrochemotherapy. *(In preparation)*

2 Scientific communications

2.1 Conference papers and oral communications

In vivo Studies on the Combination of Electrochemotherapy and Non-Thermal Plasma-Treated PBS. *Journées du GDR HAPPYBio Teleconference*, GDR HAPPYBio, Nov. **2020**, France.

In vitro Studies on the Combination of Pulsed Electric Fields and Non-Thermal Plasma. *34th Bioelectrics Consortium Teleconference*, Sep. **2020**.

Cells Electropermeabilization Enhancement by a Grounded and Compensated Cold Plasma-Treated Liquid. *The 3rd World Congress on Electroporation and Pulsed Electric Fields in Biology, Medicine, and Food & Environmental Technologies*, Sep. **2019**, Toulouse, France.

(Joined oral communication) Enhancement of Electrochemotherapy with a New Source of Non-thermal Atmospheric Pressure Plasma. *6th International Workshop on Plasma for Cancer Treatment (IWPCT)*, Apr. **2019**, Antwerp, Belgium.

Cell Electropermeabilization Enhancement by Non-Thermal Plasma-Treated Liquid. *Journées du GDR HAPPYBio*, GDR HAPPYBio, Nov. **2019**, Nouan le Fuzelier, France. ⟨hal-02413786⟩

(Joint oral communication) To Ground or not to Ground: a key question during plasma treatments. *Journées du GDR HAPPYBio*, GDR HAPPYBio, Nov. **2018**, La Rochelle, France. ⟨hal-01946034⟩

Characterization of Atmospheric Pressure Multijet Plasma Source Effects on Mice Skin. *7th International Conference on Plasma Medicine (ICPM7)*, ISPM, Jun. **2018**, Philadelphia, United States. ⟨hal-01942998⟩

Potential of Electrochemotherapy with Cold Plasma for Cancer Therapy. *5th IWPCT*, Mar. **2018**, Greifswald, Germany.

In vitro Studies of the Antiviral Effects of Marine Active Ingredients. *Electroporation-based Technologies and Treatments (EBTT) International Scientific Workshop and Post-graduate Course*, Nov. **2017**, Ljubljana, Slovenia.

2.2 Poster communications

Augusto Stancampiano, Jean-Michel Pouvesle, Thai-Hoa Chung, *et al.* Time-resolved measurement of the electric field induced by a plasma gun device in a conventional electroporation setup. ICPM7, Jun. **2018**, Philadelphia, United States. ⟨hal-01943189⟩

Thomas Maho, I Goard, Xavier Damany, Thai-Hoa Chung, *et al.* Atmospheric Pressure Multijet Plasma Source for Plasma Medicine Applications. ICPM7, Jun. **2018**, Philadelphia, United States. ⟨hal-01943164⟩

Thai-Hoa Chung, Claire Lethias and Bernard Verrier. *In vitro* Studies of the Antiviral Effects of Marine Active Ingredients. EBTT, Nov. **2017**, Ljubljana, Slovenia.

RÉSUMÉ

Malgré la panoplie des thérapies anticancéreuses, de nombreuses limites demeurent à ce jour. Les stratégies thérapeutiques anticancéreuses présentent des problèmes de spécificité vis-à-vis des cellules tumorales provoquant ainsi des effets secondaires inattendus et/ou graves. Le ciblage précis des tumeurs par des traitements locaux n'est pas toujours possible. Le développement de la multirésistance et la faible induction de la mort cellulaire immunogène restent des facteurs limitants. Ainsi, afin de favoriser l'éradication des cancers, d'autres stratégies thérapeutiques basées sur de nouvelles approches sont nécessaires, notamment la combinaison de différentes approches telles que des modalités physiques qui permettent un traitement local moins assujetti au développement de résistances dans les cellules cancéreuses. Au cours des trente dernières années, l'électrochimiothérapie (**ECT**) - une éradication locale des tumeurs basée sur la technologie d'électroporation - est largement utilisée en Europe en médecine humaine et vétérinaire avec des effets secondaires systémiques atténués. Pendant ce temps, les plasmas non thermiques ou plasmas froids (**NTP** pour non-thermal plasmas) prennent de l'ampleur pour être appliqués dans les sciences de la vie, en particulier en oncologie, grâce à leur potentiel en tant que sources riches d'espèces réactives d'oxygène et d'azote, entre autres. Étant une nouvelle branche de médecine spécialisée, les plasmas froids ont récemment donné naissance à la recherche pré-clinique et clinique des plasmas froids – nommée le « plasma médecine », en tant que soins palliatifs en clinique. Néanmoins, peu de choses est connu sur les effets anticancéreux des plasmas froids et il y a encore des défis à surmonter pour l'oncologie utilisant de l'ECT et des plasmas froids.

Cette thèse était dédiée à l'amélioration de l'ECT par le plasma médecine. En effet, bien que l'ECT soit un traitement anticancéreux ciblé bien établi et standardisé, compte tenu de sa nature, elle présente encore certains inconvénients inhérents, par exemple, un certain inconfort en raison de l'application de champs électriques pulsés intenses (**PEFs** pour pulsed electric fields). L'approche pluridisciplinaire de ma thèse, à l'interface de la physique, chimie, biotechnologies et médecine, a été soutenue par un consortium de trois laboratoires de recherche dans le cadre du projet ANR (Agence Nationale de la Recherche) INCa PlanCancer N° 17CP087-00 : mon laboratoire d'accueil - UMR 9018 METSY (Aspects métaboliques et systémiques de l'oncogenèse pour de nouvelles approches thérapeutiques, ex-UMR 8203

Laboratoire de Vectorologie et Thérapeutiques Anticancéreuses) situé à l'Institut Gustave Roussy (Villejuif, France), le GREMI (Groupe de Recherche sur l'Énergétique des Milieux Ionisés, UMR 7344, CNRS / Université d'Orléans, France) et le LPGP (Laboratoire de Physique des Gaz et des Plasmas, CNRS / Université Paris-Saclay, Orsay, France).

Pour le projet, le GREMI a conçu et fabriqué un nouveau dispositif de plasmas froids multijet à hélium avec un circuit mis à la terre et compensé pour des utilisations stables en *in vitro* et *in vivo*. Une série d'expérimentation *in vivo* a été réalisée pour tester ces multijets de plasmas froids sur la peau de deux lignées de souris (Nude et C57Bl/6J), appelant le traitement **NTP directe**. J'ai notamment étudié le **NTP indirect**, c'est-à-dire des liquides traités aux multijets de plasmas froids et utilisés par la suite comme un traitement anti-cancéreux pour différents modèles *in vitro* et *in vivo*. Les expérimentations de NTP indirect étaient notamment réalisées avec le PBS (Ca^{2+}, Mg^{2+}) recevant différents temps de traitement par les multijets de plasmas froids, donnant différents « plasma-treated PBS » ou « pPBS **»**. En combinant ces pPBS avec les µsPEF, nous avons **réussi à réduire l'amplitude des impulsions électriques *in vitro* et *in vivo*** par rapport à celle utilisée dans l'ECT en clinique ou aux NTP en monothérapie, tout en maintenant l'efficacité anti-cancéreux. De plus, **en *in vivo* le traitement combiné les pPBS et ECT a amélioré l'efficacité de l'ECT**. La stabilité, les composants et le pH des liquides traités aux plasmas froids dans différentes conditions de stockage ont également été étudiés afin d'établir les meilleures conditions de production et de stockage où ces liquides pourraient être préparés de manière reproductible et stables pour différentes utilisations. Toutes ces études dans le cadre de la nouvelle approche combinant le NTP et les µsPEF ont contribué à compléter la panoplie des thérapies anticancéreuses.

Pendant trois ans, ma thèse a donné lieu à la publication de deux articles scientifiques, la soumission d'un troisième article, un article en préparation, et diverses communications scientifiques lors de conférences et ateliers scientifiques nationaux et internationaux listés ci-dessus.

OUTLINE

ACKNOWLEDGEMENTS

Ayant parcouru un long chemin avant d'arriver à mon doctorat, je souhaite que toutes personnes mentionnées ci-après aient la certitude de ma profonde gratitude pour avoir partagé ma vie professionnelle et personnelle.

Pour ces trois années de doctorat, mes remerciements vont en premier à **Lluis Mir**, ancien directeur de notre UMR mais surtout mon directeur de thèse, sans qui cette thèse n'aurait pas vu lumière. Lluis, je vous remercie d'avoir été patient, pédagogue, compréhensible et par-dessus tout, disponible. J'ai apprécié nos conversations scientifiques (en admirant votre passion pour la science), politiques et sur la langue française (pendant lesquelles j'ai enrichi mon vocabulaire). Merci pour le Grand Maître que vous êtes.

Je remercie chaleureusement mon co-encadrant de thèse, **Franck André**, qui a su m'accompagner tout au long de ma thèse malgré son agenda chargé. Cet accompagnement allait de la paperasse pour mon recrutement bien avant notre rencontre, au travail quotidien au laboratoire où ses conseils m'étaient précieux. Un Franck (très) calme, un Franck gentil, un Franck positif, un Franck polyvalent, un Franck omniprésent !

Je ne pense pas pouvoir avoir mieux comme encadrants de thèse que Lluis et Franck. Qu'ils soient aussi remerciés de m'avoir fait partager leurs brillantes intuitions. C'est à leurs côtés que j'ai compris ce que rigueur et précision voulaient dire pour une thèse en sciences.

Mes sincères remerciements vont aux membres de mon jury de thèse qui, malgré les circonstances particulières causées par la pandémie de la Covid-19, ont accepté d'examiner mon travail et d'assister à ma soutenance de thèse :

- Au Professeur **Emmanuel Odic** – d'avoir accepté d'être Président du jury, d'avoir partagé ses avis très constructifs et de m'avoir fait part de ses compliments pour la qualité de mon travail.
- Aux Docteurs **Anne-Laure Bulteau** et **Thierry Dufour** –de l'honneur que vous m'avez fait en acceptant d'être rapporteurs de ma thèse, d'y avoir consacré votre temps précieux pour partager des observations très constructives non seulement pour mon manuscrit de thèse mais aussi pour la suite du projet ANR dont ma thèse faisait partie. Je souhaite remercier particulièrement Thierry qui était également mon référent pour ces trois années de doctorat. Thierry, merci pour ta disponibilité, ton soutien et tes encouragements. Madame Bulteau, je suis touchée de la confiance que vous m'avez accordée, merci de m'avoir confié votre projet de recherche à travers duquel j'ai découvert le LVMH Recherche.
- Au Docteur **Marie-Pierre Rols** –d'avoir examiné ma thèse avec grande attention et d'y avoir apporté ses observations de qualité. Marie-Pierre, je garde une belle image de ta douceur en qualité de Directrice de recherche pionnier dans le domaine des impulsions électriques appliquées à la biologie.
- Aux Docteurs **Muriel Golzio** et **Pierre-Marie Girard** –d'avoir assisté à ma soutenance de thèse et partagé vos avis précieux.

Que tous les membres du jury ainsi que tous les collaborateurs et amis, famille sachent que leur présence à ma soutenance de thèse, ensemble avec l'estime qu'ils portaient pour mon travail, a fait de ce jour un des plus beaux jours de ma vie.

As a matter of course, my profound gratitude to all my collaborators for their substantial contributions and professional cooperation:

- La dream team GREMI, toujours dynamique, sportive et joyeuse : **Éric,** un chef exceptionnel, discret mais qui ne manque pas d'humour ; **Augusto**, grazie mille per il tuo tempo e pazienza, la tua professionalità, per non parlare del tuo incoraggiamento al momento giusto; **Claire**, j'ai toujours admiré tes tresses et j'espère que tu m'en feras une quand mes cheveux seront suffisamment longs (en tout cas, tu me l'as promis !) ; **Sébastien**, merci pour ton soutien au niveau technique, sans toi nous n'aurions pas eu ces machines de plasmas, tout simplement ; **Thomas**, même si je n'ai pas eu l'opportunité de travailler avec toi, j'apprécie beaucoup tes présentations lors des congrès et qui reflètent la qualité de ton travail ; et en dernier pour un plus grand remerciement, **Jean-Michel** que j'estime tant, merci pour ta gentillesse et ta douceur envers nous – les thésards que tu as toujours su soutenir et encourager, merci pour les discussions très sympathiques sur le Viêt Nam, j'ai vu que mes observations t'ont fait rigoler. Tu fais partie des professeurs que j'ai pu tutoyer directement dès la première rencontre sans réfléchir (Amina m'a dit la même chose, tu sais que nous t'apprécions beaucoup !). Mieux qu'un collaborateur, tu étais un « mentor » pour moi pendant cette thèse.
- L'équipe du LPGP : **João**, **Kristaq**, **Kyriakos**, **Gérard**, **Thibault**. Merci beaucoup pour ces belles années de thèse en collaboration avec vous. Toujours disponibles pour nous accueillir à Orsay et pour me préparer des échantillons quand la fameuse machine de plasma était capricieuse. I do not, unfortunately speak Greek but my sincere gratitude to Kristaq and especially to Kyriakos for being so kind. You know how to turn a long experimentation day interesting.

Je tiens à remercier tout particulièrement **mes collègues à l'IGR** avec qui j'ai partagé un « quotidien de thèse ». Ce n'est pas le plus simple des « quotidiens » et pourtant, grâce à leur compagnie, de proche ou de loin, ce quotidien était le plus rassurant. Dans l'ordre de connaissance, puisque 3 ans est mine de rien une longue période au cours de laquelle j'ai eu l'opportunité de rencontrer (ou croiser, comme disent les français) beaucoup de personnes :

- **Isabelle**, notre gestionnaire qui a su gérer toutes nos démarches administratives, « elle est un amour ». Isabelle, merci également de m'avoir confié ta plante d'araignée qui maintenant pousse en pleine vitesse chez moi. J'espère que mon orchidée se plaît dans ton bureau baigné de lumière.
- Chère **Amina**, ma « coloc' de bureau » : qui peut croire, en nous voyant nous chamailler au bureau, que j'étais invitée à ton mariage ? Ce n'est pas pour rien que tout le monde a dit que l'on était comme un vieux couple ! Merci à toi pour ta bonne humeur de (presque) tous les jours, pour avoir été positive et optimiste, pour ta joie de vie (cela est contagieux), et particulièrement d'avoir pris le temps de me connaître et de me comprendre (pour autant). J'ai beaucoup de chance de t'avoir comme collègue et maintenant, une amie chère.
- Merci **Adeline** de m'avoir accompagnée au début de ma thèse pour les manips *in vivo* durant lesquelles j'ai beaucoup appris, en grande partie grâce à ta patience et gentillesse ; merci **Tomás** (ce qui m'a manqué depuis ton départ de l'équipe : « Holà, chica ! » puis « Allez ! Il faut travailler hein ! » ou encore « Réfléchis ! », puis pendant les pauses de café j'aurais pu sentir les arômes de mon café vietnamien préparé de façon très vietnamienne par un espagnol) ; un grand merci à l'équipe d'animalerie de s'être occupé de mes souris (surtout **Mélanie** de m'avoir accompagnée dans les grandes expérimentations) ; merci à Léna, Alain, Thierry, Félix, aux filles chez « les voisins » (Marie, Célia, Suzan, Linda), aux **équipes de l'ex-UMR 8203** (David Castel, Jacques Grill et Birgit Geoerger) ainsi que les équipes formant notre **nouvelle UMR 9018** (Catherine, notre directrice de l'Unité ; Nazanine, ma cheffe d'équipe ; Karim, Pierre, Yegor, Svetlana : merci à tous les chefs d'équipe de leur soutien ; un bonjour dans le couloir

ou un au revoir à 20h du soir en passant demander aux étudiants si tout allait bien, ça fait partie d'une vie agréable au labo).

- **Leslie**, ma chère, je me rends compte de la chance que l'on a (et que j'ai) de t'avoir dans l'équipe. Heureuse d'avoir passé la moitié de ma thèse à tes côtés. Pas besoin d'être dans le même projet ni dans le même bureau pour avoir ton soutien en permanence. En plus, tu as un humour qui « colle » bien avec le mien donc si jamais je n'ai pas encore eu l'opportunité de te le faire savoir, saches que je me sens en pleine de sécurité quand je suis avec toi (j'en n'ai pas davantage d'explication). Merci à cette thèse de m'avoir offert toi et Amina comme collègues et amies.
- **Céline**, **Giorgia**, **Jean-Rémi**, **Kenza**, **Camille**, **Alberto**, **Florian**, **Bảo Trâm**, **Valentin**, **Aurore** : notre labo est formidable grâce à vous. Toujours souriants même quand je débarquais à l'imprévue pour vous emprunter du matériel ou vous poser mes questions naïves. Merci du fond du cœur d'avoir pris le temps de me connaître et « bienvenue » la personnalité que j'ai. Je tiens à remercier ma compatriote pour ses Bubble Tea qui m'ont réconfortée, pour son talent culinaire. Bé Trâm, toi qui es si calme, si douce, toi qui as su montrer à nos collègues la vraie « cliché » d'une vietnamienne (ce que je n'ai pas pu assurer), je suis heureuse de t'avoir rencontrée.

Il est peut-être out of scope, mais mes pensées vont aux différentes lignées de cellules et souris que j'ai pu étudier tout au long de ma thèse. Elles étaient, la plupart du temps, très collaboratives et « gentilles », si je peux le dire de cette manière pour leur remercier d'avoir contribué au succès de ce travail. Merci à la plus belle ville du monde, Paris mon amour, pour ces belles années !

A mes chers anciens collègues au CEA qui sont, depuis mon stage en 2012, devenus mes amis. Vous m'avez vue traverser certaines (grandes) épreuves et m'ont aussi vue rigoler très sérieusement. Je rédige ces remerciements avec une grande pensée à vous : **Hamed**, mon maître de stage, toi qui étais l'origine de ma passion pour les nanotechnologies, le stage dans ton équipe a été décisif pour mon parcours professionnel, je te remercie particulièrement pour ton soutien. Nous avons de la chance de t'avoir comme Directeur (j'en suis sûre, tu vas encore me dire « La chance, c'est aussi nous qui la provoquons ! ») ; **Willem**, mon co-encadrant de stage et surtout, un brillant chercheur très humble pour qui j'ai beaucoup d'estime ; **Dominik** - mon Domichou (si je pouvais, j'aurais déposé un brevet sur ce surnom), toi qui es toujours aussi doux, aussi gentil, toujours à mon écoute, je t'apprécie beaucoup et te souhaite le bonheur où que tu sois, à Paris ou à München ; **David**, merci de m'avoir fait découvrir Mestre, la sangria et le cap'b ; Aura, Joana, Rana, Shatha, puis enfin, **Masha** et son compagnon Joseph (the perfect couple dont l'un me prépare un superbe magret de canard bien rosé au BBQ en plein hiver et l'autre me sert de l'alcool, et qui m'ont confié deux charmantes demoiselles-chats pendant une semaine sans rien me payer au retour à part des BBQ digne d'une étoile Michelin. A quand le prochain ?).

A **Astrid** ma coloc', je te remercie pour ta gentillesse, pour ton grand cœur. Nous n'avons pas vraiment le même caractère, n'empêche que j'étais heureuse d'avoir partagé avec toi notre charmant appartement parisien (ainsi que la passion pour le vintage) et je t'en remercie. C'est aussi en partie grâce à toi que Franck et moi sommes rencontrés, j'ai vu que Dieu a fait des merveilles en me guidant vers une coloc' avec toi.

A tous mes amies et amis grâce à qui je ne me suis jamais ennuyé en trois ans et trois mois : la thèse n'y était pas pour rien, mais vous vous êtes bien chargé du reste.

A **Gia Thụy**. Cảm ơn anh đã bên cạnh, yêu thương, chăm sóc em suốt 7 năm. La vie est faite de séparation, l'importance est de vivre des moments sincères et inoubliables. Je suis touchée de la dédicace me concernant dans ta thèse et t'en remercie. Sache que je te souhaite toujours le meilleur.

A **cô Mai et famille** – ma seconde famille qui m'a chaleureusement accueillie dès mon premier jour en France : cảm ơn cô và cả nhà đã luôn thương yêu và quan tâm đến con, xem con như con cháu trong đại gia đình. Tạ ơn Chúa đã dẫn đưa con đến với gia đình cô.

A mes chers amis **chị Thủy** et **Quentin** : Je ne peux trouver les mots justes et sincères pour vous exprimer mon affection, vous êtes pour moi des amies et au-delà, sœur et frère de cœur sur qui je peux compter. La chance que j'aie de vous avoir dans ma vie, je la chérie. En témoignage de l'amitié qui nous unit et des souvenirs de tous les moments que nous avons passés ensemble, remplis de joie et parfois des larmes, je vous dédie cette thèse. Une tendre pensée à chị Thủy (sans qui je n'aurais pas connu Quentin et anh Quang) : merci de ton soutien, avec l'amour d'une grande sœur tu as su veiller sur moi, et par-dessus de tout, merci de ta confiance ; sache que je suis la marraine la plus fière et heureuse du monde, merci de m'avoir confié ton petit Lucas.

A **ma belle-famille** : Annie, Jean-Pierre, Lionel et Maëva, merci de m'avoir si bien accueillie dans votre famille et du soutien sans faille que vous m'avez témoigné. Merci pour les taquineries accompagnées de délicieux repas préparés avec amour et d'excellents vins servis avec générosité (je ne dénonce personne, promis !). A Jean-Pierre et Annie, merci d'avoir mis au monde un être aussi extraordinaire que votre fils, merci pour l'éducation que vous lui avez offerte et qui fait qu'aujourd'hui, Franck est une si belle personne.

Je dédie cette thèse à ma famille – mon rempart. Votre soutien fut une lumière dans tout mon parcours. Aucune dédicace ne saurait exprimer l'amour et l'estime que j'ai toujours eue pour vous, ma considération pour vos encouragements et votre bonté exceptionnelle.

A **ông Nội**, mon grand-père défunt qui a pris soin de moi depuis ma naissance, qui m'a ramenée à l'école tous les jours jusqu'à son dernier jour. Cette thèse est pour toi.

A **mes parents**, je vous aime, même si je n'ai jamais su exprimer mes sentiments pour vous. Cảm ơn ba đã chở con đi học từ sáng đến tối, đã khó nhọc nuôi nấng chị em con. Cảm ơn mẹ đã hy sinh rất nhiều cho gia đình mình, đã sẵn sàng hy sinh mạng sống của mình để cho con có chị, có em. A maman, je te dédie ce doctorat. Ce modeste travail est le fruit des sacrifices que tu as déployés pour mon éducation et ma formation. Tous les enfants du monde auraient aimé être à ma place.

A **cu Bi**, mon petit-frère d'amour. Je remercie papa et maman de m'avoir offert le plus beau cadeau que j'aurais souhaité qui est toi. Cheers to a remarkable man and the most incredible brother one could ask for. I am the luckiest having you by my side. Proud of you and thank you for your love!

A **Franck**, l'homme de ma vie. Tu m'as dit en rigolant de te remercier de m'avoir supportée pendant tout ce temps. Lors de ma soutenance, Lluis a bien félicité notre couple d'avoir traversé ensemble ces trois ans, nous avons peut-être vu le pire. Donc je veux simplement que tu saches que chaque jour passé à ton côté est un cadeau. Que puis-je souhaiter de plus ?

Louange à Dieu qui m'aime inconditionnellement.

Et pour terminer, c'est toujours avec bonne humour (Vous me connaissez !) :

Says here you should go to hell but since you have a PhD we'll count that as time served

ABBREVIATIONS

1D:	one dimension
2D:	two dimensions
3D:	three dimensions
ΔE:	voltage gradient
$\Delta\psi_0$:	transmembrane resting potential
$\Delta\psi_i$:	induced transmembrane potential (by an electric field)
λ:	(in physics, electronics engineering, and mathematics) the wavelength of any wave
ɵ:	angle

A

ALDH:	aldehyde dehydrogenase
APPJ:	atmospheric pressure plasma jet
AQP:	aquaporins
Ar:	argon
ATM:	ataxia-telangiectasia mutated
ATP:	adenosine triphosphate

B

B16-F10:	murine melanoma cell
BLM:	bleomycin

C

C:	Celsius
CA(P)P:	cold atmospheric (pressure) plasma
CARs:	chimeric antigen receptors
CDDP:	*cis*-diamminedichloridoplatinum (II) or *cis*-Platin
CHO:	Chinese hamster ovary cell
CNRS:	Centre National de la Recherche Scientifique
CR:	complete response
CRT:	calreticulin
CT:	computed tomography

D

d:	cell membrane thickness
DBD:	dielectric-barrier discharge
DCs:	dendritic cells
DC-3F:	Chinese hamster lung fibroblasts
DEP:	dielectrophoresis
DMEM:	Dulbecco's Modified Eagle's Medium
DNA:	deoxyribonucleic acid
DOPC (18:1 (Δ9-Cis) PC)	1,2-dioleoyl-sn-glycero-3-phosphocholine ($C_{44}H_{84}NO_8P$)
dsDNA:	double-stranded DNA
DNA-PKCs:	DNA-protein kinase catalytic subunit
Drp1:	dynamin-related protein 1
DSB:	double-strand breaks

E

E:	electric field amplitude
ECT:	electrochemotherapy
EGT:	electrogenetransfer
EPR:	enhanced permeability and retention
EPs:	electric pulses
ER:	endoplasmic reticulum
ESOPE:	European Standard Operating Procedures of Electrochemotherapy

F

FACS:	fluorescence-activated cell sorting
FBS:	foetal bovine serum
FDA:	food and drug administration

FTIR: Fourier transform infrared spectroscopy

G

GC: Golgi complex
GFP: Green fluorescent protein
GMP: good manufacturing practices
GUV: giant unilamellar vesicle

H

H_2O_2: hydrogen peroxide
HDI: human development index
He: helium
HF: high frequency
HMGB1: high-mobility group protein 1
HRR: homologous recombination repair
HSP70: 70 kDa heat shock proteins
HV: high voltage

I

IARC: International Agency for Research on Cancer
IC_{50}: half maximal inhibitory concentration
ICCD: intensified charge coupled device
ICD: immunogenic cell death
IFN: interferon
IL: interleukin
IRE: irreversible electroporation
i.p.: intraperitoneal
i.t.: intratumoural
i.v.: intravenous

K

K: Kelvin

L

LIF: laser-induced fluorescence
LPB: murine fibrosarcoma cell
LPFS: local progression-free survival
LV: low voltage

M

MAM: mitochondria-associated ER membranes
MD: molecular dynamics
MEM: minimum essential medium
MHCD: micro-hollow cathode discharge
MMP-9: matrix metallopeptidase 9
MRI: magnetic resonance imaging
mRNA: messenger-RNA
mTOR: mammalian/mechanistic target of rapamycin

N

NAD^+: nicotinamide adenine dinucleotide
NASA: National Aeronautics and Space Administration
NHEJ: non-homologous end joining
$NO^{\bullet}$: nitric oxide (or nitrogen oxide or nitrogen monoxide)
NO_2: nitrogen dioxide
NO_2^-: nitrite
NO_3^-: nitrate
NOS: nitric oxide synthase
NTP: non-thermal plasmas

O

$^1O_2$: singlet oxygen
$O_2^{\bullet -}$: superoxide ion
O_3: ozone (or trioxygen)
$^{\bullet}OH$: hydroxyl radical
ODNs: oligodeoxynucleotides
$ONOO^-$: peroxynitrite
OR: objective response

P

PAL: plasma-activated liquid
PAM: plasma-activated medium
PBS: phosphate buffer saline
pPBS: plasma-treated PBS 1X
PDGR: platelet-derived growth factor

pDNA	plasmid DNA
PDK1:	3-phosphoinositide-dependent protein kinase-1
PEF:	pulsed electric field
PEG:	polyethylene glycol
PET:	positron emission tomography
PMJ:	plasma multijet
PR:	partial response
PRDM1 α:	positive regulatory domain zinc finger protein 1
P/S:	Penicillin/Streptomycin
PTL:	plasma-treated liquid(s)
PTM:	posttranslational modification

R

r:	radius
RECIST:	Response Evaluation Criteria in Solid Tumors
r.o.:	retro-orbital
RLS:	Ringer's lactate solution
RPMI medium:	Roswell Park Memorial Institute medium
RLS:	Ringer's lactate solution
RNA:	ribonucleic acid
RNS:	reactive nitrogen species
ROI:	region of interest
RONS:	reactive oxygen and nitrogen species
ROS:	reactive oxygen species
RF:	radio frequency

S

s:	second
s.c.:	subcutaneous
SHG:	second harmonic generation
shRNA	short hairpin-RNA
siRNA	small interfering-RNA
SOP:	standard operating procedure
slm:	standard litre per minute
SP:	secretory pathway
SSB:	single-strand break

T

t:	time
T:	temperature
TIRF:	total internal reflection fluorescence microscopy
TMV:	resting transmembrane voltage
TNF:	tumour necrosis factor
TRPM2:	transient receptor potential cation channel, subfamily M, member 2
ttt:	treatment

U

UPR:	unfolded protein response
US:	ultrasound
UV:	ultraviolet

V

VEGF:	Vascular endothelial growth factor

W

w/:	with
w/o:	without
WT:	wild-type
WHO:	World Health Organization

TABLE OF FIGURES

TABLE OF TABLES

STATE OF THE ART

As a multidisciplinary thesis, this research work covered the field of biotechnologies, biomedicine, physics and chemistry for pre-clinical studies of novel medical physics approaches against cancer. Before presenting the achievements during those three years of research, state of the art will be introduced to give insight into the medical physics era with a particular interest in electroporation-based technology and the non-thermal plasma domain. The main applications of those two technologies, both general and medical, focusing on oncology, will also be presented.

1 From iatrophysics to medical physics: then and now

Modern medical practice and research depend significantly on technology, and hospitals are equipped with physics-based devices for clinical measurement, diagnosis, and treatment. Today, the exertion of physicists in medical institutions generally refers to the term medical physics, which originated from iatrophysics. It is essentially related to medical applications of radiation, diagnostic imaging, and clinical measurement. Although the implication of physics in clinics was only instigated this last century, the relation between physics, biology and medicine has a much longer, more prosperous and more profound heritage, dating back to the earliest recorded period of medical history. Even if historical origins are often arguable, thus difficult to determine, this chapter will trace a brief history of the contribution that physics has made to medical sciences, from ancient Greece to the study of the human body mechanics by da Vinci in the late 15th century to the emergence of radiology, phototherapy and electrotherapy at the end of the 19th century, with particular focus on two physical-based technologies of the 20th century, the electroporation and non-thermal plasma technologies, being the centre of this thesis for their applications in oncology.

1.1 A historical perspective

In Classical Greece, Hippocrates (c. 460 – c. 370 BC) – the Father of Medicine, prescribed sunbathing (heliotherapy) for medical and psychological purposes, establishing the therapeutic use of ultraviolet (UV) radiation. Throughout the centuries, the discovery and application of physics have been fundamentals for scientists to explore the living's functions. Electrophysiology, biomechanics, cardiology, ophthalmology, neurology, audiology, physiotherapy, orthopaedics, and radiology directly apply physics to the medicine field (Keevil, 2012). Other specialities such as environmental health, dermatology, and even general surgery have medical physics sources.

Leonardo da Vinci (1452–1519), one of the most famous polymaths of human history, could be considered the first medical physicist with his detailed studies of human body mechanics. Da Vinci described mechanical science as "the noblest and above all others the most useful", bringing physics closer to clinical engineering and medicine. However, science had to wait for more than a hundred years later to demonstrate by William Harvey (1578-1657) that blood flows rapidly around the human body under the action of a single mechanical pumping system

of arteries and veins (Harvey, 1628). At the same time, the microscope of Anton van Leeuwenhoek (1632–1723) opened up new vistas of biological structure, and the pioneering work of Santorio Sanctorius (1561–1636) on **clinical measurement of temperature, pulse rate, and body mass** are early examples of modern clinical practice (Porter, 1997). René Descartes (1596–1650) and later materialist philosophers of the 17th century stated that creatures, either human beings or animals as mechanisms without a soul. This early school of thought merely interested in fundamental issues about the body's function and the nature of life, leading to the development of the **biomechanics** field (Keevil, 2012). Indeed, following Harvey's work, Giovanni Alfonso Borelli (1608–79) examined the human body in its static as well as dynamic positions, from the structure to the motion, balance, and forces vis-à-vis almost all the principal joints, with the recognition that the muscles balance the body-weight (*Figure **1a***). Borelli's famous *De motu animalium* (published posthumously in 1679) is the first comprehensive treatise on biomechanics. Borelli was probably the first to determine man's centre of gravity experimentally (Marquet, 1992). The following century saw the first introduction of the term Medical Physics (or, more accurately, ***Physique médicale***) in Paris in **1778** by Félix Vicq d'Azir (1748-94), the general secretary of the Société royale de médecine (Parent, 2007) which set Paris on the road to becoming the leading centre for medical training and research in Europe for the first half of the 19th century (Société royale de médecine, 1790). We find Mauduyt de la Varenne (1732-92) making a critical study into the **medical uses of electricity** (Mauduyt, 1784) following the demonstration of charge storage in a Leyden Jar in 1746 by Pieter van Musschenbroek (1692-1761), and the observations of Abbé Jean-Antoine Nollet (1700-70) on the **biological effects of electricity** in his experimental animals and plants after electrification (*Figure **1b***) (Nollet, 1749). Physicists had rapidly engaged in exploring its possible medical applications. In Geneva, Jean Jallabert (1712-68) was amongst several who reported successful treatment of paralysis using electric shocks (Jallabert, 1749). In 1786, Italian physician, physicist, biologist and philosopher Luigi Galvani (1737–98) discovered "**animal electricity**" in his famous experiments with the muscles of dead frogs' legs twitched when struck by an electrical spark. This one of the first forays into the study of bioelectricity has made Galvani the pioneer of **bioelectromagnetics. Together** with Alessandro Volta (1745–1827), who demonstrated his electric pile in 1800, they founded the **electrophysiology** science (Porter, 1997).

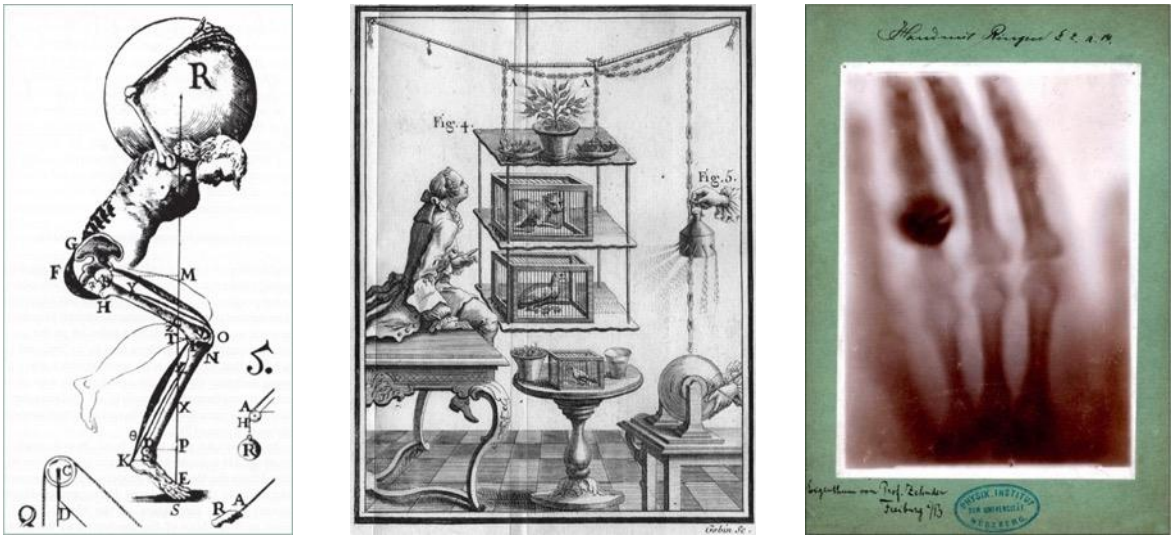

(a) (b) (c)

Figure 1| Three discoveries in physics that have revolutionised modern medicine

(**a**) Giovanni Borelli's representation of the body as a mechanism in his *De Motu Animalium*: how muscles balance the body, and a load carried on the neck. "If the spine of a stevedore is bent and supports a load of 120 pounds carried on the neck, the force exerted by Nature in the intervertebral disks and the extensor muscles of the spine is equal to 25,585 pounds. The force exerted by the muscles alone is not less than 6404 pounds". (Marquet, 1992). (**b**) Abbé Nollet's experiment on animals and plants (Nollet, 1749). Nollet measured the change in weight of cats and small birds after placing them either near an electrified body or within an electrified cage. Electrified animals lost more weight than the controls (Duck, 2014). (**c**) Hand mit Ringen (Hand with Rings): a print of one of the first X-rays by Wilhelm Röntgen (1845–1923) of his wife Anna Bertha Ludwig's left hand on November 8th, 1895. This first-ever X-ray image was presented to Professor Ludwig Zehnder of the Physik Institut, University of Freiburg, on January 1st, 1896. From Wikimedia Commons, the free media repository.

The early 19th century was marked by critical investigation of physics in biomedicine and physiology, from the famous **wave theory of light** by Thomas Young (1773–1829) to the invention of the **ophthalmoscope** by Hermann von Helmholtz (1821–94) and the invention of the **stethoscope** in 1816, the most iconic of medical instruments, by René Laennec (1781–1826). A complete, accurate and concise **definition of medical physics** in French arose in the 1814 revised edition of Nysten's medical dictionary (Nysten, 1814):

> *Physics applied to the knowledge of the human body, to its preservation and to the cure of its illnesses ("Physique appliquée à la connaissance du corps humain, à sa conservation et à la guérison de ses maladies").*

Nevertheless, the term "medical physics" took more than a decade to first appear in English in one of the most influential textbooks ever written on general science *Elements of Physics* (Arnott, 1827). This has created a shared understanding of the connection between physics and medicine, which marked the beginning of medical physics as a coherent discipline. Neil Arnott (1788-1874) was also the inventor of the water bed – labelled the "Hydrostatic Bed" – first used

professionally in 1873 at St Bartholomew's Hospital (London, UK). From the late 19th century onwards, fundamental physics was a compulsory element in medical education in the UK, recognising the growing importance of physics in medical practice.

The late 19th century saw a historical revolution in medical physics since, in the early evening of November 8th, 1895, an illuminating accident led to the discovery of "a new kind of ray" by Wilhelm Röntgen (1845–1923) which changed everything (Stanton, 1896). The first **X-ray image** Röntgen took of his wife Bertha's hand with her wedding ring visible (*Figure **1c***) is one of the most famous scientific images in history. Röntgen's discovery of a new form of energy would be named after him. Still, he always preferred the term X-radiation or X-rays – from the mathematical designation "X" denoting something unknown – as no one understood these great rays. Researchers worldwide could experiment on X-rays to develop body imaging, amongst others, as Röntgen refused to patent his findings, convinced that his "inventions and discoveries belong to the world at large" (from Nobelprize.org). Within four years since the discovery that earned Röntgen the first Nobel Prize in 1901, and of which the medical implications were immediately realised, human history witnessed some of the most significant discoveries in life science. A few months after Henri Becquerel (1852–1908) discovered radioactivity (uranic rays) in 1896, Pierre and Marie Curie (1859–1906 and 1867–1934, respectively) (*Figure **2a***) discovered **radium** and **isolated radioactive isotopes**. They shared a Nobel prize in Physics in 1903 (and later a second Nobel prize for Madame Curie in 1911, this time in Chemistry). None of these investigations was uplifted by the prospect of medicine. Still, their medical potential was recognised without delay, with the first use of **radiography** on the battlefield in March 1896 and by the next month, the creation of the first scientific journal dedicated to **medical imaging**, *Archives of Clinical Skiagraphy* (from Greek σκια for a shadow - an early term for radiography) (Keevil, 2012). From then on, the use of ionising radiation in medicine was widely recognised, in particular via the rapid progress of radiotherapy and X-ray imaging. The **first cancer treatment by X radiation** was performed in Savoie, France, by Dr Victor Despeignes (1866-1937) for a patient with an epigastric tumour. That cancer had shrunk by about 50% (Sgantzos *et al.*, 2014). Inspired by this, radiologist Jean Bergonié (1857-1925) and histologist Louis Tribondeau (1872-1918) have laid the first biological basis for the use of X-rays, demonstrating that cancer cells are more sensitive to X-rays than healthy cells (formulating the following law: "X-rays are more effective on cells which have a greater reproductive activity; the effect is greater on those cells which have a long lineage, on those

cells the morphology and the function of which are least definitively fixed") (Bergonié *et al.*, 2003).

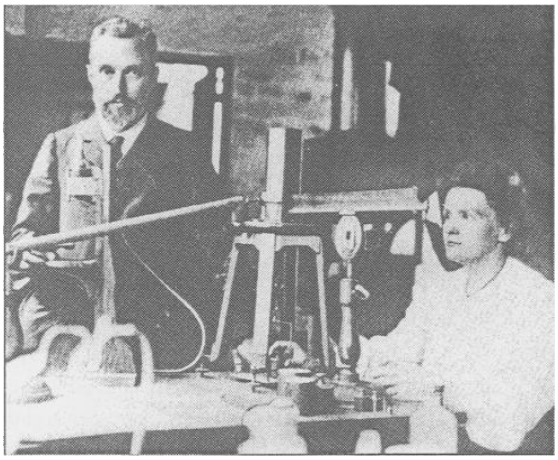

(a)

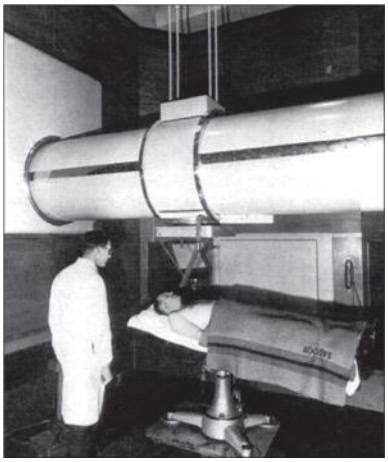

(b)

Figure 2| Portrait of Pierre and Marie Curie and a photograph of one of the first radiotherapy units in clinics (**a**) Pierre and Marie Curie, in their humble Paris laboratory in 1899, with Marie Curie proceed to the measurement of a radioactive sample. With the right hand, she lifts progressively the weight applied to the quartz; in the left hand, she holds the chronometer (Adloff, 1999). (**b**) One of the world's first megavoltage radiotherapy units at St Bartholomew's Hospital, London, UK, in 1937 (Keevil, 2012).

Occurring after, and mainly because of World War II (1939-1945), **nuclear medicine** was one of the greatest innovations in radiotherapy that extended the applications of medical physics, especially in the treatment of cancer. ^{131}I produced at the Berkeley cyclotron (Berkeley CA, USA) was the first radioisotope used in the clinic for thyroid investigations in 1939, then for treating **hyperthyroidism and thyroid cancer** (Hamilton *et al.*, 1939). *Figure 2**b*** depicted one of the world's first **megavoltage radiotherapy** units implemented at St Bartholomew's Hospital in London in 1937 (Keevil, 2012). Imaging techniques and standardisation operating procedures have also benefited from tremendous technological development: **ultrasound imaging** in the 1930s for non-destructive examination followed by medical applications in the 1950s (Wells, 2001); positron emission tomography (**PET**), invented in the 1950s; electron linear accelerators (**linacs**) for delivery of megavoltage x-rays, a spin-off from war-time research on the radar, used at Hammersmith Hospital (London, UK) by 1953; **nuclear tomographic imaging**, also known as single-photon emission computed tomography, developed in the 1960s, etc. One of the most significant advances in medicine in the last millennium is the invention of the **X-ray computed tomography** (**CT**) scanner in 1973 by Godfrey Hounsfield (1919–2004) and Allan Cormack (1924-98). The revolution that CT brought about in medical imaging has been surpassed only by the invention of **magnetic resonance imaging** or **MRI** in 1973 (Lauterbur, 1973; Mansfield *et al.*,

1973). Based on nuclear magnetic resonance (NMR) that applies magnetic fields rather than ionising radiation, MRI is a powerful and flexible technique for imaging physiological and mechanical function and structure, such as the **brain** with its consciousness, a notion which Descartes and fellows of the past centuries ignored. Following those imaging techniques, **multimodality imaging** – true imaging fusion – garnered momentum for **clinical oncology** with the complementary capabilities of PET and CT (Beyer *et al.*, 2000) or, more recently, PET and MRI (Marsden *et al.*, 2002) in one imaging system. Another essential invention in physics and medicine history was the **laser** (an acronym for "light amplification by stimulated emission of radiation"). The medical applications of laser (laser medicine) were settled within a year of constructing the first functioning laser in 1960 (Müller *et al.*, 2006), starting in ophthalmology and dermatology, followed by surgery and in **photodynamic therapy**.

Many physics-based medical innovations, such as CT and PET, have resulted from focused research with clinical purposes in mind. Nonetheless, generally significant developments have been unpredictable spin-offs from basic science research. Their translation into clinical practice, if this takes place, has not always been as rapid or straightforward. On the other hand, by focusing on these historical events, we can easily forget that other medical applications of physics have their origins at this same time. The therapeutic use of infrared (**IR**) and ultraviolet (**UV**) radiation was pioneered by the Nobel prize-winning Danish doctor Niels Ryberg Finsen (1860-1904), who introduced the “red room” treatment for smallpox lesions in 1893, and who, in 1895 showed that *Lupus vulgaris*, a disfiguring form of tuberculosis, responded to treatment with concentrated light radiation. Thus, **phototherapy** was born. Another investigation on the biological responses of electrical currents and the problem of industrial deaths from electrocution was performed by Arsène d’Arsonval (1851- 1940), professor of biophysics at the Collège de France (Paris, FR), who introduced the first **clinical high-frequency heat therapy** unit, in the Hôtel Dieu, in 1891. Thus, **modern electrotherapy** was born. At the same time and following the path of Abbé Nollet, who reported the first systematic observations of the appearance of red spots on animal and human skin exposed to electric sparks (Nollet, 1749), Ritter in 1802 (Noah, 1849), Frankenhaeuser & Widén in 1955 (Frankenhaeuser *et al.*, 1956), and Stämpfli & Willi in 1957 (Stämpfli *et al.*, 1957) reported that nerve membrane “**electrical breakdown**” might explain the electrical conductivity changes in nerves which electric fields have damaged. The bio-medical application of **pulsed electric fields** began quickly in 1982 with the seminal work of Neumann and colleagues to temporarily **permeabilise cell membranes** to

deliver foreign DNA into cells (Neumann *et al.*, 1982). They termed the phenomenon "**electroporation**". Thus, **electroporation-based technology** was born.

Another modern science, **plasma science,** finds its fundamentals established in 1879 by Sir William Crookes (1832-1919) when he was experimentally ionising gas in an electrical discharge tube thanks to the application of high voltage through a voltage coil (Crookes, 1879). Crooks designated the **ionised gas** "radiant matter". Almost fifty years later, in 1927, when Irvin Langmuir (1881-1957) observed that the flow of certain highly ionised gases in a closed atmosphere resembled that of blood flowing through the vascular system, he proposed, "*We shall use the name **plasma** to describe this region containing balanced charges of ions and electrons*" (Langmuir, 1928). This observation gave birth to the current plasma term, whose technology has since been applied in many domains over the past few decades, including medicine. Thus, **non-thermal plasma technology** was born.

A broad and necessarily selective history of physics's contribution to medicine has been presented. Even briefly introduced, this contribution is undoubtedly essential and diverse. With specific respect to the clinic, most contemporary medical procedures involving those physical inventions have been refined over decades and now are considered safe and beneficial. We now stand on the brink of a new revolution in post-genomic personalised medicine, with physics-based technologies again at the forefront. The following sections of this chapter will offer a general view of **electroporation-based and non-thermal plasma technologies** that have garnered the rising interest of physicists, biologists, and physicians for their potent applications in various life science fields, including for medical research against cancer – the centre of this thesis.

1.2 Electroporation-based technology

1.2.1 History of cell membrane impermeability rupture by electric pulses

The appearance of red spots on animal and human skin exposed to electric sparks observed by Abbé Nollet (Nollet, 1749) (see history in **Chapter 1.1**) could be considered the first systemic observations of the thermal damage tissues by pulsed electric fields. This marks the beginning of the history of the **electropulsation phenomenon**. Over the next two centuries, as mentioned above in that history, this effect was reported in a series of investigations: from Frankenhaeuser and Widén (Frankenhaeuser, 1956) to Stämpfli and Willi (Stämpfli, 1957) for the excitable

membrane at the Ranvier nodes, followed by a study by Stämpfli where he compared the phenomenon to the breakdown of the dielectric field of a capacitor and reported that under certain conditions, **membrane breakdown** is **irreversible** whereas in others it is **reversible** (Stämpfli, 1958). In 1967, a pivotal study by Sale and Hamilton on non-excitable cells of micro-organisms under electric fields (Hamilton *et al.*, 1967; Sale *et al.*, 1967) set the basis for the field of **irreversible electroporation**. The observations reported by Sale and Hamilton laid the foundation for many future studies in electroporation in general. Kinosita and Tsong, in the 1970s showing **high-amplitude pulsed electric fields (PEFs)** could be tuned to **generate defects** of different sizes in erythrocyte membranes ("**pores**") and that those pores eventually resealed, allowing for selective internalisation of naturally impermeant molecules (Kinosita *et al.*, 1977a., Kinosita *et al.*, 1978). These researchers also demonstrated the increase in conductivity that follows the application of high voltage (HV) pulses and the ability of the electric fields to directly cause haemolysis (Kinosita et al., 1977b., Kinosita *et al.*, 1977c). These early contributions supported **the theory of aqueous pore formation**, published the following year (Sugár, 1979). Those studies were followed by similar ones for planar lipid bilayers in 1979 (Benz *et al.*, 1979) and lipid vesicles in 1981 (Teissié *et al.*, 1981).

Less than ten years later, as presented in the previous section, Neumann and colleagues managed to use short and intense electric pulses to introduce DNA into a mouse lyoma cell line in suspension to **induce the expression of the exogenous gene carried by the DNA** (Neumann, 1982; Wong *et al.*, 1982), coining the term "**electroporation**" and opening the gate for what was called electrogenetherapy (EGT) henceforth. The same year witnessed the use of reversible electroporation to produce a fusion between cells (Zimmermann, 1982). More than two years were necessary before the second publication on the successful electrotransfer of DNA to eukaryotic cells *in vitro* by Potter and colleagues (Potter *et al.*, 1984), achieved using the ISCO 494 generator - a piece of classical laboratory equipment for proteins and DNA gels electrophoresis. Ever since, microbiologists have employed electrophoresis power supplies as accessible equipment to perform gene transfection in bacteria by electroporation. Another remarkable discovery of PEFs in biology, which has revolutionised the medical field, was the **introduction of cytotoxic agents into malignant cells** after electroporation, an investigation pioneered by our group in 1987-1988 (Mir *et al.*, 1988; Orlowski *et al.*, 1988). Those studies paved the way for the potential of PEFs in cancer treatment since the studied **hydrophilic molecules** (anticancer drugs netropsin and **bleomycin**) could not cross the plasma membrane

in ordinary conditions but diffuse directly into the cytosol under the delivery of PEFs that transiently permeabilised the cell membrane. Indeed, only a few years later, in 1991, our group published two breakthrough papers on the use of reversible electroporation in oncology, an *in vivo* study (Mir *et al.*, 1991a) and **the first clinical trial** in the field (Mir *et al.*, 1991b). We termed that application "**electrochemotherapy**" or **ECT**. Note that there were also important series of studies: the demonstration of irreversible electroporation in the case of tissue electrical trauma (Gaylor *et al.*, 1988; Lee *et al.*, 1987., Lee *et al.*, 1988), the first skin electroporation used for **transdermal drug delivery** (Prausnitz *et al.,* 1993), the first *in vitro* application of HV pulses of **sub-microsecond duration** (60 ns) (Schoenbach *et al.*, 1997), the first report of the blood flow blockage in the area where applied PEFs during tissue reversible electroporation (Ramirez' *et al.,* 1998), a phenomenon that our group later referred to as the **vascular lock** (Gehl *et al.*, 2002).

The fundamental principles introduced by those investigations still underlie our current understanding of the electropulsation phenomenon, whose mechanisms will be briefly discussed in the next section.

This cell membrane rupture of impermeability by the electric pulses has resulted in the electroporation-based technology, whose versatility has found its applications in daily life and biomedicine. Those applications will be further described in **chapters 2 and 3**, focusing on electrochemotherapy as this thesis's primary field of study.

1.2.2 A mechanistic perspective

1.2.2.1 Electropermeabilisation at the cell level

Let us look back at our cellular membrane, whose detailed organisation remains somewhat elusive. Typical mammalian **plasma membranes** (PM) contain hundreds of different lipids with a highly non-uniform lateral mixing (Ingólfsson *et al.*, 2014). Of only 5 nm of thickness with a eukaryotic cell of about 15 to 50 µm in diameter, the PM regulates all the exchanges between the outside and the inside of the cell in an exact manner. In particular, the PM acts as a barrier that prevents the free diffusion of not only vitally essential molecules, such as all the substrates or products of the cell metabolism, ions, sugars, and amino acids, but also other large hydrophilic molecules. Life would not be possible without controlling the transport of substances across the cell membrane. Together with the small hydrophilic molecules that are

not transported through channels or pumps of the PM, these molecules (termed "non-permeant" molecules) can only reach specific cell compartments of the cell (but neither the cytosol nor the nucleosol) by endocytosis/exocytosis.

To allow the uptake of those non-permeant molecules, perturbations must be initiated at the PM level, *i.e.*, concerns that transiently break up the PM impermeability. One of the most popular and practical methods to reversibly permeabilise the PM consists of applying **adequate PEFs** – a theory firstly elaborated by Neumann and colleagues, as mentioned above, and which they termed "**electroporation**". Their electroporation theory states that the electric pulses-induced transmembrane voltage difference can enlarge the normal fluctuations of the PM, resulting in their large hydrophobic pores. These pores become hydrophilic by rotating the lipids at the limits between the lipid bilayer and the aqueous medium that tries to fill the hydrophobic "pore" (conduit).

To explain this theory as early as it was reported, some 1D approximations of the PM were analytically modelled (Bernhardt *et al.*, 1973; Litster, 1975). If considering the cell as a 1D model (*Figure **3a***) at a physiological state, the cell PM has a **native transmembrane potential difference** or $\Delta\psi_O$, whose value depends on the species and the cell type (Escoffre *et al.*, 2012). $\Delta\psi_O$ is found generally around -70 mV for excitable cells. The exposure of living cells to short-duration and intense electric HV pulses induces **electrophoretic movement** of ionic charges (mostly small ions) on both sides of the plasma membrane, *i.e.,* an **induced transmembrane potential** ($\Delta\psi_i$). This generates a transient increase in the permeability level of the PM.

$\Delta\psi_i$ is defined by the Schwan equation (a derivation of Laplace's equation published by H. Schwan (Schwan, 1957)):

$$\Delta\psi_i = {}^3/_2 \times E_{ext} \times r \times \cos(\Theta)$$

where (Gimsa *et al.*, 2001; Kotnik *et al.*, 2000; Schwan, 1957):

E_{ext}: the external electric field strength

r: the radius of the cell

Θ: the polar angle between the field line and a normal from the centre of the cell (approximated by a sphere) to the point of interest on the cell membrane

When the transmembrane potential difference net value (the sum of the vectorial values of the induced and resting potential differences or $\Delta\psi_O + \Delta\psi_i$) is more significant than **200 to 300 mV**, there will be the formation of **short-lasting pores** in the PM with chemical modification of the lipids. These transient permeation structures are generated at the cell membrane level

because the membrane structure has to endure the electro-compressive forces caused by this potential difference. Under the electric field, water dipoles orient and form almost single molecule-thick columns that penetrate the lipid tails' layer. Phospholipid heads also move towards the interior of the PM, and columns rapidly enlarge to form hydrophilic conductive large pores ("**pre-pore**"), resulting in its permeabilisation.

With time, there are many more studies investigated not only in *in silico* using molecular dynamics (MD) simulations (some will be discussed in the next section) but also *in vitro* to better under the electroporation phenomenon (Azan *et al.*, 2017; Breton *et al.*, 2012a; Gabriel *et al.*, 1997; Kinosita, 1977a; Kotnik *et al.*, 2019; Rols *et al.*, 1998a; Teissié *et al.*, 1993). However, electroporation is always well described by the equation of Schwan, indicating that the value of the induced change is proportional to the cell radius and the scalar value of the external electric field.

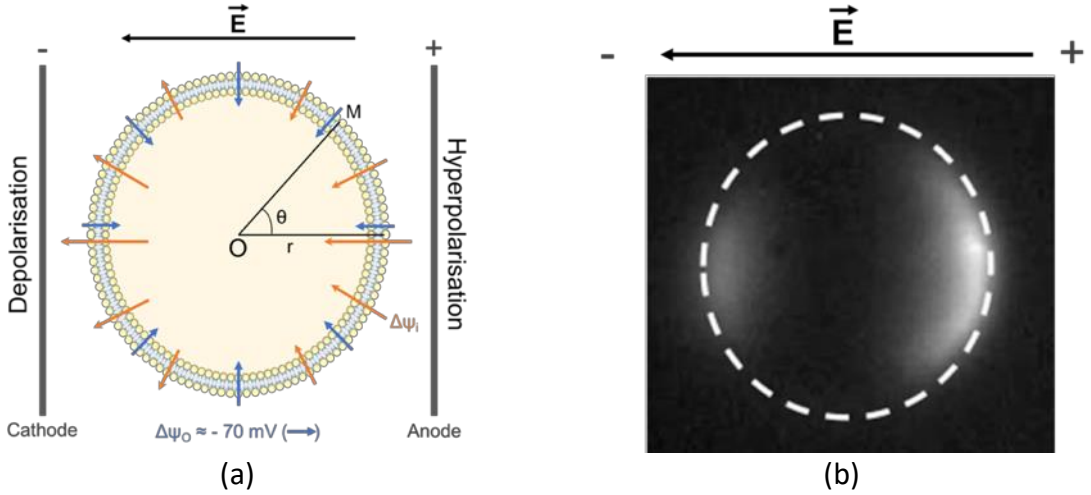

Figure 3| The physical principle of electroporation on a cell

(**a**) The cell plasma membrane naturally has a native transmembrane potential difference or $\Delta\psi_O$ (blue arrows) which value depends on the species and the cell type. Considering the cell as a sphere of a radius r, its plasma membrane as a very thin spherical dielectric bilayer shell, when electric pulses are applied, an induced transmembrane voltage $\Delta\psi_i$ is created (orange arrows). The cell permeabilisation appears only on the part of the plasma membrane where the potential difference has been brought above its critical value of *ca.* 200-300 mV, *i.e.*, $|\Delta\psi_O + \Delta\psi_i \approx 200 - 300\ \mathrm{mV}|$. The $\Delta\psi_i$ effect is position-dependent on the cell surface (dependent on the angular parameter Θ), hence, under an applied electric field, the side of the cell facing the anode (+) is hyperpolarised while the one facing the cathode (-) is depolarised. (**b**) The localisation and asymmetry of electropermeabilisation can be detected by propidium iodide uptake in a CHO cell submitted to a train of 10 electric pulses, 5 ms, 1 Hz at 700 V/cm. Adapted from (Bernhardt, 1973; Escoffre, 2012; Kinosita, 1977a; Teissié, 1993).

The **resting transmembrane potential** is essential for the permeabilisation threshold and the succession of events. Permeabilisation will initially happen at the pole of the cell facing the anode (the positive electrode), where the capacitance of the membrane is first exceeded when an external electric field is applied. The second event is the permeabilisation of the pole of the

cell facing the cathode (the negative electrode). The extent of permeabilisation (area of the permeabilised membrane) on the pole facing the anode can be controlled by **pulse amplitude**, *i.e.*, the higher the pulse amplitude, the greater the area through which diffusion can take place (Gabriel, 1997). The degree of permeabilisation can be controlled by the **pulse duration** (and pulse number), *i.e.*, the longer the pulse, the greater the perturbation of the membrane in a given area (Gabriel, 1997). Depending on the electric field strength and the duration of the exposure of cells, the membrane electroporation can be **either reversible or irreversible**, **with or without thermal damage** (*Figure **4***).

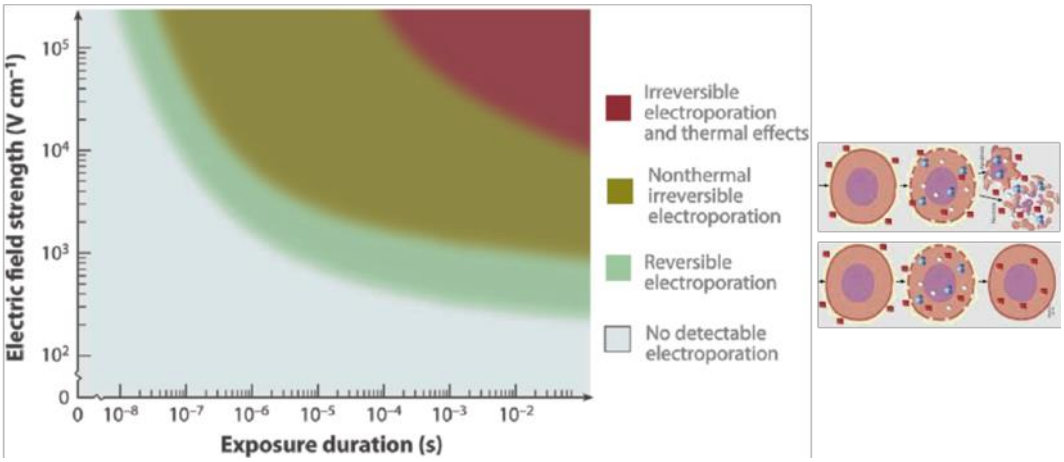

Figure 4| Schematic of different effects on cells exposed to electric fields, including the consequent thermal effects

Reversible electroporation, irreversible electroporation and thermal damage zones are displayed as functions of electric field strength and pulse length (exposure duration). Note that the field scale is logarithmic and approximative. Figure adapted from (Bower *et al.*, 2011; Yarmush *et al.*, 2014)).

- Reversible electroporation is defined as the **temporary permeabilisation** state of a cell exposed to an electric field. The presence of the electric field disturbs the phospholipid bilayer, allowing molecules to reach the cell interior through the cell plasma membrane. The cell membrane will recover its initial state afterwards (*Figure **4***, lower panel).
- Irreversible electroporation also referred to as non-thermal irreversible electroporation or **IRE**, is defined as the **permanent permeabilisation** state of a cell exposed to HV electric pulses. It induces the loss of homeostasis (lethal biochemical imbalance) and apoptotic-like cell death by irrecoverable disruption of the cell membrane (*Figure **4***, upper panel). Consequently, sooner or later, all molecules will

be able to freely cross the cell membrane when it cannot fully recover its initial impermeability.

1.2.2.2 Electroporation of the lipid bilayer: molecular mechanisms

Since electroporation, as it is called, is a succession of events, our group also proposed the term **electropulsation** (comprises cell electroporation followed by cell electropermeabilisation) to better describe the action of PEFs on the cell membrane. The kinetic of electropulsation phenomenon can be described in five major steps, with timescale (Kotnik, 2019; Rols *et al.*, 1990; Teissié *et al.*, 2005):

- Initiation or creation of pores (ns for the conductivity, and µs for the permeability): the applied PEF induces a membrane potential difference and reaches the critical value ($E = E_{Poration}$). The plasma membrane is destabilised (mechanical stress with a magnitude that depends on the buffer composition), some membrane defects are generated and permeabilisation begins.
- Expansion (up to µs): these defects expand on the cell surface as long as the PEF strength is larger than a critical value ($E > E_{Poration}$) and the density of the defects increases as long as the field is present (cumulated duration);
- Stabilisation and partial recovery (µs for the conductivity, and ms for the permeability): points of cell permeabilisation for small molecules remains but the membrane retrieves its organisation as soon as the PEF is subcritical ($E < E_{Poration}$);
- Resealing (seconds to minutes at about 20-37°C, and hours at about 4°C): once the PEF is turned off ($E < E_{Poration}$ until $E = 0$), the membrane gradually loses its permeability (the annihilation of leaks is slow), returning to its initial impermeable state (unless damages are irreversible, leading to the loss of cell viability after this step);
- Memory (hours): some structural changes and physiological properties recover on a much longer time scale while the cell viability is preserved.

MD simulation was employed to simulate and understand the effect of PEFs at the cell membrane level (*Figure **5***), offering a better visualisation of the electroporation (Delemotte *et al.*, 2012; Tarek, 2005). This computational methodology simulates the evolution of the atoms composing the cell membrane and its surroundings for tens of nanoseconds. Pore generation can occur during the computational time if the force corresponding to the simulated electric

field is high enough. This process is stochastic, and simulations often require a high field amplitude. Since, in the calculations of MD, each molecule is considered, the region of interest is limited by the number of elements that the computer can handle simultaneously; thus, the constraints in both sample size and the duration of the simulation (especially that of ns timescale) (Azan, 2017). Otherwise, too heavy MD simulations have to be run, with a computational cost challenging to afford. Using MD simulation, Vernier and colleagues have demonstrated that electroporating fields target oxidatively damaged areas in the cell membrane (Vernier *et al.*, 2009); Yusupov *et al.* also revealed the synergistic effect of electric field and lipid oxidation on the permeability of cell membranes (Yusupov *et al.*, 2017), elucidating the dynamics of the permeation process under the influence of combined lipid oxidation and electroporation.

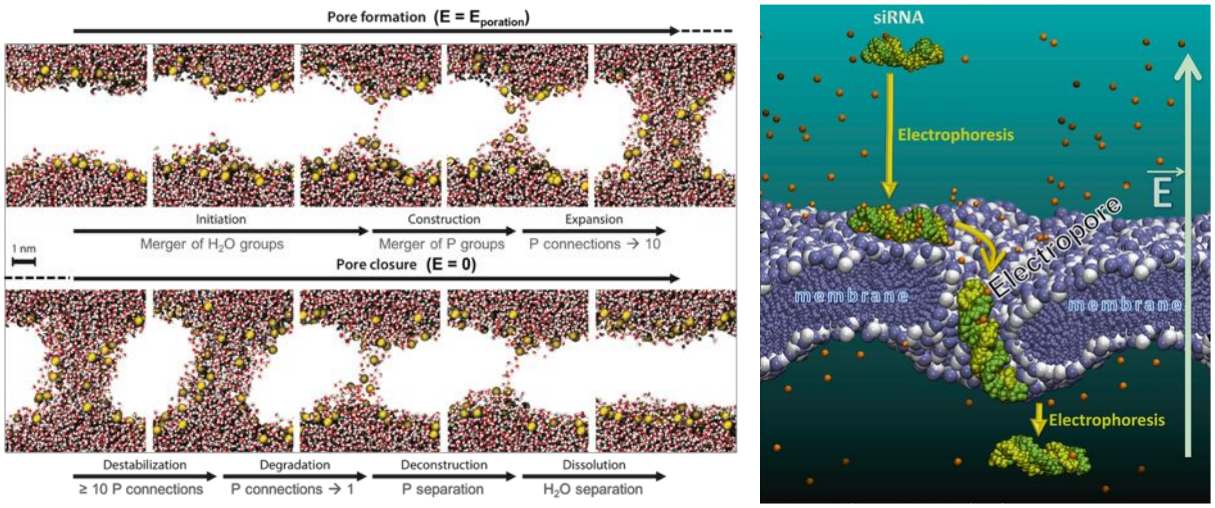

Figure 5| Molecular dynamic simulation of the electropulsation phenomenon in the lipid bilayer

(**a**) Life cycle of an electrically induced pore in the lipid bilayer. For simplicity and clarity, only water molecules (H_2O, represented by red and grey spheres) and phosphorus atoms of the polar fatty acids (P, represented by large green spheres) from the lipid headgroups are shown (apolar tails of phospholipids not represented) Stages of pore formation and closure are displayed in their order of appearance but disregarding the differences in their characteristic timescales. The formation of pores begins with the onset of the electric field (E), and closure begins as the field ceases (E = 0). Figure adapted from (Kotnik, 2019; Levine *et al.*, 2010). (**b**) Electrotransfer of a double-stranded siRNA (yellow and green spheres) through an aqueous pore within a model DOPC membrane (headgroups showed as blue and grey spheres and hydrophobic tails as cyan lines) driven by nanosecond electric pulses. When being submitted to a pulse of sufficient field strength, the siRNA is dragged by electrophoresis towards the membrane and several of the siRNA phosphate groups strongly associate with the cholines of the phospholipid headgroups. If the siRNA is close to an electropore (*i.e.*, a field-induced hydrophilic pore), the siRNA can slide electrophoretically along this pore, against the field direction, being finally detached from the membrane phospholipids by electrophoresis. In the simulation, the translocation of a 23 bp siRNA can be completed within less than 10 ns under a transmembrane potential difference of 1.6 V. For clarity, water molecules are omitted, and the lipid headgroups initially in interaction with the siRNA strand are depicted in red to highlight their lateral diffusion. (Breton *et al.*, 2012b; Mir, 2014)

*Figure **5a*** illustrates an electropore in a lipid bilayer (Kotnik, 2019; Levine, 2010). **Pore creation** in an electric field begins with introducing water into the bilayer, followed by the reorganisation of the phospholipid head groups in each leaflet around the defect (**pore construction**). Migration of additional water and head groups into the created pore continues until an arbitrarily defined mature pore structure is formed (**pore maturation**). Pore annihilation begins with the removal of the "porating" electric field. The pore structure is quasi-stable at this time (**pore destabilisation**). Still, soon after that, there is a decrease in pore size as head groups and water begin to migrate out of the membrane interior (**pore degradation**). The head groups separate again into two groups (**pore deconstruction**). Water quickly follows (**pore dissolution**), and the intact structure of the bilayer is restored. *Figure **5b*** illustrates the mechanism of electrotransfer of a double-stranded siRNA through an aqueous pore within an

artificial lipid membrane of a giant unilamellar vesicle (GUV) synthesised with 1,2- dioleoyl-sn-glycero-3-phosphocholine (DOPC), under nanosecond pulses (Breton, 2012b; Mir, 2014). Despite the constraints of heavy MD simulations, our group succeed to predict the electropulsation phenomenon with ns pulses (Breton, 2012b).

For the *in vitro* study of the electroporation phenomenon, there are several techniques developed to detect plasma membrane electroporation. Those physical and chemical methods are highlighted in the graphic shown in *Figure **6*** (Napotnik *et al.*, 2017).

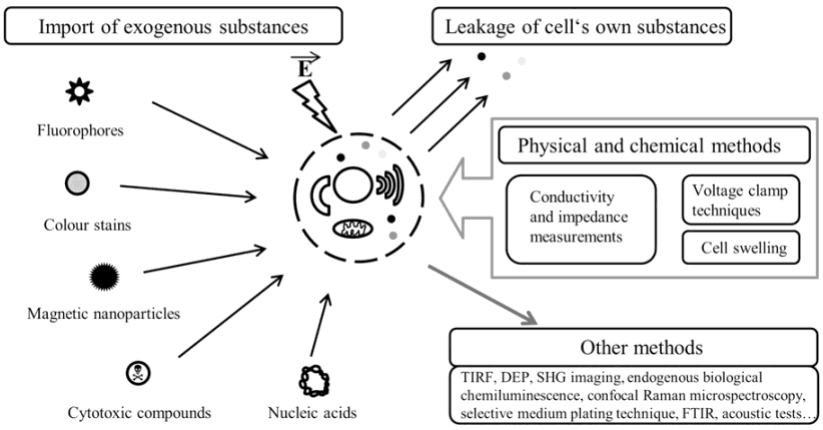

Figure 6| Different methods employed for *in vitro* detection of plasma membrane electroporation
Abbreviations: TIRF – total internal reflection fluorescence microscopy, DEP – dielectrophoresis, SHG – second harmonic generation, FTIR – Fourier transform infrared spectroscopy. Graphic adapted from (Napotnik, 2017).

1.2.3 Electric pulse generator and electrodes

The delivery of EPs to cells or tissues can be performed using both home-made *(Zerbib et al.*, 1985) or commercially available electric pulse generators. Some CE approved generators authorised for application in humans are presented in *Figure **7***.

The Cliniporator™ was produced by IGEA®, an Italian spin-off company of the University of Modena, in 2006 during the ESOPE project (European Standard Operating Procedures of Electrochemotherapy). The NanoKnife 3.0 Generator is a product of AngioDynamics, Inc. (New York, US), employing IRE technology for surgical ablation of soft tissue (US) and cell membrane electroporation (CE). The computer-controlled Cliniporator™ allows the setting and controlling pulse parameters on a screen and monitoring and storage of delivered current and voltage parameters for immediate management and later retrieval and analysis. Furthermore, this square-wave pulses Cliniporator™ can deliver a high pulse frequency, enabling the use of more complex electrodes (Marty *et al.*, 2006).

(a) (b) (c)

Figure 7| Some electric pulse delivery units
(**a** and **b**) The Cliniporator™ (IGEA® Clinical Biophysics, Carpi, Italy). (**c**) The NanoKnife 3.0 System (AngioDynamics, Inc., New York, US).

Many preclinical (André *et al.*, 2008; Čemažar *et al.*, 2009) and clinical (Gehl *et al.*, 2006; Snoj *et al.*, 2009; Spanggaard *et al.*, 2013) studies using electroporation involved the Cliniporator™. This computer-controlled medical device provides two types of EPs:

- short (microsecond time scale), high voltage (HV, 100-1000 V) pulses
- long (millisecond time scale), low voltage (LV, 20-200 V) pulses

Considerable advances have been made in the fabrication of electroporation equipment for pre-clinical studies and clinical uses, among which has found the **electrodes** – one essential aspect of the electroporation (Gehl *et al.*, 1999; Gilbert *et al.*, 1997). Four types of fixed geometry electrodes are available (*Figure **8***):

- Non-invasive plate electrodes
- Invasive parallel row needle electrodes
- Invasive hexagonal needle electrodes
- Invasive finger electrodes

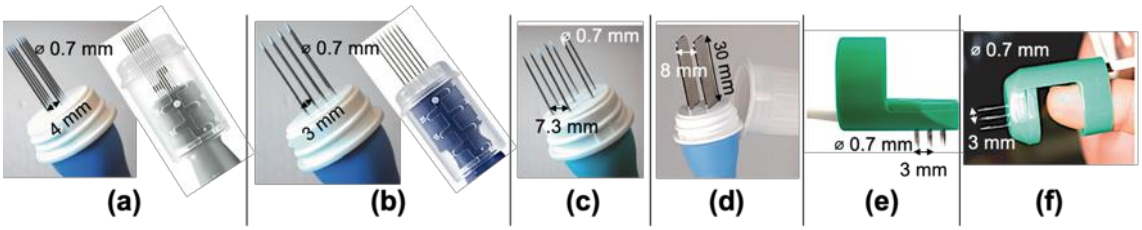

Figure 8| Different fixed geometry electrode configurations are available for ECT of different nodules with different depths, sizes, and shapes

(**a** and **b**) Adjustable (**a**) linear and (**b**) hexagonal configuration needle electrodes, 10 to 30mm in length for treatment of lesions up to 3 cm deep (recommended voltage 400 V). (**c**) Hexagonal needle electrodes, 10 to 40mm in length (recommended voltage 730 V). (**d**) Plate electrodes, 30mm length (recommended voltage 960 V). (**e** and **f**) Finger electrodes with (**e**) perpendicular or (**f**) axial needles, 5 to 10mm in length (recommended voltage 400 V) for the treatment of small lesions in anatomical cavities (up to 1 cm deep). Figure adapted from "Electrodes and Accessories" of the IGEA® Clinical Biophysics (Carpi, Italy) and (Miklavčič *et al.*, 2014).

For successful therapy, the entire target tissue must be exposed to the local electric field strength above the reversible threshold. There are thus electrodes developed recently for the treatment of **deep-seated tumours**. Those will be presented in **chapter 3**. The choice of the EP type and the choice of the electrodes will also be addressed in sections dedicated to electrochemotherapy (ECT) and electrogenetransfer (EGT). The efficiency of ECT strongly depends on the local electric field distribution inside the target tissue.

1.3 Non-thermal plasma technology

1.3.1 Plasma and the introduction of non-thermal plasma in biology and medicine

There are four fundamental states of matter: solid, liquid, gas, and plasma (*Figure **9a***). As the energy exerted on atoms increases, the thermal motion of atoms in the solid aggravates and finally overcomes the restrictive interaction between particles in the solid such as ionic bonds and forms liquid. Similarly, when the atoms in liquid obtain adequately significant energy to overcome the restrictive Van der Waals force from surrounding atoms, these liquid atoms will transfer into gas atoms. The translational energy of atoms in gas is much larger than that in liquid and solid. When the enthalpy is large enough for the electron to overcome the electrostatic potential barrier, the electron will be stripped away, creating a free electron and a positively charged ion (an ionisation process). The field energy causes the free electrons to accelerate and ionise the gas atoms and molecules, which release more free electrons that provoke new ionisations. At the same time, excited electrons produce molecular dissociations, forming new atoms and free radicals, which can excite atoms and molecules to higher energy

levels. When returning to a more stable state, excited atoms and molecules emit excess energy in broad-spectrum electromagnetic radiation, such as ultraviolet (UV) radiation. As a result, the plasma is constituted essentially by molecules and atoms in an excited state, positive and negative ions, free radicals, electrons, UV radiation and reactive oxygen and nitrogen species (RONS), such as atomic oxygen (including ozone (O_3)), superoxide (O_2^-), hydroxyl radicals ($^{\bullet}OH$), singlet oxygen ($^1O_2$), nitric oxide ($NO^{\bullet}$) or nitrogen dioxide (NO_2). Plasma is thus defined as an ionised gas in which many atoms have lost one or several electrons and exist in a mixture of free electrons and positive ions (Eliezer *et al.*, 2001).

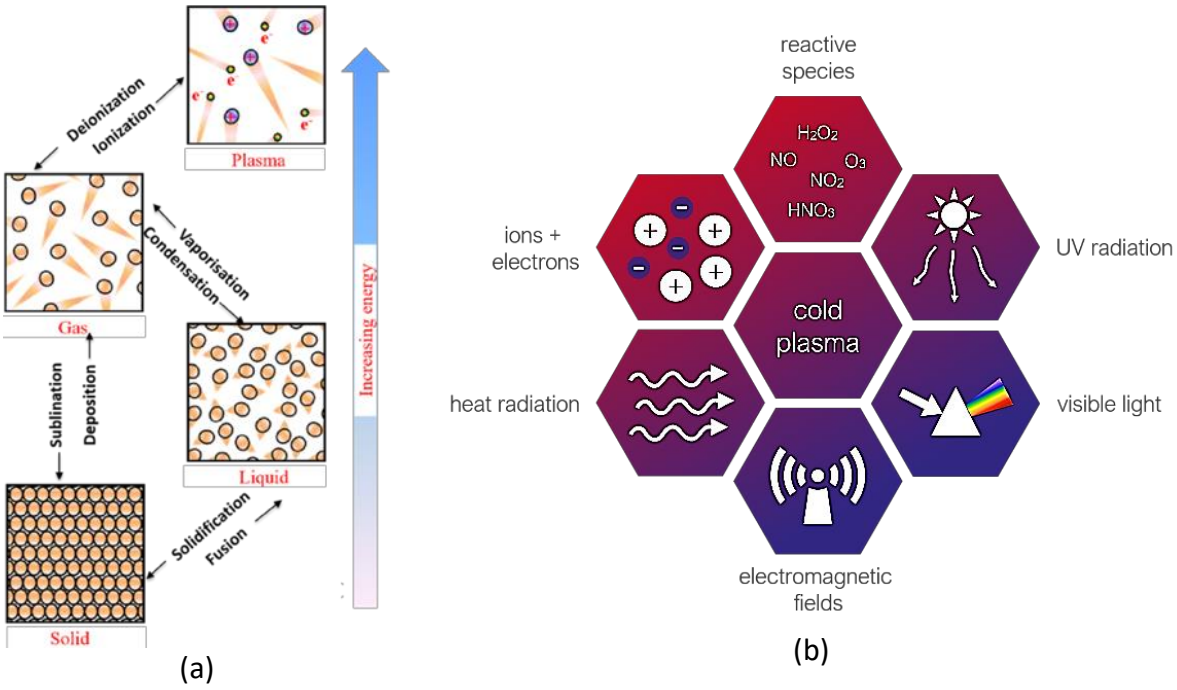

Figure 9| Schematic illustration of non-thermal plasma

(**a**) The four fundamental states of matter. The triangular tails represent the thermal motion strength of particles. Scheme adapted from (Yan *et al.*, 2017). (**b**) Different components of non-thermal plasma (also called cold plasma) (scheme from www.terraplasma.com/en/cold-plasma/).

In simple terms, plasma is an electrified gas with a chemically reactive media mixing a large number of different species such as electrons, positive and negative ions, free radicals, gas atoms and molecules, in the ground or any higher state, of any form of exciting species. Plasma is formed when a high voltage or temperature knocks off the outermost electrons from an atom, which in turn knock off electrons in the neighbouring atoms.

Temperature (enthalpy) increases when matters transform from solid to liquid to gas and plasma. The plasma temperature is determined by the thermal motions of electrons and heavy particles (atoms and ions); hence plasma is generally distinguished into two main groups: the

high temperature or fusion plasmas and the low temperatures or gas discharges. The low-temperature plasma is further divided into two groups, resulting in a classification of three distinctive kinds of plasma:

- High temperature (equilibrium) plasma: intensive collisions between all particles (electrons, ions and neutral species) increase their density. All particles have the same temperature and thus are in thermal equilibrium.
- Thermal (quasi-equilibrium) plasma: plasma in a local thermal equilibrium state.
- Non-thermal (non-equilibrium or cold) plasma: generated at reduced pressures, the heavy particle temperature of NTP ranges between +25°C and +50°C (usually less than 40°C at the point of the application). All particles are not in thermal equilibrium. The major components of a non-thermal plasma are electrons, ions, and radicals such as reactive oxygen and nitrogen species (ROS, RNS or also called RONS), mild thermal radiation, UV photons and visible light (*Figure **9b***).

Typical classification and parameters of plasma with some common applications are listed in *Table **1*** (this table contains some applications of plasmas that are presented in more detail in the next **chapter 2.2**).

Classification	Temperature (K)	Electron density (m^{-3})	Examples of discharge type	Applications
High-temperature (equilibrium) plasma	$T_e \approx T_{ion} \approx T_{gas} = 10^6–10^8$	$n_e \geq 10^{20}$	Laser fusion Tokamak	Fusion plasma for energy
Thermal (quasi-equilibrium) plasma	$T_e \approx T_{ion} \approx T_n \approx T_{gas} \leq 2 \times 10^4$	$n_e \geq 10^{20}$	Plasma torch, arc plasma, Radio-frequency (RF) inductively coupled discharges, Microwave plasma	Radiation, welding and cutting, waste treatment, material processing, etc.
Low-temperature (or non-thermal or non-equilibrium) plasma	$T_e \geq T_{ion} \geq T_n \approx T_{gas} = 300–1000$	$n_e \approx 10^{10}$	Glow or corona discharges, dielectric barrier discharge (DBD), micro-hollow cathode discharge	Ozoniser, volatile organic compound treatment, surface modifications (coating, etching, activation, cleaning, nitration, etc.),

	(MHCD), atmospheric pressure plasma jet (APPJ), plasma needle	Illumination (plasma screen, fluorescent lamps, etc.), plasma agri-food, plasma medicine

***Table 1**| Typical classification of plasma with some applications*
Adapted from (Sakudo *et al.*, 2019)

In nature, we find plasma in lightning as temporary electrical discharges, the solar wind or the northern light (aurora borealis). More than 99% of the Universe is composed of plasma. Our Sun is in a gigantic plasma ball whose core reaches 108 K, and since almost all of the stars that we observe in the sky are suns, they are in the high-temperature plasma state. Thunderstorm lightning is an example of thermal plasma that can find a temperature of approximately 2×10^4 K. For daily life applications, we see the plasma technology applied for microplasma welding (a method used to join paper-thin sheets of metals, *e.g.,* for the manufacture of stainless-steel water storage tanks or kitchen implements), plasma spray (the only process to coat any material onto any other one), printers (plasma makes plastics attract or repel liquids), neon lights, and plasma TV. Examples of plasma physics applications for applied sciences are international communications, energy power generators, and the nuclear fusion bomb (the hydrogen bomb).

Plasma Science and technology have offered a valuable contribution to human health for more than 50 years. Since thermal plasma can reach up to several thousand Celsius degrees, it is used in applications where high temperatures are required, such as casting processes in the metallurgical industry or chemical synthesis processes (*e.g.*, production of acetylene from natural gas). **Non-thermal plasma** (**NTP**), with temperatures close to ambient temperature, is, on the contrary, suitable for the treatment of heat-sensitive materials even though the mean electron energies of NTP is about 20 eV, considerably higher than those of the components of the ambient gas. NTP thus finds its utilisation in **biotechnology and medicine**, starting with experiments conducted in the 1960s and 1970s for biological applications. For example, NASA (The National Aeronautics and Space Administration) investigated oxygen plasma to destroy natural matter and inactivate microorganisms for space applications (Bol'shakov *et al.*, 2004; Mogul *et al.*, 2003). After decades of experience in biomaterials, in 1971, scientists began working with a device that took advantage of "the plasma state" properties to produce simultaneous division of tissue and coagulation of blood vessels. Thermal plasma, *e.g.*, plasma knife (plasma scalpel), was first demonstrated to heal the wound of mouse skin (Link *et al.*,

1973) and a few years later, was used for surgery — the work pioneered by Glover and colleagues in 1978 (Glover *et al.*, 1978., Glover *et al.*, 1982). Despite this historical connection, thermal plasma is typically associated with high energy physics or low-pressure processes employed in the semiconductor industry while being rarely used in medical applications directly. The few known uses of thermal plasma in medicine are based mainly on the high temperature generated by conventional thermal discharges. One good example of this is the Argon Beam or Argon Plasma Coagulator (APC), developed primarily to cauterise wounds (Ginsberg *et al.*, 2002). This device generates thermal plasma in flowing argon through HF (≥ 350 kHz) electrical discharge ionisation. The argon flow takes thermal plasma outside the ionisation tube, creating a jet that impinges onto the tissue. The high temperature of the thermal plasma (about 10,000 K) leads to rapid cauterisation and tissue desiccation. This APC technique has been employed successfully in open surgery and endoscopy for haemostasis and thermal devitalised pathological tissues, *e.g.*, in the otorhinolaryngology (Bergler, 2003; Grund *et al.*, 1994; Peng *et al.*, 2018). The procedure is yet painful, but significant thermal tissue damage (up to 7 mm deep) results in prolonged healing (Ginsberg, 2002; Vargo, 2004). Today's medical community is shifting the preference toward non-equilibrium room temperature (RT) discharges where **thermal damage is minimised or eliminated**. Fridman and colleagues' study has introduced **direct NTP** treatment of living tissue where sterilisation occurs without any visible or microscopic damage, and blood is coagulated in an open wound without damaging the surrounding tissue (Fridman *et al.*, 2006) (see *Figure **12*** in **chapter 2.2**). Initial steps in eliminating thermal damage by NTP have been made earlier, *e.g.,* pouring saline over the arc to cool it off, preventing any significant tissue desiccation. A more sophisticated NTP-based surgical tool that has recently been reported is the Pulsed Electron Avalanche Knife (PEAK), where thermal damage to the tissue was reduced by keeping the current pulses short (microseconds) and the electrode thin (microns) (Miller *et al.*, 2003). The resulting streamers (micro-sparks) of NTP, forming under the micro-wire, deposit significant energy into the tissue, rupturing it quickly without destroying surrounding areas, thus performing the precision cutting. Further advances in the non-thermal direction have been made by further size reduction of the needle tip and **introduction of noble gases**, where discharge power can be significantly lower. A discharge capacity of a much gentler, non-thermal interaction with tissue, "plasma needle", has been proposed to treat dental cavities and skin disorders demonstrated to destroy cells and bacteria in a highly localised manner without disturbing the nearby tissues

(Stoffels *et al.*, 2002). It involves a "glow" discharge igniting at the end of a sharp pin in flowing helium upon applying an RF electromagnetic excitation (about 13 MHz). This discharge operates near RT, dissipating milliWatts in several cubic millimetres. Physicists, chemists, engineers and even medical doctors have actively engaged in the race for the research and development of NTP devices suitable for applications in biotechnology and medicine. Details of those innovative devices and their implications in different fields will be discussed later in **chapters 2 and 3**.

1.3.2 Plasma sources and diagnostics

1.3.2.1 Primary sources of NTP for biological applications

NTP in biomedical applications is mainly generated by electrical discharge methods whose type of discharge depends on the waveform and the frequency of the power source, such as direct current (DC) and alternating current (AC) discharge, as well as ambient gas pressure, such as low-pressure and atmospheric pressure plasma, and the precise shape and configuration of the electrodes. Electrical discharge methods are generally categorised into glow discharge, corona discharge, atmospheric pressure plasma jet (APPJ), dielectric barrier discharge (DBD), micro-hollow cathode discharge (MHCD), DC discharge, and pulse discharge or high/low-frequency discharge. *Table **2*** lists some of those working at atmospheric pressure NTP and used for biomedical applications (Sakudo, 2019).

Discharge type (at atmospheric pressure)	Conditions (V, A, Freq, Gas and gas flow)	Pressure (atm)	Gas temperature (C)
DC corona discharge	5–30 kV direct current (DC) (positive and negative); 10–250 µA; dry or wet; O2, N2, Ar, He at 10 $L.min^{-1}$	1	RT
APPJ microwave	P = 2.5 W; 2.45 GHz; $He/O_2/N_2$ at 2.0/1.2/1.5 $L.min^{-1}$	1	Max. 50.8°C on a dentine surface; 20°C on an agar surface
DBD (Flexible sheet-type)	±2.5 kV; 5 kHz; air, humidity 64.4%	1	about 50°C
MHCD jet	1.5–2.5 kV DC; 20 mA; air (0.1–8 $L.min^{-1}$)	> 1	RT (220 $mL.min^{-1}$); > 55°C (5 mm from nozzle, 220 $mL.min^{-1}$)

***Table 2**| Different electrical discharge methods for atmospheric pressure NTP generation. Adapted from* (Sakudo, 2019).

There is no universal prerequisite for the composition of plasmas. Most NTP is produced with noble gases, commonly pure helium or argon but can also be made from the air or other mixtures. There are, however, limits to the production of plasmas concerning electric current, UV radiation (maximum dose allowed) and the output of RONS (limits for O_3, NO_2, NO etc.) for the safety of their utilisation (Heinlin *et al.*, 2010).

Two predominant sources of NTP discharge devices used in biomedicine can be distinguished (Heinlin, 2010; Hoffmann *et al.*, 2013; Pouvesle *et al.*, 2013):

- Direct plasma discharge sources, typically **dielectric barrier discharge** (**DBD**), use the target area as a counter electrode (*Figure **10a**)*, creating relatively homogenous plasmas that contain **high concentrations of plasma-generated species** with relatively **weak UV radiation**. The electrical discharge between two electrodes of a DBD (an HV electrode and a grounded one) is isolated by an insulating layer (barrier). DBD devices must also be charged only with bipolar or HV pulses to ensure capacitive coupling. Since the target itself (tissue/skin/biological sample) serves as an electrode, the electrical current flow through the target (body). The distance between the DBD and the biological target is typically **1 mm**. DBD is one of the most, if not the most, popular devices to generate NTP. Originally called silent (inaudible) discharge, DBD was also known as partial discharge or ozone production discharge, as it was firstly reported in 1857 by Ernst Werner von Siemens (1816-92). He generated ozone by subjecting a flow of oxygen or air to the influence of a DBD maintained in a narrow annular gap between two coaxial glass tubes. This was achieved by an alternating electric field of sufficient amplitude (Kogelschatz, 2003).
- Indirect discharge sources, typically **plasma jets** (*Figure **10b and c***), refer to various discharge systems (hence numerous configurations) used in plasma science. The plasma jet commonly refers to a system where the carrier gas discharge (noble gas/air) is operated in a non-sealed electrode arrangement, generating a relatively more robust **UV radiation** and **lower density of reactive species on the target** in comparison to the DBD. The gas temperature at the production site of the jets is around **40-60°C**. The plasma jets can be categorised according to discharge geometry, electrode arrangement, excitation frequency or pattern (Winter *et al.*, 2015). Thanks to the configuration of the plasma jet, the distance between the

production site of the jet and the biological target can easily be greater (up to **a few centimetres**) than that using the DBD.

- Moreover, larger surfaces can also be created by joining single jets or multi-electrode systems. Recently, the team of Robert at the GREMI (Orléans, France) has developed NTP multi-jet systems using two different setups based on a single plasma source, offering a large treatment surface covered by multiple single jets (*Figure **10c***) (Robert *et al.*, 2015). **This thesis used one of the NTP multi-jet systems from the GREMI.**

Another NTP discharge source, the hybrid plasma devices or coronal barrier discharges, combines both principles described above but are currently applied only at the practical level. Other sources for the plasma generation are corona pin electrode, HF discharge, gliding arc, pen-type Tsukuba mild plasma, and Nagoya non-equilibrium atmospheric pressure plasma (NEAPP). Different NTP sources are recapitulated in the review of *(Braný et al.*, 2020; Tanaka *et al.*, 2017b). The four specific types of NTP devices having CE approval for clinical practice will be described in **Chapter 3.3**.

(a) (b) (c)

Figure 10| Photographs of different NTP devices available for pre-clinical and clinical investigations

(**a**) The floating-electrode dielectric barrier discharges (FE-DBD), electrically safe for treatment where the target is the counter electrode, here a finger (Fridman, 2006). (**b**) The CE-certified argon plasma jet kINPen® MED developed by the Institute of Plasma Physics (INP) Greifswald and manufactured at Neoplas tools GmbH (Greifswald, Germany) (Isbary *et al.*, 2013a). (**c**) Some NTP multijet devices developed by the GREMI (Orléans, France): a hand-held NTP multijet (left panel), and an NTP jet array consisting of two branches that deliver 13 and 21 secondary jets in ambient air over a grounded target. The full assembly is connected to a single plasma gun reactor flushed with a 2 slm helium flow rate (Maho *et al.*, 2018; Robert, 2015).

Although the control of the plasma composition remains an important challenge, the direct discharge sources can control the plasma composition more easily as compared with other discharge devices. Nonetheless, their major disadvantage is the application distance (between the electrodes) which must remain within a close range, generally less than 3 mm, thus limiting its use for small areas of the human body. To that, even if the concentration in RONS generated by the indirect discharge sources is lower than that of direct discharge sources and the plasma

generated is less controllable, the use of different specific carrier gases, the variation of the distance to the target, the configuration of the electrodes, amongst several other characteristics, make plasma jet possible to obtain changes in plasma composition using classical plasma jets (Isbary *et al.*, 2013b).

1.3.2.2 Plasma experimental observations and diagnostics

As discussed above, one of the essential properties of NTP is its high chemical reactivity at low gas temperatures and even at RT. These properties are necessary for interaction with biological targets. For essential applications such as plasma medicine, the knowledge of the fluxes of the discharge species and the relevant elementary processes, *i.e.,* plasma observations and diagnostics, are essential. Having usually small dimensions (typical from micrometre to the millimetre) and non-uniform distributions of the species densities, amongst other parameters (Schulz-Von Der Gathen *et al.*, 2008), NTP is not easy to characterise. Non-invasive optical diagnostic techniques with the high special resolution are, to date, the methods of choice for the diagnostics of NTP and for the slightest disturbance of the plasma properties. Those techniques are selectively described in the review of (Lu *et al.*, 2016). To cite some:

Plasma experimental observations by:

- Fast imaging: can be obtained with phase-resolved imaging or optical emission spectroscopy (to image dynamic processes in plasma with picosecond time resolution at MHz acquisition rates) or with gated and triggered intensified charge-coupled device (ICCD) cameras (to detect and monitor plasma bullets with pico- to nanosecond precision) or with streak cameras (high time resolution (but 2D) for the monitoring of highly-dynamic breakdown processes)
- Laser-induced fluorescence (LIF) spectroscopy: single- and two-photon absorption laser-induced fluorescence, scattering techniques (Rayleigh scattering, Thomson and Raman scattering), optical emission and optical absorption spectroscopies, selected non-optical methods (molecular beam mass spectrometry, flow visualisation, electron paramagnetic resonance spectroscopy)

Plasma electrical characterisation:

- Voltage-current characteristics: the temporal behaviour of the voltage is measured using an HV probe and a voltage divider (with specific characteristics) for voltages above 500 V; the temporal behaviour of an electric current is calculated using

voltage measurements across known impedances (another method is to measure pulsed and alternative currents using current transformers and Rogowski coils). The DIN SPEC 91315:2014-06 (Deutsches Institut für Normung e.V. Berlin, DE) is implemented to characterise plasma sources with their biological performance (*e.g.,* risk and safety potential).

- Electric field: investigated by an electro-optic sensor equipped with an isotropic crystal probed by a laser beam. One example is the Kapteos eoProbe™ from the Kaptéos Society (France). This Ultra-Wide Band sensor allows accurate electric field measurements in almost any location and environment (air, liquids, gases, vacuum) under harsh conditions.

Besides, electron paramagnetic spectroscopy can detect radical species generated in the plasma by measuring unpaired electrons (dangling bonds, radicals, transition metal complexes, etc.).

1.3.3 Principles of non-thermal plasma treatment in biomedicine

NTP has a myriad of potential not only in the physics and material industry (ozone generation, gas purification, electrostatic precipitation, combustion and surface functionalisation of materials, etc.) but also in biotechnology and medical applications. Alongside well-known applications such as using low energy plasmas for decontamination, sterilisation or even wound healing or using higher energy plasmas to cut bones during an operation or for blood coagulation, etc., therapeutic applications of NTP are under research. They have recently garnered significant interest, especially in the cancer treatment (Fridman *et al.*, 2008).

Despite that wide range of applications, the interaction and thus the effects of NTP on microorganisms or living tissues and cells are not fully understood. Whether there are or not distinctive effects of NTP treatment on bacteria, microorganisms or cells, the biological impact of NTP could be explained by the generation of a large number of different species within the plasma region and the afterglow (electrons, ions, gas atoms and molecules of any form of exciting species, UV and heat radiation, electromagnetic fields, and especially free radicals), as shown in *Figure **9b***. If the plasma is in contact with a biological target (*e.g.*, microorganisms, skin, tissue, cells) or is exposed to a liquid (*e.g.,* water, saline solutions, cell culture media, etc.),

those species that are delivered from the plasma to the targets will interact across different regions in the gaseous and liquid states, generating a “cocktail” of reactive species of varying life span and characteristics. And yet radicals are essential to induce physiological outputs in living cells and tissues (Trachootham *et al.*, 2009).

For example, depending on the plasma dose and voltage value producing the plasma discharges, NTP may trigger either physical destruction of the bacteria or a programmed cell death (Lunov *et al.*, 2016; Sakudo, 2019). In general, the effects of NTP treatment were mainly attributed to (Bourke *et al.*, 2017; De Geyter *et al.*, 2012): UV-based DNA damage in combination with the erosion of microorganism structures by UV-based photo-desorption and etching processes by reactive species; the deleterious impact of ionised particles on the membranes (membrane damage, membrane perforation by etching due to highly reactive gas radicals); ion accumulation increases the eternal electrostatic pressure that destroys mechanically rigid bacterial wall structures; or interactions with RONS leading to oxidative damage and modification of cytoplasmatic membrane, proteins, and DNA, etc. Indeed, according to the current state of knowledge, the biomedical effects of NTP were mainly based on the action of reactive oxygen and nitrogen species (RONS) and attributed to redox-controlled cellular processes (Bauer *et al.*, 2016; Graves, 2012a., Graves, 2017; Privat-Maldonado *et al.*, 2019; Von Woedtke *et al.*, 2019). That applied **redox biology** will be further discussed in **chapter 3.3**, focusing on cancer cells.

The three most essential effects offered by NTP treatment for biomedical applications are consistently reported in various studies using different plasma sources and devices under varying plasma parameters and treatment conditions (Bekeschus *et al.*, 2018b; Braný, 2020; Dubuc *et al.*, 2018; Liao *et al.*, 2017; Von Woedtke, 2019; Weltmann *et al.*, 2016):

- Inactivation of a broad spectrum of microorganisms, including multidrug-resistant pathogens
- Stimulation of cell proliferation and angiogenesis via redox-regulated pathways where pro-angiogenetic factors are promoted (effects occur with a low NTP treatment intensity and time)
- The initialisation of (programmed) cell death, even triggering ICD with higher NTP treatment intensity and time, primarily in cancer cells.

The cellular effects of RONS can be summed up as follows:

- Reactive Oxygen Species (ROS) such as O, O_2-, O_3, OH, H_2O_2… have several effects on cell membrane: Peroxidation of lipids, oxidation of proteins (chain of amino acids) that play the role of gateways between the exterior and interior of the cells, DNA oxidation, ...
- Reactive Nitrogen Species (RNS) such as N, NO, NO_2, NO_2^-, NO_3^-, N_2O_5 ... affect the cell signalling.

Nevertheless, it is worth to be pointed out that almost all those observed effects were from nearly all studies whose plasma devices that are in-lab-made designed and developed, *i.e.*, their plasma devices have different forms of plasmas electrode source designs, types of energy used (RF, DC and microwave), the frequency used (ns or µs, at Hz range or kHz range), the gas used (argon, helium or nitrogen, etc. *versus* air), not speaking of the time of treatment (contact time between the plasma and the target). Those different parameters are the primary sources of the physical and chemical properties of the plasma generated and, *in fine,* their reported therapeutic effects.

In need of communal efforts to tackle major obstacles essential to move forward in medical-oriental plasma research, five major fields were identified in the Future in Plasma Science II (FIPS) workshop in February 2016 in Greifswald (Germany): (**1**) plasma-based biomedical materials, (**2**) plasma decontamination, (**3**) plasma biology, (**4**) plasma wound healing, and (**5**) plasma oncotherapy (Bekeschus *et al.*, 2018a). At least the most important, those applications will be discussed over the following two chapters.

2 Biophysical-based treatments, except for cancer treatment

After a long-winded road of discovery from physicists laying down the theoretical fundamental of pulsed electric fields (PEFs) and non-thermal plasmas (NTP), through uncountable pre-clinical investigations with various models, from artificial ones to 2D and 3D cells *in vitro* and finally to animals *in vivo*, PEFs and NTP technologies came to be applied extensively in different fields, including medicine.

This chapter introduces the leading and most known applications of those technologies in the biomedical field except oncology. Their applications in oncology – the focus of my thesis – will be addressed in detail in the next chapter.

2.1 Electroporation-based treatments

2.1.1 General applications of electroporation

The use of the electric field in agriculture research has a long history (Bertholon, 1783). Ever since, positive effects of PEF have been described in fungi, soy, microalgae, and other cells (Wohlgemuth *et al.*, 2019). Controllable and reliable growth and compound stimulation have been achieved under nsPEF conditions (and only) while maintaining techno-functional properties of the remaining compounds, as demonstrated for foaming, emulsification, and colour compounds (Buchmann *et al.*, 2019), with a yet unknown specific mechanism. Operated at relatively high field amplitude PEFs (up to 80 kV/cm), electroporation is an alternative to conventional non-thermal technology in food processing and biorefinery. It improves food quality and preservation by reducing the cost of energy by lowering treatment temperature and shortening processing time, and inactivating microorganisms such as vegetative bacteria and yeast cells selectively (Sitzmann *et al.*, 2017). A typical example of electroporation in food manufacturing is the production of French fries with pre-treatment through a gauntlet of PEFs – a machine known as the E-FLO™ (Heat and Control, 2019). This PEF process allows sugars and amino acids to be released from the potato before cooking, which lessens acrylamide – a hazardous substance categorised as “probably carcinogenic to humans” by the WHO. Besides creating a healthier product, PEF treatment also increases the amount of starch in the outer layers of the potato, resulting in a crunchier chip, and also reduces the time and need to blanch the potatoes before cooking. Moreover, cooking and kitchen operations assisted by PEF have found their places in daily life with commercialised products, such as the Nutri-Pulse® E-cooker

utilised for fast preparation of fish, meat, and vegetables at a moderate PEF strength (10-180 V/cm) upon heating above only 40–50 °C (Blahovec *et al.*, 2017; IXL Netherlands BV and IXL e-Cooker BV).

In recent years, besides utilising PEF for pasteurising liquid food products (such as juices, milk or liquid egg products), other applications have been increasingly investigated, particularly regarding its potential for improving mass transfer, offering higher extraction yields and valuable compounds recovery. Electroporation is thus applied in juice and oil production processes (biorefinery), for fermentation by raising yeast metabolism, for vinification as elimination of pathogenic microorganisms, reduction of maceration time, the release of polyphenolic compounds into grape juice, acceleration of wine ageing and inactivation of oxidative enzymes (Ozturk *et al.*, 2017), for accelerating the drying process in vegetables or meat via the acceleration of water transfer, for cryopreservation (efficient permeabilisation of cryoprotectant into the cell for freezing tolerance of spinach leaves) or for meat curing (infusion of curing agent such as salt) (Gómez *et al.*, 2019; Mahnič-Kalamiza *et al.*, 2014; Toepfl *et al.*, 2005).

2.1.2 Medical applications of electroporation, except for cancer applications

2.1.2.1 Electrogenetherapy (gene transfer mediated by electroporation)

2.1.2.1.1 Historical aspects of electrogenetherapy

The concept of gene therapy arose in the mid-60s when the benefit of therapeutic genes to genetically modify viruses with the replacement of deleterious viral genes was evoked (Tatum, 1966). Five years later (*i.e.*, forty years ago), the potential of the delivery of genetic material to the nuclei of cells to generate a therapeutic effect has been recognised (Rogers, 1971), either for the correction of a defective gene by silencing it or by providing a functional replacement or for the introduction of a gene that encodes a foreign therapeutic protein or whose expression provokes cell death. Gene therapy has evolved to encompass not only the delivery of therapeutic DNA (plasmid DNA or pDNA) but also messenger- (mRNA), micro- (miRNA), short hairpin- (shRNA) and small interfering RNAs (siRNA) and oligodeoxynucleotides (ODNs). On its journey to target cell nuclei, nucleic acids encounter several biological barriers, such as the extracellular matrix, the cell membrane, the cytoplasm, and the nuclear envelope whose nuclear pores are impermeable to molecules more significant than 70 kDa (*ca.* 10 nm Ø)

(McCrudden *et al.*, 2013; Melchior *et al.*, 1995). These are the main reasons gene therapy has yet to be successfully translated. Significant effort has been allocated to developing viral and non-viral techniques for the vectorisation of nucleic acids. Non-viral strategies are making meaningful progress in the quest for a prominent gene delivery vehicle in the clinical medicine (Nakayama *et al.*, 2015), amongst which we find **electrogenetransfer** (**EGT**), also known as **gene electrotransfer** (**GET**), proven to be one of the most efficient and safest techniques (Spanggaard, 2013; Villemejane *et al.*, 2009).

Based on electroporation technology, pioneer works regarding EGT were performed in 1982 by Neumann and colleagues for *in vitro* induction of exogenous gene expression, as presented in previous sections, followed by numerous investigations up to date to develop and improve this physics-based gene therapy. The development of a square-wave pulse generator with modulable intensities by Teissié (Zerbib, 1985) found its application not only in the transformation of bacteria with plasmid DNA (Fiedler *et al.*, 1988) but also in the transfection of animal and plant cells, as well as the delivery of genes into animal and human tissues (André *et al.*, 2004; André, 2008; Daud *et al.*, 2008; Gothelf *et al.*, 2010; Mir *et al.*, 1999., Mir *et al.*, 2005; Rols *et al.*, 1998b; Rosazza *et al.*, 2016; Spanggaard, 2013).

2.1.2.1.2 Mechanisms and applications concerning other gene delivery strategies

Mechanisms of EGT

Electroporation is a crucial component of EGT, where the electric pulses are used to electropermeabilise the cell membranes and also to favour the electrophoretic transfer of extracellular genetic materials into the cells while securing the cell viability afterwards (Rols, 1998b; Satkauskas *et al.*, 2002; Titomirov *et al.*, 1991). The seven major steps of EGT are: (**1**) Plasmid DNA is delivered to the tumour environment; (**2**) EPs permeabilise the cell membrane; (**3**) pDNA interacts with cell plasma membrane on cathode facing site (Faurie *et al.*, 2010); (**4**) pDNA is inserted into cell membrane via actin cytoskeleton (Rosazza *et al.*, 2011); (**5**) Plasmids are internalised by endocytosis, and microtubules actively transport DNA molecules through the cytoplasm; (**6**) DNA leaves endosomes and crosses the nuclear envelope (Lechardeur *et al.*, 2006); (**7**) After DNA expression, the proteins are released into the cytoplasm.

EGT has a different electrotransfer mechanism than small molecules (smaller than the usual size of plasmid) electrotransfer, such as drugs. Simple diffusion happens through the cell

membrane after permeabilisation for drugs and other small molecules. Diffusion will occur as long as the cell membrane is permeabilised, i.e., after the pulses have been delivered. On the contrary, DNA (and other nucleotides too large to pass through the hydrophilic pores by diffusion) are polyanions with an overabundance of negative charges, enabling the molecules to move in an electric field. In ***in vivo***, the membrane of muscle cells or tumour cells remains permeabilised for several minutes after the delivery of a train of eight square wave pulses of 100 µs duration each, as discussed above in **chapter 1**. However, no transfection (or at least no more transfection than the one obtained by the injection of naked DNA in the absence of PEFs) is found in DNA is injected into the tissue **after** the delivery of the electric pulses (Gehl, 1999; Mir, 1999; Satkauskas, 2002). Thus, DNA must be present **at the time** of the delivery of PEFs. However, moving DNA is insufficient; the cell membrane must be permeabilised to allow the DNA molecule's passage. Hence, optimisation of pulses is necessary to achieve either a greater **degree of permeability** of the cell membrane (for passive diffusion) or a greater **degree of electrophoretic effect**. Our group has demonstrated that generally, a series of short high voltage pulses (*e.g.*, eight pulses of 0.1 ms duration each, at 1000 V/cm voltage to electrode distance) is optimally used for drug delivery (Gothelf *et al.*, 2003), while a combination involving permeabilising short HV pulses and electrophoretic long LV pulses (*e.g.*, one short pulse of 0.1 ms duration, at 800 V/cm and one long pulse of 400 ms duration, at 80 V/cm) are used for very effective DNA transfer (André, 2008). There are also studies displaying efficient electrotransfer in several tissues (tumours, liver, skeletal muscle) using long pulses only, ranging from 5 ms to 50 ms (see review (Mir, 2014)).

Applications of EGT

The EGT is used in research and medicine for many applications such as transfection of reporter genes, gene therapy, DNA vaccination and generation of iPS. DNA vaccination consists of injecting a DNA sequence coding for a pathogenic cell epitope (*e.g.,* cancerous cell), leading to the activation of the immune system against the cells exposing that epitope. With the possibility of multi-potent vaccines, the high level of safety due to the absence of viral elements and the stability of the DNA molecule in lack of need for cold storage, DNA vaccines offer considerable advantages and the possibility to produce good manufacturing practices (GMP)-grade plasmid DNA (GMP-DNA) for direct gene transfer into humans (Gothelf *et al.*, 2012). For example, a recent study done in our laboratory by Calvet *et al.* used a plasmid that encodes a

modified form of the human telomerase reverse transcriptase gene (hTERT) and its intradermal electrotransfection in mice. The transgene expression was 100-fold higher when combined with EGT than when the DNA was injected alone. After optimising the electrical parameters (choice of suitable electrodes, HV pulse intensity and the best combination of HV-LV), the telomerase antigen will be used as a cancer DNA vaccine called INVAC-1 (Calvet *et al.*, 2014a).

Since LV pulses application is favourable for the delivery of DNA vaccines (André, 2008; Gothelf, 2012; Mir, 2009), it is worth highlighting the most recent news related to EGT and the ongoing COVID-19 pandemic. On November 24th, 2020 – a week before the end of this thesis writing, when the world is facing the SARS-CoV-2 virus that has already infected *ca.* 64.5 M people and taken more than 1.5 M lives, for less than a year since the first confirmed case (updated statistics from WHO Coronavirus Disease (COVID-19) Dashboard), the US. Food and Drug Administration (FDA) has announced to clear the Cliniporator™ platform for use in the upcoming Phase 1 trial investigating CORVax12, a DNA-encodable vaccine candidate for COVID-19. CORVax12 of the US. biotechnology OncoSec Medical Incorporated combines TAVO™ (tavokinogene telseplasmid), a DNA plasmid-based IL-12, with the National Institute of Health (NIH)'s SARS-CoV-2 virus "spike" protein. Furthermore, OncoSec announced that it had licensed the exclusive rights to the Cliniporator™ electroporation or gene electrotransfer platform from IGEA Clinical Biophysics, a license encompassing a broad field for gene delivery in oncology. The unique approach with CORVax12 delivered by the Cliniporator™ brings new hope to better protection against COVID-19 and other virus diseases.

2.1.2.2 Irreversible electroporation

First reported with persuasive results in 1987-88, irreversible electroporation (or IRE), as presented above in **section 1.2**, is permanent electroporation with promising clinical achievements. Research conducted by Davalos and co-investigators tested this phenomenon using a mathematical model and *in vivo* conditions, showing that IRE could indeed induce cell death without using a thermal energy (Davalos *et al.*, 2005), leading to the first successful *in vivo* IRE procedure on mice tumours (Al-Sakere *et al.*, 2007). Clinical applications of IRE were followed *(were following?)*, wherein micro- to millisecond HV pulses were delivered to induce cellular necrosis or apoptosis while mitigating deleterious thermal effects of ablated tissues and neighbouring (Rubinsky *et al.*, 2007). IRE finds its applications primarily for cancer treatment, but those will be presented later in **chapter 3.1**. Other applications in medical treatment (except

oncology) of IRE are: cardiology (prevent arterial restenosis following angioplasty) or hypertension treatment through the renal sympathetic nerve denervation (Rolong *et al.*, 2017; Rubinsky, 2007). Nevertheless, this treatment modality has to proceed with caution since adverse effects have been reported on patients, such as cardiac arrhythmias, complete heart block, increasing pacing thresholds or atrial and ventricular electrical and mechanical dysfunction (directly related to the PEF strength) (Aras *et al.*, 2018), whence the adoption of electrocardiogram (ECG)- synchronised delivery of pulses to gate IRE with R-wave of ECG to deliver the PEFs during the absolute refractory period of the ventricles (Deodhar *et al.*, 2011). A systemic review reported an improvement in cardiac safety of ECG-gated IRE Field (Scheffer et al., 2014), but no systemic evaluation of short and long-term cardiac injury associated with this combined technique.

IRE is a technology of ongoing development to enhance existing treatments or for novel applications, such as tissue engineering or dermatology (regenerative medicine, scarless skin regeneration, skin rejuvenation, wound healing, and wound burn disinfection), etc. (Rolong, 2017).

The application of PEFs in cancer research and treatments will be expressly detailed later in section 3.2.

2.2 Non-thermal plasma technology for biological applications

2.2.1 General applications of NTP

NTP is a cutting-edge technology that has gained considerable attention during the last decade for different applications in various fields of research and development and innovative industry. Similar to electroporation technology discussed above, NTP is a promising technology for **surface modification** (Foest *et al.*, 2005) or in agriculture and food industry sectors thanks to not only its effectiveness in **microbial pathogens inactivation** such as spoilage fungi, bacterial in addition to degrading toxins but also its simple design, ease of use (especially at room temperature), cost-effective operation with short treatment times, lack of toxic effects, and significant reduction of water consumption (López *et al.*, 2019; Sakudo, 2019). Plasma agriculture possesses great potential in **stimulating seeds germination and plants growth**, **tailoring plants' dormancy** and **improving plants' resistance to common diseases** (Adhikari *et al.*, 2020a., Adhikari *et al.*, 2020b). The research team led by Dr T. Dufour has demonstrated the

ability of NTP treatment of tap water or demineralised water and liquid fertiliser (used to irrigate seeds) to increase plant growth and promote seed germination (Judée *et al.*, 2018; Zhang *et al.*, 2017). The advantage of the concept of a contact-free application of NTP to sterilise, for example, Candida biofilm-contaminated surfaces and devices in health care settings (Maisch *et al.*, 2012) might have a positive impact on preventing community-acquired and nosocomial infections in health care facilities. NTP also acquires strong microbicidal properties, including those against bacterial spores. Yost and Joshi used FE-DBD plasma to treat PBS and the resulting plasma-treated PBS induced severe oxidative stress in *Escherichia coli* as a consequence of a direct and non-specific attack of $^{\bullet}OH$ (generated from H_2O_2 and $O_2^{\bullet-}$) on various microbial structures and components, including rapid loss of membrane potential and membrane integrity, lipid peroxidation and DNA damage (Yost *et al.*, 2015). Guo *et al.* demonstrated that plasma pre-treatment enhances the sensitivity of methicillin-resistant *Staphylococcus aureus* to antibiotics. The short-lived RONS generated by NTP played a primary role in inducing the increase of many species of RONS in the bacteria cells (Guo *et al.*, 2018a). The same group is also assumed, together with some other studies, that NTP is effective in the **virus inactivation** (Ahlfeld *et al.*, 2015; Guo *et al.*, 2018b; Volotskova *et al.*, 2016). Similar modes of action of NTP have determined its application in the food industry. Treatment with NTP is used for food preservation or to decontaminate various kinds of foods with minimal impact on the food quality, even if it has been demonstrated that its effectiveness as a food decontamination technique varies amongst different foods (López, 2019). NTP can also **sterilise contaminated matter** (Laroussi, 1996) or **decontaminate abiotic surfaces** such as stainless steel, various packaging materials, paper, glass and plastics of diverse nature. Notably, the NTP jet is also used medically for **disinfection and sterilisation of medical instruments** (Sakudo, 2019).

Nevertheless, the rapid industrial implementation of NTP still faces some issues and unanswered questions, such as its impact on the nutritional and sensory quality of treated products; our knowledge of the NTP components and reactive species responsible for the antimicrobial activity; possible toxicity of (or some of) the chemical species generated, its scale-up by designing fit-for-purpose apparatus, etc.

2.2.2 Medical applications of NTP except for cancer applications

2.2.2.1 Plasma in dentistry: from sterilisation to whitening

Conventional treatments such as unique teeth brushing products, fluoride uptake, antibiotics, and vaccines for oral disease or infections (dental caries, periodontal and intraoral illness caused by bacteria) still have limitations. Therefore, with antibacterial capacity, NTP is an inexpensive approach for treating dental diseases. It has been demonstrated that NTP sterilised biofilms efficiently on root canals, dental implants or oral mucosa and eradicated bacteria and microbes. Given its characteristic, the NTP jet can access small irregular structures and narrow channels within the diseased tooth to be cleaned, *e.g.,* for the treatment of dental caries or for root canal disinfection (a property that is proven as more advantageous than lasers, by some studies) (Arora, 2013). NTP is also used to assist in cleaning and optimising tooth and implant surfaces to improve bone integration or restore the adhesive of dental composite. It was observed that NTP treatment could modify the dentine surface and increase the dentine/adhesive interfacial bonding (Ritts *et al.*, 2010; Stancampiano *et al.*, 2019).

Numerous methods are available in dentistry to restore natural tooth colour, amongst which found NTP – is considered “the next-generation technology” (Arora, 2013). NTP has been tested for its tooth bleaching effect and has produced successful results, shedding light on the chemical effect of NTP exposure. Indeed, hydrogen peroxide (H_2O_2), one of the oldest bleaching techniques, has long been used for tooth whitening by producing free radicals, which have also been found in NTP treatment.

2.2.2.2 Skin decontamination

Similar to its capacity to disinfect or sterilise a wide range of targets, ranging from material to biological targets, NTP showed antiseptic effects on bacteria, yeast, and fungus, as described above in section 2.2.1. Thus, NTP is also used to decontaminate skin thanks to the abundant production of free radicals, which are toxic to organisms at a critical concentration (Klebes *et al.*, 2014).

2.2.2.3 Skin wound healing

Since NTP demonstrated its antiseptic effects in the decontamination of skin, it can support wound healing by stimulating of proliferation and migration of wound relating skin cells, by activation or inhibition of integrin receptors on the cell surface or by its pro-angiogenic effect

(Haertel *et al.*, 2014) (*Figure **11***). The first prospective randomised controlled phase II trial to decrease bacterial load with 5 min daily argon NTP and standard wound care on chronic wounds in 36 patients resulted in a significantly less bacterial load (*Figure **11d***) (Isbary *et al.*, 2010). Another randomised controlled trial engaging 50 patients demonstrated the healing effect of NTP in pressure ulcers with a significantly better pressure ulcer scale for healing scores and exudate (Chuangsuwanich *et al.*, 2016).

NTP has been demonstrated *in vitro* and *in vivo* to be able to change the gene expression of key molecules of the wound healing machinery (activation of angiogenesis-related molecules in skin keratinocytes, fibroblasts and endothelial cells), thus improving the wound healing (Arndt *et al.*, 2013b., Arndt *et al.*, 2018; Kubinova *et al.*, 2017).

Figure 11| Example of wound healing treatment in clinics with NTP
Visualisation of (**a** to **c**) a 61-y-o patient with venous ulcers receiving a daily therapy of 2 min MicroPlaSter®: (**a**) wounds before plasma treatment, (**b**) after 7 and (**c**) after 11 treatments. At the beginning of NTP treatment, *Klebsiella oxytoca* and *Enterobacter cloacae* were detectable, after the 11th treatment (23 days later) swabs were sterile. Adapted from (Heinlin, 2010) and (**d**) the MicroPlaSter® plasma torch (Microwave 2.46 GHz, 86 W; Ar 2.2 slm; distance to torch 2 cm) used in the treatment of a chronic infected wound (Isbary, 2010).

Besides the effectiveness in skin decontamination and the healing of skin wounds, mild NTP treatments have shown to enhance the expression of collagen I, fibronectin, and vascular endothelial growth factor (VEGF) in fibroblasts significantly to boost angiogenesis and repair of connective tissues, hence application in dermatology as rejuvenation (Choi *et al.*, 2013; Foster *et al.*, 2008).

2.2.2.4 Blood coagulation

Haemorrhage or blood loss is considered a significant issue during surgical intervention, especially in patients under anticoagulant therapy (Van Der Meer *et al.*, 1993). To treat and prevent blood clots, new oral anticoagulants (blood thinner) such as rivaroxaban (Xatelro®) are increasingly prescribed instead of former anticoagulative therapy using vitamin K antagonists

(*e.g.*, warfarin) (Carter *et al.*, 2013). However, there still is a need for pro-coagulant therapy (Weiner *et al.*, 2003) due to the lack of proper antidotes (Riley *et al.*, 2017).

Besides the capacity to sterilise and disinfect living tissues, NTP has been suggested as an alternative haemostatic direct treatment to meditate haemorrhage during surgery, an application similar to the one fulfilled by the extensively used electrical knives. An *ex vivo* investigation pioneered by Fridman and colleagues fifteen years ago showed blood coagulated from oozing haemorrhage of human spleen using FE-DBD (Fridman, 2006) (*Figure **12***). The tissue integrity was preserved in that study. The group pursued their investigation of the mechanisms of blood coagulation by NTP. It attributed a central role to a plasma-induced fibrin clot (Kalghatgi *et al.*, 2007). This mechanism was also speculated in another study on blood plasma sample (Ke *et al.*, 2016). However, a recent *in vivo* study rejected that proposed mechanism and emphasised the critical regulator role of platelets in the haemostasis facilitated by the kINPen® MED via the increased activation of platelets by the RONS oxidation (Bekeschus *et al.*, 2017). Although the mechanisms of NTP blood coagulation are yet unrevealed, and NTP treatment could only offer a limited treatment zone, practical results of NTP already open the gate for clinical benefits of tissue-tolerable NTP as a coagulant agent in surgery.

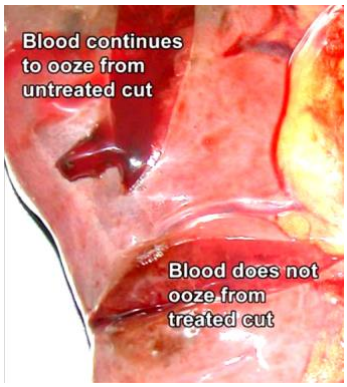

Figure 12| A photograph of a human spleen before and after thirty seconds of treatment with FE-DBD showing blood coagulates without tissue damage

Top cut: blood continues to ooze from an untreated area; bottom cut: blood coagulates while the wound remains wet (Fridman, 2006).

The application of NTP in cancer research and treatments will be expressly detailed later in section 3.3.

3 Biophysical-based treatments in cancer therapy

This chapter will get a glimpse of cancer with its updated basic facts. It will then focus on the applications of the electroporation-based approaches and the non-thermal plasma technologies against cancer.

3.1 Cancer at a glance

3.1.1 The landscape and epidemiology of cancer

Characterised by uncontrolled growth and spread of abnormal cells, cancer – a generic term for malignant tumours and leukaemias – is a group of diseases with the highest impact on global health. According to the World Health Organization (WHO), cancer is the second leading cause of death globally (behind ischaemic heart disease and stroke). Cancer occurs principally in low- and middle-income countries (approximately 70% of the world's cancers). Note that all the statistics mentioned in this section are from, if not otherwise stated, the WHO (World Health Organization, 2018., World Health Organization, 2020), the WHO Cancer Fact Sheet, the (American Cancer Society®, 2009), and from (Siegel *et al.*, 2020)

In 2018, the WHO estimated 18.1 million new cases and 9.6 million deaths from cancer (*Figure **13a***), in which the ten most common cancers for both sexes are responsible for 60-70% of cancer cases and deaths (*Figure **13b***). By 2040, those figures will nearly double, with the most significant increase in low- and middle-income countries. Around one-third of deaths from cancer are due to the five leading behavioural and dietary risks: high body mass index, low fruit and vegetable intake, lack of physical activity, tobacco use, and alcohol use. Tobacco use is the most critical risk factor, responsible for approximately 22% of cancer deaths. Female breast cancer (11.6%), lung cancer in men (11.6%) and colorectal cancers (10.2%) are the most frequently diagnosed cancers worldwide. Due to increasing life expectancy, epidemiological and demographic transitions, and frequency of diagnosis, the global numbers of new incidence and mortality continue to rise (van Hoeve *et al.*, 2015). Despite all the recent technological improvements, recurrence and metastasis remain the principal cause of death from cancer.

The causal factors triggering cancer, either external (tobacco, chemicals, infectious organisms, radiation, etc.) or internal (inherited mutations, mutations that occur from metabolism, hormones or immune conditions, etc.), may act together or in sequence to initiate or promote carcinogenesis, with ten or more years passed between the exposure to those factors (especially the external ones) and the detection of cancer.

The World Cancer Research Fund and the American Institute for Cancer Research have determined additional cancer causes, including beta carotene, red meat, processed meats, low fibre diets, not breastfeeding, obesity, increased adult height and sedentary lifestyles (Blackadar, 2016). In that excellent review article tracking back the history of the cause of

cancer, Blackadar was surprised himself when he discovered that natural factors (hormones, UV radiation, parasites, fungus, bacteria, wood dust, alcohol, food preparation technique, herb, etc.) are an additional and relatively underappreciated and woefully ignored cause of cancer.

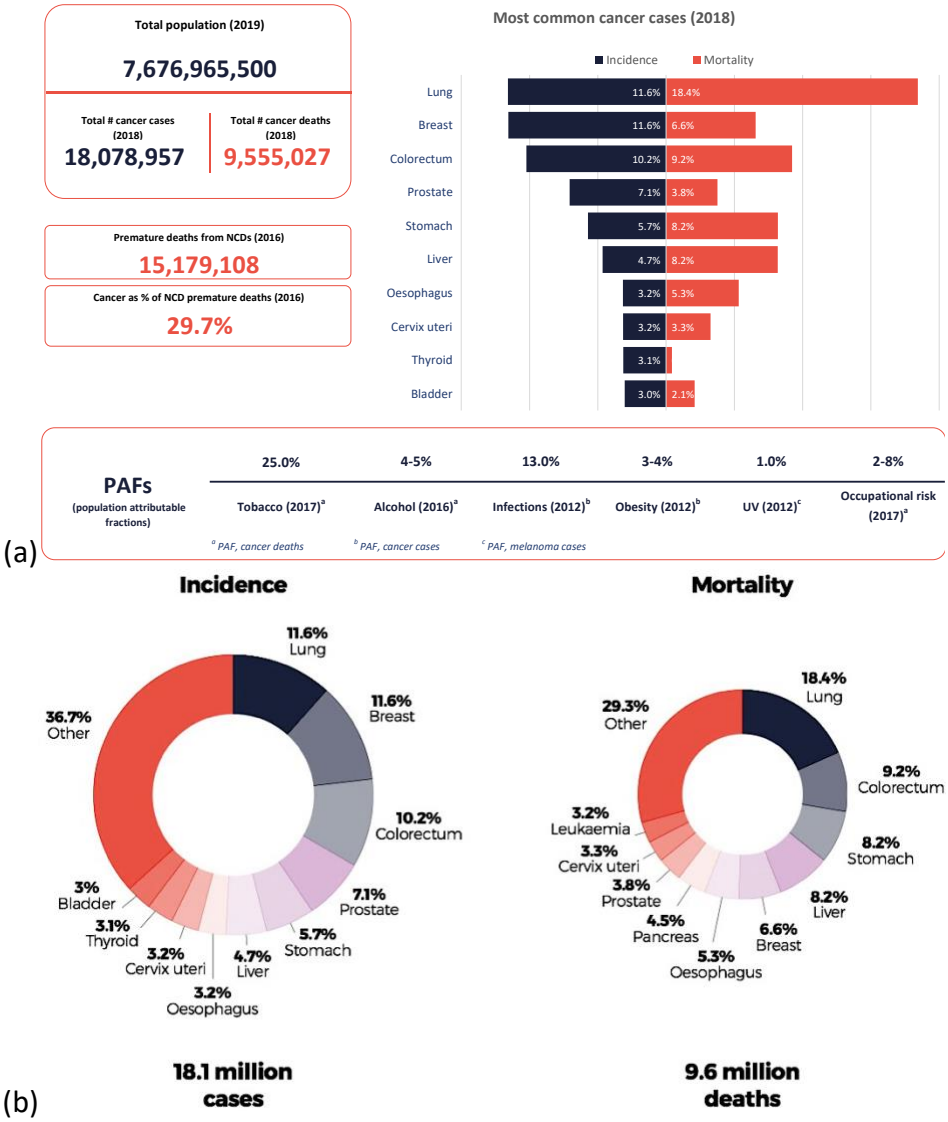

Figure 13| The burden of cancer (the WHO cancer report 2020 on global profile)

(**a**) Estimated global burden of cancer and (**b**) distribution of cases and death by the leading 10 cancer types for both sexes in 2018 (World Health Organization, 2020).

Rather than responding appropriately to the signals that control normal cell behaviour, cancer cells grow, divide, and proliferate uncontrollably, invading normal tissues and organs and eventually spreading throughout the body (metastasis). That is to say, all cancers involve the malfunction of genes that control cell growth and division. However, only about 5% of all cancers are strongly hereditary, in that an inherited genetic alteration confers a very high risk of developing one or more specific types of cancer. Most cancers do not result from inherited

genes but genetic damages occurring during one's lifetime. Genetic damage may result from both internal and external factors.

Cancerologists and oncologists distinguish the two following risks for an individual to develop cancer:

- Lifetime risk is the probability that an individual, throughout a lifetime, will develop or die from cancer (*e.g.*, in the US, men have slightly less than a 1 in 2-lifetime risk of developing cancer compared to women, whose risk is a little more than 1 in 3);
- Relative risk refers to measuring the strength of the liaison between risk factors and particular cancer by comparing the risk of developing cancer in persons with a specific exposure or characteristic to the risk in persons who do not have this trait. For the two most common cancers, the American Cancer Society estimated that male smokers are about 23 times more likely to develop lung cancer than non-smokers, *i.e.*, their relative risk is 23; and women who have a first-degree relative (mother, sister or daughter) with a history of breast cancer have about twice the risk of developing breast cancer as compared with women who do not have this family history.

There is no better way against disease than to prevent it after studying its causation or origination (aetiology). Humans have won the battle against deadly diseases throughout history, including smallpox and polio, by vanquishing them through prevention. The actual cancer control continuum defined by WHO, shown in *Figure **14***, clearly sets a global priority on cancer prevention. Primary prevention of cancer consists of modifying factors that increase the risk of cancer (*Figure **15***). Early detection aims to identify cancer or precancerous lesions as early as possible by one of two distinct approaches: early diagnosis or screening. The main diagnostic steps are assessing the anatomical extent of the disease and the cancer type and subtype. Standard cancer treatments are systemic surgery, therapy (*e.g.*, chemo-, endocrine and targeted therapy), radiotherapy, nuclear medicine, bone-marrow transplantation and cancer cell therapy. Survivorship care is the provision of services after completion of cancer treatment and includes surveillance to identify diseases and their families. It is part of the management strategy for a cancer diagnosis.

Figure 14| The cancer control continuum
Adapted from (World Health Organization, 2020).

Figure 15| European code against cancer: 12 ways to reduce cancer risk
With technical support from International Agency for Research on Cancer (IARC) and the European Code against Cancer, the approach used in the European Union is a simple, clear, comprehensive, evidence-based set of 12 ways to reduce cancer risk (World Health Organization, 2020).

Even if the WHO indicates that at least 30-50% of all cancer deaths are preventable with current knowledge and interventions (Danaei *et al.*, 2005), the journey towards achieving cancer prevention remains challenging and full of obstacles. Effective screening methods are available for only a few cancers, and advances in cancer treatment have not been as practical as those for other chronic diseases, not speaking of the cost of treatment (the total annual economic cost of cancer in 2010 was estimated at approximately US$ 1.16 trillion). Moreover, as stated earlier, ten or more years pass between the exposure to cancerous factors (especially

the external ones) and the detection of cancer; late-stage presentation and inaccessible diagnosis and treatment are common. Humankind has thus likely to treat and live with cancers rather than prevent them.

Recognising the rapidly increasing global burden, governments have increased the importance of comprehensive cancer control. Firm commitments have been made in United Nations and World Health assemblies during the past decade. The set priorities, which have to be feasible, evidence-based, comprehensive and inclusive, are: strengthen tobacco control to reduce cancer death by 25%; vaccinate against HPV and hepatitis B, reaching >90% coverage; screen for cervical cancer with >70% participation; focus on early diagnosis and treatment for curable cancers, *e.g.,* some childhood cancer to save 1 million lives by 2030; scale-up capacity to manage 200 million cancer cases in next decades; provide palliative care for all. There is also a global initiative for childhood cancer to ensure the survival of at least 60% of children with cancer by 2030, thereby saving an additional one million lives and reducing suffering for all.

3.1.2 The development of cancer

Types of cancer

Cancer can result from uncontrolled proliferation of any of the different kinds of cells in the body, resulting in numerous distinct types of cancer, varying substantially in their behaviour and response to treatment. The International Classification of Diseases (revision 11) lists **more than 600 types of cancer**, most of which require unique diagnostic and management approaches (World Health Organization, 2020). The most critical issue in cancer pathology is the **distinction between benign and malignant tumours**. A tumour is an abnormal proliferation of cells, which may be either benign or malignant. A benign tumour, such as a common skin wart, remains confined to its original location, neither invading surrounding normal tissue nor spreading to distant body sites. However, a malignant tumour can invade surrounding normal tissue and spread throughout the body via the circulatory or lymphatic systems (**metastasis**). Only malignant tumours are appropriately referred to as cancers, with their dangerous ability to invade and metastasise specific organs, including lung, liver, brain, and bone (Cooper, 2000).

Figure 16 highlights different stages of metastatic progression.

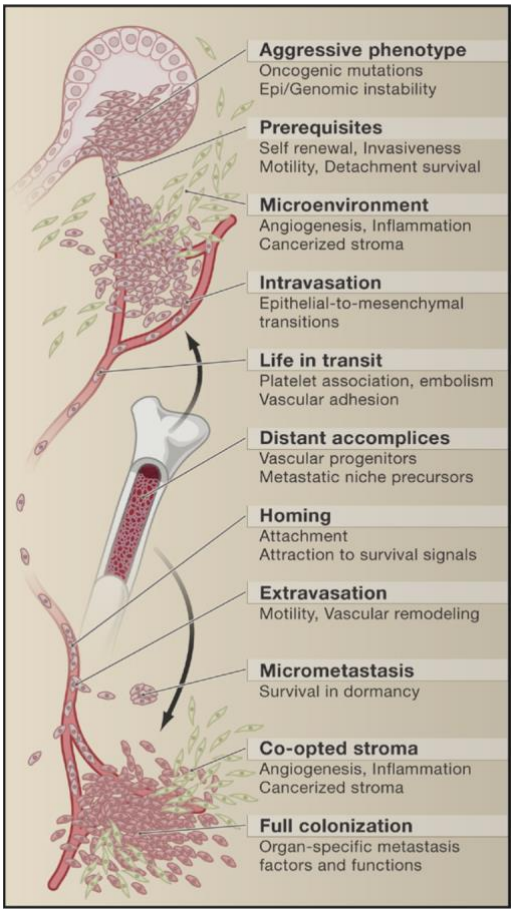

Figure 16| Stage of metastatic progression.

Metastasis proceeds through the progressive acquisition of characters that allow malignant cells originating in one organ to disseminate and colonise a secondary site. Although these traits are depicted as part of a continuous biological sequence, their acquisition during metastatic progression need not follow this particular order. Although, in some cases, several factors may be crucial to implementing a single step in this cascade, other mediators of metastasis may facilitate the execution of multiple stages simultaneously. Likewise, the specific steps of this sequence that are rate-limiting for metastatic progression may also vary from one tumour to another (Gupta *et al.*, 2006).

Both benign and malignant tumours are classified according to the type of cell from which they arise, mostly three main groups: **carcinomas**, **sarcomas**, and **leukaemia** or lymphomas (their definition are given in the *Glossary & Key Terms* found at the end of this thesis manuscript). Note that carcinomas, which are malignancies of epithelial cells, comprise approximately 90% of human cancers, as opposed to sarcomas (solid tumours of connective tissues), rare in humans. Tumours are further classified according to the tissue of origin and the type of cell involved. For example, fibrosarcoma arises from fibroblasts and erythroid leukaemia from precursors of erythrocytes (red blood cells). The most common cancer type varies amongst countries. Certain cancers are much more common in countries at the lower end of the human development index (HDI) than in high-HDI countries, *e.g.*, cervical cancer and Kaposi sarcoma.

The development of cancer (Cooper, 2000)

Tumour clonality has been demonstrated as one of the fundamental features of cancer, *i.e.*, the development of tumours from single cells that begin to proliferate abnormally.

Cancer development is a multistep process involving mutation and selection for cells with progressively increasing capacity for proliferation, survival, invasion, and metastasis at a cellular level, as described above in ***Figure 16***. This progress could be resumed in two significant steps: **tumour initiation**, probably the result of a genetic alteration leading to abnormal proliferation of a single cell (Cell proliferation then leads to the outgrowth of clonally derived tumour cells), and **tumour progression** that continues as additional mutations occur within cells of the tumours. Some of these mutations present a selective advantage to the cell (*e.g.*, more rapid growth). The descendants of a cell bearing such a mutation will become dominant within the tumours - a clonal selection process. The clonal selection continues throughout tumour development, so tumours continuously become more rapidly growing and increasingly malignant.

Ninety per cent of cancer deaths are not caused by the primary tumour but because **metastasis** (Torre *et al.*, 2015). The primary tumour selectively and actively modifies organs of future metastasis before the occurrence of metastatic spread. Tumours induce the formation of microenvironments (pre-metastatic niches) in distant organs that are favourable to the survival and outgrowth of tumour cells before they arrive at these sites (Peinado *et al*., 2017). Metastases are usually multiple and resistant to conventional therapies, jeopardising successful surgical resection, chemotherapy and radiation treatment.

3.1.3 The hallmarks of cancer

In human oncology, one of the most pervasive characteristics of tumours is **genomic instability** (Hanahan *et al.*, 2011), leading to the generalised loss of growth control of malignant cells - the net result of accumulated abnormalities in multiple cell regulatory systems, reflecting in several characteristics of cell behaviour that distinguish cancer cells from their normal counterparts (expression of neoantigens, differentiation antigens or cancer-testis antigens, which can lead to the presentation of peptides bound to major histocompatibility class I (MHCI) molecules on the surface of cancer cells) (Chen *et al.*, 2013).

Current conceptualisation identified the **eight hallmarks of cancer** or what are arguably necessary conditions to manifest malignant disease are (Hanahan *et al.*, 2017):

- Sustaining proliferative signalling: In physiological conditions, proliferation is regulated by growth factors produced in an autocrine, endocrine or paracrine

fashion. Unlike noncancerous cells, cancer cells are endowed with extensive proliferation capacity by making their growth factors;

- Evading growth suppressors: Unlike noncancerous cells, cancer cells may keep growing in the presence of inhibitory signals from the surrounding environment;
- Resisting cell death: When an event irreversibly damages noncancerous cells, these latter will trigger apoptosis (programmed cell death). Contrariwise, cancer cells often present mutations on genes responsible for sensing such damages or triggering cell death;
- Enabling replicative immortality: Noncancerous cells cannot divide more than a defined number of times due to telomere shortening (Hayflick limit). Contrariwise, cancer cells can reactivate the telomerase to synthesise telomeres continuously and thus escape senescence;
- Inducing angiogenesis: Cancer cells require sufficient nutrients and energy to sustain their growth. By releasing factors that promote the creation of new blood vessels, they ensure their blood supply;
- Activating invasion and metastasis: by downregulating the expression of adhesion molecules and secreting proteases, cancer cells can invade surrounding tissues or even reach the blood flow through which they may colonise distant tissues;
- Deregulating cellular energetics and metabolism: cancer cells can alter their utilisation of energy sources—notably glucose—to support their proliferation;
- Avoiding immune destruction: incipient neoplasia could find ways to circumvent active surveillance by the immune system that would otherwise eliminate the proliferation of premalignant cells aberrantly.

*Figure **17*** displays the interactions of the tumour cell secretory pathway with different hallmarks of cancer, rationalising the complexities and variability at all levels of consideration of this neoplastic disease with yet unknown mechanisms.

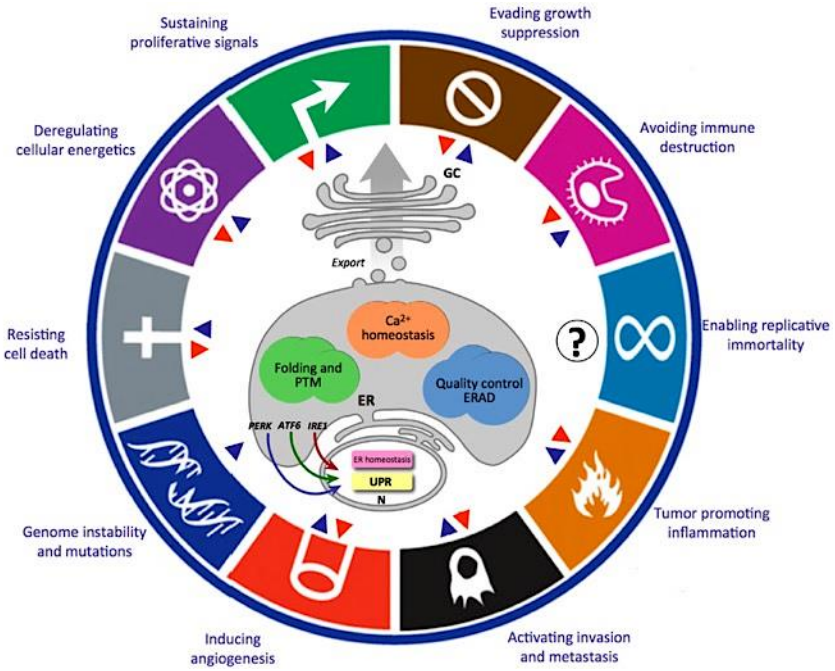

Figure 17| The interactions of the tumour cell secretory pathway with different hallmarks of cancer
Arrows indicate either positive (blue) or negative (orange) regulatory mechanisms linking the secretory pathway (SP) to the hallmarks of cancer. The question mark indicates an absence of information available in the literature on the relation between the SP and replicative immortality. Figure adapted from (Dejeans *et al.*, 2014; Hanahan, 2011).

Those capabilities are familiar to many, if not most, forms of human cancer. Each one serves a distinct functional role in supporting tumours' development, progression, persistence and constituent cells. Genome instability facilitates their acquisition with subsequent **gene mutation and tumour-promoting inflammation**. Integrating these hallmark capabilities encompasses heterotypic interactions between multiple cell types populating the "**tumour microenvironment**". The tumour microenvironment comprises cancer cells and a tumour-associated stroma, including three major classes of recruited support cells: angiogenic vascular cells, various subtypes of fibroblasts, and infiltrating immune cells. Their functions are hijacked to participate in tumour initiation, progression, and metastasis (Hanahan, 2011; Valkenburg *et al.*, 2018). Moreover, the neoplastic cells populating individual tumours are typically heterogeneous, in that cancer cells can undertake a variety of distinctive phenotypic states and undergo genetic diversification during tumour progression. Hence, the hallmarks of cancer constitute a valuable heuristic tool for elucidating mechanistic bases and commonalities underlying the pathogenesis of diverse forms of human cancer, with potential applications to cancer therapy that will be discussed after that.

As cancer remains a worldwide health problem with yet unsolved puzzle, the WHO underlines that cancer cannot be prevented or controlled by the health sector alone but requires a coordinated, multisectoral, multidisciplinary approach (World Health Organization, 2020). Hence, efforts are put not only into daily life prevention and intervention but also into the research and development of cancer therapies to diagnose better, prevent and treat cancer. Concerning traditional cancer treatment modalities, the following section will highlight advances in current anticancer therapies as multidisciplinary approaches.

3.1.4 Anticancer therapies

The development of anticancer therapies was initially based on empirical observations due to the lack of knowledge on the characteristics of cancer cells and their microenvironment, as well as their role in tumour progression. Historically cancer has been treated based on broad pathologic criteria involving various regimens of cytotoxic therapy - a ‘‘one size fits all’’ approach. Over time, better knowledge in oncology and cancerology has been acquired, thus allowing the development of novel and more appropriate therapeutic strategies that consider the tumour size, stage, and other characteristics and patient preferences. The most commonly utilised anticancer therapies to date are surgery, chemotherapy and radiotherapy.

3.1.4.1 Tumour ablation

By far, surgery is the first and most considered cancer treatment modality. William Halsted’s approach to mastectomy took the medical world by storm at the turn of the last century (Halsted, 1894). Ever since ablative therapy has diverse approaches with a very similar concept but distinguished technology (Seror, 2015).

Tumour ablation can be performed with:

- Surgery: the surgical act consists of operating on the patient to remove the tumour or the affected organ and a part of the healthy tissue surrounding the tumour with the neighbouring lymph nodes and vessels to avoid any risk of cancer extension. Tumour resection remains an invasive treatment that can be unmanageable, depending on the size of the tumour mass. Nevertheless, surgery is responsible for a large part of cancer cures.
- Cryoablation (Erinjeri *et al.*, 2010): Referred to all methods of destroying tissue by freezing, cryoablation instigates cellular damage, death, and necrosis of tissues by

cold-induced injury to cells (direct mechanisms) and by change of the cellular microenvironment and impair tissue viability (indirect mechanisms). By both mechanisms, cell injury can be influenced by cooling rate, target temperature, time at the target temperature, and thawing rate. Indeed, this invasive cancer treatment targets the lesions, under imaging guidance, by percutaneous or laparoscopic insertion of cryoprobes (one or several) cooled with liquid nitrogen. Almost all tissues exhibit subsequent cell death via a rapid cooling below −40°C (some techniques also use high-pressure room temperature argon gas to reach -80°C of cryoprobes). Since the cooling of tissues and nerves provide an anaesthetic effect, cryoablation tends to be less painful than the heat-based thermal ablation techniques like radiofrequency or microwave ablation that will be next discussed.

- Hyperthermia: As introduced in **chapter 1.1.**, the application of radiofrequency (**RF**) energy and its thermal effects on tissue were described in 1891 by d'Arsonval. Employing RF or micro-wave, these techniques are used for tumours whose localisation does not allow surgical intervention. Based on thermal destruction, hyperthermia is governed by three phenomena: thermal production, *i.e.*, the energy delivered as well as its interaction with the tissues; thermal conduction, *i.e.*, how the heat is dissipated by transmission due to the physical contact between the target tissue and the surrounding tissues (it differs from one tissue to another); thermal convection, *i.e.*, the dissipation of heat via its transport by the fluids which pass through the tissues (thus, blood vessels more significant than 2-3 nm act as heat sinks (Ringe *et al.*, 2015)). RF ablation takes advantage of the heat produced by applying a high-frequency electric current, *c.a.* 460-480 kHz (Hong *et al.*, 2010), reaching around 60 to 100°C at the treated site. Depending on the tumour location, the RF is delivered percutaneously or by laparoscopy employing multiple curved uninsulated electrodes deployed from the needle tip central cannula (an umbrella shape). RF ablation is the primary technique used today to treat hepatic tumours (Pepple *et al.*, 2014). Nevertheless, certain parts of the tissues, such as blood vessels and the hepatic bile ducts, strongly dissipate the deposited heat, interfering with the treated areas' proper heating effects. On the other hand, microwave ablation radiates into the tissue through an interstitial antenna. For medical purposes, the frequency of microwave ablation varies between 915 and 2450 MHz. It causes the

very rapid oscillations of the dipoles, thus causing friction of the water molecules in the tissues, leading to a temperature rise of up to 180 °C in the target tissues (without current passage). That temperature rise is more rapid than in RF ablation. Besides, not like RF ablation, microwave ablation seems less prone to induce a heat sink effect when the used microwave are capable of propagating through and effectively heating many types of tissues, even those with low electrical or thermal conductivity and high baseline impedance (Lubner *et al.*, 2010).

- Irreversible electroporation (IRE) and high-frequency irreversible electroporation (H-FIRE): these recent approaches are nowadays employed when thermal ablation turns out to be too risky. IRE and HFIRE target tissues with an electroporation-based strategy (described above in **chapter 1.2.**) using a series of brief electric pulses, whose parameters cause the cell electroporation but may also result in secondary Joule heating of the tissue (Aycock *et al.*, 2019). Davalos and colleagues were the first to propose that IRE could be an efficient soft tissue ablation approach (Davalos, 2005). Those results were followed by the first successful *in vivo* application of IRE for the minimally invasive treatment of aggressive cutaneous tumours implanted, achieved by our group, using plate electrodes to deliver 80 monopolar pulses of 100 µs at 0.3 Hz with a PEF magnitude of 2500 V/cm, with minimal heating of the tissue thanks to mathematical models of the electrical and thermal fields (Al-Sakere, 2007), and the first clinical trial to treat renal tumours (Thomson *et al.*, 2011). Recently, H-FIRE has been introduced to outperform IRE by using HF voltage waveforms with integrated bursts of 0.25–10 µs bipolar pulses to more uniformly penetrate the heterogeneous system (Arena *et al.*, 2011). H-FIRE has since been used to treat intracranial malignancies in the canines (Garcia *et al.*, 2017), and low-amplitude H-FIRE waveforms have been used to transiently disrupt the blood-brain barrier (Arena *et al.*, 2014).
- Radiotherapy: ionised radiations (X-rays, gamma rays, radiations using protons, neutrons, electrons, carbon ions) used to locally target the treated tumour (see history in **chapter 1.1.**). To date, more than half of cancer patients resort to radiotherapy in their approved health care pathway, primarily in combination with other treatments such as chemotherapy or surgery. The main challenge remains to target cancer cells without specifically harming surrounding normal cells.

As for unresectable and disseminated cancerous tumours, and this is, unfortunately, the case of numerous cancer cases, there are developments and applications of other therapies introduced below.

3.1.4.2 Photodynamic therapy

Since the Ancient Indian and Chinese civilisations more than 3000 years ago, light has been employed to treat various diseases, mainly in combination with reactive chemicals, *e.g.*, vitiligo, psoriasis or skin issues (Ackroyd *et al.*, 2001). However, it was only after discovering **phototherapy** in 1895 (see history in **section 1.1.**) that the use of light and chemicals emerged.

Currently being used as an alternative treatment for the control of malignant diseases, **photodynamic therapy** (**PDT**) is based on the uptake of a photosensitiser molecule that reacts with oxygen after being excited by light in a determined wavelength and generates oxidant species in target tissues (such as radicals, singlet oxygen, triplet species), leading to cell death. The photosensitised oxidations of nucleic acids, lipids, and proteins within the cell that leads to severe alteration in cell signalling cascades or gene expression regulation have been identified as the main cytotoxic properties of PDT. The key step in terms of the performance of the photosensitiser is the formation of triplet exciting species (dos Santos *et al.*, 2019).

With well-established safety profiles and selectivity towards tumour cells for cellular and vascular-targeted PDT, verteporfin (Visudyne®) and porfimer sodium (Photofrin®) are amongst the most commonly photosensitising agents approved or in clinical trials.

3.1.4.3 Chemotherapy

Chemotherapy was first developed at the beginning of the 20th century, though it was not originally intended as a cancer treatment. Throughout World War II, it was noticed that individuals exposed to nitrogen mustard developed significantly reduced white blood cell counts. This discovery led researchers to scrutinise whether mustard agents could be used to halt the growth of rapidly dividing cells such as cancer cells. In the 1940s, two distinguished Yale pharmacologists, Alfred Gilman and Louis Goodman examined the therapeutic effects of mustard agents in treating lymphoma. First, they established lymphomas in mice and showed that the tumours could be treated with mustard agents. Then, together with Gustav Linskog, a thoracic surgeon, they injected a less volatile form of mustard gas termed mustine (nitrogen mustard) into a patient having non-Hodgkin's lymphoma. Since then, several other molecules have shown to be effective antineoplastic agents (*Figure **18***).

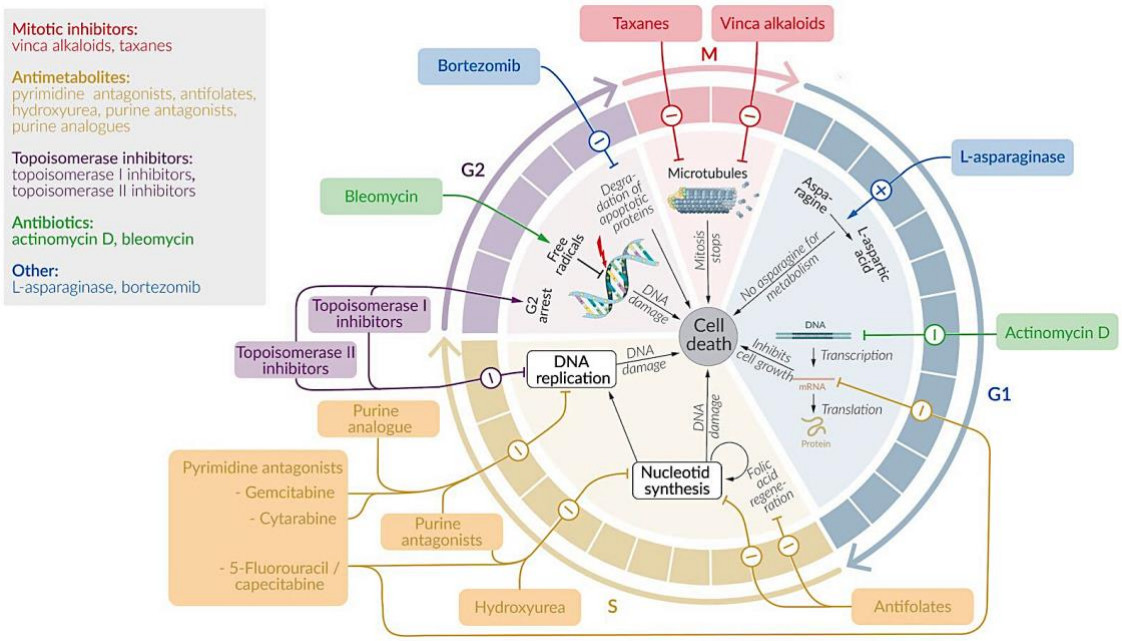

Figure 18| Classification of chemotherapeutic agents and their mechanism of action
Source: https://www.amboss.com/us/knowledge/Chemotherapeutic_agents

Chemotherapy can be used as:

- Neo-adjuvant chemotherapy: to reduce the tumour size before surgery or radiotherapy
- Adjuvant chemotherapy: to eliminate potentially remaining cancer cells after surgery or radiotherapy
- Palliative treatment, *i.e.*, to relieve symptoms caused by cancer when the latter is at an advanced stage, probably cannot be controlled, and has metastasised. This *palliation* (also called *palliative chemotherapy* or treatment with *palliative intent*) is in the hope to improve the quality of life or help the patient feel better by shrinking a tumour that's causing pain or pressure.

Chemotherapeutic agents not only damage actively dividing cells but can also affect tissues with a low mitotic potential (*e.g.*, neurons). Common adverse effects of chemotherapy occur in: gastrointestinal tract (*e.g.*, chemotherapy-induced nausea and vomiting, diarrhoea, constipation, intestinal perforation, etc), blood (*e.g.*, myelosuppression, often dose-dependent), skin (alopecia), central nervous system (*e.g.*, vomiting, chemotherapy-induced peripheral neuropathy), sexual organs (gonadal damage).

Chemotherapy is thus a non-targeted therapy or at least not a precise strategy treatment, as opposed to targeted therapies which will be discussed here below.

3.1.4.4 Targeted anticancer therapies

Despite numerous improvements in many anticancer approaches (improvement of surgical techniques, radiotherapy procedures, introduction and extension of treatments by immunotherapy, alone or in combination...), there are nevertheless many situations for which cancerous disease cannot be controlled, and side effects are unavoidable. More efficient techniques are thus needed, amongst which found targeted anticancer therapies. With cutting-edge translational research discoveries and based on either the unique characteristics of molecules, peptides, proteins, antibodies or the structures, metabolisms and other phenotypic properties of cancer, targeted anticancer therapies engage in destroying cancer cells in a more precise manner, therefore, may significantly improve the treatability of cancer.

Targeted anticancer therapies encompass a variety of direct and indirect approaches. **Direct approaches** target tumour cells directly to alter their molecular pathways by either mAbs or small molecular inhibitors. **Indirect approaches** target tumour stroma, a critical component of the tumour microenvironment, by mAbs, peptide ligands or radiolabelled chemical agents that inhibit angiogenesis or disrupt the tumour vasculature fibroblasts, macrophages, hence affecting tumoural micro-environment. In other words, there are many different types of targeted therapies for cancer, and some may fit into more than one category, but those can be distinguished into at least **two main strategies** (Bashraheel *et al.*, 2020):

- Immunotherapy based strategies:
  - ✓ Immune checkpoint inhibitors
  - ✓ Immune cytokine-based strategies
  - ✓ Tumour superantigen targeting and superantigen ligand targeting
- Enzyme or small molecules strategies:
  - ✓ Proteolysis targeting chimaera
  - ✓ Antibody-drug conjugates
  - ✓ Antibody-directed enzyme prodrug therapy

To design an appropriate targeted treatment protocol, almost all molecules are administered orally or intravenously, with molecular tests carried out before the treatment to determine the presence or absence of specific biomarkers in patients' tumours. To date, while being actively investigated for development, these targeted therapies have the US FDA approval for more than fifteen types of cancer, including the most common types, such as the cancers of

breast, lung, prostate, colon, liver, kidney, bladder, and the colorectal carcinomas, the leukaemias and the lymphomas.

The main current approaches and treatments deemed promising and even used for clinical applications in the fine-tuning of precision medicine to target cancer with maximal tumour destruction, and minimal side effects are described here.

3.1.4.4.1 Hormone-replacement therapy

Tumours require certain hormones to grow. Thus, hormone therapy is proposed to slow or impede the growth of hormone-sensitive tumours. This systemic treatment prevents the body from producing the hormones or interfering with the hormones' action. Hormone therapies have been approved for breast and prostate cancer which depend on sex hormones to grow (Lobo, 2017).

The introduction of hormonal therapy took place in 1939 by Charles Huggins, based on an early observation on the effect of oestrogens on breast cancer made by Beatson in 1896 (Beatson, 1896) treated men with prostate cancer with hormones and was able to show responses through the decreases in acid phosphatase levels (Huggins *et al.*, 1941). This exciting discovery was an essential addition to the systemic treatment of cancer and earned Huggins a Nobel Prize. Since then, many medications have been discovered to prevent cancer cells from getting the hormones needed for growth and proliferation and have been used in combination or not with other cancer treatments, such as chemotherapy or radiation therapy.

Some frequently used hormone therapy drugs in clinics to treat common cancer types, mainly breast cancer and prostate cancer, are anastrozole (Arimidex®), exemestane (Aromasin®), fulvestrant (Faslodex®), letrozole (Femara®), leuprolide (Eligard®, Lupron Depot®), tamoxifen (Nolvadex®), abiraterone (Zytiga®).

3.1.4.4.2 Signal transduction inhibitors

The primary signal transduction pathways in cancer cells are deregulated so that every cancer case itself poses new challenges for medicine. Signal transduction inhibitors, as their name indicate, block the activities of molecules that participate in signal transduction, the course by which a cell responds to signals from its environment. The signal is transmitted within the cell through biochemical reactions that ultimately produce the appropriate response(s). In some cancers, the malignant cells are stimulated to divide endlessly without being prompted by external growth factors – inappropriate signalling that signal transduction inhibitors can

perturb or even suppress. Particular examples of FDA approved mAbs are the anti-human epidermal growth factor receptor 2 (HER2) antibody trastuzumab (Herceptin®) against breast and stomach cancer and the anti-CD20 antibody Rituximab (Mabthera®, Rixathon®, Truxima®) used for a variety of B-cell malignancies.

3.1.4.4.3 Apoptosis inducers

Apoptosis is a programmed cell death process mediated by several intrinsic and extrinsic signalling pathways, which are triggered by multiple factors, including cellular stress, DNA damage and immune surveillance. Healthy cells of an organism may undergo apoptosis to get rid of unneeded or abnormal cells, but cancer cells have strategies to avoid this process. Anti-apoptotic oncogenes such as BCL2 (B-cell lymphoma 2) and BCL2L1 (BCL2-like 1) that prevent cell death (Hockenbery *et al.*, 1990) are a powerful mechanism for tumour growth and drug resistance (Rathmell *et al.*, 2002). Apoptosis inducers can get around these strategies to cause (or restore) the normal cell death of cancer cells. To date, there is a limited number of FDA-approved apoptotic inducers, which are small molecules designed to inhibit anti-apoptotic BCl-2 family members. For example, velcade (Bortezomib®) induces apoptosis in lymphoma and multiple myeloma cells. Other promising therapeutic strategies to activate cancer cell apoptosis include agents that trigger the extrinsic apoptosis pathway, target tumour suppressor pathways or the tumour microenvironment, and combination drug therapies (Carneiro *et al.*, 2020). Scientists are also investigating plant compounds like resveratrol (found in red wine) to see if they might trigger cancer cell death.

3.1.4.4.4 Angiogenesis inhibitors

To get abundant nutrients and oxygen necessary for tumours to grow, progress and metastasise beyond a specific size, cancer cells form new blood vessels from pre-existing ones by releasing pro-angiogenic chemical signals - a process named tumour angiogenesis (Teleanu *et al.*, 2019). Treatments that interfere with angiogenesis (angiogenesis inhibitors) may block tumour growth by preventing new blood supply formation. For example, the treatment of glioblastoma or hepatocellular carcinoma based on some targeted therapies such as Pazopanib (Votrient®), Sorafenib (Nexavar®), or Sunitinib (Sutent®) inhibits angiogenesis interfere with the action of vascular endothelial growth factors (VEGF), a substance that stimulates new blood vessel formation (angiogenic activator) or platelet-derived growth factors (PDGF), that interact with cell surface tyrosine kinase receptors important for regulating cell proliferation, cellular

differentiation, cell growth and development. Other angiogenesis inhibitors support the removal of existing vessels, *i.e.*, at the end of an inflammatory response. Those chemical signals, such as angiostatin, endostatin, platelet factor 4 (PF4), thrombospondin-1 and 2, IL-12, etc., facilitate the termination of neovascularisation through anti-apoptosis gene suppression (Mousa *et al.*, 2017).

The FDA has approved several angiogenesis inhibitors to treat cancers, with some being used in conjunction with other anticancer chemotherapeutics (Rajabi *et al.*, 2017). The most applied amongst the currently available anti-angiogenic drugs of enzymatic or mAb origin are bevacizumab, sunitinib, pazopanib, endostar, regorafenib, axitinib, sorafenib, ranibizumab, and aflibercept (Teleanu, 2019).

3.1.4.4.5 Immune cytokine-based therapies

As discussed above, in the hallmarks of cancer, tumours can develop mechanisms to escape the immunologic detection and elimination (Palucka *et al.*, 2016). Therefore, anticancer immunotherapy seeks to stimulate the immune system to favour anticancer immunity and decrease the control of cancer cells over immunity. Some immunotherapies use mAbs to recognise specific molecules on the surface of cancer cells and bind to those target molecules, resulting in the immune destruction of cancer cells. Other mAbs bind to specific immune cells to help these cells better kill cancer cells.

Since the discovery of anti-tumour activity of interferon α (IFN-α) against several cancer cell lines in 1970 (Gresser *et al.*, 1970), scientists have investigated many cytokines such as (in conjunction with electroporation approaches) interleukin 2 (IL-2) or into IL-12, in preclinical studies (Cha *et al.*, 2012; Mir *et al.*, 1992., Mir *et al.*, 1997) and clinical trials in both human (Daud, 2008; Greaney *et al.*, 2020) and veterinary (Mir, 1997; Pavlin *et al.*, 2012), exploiting their ability to stimulate immune responses, either innate or adaptative, against cancer. Indeed, whereas systemic IL-12 is associated with potentially life-threatening toxicity (Atkins *et al.*, 1997; Leonard *et al.*, 1997) as part of the incapability of cytokines (which are peptides) to cross the cell lipid bilayer to enter the cytoplasm, the intratumoural plasmid IL-12 electroporation therapy is safe, well-tolerated and can induce tumour regression at distant sites, especially in a patient with metastatic melanoma. Those strategies using electroporation technology to overcome the plasma membrane impermeability were described in **chapters 1 and 2** and are part of gene therapy in cancer treatment which will be mentioned in the next section.

Despite some drawbacks of cytokines as monotherapies, the (mild) anti-tumour activities shown by the IL-2 and IFN-α led to their FDA approval to treat several types of cancer. For example, IL-2 has been approved for the treatment of advanced renal cell carcinoma and metastatic melanoma, and IFN-α for the treatment of hairy cell leukaemia, follicular non-Hodgkin lymphoma, melanoma and AIDS-related Kaposi's sarcoma (Bashraheel, 2020)

As one of the fastest-growing categories of protein therapeutics with an increasingly improved safety profile, monoclonal antibodies (mAbs) technologies can cause a specific cancer cell death via the delivery of toxic molecules. Once the mAb has bound to its target cell, the toxic molecule linked to the Ab (such as a radioactive substance or a cytotoxic chemical) is taken up by the cell, ultimately killing that cell. Cells that lack the target for the antibody will not be affected by the toxin - *i.e.*, the vast majority of cells in the body.

Nevertheless, mAb-based medicines also have limitations that halt their clinical utilisation. To date, the most prominent challenges consist of the short pharmacokinetic properties of mAbs and stability issues during their production (manufacturing, transport and storage) that can lead to aggregation and protein denaturation (Awwad *et al.*, 2018). Cytokines have other disadvantages for several types of cancer treatment (low response rate, modest efficacy and high toxicity due to the need for high doses of IL-2 and IFN-α). Therefore, besides the use of excipients (*e.g.*, surfactants and amino acids) or the production of more stable constructs (*e.g.*, protein scaffolds and bispecific molecules), many strategies are being pursued to improve the pharmacokinetic and stability profiles of mAbs, such as Fc fusions, PEGylation, and combination with other therapies (Bashraheel, 2020).

3.1.4.4.6 Cellular adoptive immunotherapy

Cellular adoptive immunotherapy (also called adoptive T cell therapy, adoptive cell transfer or T-cell transfer therapy) is immunotherapy in which genetically modified autologous T cells could be intravenously re-infused into patients to produce substantial clinical benefit, at least in specific B cell malignancies (Grupp *et al.*, 2013), bypassing vaccination. The most well-developed therapy is the chimeric antigen receptor T-cell (CAR T-cell or "CARs") therapy in which patient's T cells are transfected with a construct encoding an antibody against a tumour surface antigen (typically CD19) fused to T cell signalling domains, resulting in a potent antitumour activity in, *e.g.*, lymphoid malignancies (Kochenderfer *et al.*, 2013). With a similar principle, there is tumour-infiltrating lymphocyte (TIL) therapy that employs these lymphocytes,

already primed to recognise the tumour cells and destroy the tumour itself. TILs are collected from the tumour during a biopsy or surgical resection and grown in considerable numbers in a laboratory with IL-2 that promotes rapid TIL growth before infusing into the patient (Geukes Foppen *et al.*, 2015).

Multiple approaches to cancer therapy exist, but few are as complicated as immune-based therapy. *Figure* ***19*** depicts some therapies currently under preclinical or clinical evaluation to target the cancer-immunity cycle (Chen, 2013).

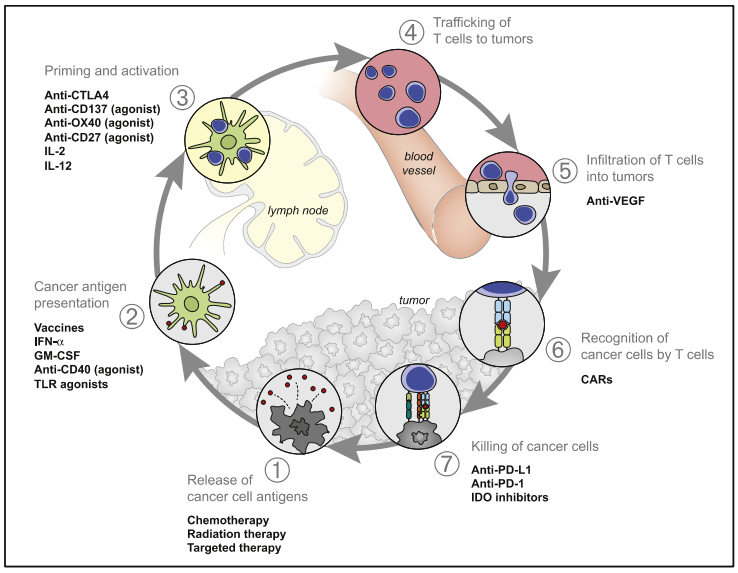

Figure 19| Examples of some therapies currently under preclinical or clinical evaluation that might affect the cancer-immunity cycle

Abbreviations: CARs: chimeric antigen receptors; CTLA4: cytotoxic T-lympocyte antigen-4; GM-CSF: granulocyte macrophage colony-stimulating factor; IDO: indoleamine 2,3-dioxygenase; IFN: interferon; IL: interleukin; PD-L1: programmed death-ligand 1; VEGF: vascular endothelial growth factor. Although not illustrated, intratumoral T regulatory cells, macrophages, and myeloid-derived suppressor cells are key sources of many of these inhibitory factors (Chen, 2013).

3.1.4.5 Vaccination

Vaccination allows immune cells to better irradicate cancerous cells by efficiently recognising antigens presenting on those cell surfaces. Here vaccination is not a preventive approach but one more treatment of established, slow-growing (or otherwise already treated) tumours. The anticancer vaccines could be either from the patient's tumour cells (antigen-presenting cells or APCs) or from DCs that stimulate the immune system to respond to an antigen present on cancer cells. More recently, a novel approach called oncolytic virotherapy was proposed and which uses oncolytic virus (natural or engineered) to enhance systemic antitumour immune responses (Andtbacka *et al.*, 2015). These oncolytic viruses have tumour selectivity and, through genetic engineering methods, the capacity of being transformed to express tumour-killing factors only in the cancer cells while being non-pathogenic for the non-cancerous counterparts. They have been ever since used in combination with other anticancer therapies (Cao *et al.*, 2020).

3.1.4.6 Gene therapies

Gene therapies, as their name indicate, are treatments dealing with nucleic acids rather than chemical agents for therapeutic ends. Gene therapy is sometimes considered a targeted therapy because, like cancer vaccines, this therapy, for anticancer aims, interferes with the growth of specific cancer cells.

It has been nearly half a century since the introduction of the gene therapy concept for human genetic disease (Friedmann *et al.*, 1972) and almost twenty years since the beginning of the successful clinical translation of gene therapies in the 2000s. In between those historical moments, the early development of gene delivery vectors such as an adeno-associated virus (AAV) and replication-defective retroviruses, coupled with encouraging results in preclinical disease models, was hindered by, unfortunately, therapy-related severe toxicities in the initial clinical trials in the early 1990s, including inflammatory responses to the virus vectors and malignancies caused by vector-mediated insertional activation of proto-oncogenes (Dunbar *et al.*, 2018).

Building on decades of pre-clinical research and clinical assays, with manufacturing advances, gene therapies have begun to be improved using plasmid or non-viral vectors as an alternative to classical viral gene delivery. The delivery of nucleic acids is enhanced by various approaches, including a polymer or lipid conjugation, particle-mediated delivery, hydro-dynamic delivery, ultrasound or electroporation (Dunbar, 2018; Heller *et al.*, 2010., Heller *et al.*, 2015). These safer and more efficient plasmid vectors were used to transduce autologous hematopoietic stem cells in patients with immunodeficiencies, hemoglobinopathies, and metabolic and storage disorders. The US FDA approved the first gene therapy products in 2017, with CAR–T cells (described above in section “cellular adoptive immunotherapy”) to treat B cell malignancies and AAV vectors for *in vivo* treatment of congenital blindness (Dunbar, 2018).

Up to 2019, twenty approved human gene and cell-based gene therapy products have already been approved in clinics and markets of mainly North America, Europe and Asia (Shahryari *et al.*, 2019), primarily based on AAV and lentiviral vectors, and over two thousand human gene therapy clinical trials have been reported worldwide (http://clinicaltrials.gov).

Even if all those abovementioned targeted therapies have been proven efficient in various cancers, targeted therapies can instigate serious side effects. Common ones are diarrhoea, hepatitis (amongst other liver problems), and changes to the patient’s skin, hair, and nails. The

toughest for most cancer patients is skin problems because targeted cancer therapies attack the same growth factors and blood vessels needed for healthy skin.

3.1.4.7 Personalised medicine

After decades of research, scientists now understand how genetic changes in patients' tumours can cause cancer to grow and spread. They have also discovered that the changes that drive cancer in one person may not occur in others who have the same type of cancer, *i.e.*, individuals with the same disease respond differently to the same therapy. Moreover, the same cancer-causing changes may be found in different categories of cancer. Until recently, cancer patients with the same type and stage of cancer were receiving the same treatment. Thus, the inefficiency of the therapies has been observed in numerous cases.

Personalised medicine, also known as precision medicine, allows the selection of a treatment based on the patient's genetic makeup. For cancer, the treatment is tailored to consider the genetic changes that may occur in the individual's tumour, *i.e.*, the approach takes advantage of knowing the genetic changes in a patient's tumour to determine its selective treatment. Hence, personalised medicine could be defined as the targets involved in targeted therapy, with similar strategies to target cancer as described above.

Despite the richness of therapies, challenges remain to this day in oncology. The employed anticancer therapeutic strategies present indeed problems of specificity for tumour cells or a lack of validated biomarkers and also insufficient characterisation of the patient populations appropriate for treatment, amongst others, thus causing considerable side effects. The precise targeting of tumours by local treatment is not always practicable. Furthermore, cancer recurrence or the development of multidrug resistance and the weak induction of immunogenic cell death, amongst other issues, remain to limit factors. Therefore, different therapeutic strategies based on new approaches are required, particularly physical modalities that allow local treatment and are less prone to developing resistance in cancer cells. Several strategies **potentiate anticancer drugs' distribution in tumours, improving** their therapeutic index. Recent years have witnessed a considerable increase in research, development and application of anti-cancer therapies based on physical principles, amongst which **electrochemotherapy** and **non-thermal plasma technology** have raised great excitement. These approaches offer eradication of cancerous tumours, directly or indirectly, and in the case of electroporation, a safe and efficient vectorisation technique for delivering molecules of therapeutic interest (*e.g.*,

nucleic acids, drugs, ions). The following two sections are interested in electrochemotherapy, an anti-cancer treatment based on electroporation, and non-thermal plasma technology applied in oncology.

3.2 Electrochemotherapy

3.2.1 Basic knowledge

Electrochemotherapy (ECT) enhances the delivery to the tumour site of very low- or non-permeant chemotherapeutic agents, at a low dose in the tumour site, by the local exposure to **electric pulses** transiently permeabilise the tumour cell membrane. ECT selectively kills the tumour cells and accordingly reduces associated systemic side effects. Being the first electroporation-based application in the targeted drug administration (Mir, 1991b), ECT is a non-thermal, safe and efficient established local eradication of solid tumours. The effectiveness of ECT has made it nowadays widely utilised in more than 150 clinics in the European Union and abroad in the human (Campana *et al.*, 2019a; Probst *et al.*, 2018) and veterinary oncology (Čemažar *et al.*, 2008). ECT indeed has an excellent therapeutic index over other chemical-based anti-cancer treatments, *i.e.*, very low concentrations of the chemotherapeutic agents are needed to achieve antitumour effectiveness; thus, eventual systemic toxicity is spared.

The theory of ECT is based on the properties mentioned above of **reversible electroporation** (see **chapter 1.2** and *Figure **20***) combined with the therapeutic efficiency of chemotherapeutic molecules (Escoffre, 2012; Mir, 1991a).

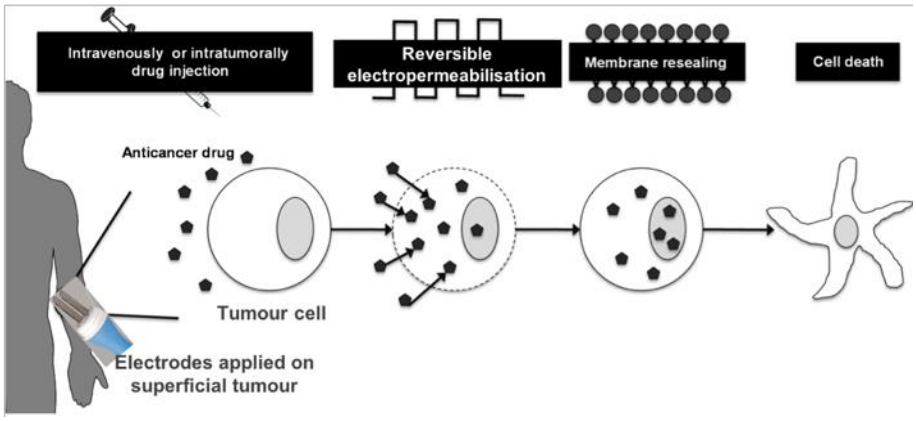

Figure 20| Principle of electrochemotherapy

Low- or non-permeant cytotoxic drugs (BLM or *cis*-Pt) are i.v. or i.t. administered to a patient, then short intense electric pulses are applied to the tumour via electrodes connected to an electric pulse generator, resulting in tumour cell electropermeabilisation and, therefore, in an increased internalisation of chemotherapeutic drugs in the cytosol, leading to necrotic/apoptotic cell death by drug cytotoxicity, systemic anti-tumour reaction (Calvet *et al.*, 2014b); vasoconstriction of the tumour neovasculature to the ischemia of the tumour cells (Jarm *et al.*, 2010). Scheme adapted from (Escoffre, 2012).

In general, a patient receiving ECT will first get an intravenous or intratumoural administration of an anti-cancer drug, commonly used bleomycin (BLM) or *cis*-platin (*cis*-Pt), resulting in an even distribution over the vascular system and extracellular space of the tissue. **Electrodes** located around (see *Figure **8***) or inside the tumour (see *Figure **24***) will deliver defined **electric pulses,** which enable diffusion through the plasma membrane of the otherwise very low or non-permeant anti-cancer drug into the target cells. After a short time ranging from a few seconds to several minutes after exposure to the PEF, the plasma membrane permeability will return to its initial state. The specific anticancer chemotherapeutics will elicit DNA single- and double-strand breaks (bleomycin) or intra- and inter-strand DNA bonds (*cis*-platin). Those cytotoxic effects are much more pronounced in **fast-dividing tumour cells** than in quiescent (non-malignant) cells because unrepaired strand breaks mainly affect dividing cells (Mir, 2006; Tounekti *et al.*, 2001). Therefore, this mechanism of action only requires two main conditions to achieve an efficient ECT: first, although low, a necessary concentration of cytotoxic drug has to reach the tumour, and second, the whole tumour nodule has to be covered by a permeabilising pulsed electric field (PEF). Similar to EGT, the electroporation parameters should be carefully chosen in ECT to avoid “excessive electroporation” because cells should survive the electroporation process.

Benefits arising from this combination therapy of pulsed electric fields (PEFs) and chemotherapeutic agents include a considerable reduction of the dose of a cytostatic drug due to locally increased cytotoxic effect (BLM, 1000-fold and *cis*-platin, 80-fold increase of toxicity)

(Gehl *et al.*, 1998; Orlowski, 1988; Poddevin *et al.*, 1991), as, in the case of the bleomycin, a few hundreds of molecules per cell only are sufficient to induce cell death in a single treatment session. ECT is used in clinics to treat almost all types of tumour nodules, as all cells are permeabilised by electric pulses of appropriate electric field amplitude and bleomycin is effective on all dividing cells, whatever their origin. Beyond its effectiveness and benefits mentioned above, ECT is a repeatable and minimally invasive intervention that is easy and quick to perform (about 25-30 minutes), thus offering a short hospitalisation and mitigating the symptom burden.

Our group published the first clinical study on ECT in 1991, demonstrating this target anti-cancer modality's feasibility, safety, and effectiveness (Mir, 1991b). This pioneered study enthused groups in the United States (Tampa), Slovenia (Ljubljana), and France (Toulouse and Reims) to accomplish further clinical studies (Domenge *et al.*, 1996; Heller, 1995; Rudolf *et al.*, 1995), which were then compiled in a joint paper published seven years later (Mir *et al.*, 1998).

Figure 21| Photos demonstrating a complete response to ECT in a patient with cutaneous metastasis from malignant melanoma

Photos of the course of treatment for a patient treated with i.v. bleomycin and type III (hexagonal) electrodes under general anaesthesia. Before treatment (left panel), the metastasis was ulcerated with consequently haemorrhage, pain and discomfort. One month after treatment (middle panel), the lesion was covered by a crust. Around the crust, needle marks in normal tissue are visible, because the tumour was covered including a margin of normal tissue. Whereas the tumour area became necrotic, the normal tissue was very little affected, indicating a therapeutic window. Six months after treatment (right panel), complete regression of the treated nodule has been observed. The crust fell off after 10 weeks, revealing normal skin that had healed underneath the nodule (from Gehl J., Ugeskrift for Laeger, 2005).

The current and potential applications of ECT are focused on: *(i)* **primary tumours** (breast, ovary, colon-rectum, pancreas); *(ii)* **cutaneous metastasis** (melanoma and non-melanoma skin cancer, breast, head and neck) and *(iii)* **non-cutaneous metastasis** (bone, liver, brain, soft tissue sarcomas) (Esmaeili *et al.*, 2019).

3.2.2 Chemical aspects of ECT

3.2.2.1 Bleomycin

First isolated from *Streptomyces verticillus* collected from the soil in a coal mine in Japan by Umezawa and colleagues in 1966, bleomycin (BLM) forms a family of glycopeptide antibiotics with antitumour activity (Umezawa *et al.*, 1966). BLM is, therefore, employed in the treatment of, amongst others, Hodgkin's disease, non-Hodgkin's lymphoma and testicular cancer (Tounekti *et al.*, 1993). BLM is the most commonly used drug combined with chemotherapy against lymphomas, squamous-cell carcinomas, and germ-cell tumours in clinics. BLM is administered intravenously, subcutaneously or intramuscularly, as it is not absorbed from the gut. The primary target for the cytotoxic action of BLM is DNA.

The BLM family comprises at least thirteen small water-soluble glycopeptide antibiotics, all members have an identical core structure but differ in their configuration of sugars and positively charged tails. Some clinically administered forms of BLM are bleomycin sulfate injection under brands named *e.g.*, Blenoxane (Bristol-Myers Squibb) or Bleomycine Bellon (Sanofi). Due to its hydrophilic nature, bleomycin is normally not bound to plasma proteins, and its entry into the cells is limited and primarily mediated by endocytosis (Pron *et al.*, 1999). Once inside the cell, BLM becomes a very potent drug. Nevertheless, this high intrinsic cytotoxicity is limited because as a large and hydrophilic molecule, BLM is unable to cross cell plasma membranes by free diffusion (Mir *et al.*, 1996; Orlowski, 1988; Poddevin, 1991).

Studies indicate that the positively charged tail of BLM might be key to cellular uptake. The BLM require cofactors which are a reduced transition metal (Fe(II) or Cu(I)), oxygen and a one-electron reductant to generate “activated” bleomycin. Once activated, BLM can catalyse oxidative damage to the ribose or the deoxyribose of nucleotides in the DNA or double-stranded RNA, which further leads to single- and double-stranded DNA breaks and cell apoptosis (Chen *et al.*, 2005). Those damages are reminiscent of those generated by ionising radiation.

Other main points:

- The eukaryotic cellular responses to BLM administration are complex. They are cell-line- and genotype-dependent, with extended cell-cycle arrest, apoptosis and mitotic cell death as the most common outcomes (Tounekti, 2001).

- In concert with chemical synthesis, biosynthetic genes for BLM have been identified. Some of the proteins in the pathway have been characterised, opening the gate to making libraries of BLM analogues.
- BLM is more toxic in fast-dividing cells as compared with quiescent cells because unrepaired strand breaks mainly affect mitotic cells (Tounekti, 1993)

BLM is inactivated in normal and tumour tissues by bleomycin hydrolase, a cysteine protease that cleaves the ammonia group from BLM (Sebti *et al.*, 1988; Umezawa *et al.*, 1974). This enzyme is active in all tissues but is found at deficient activity in the skin and lung, which may explain these being the most common sites of toxicity by BLM. Indeed, the side effects of the BLM are tissue-specific and dose-dependent and encompass lung inflammation which often advances to the lung fibrosis (Brömme *et al.*, 1996; Fyfe *et al.*, 2010).

In clinical practice, side effects of BLM are dose-dependent and include mainly lung fibrosis and skin toxicity (erythema, peeling, hyperkeratosis). These results are probably from the poor expression of bleomycin hydrolase in these tissues, an enzyme responsible for BLM degradation. However, contrary to many anticancer drugs, neither digestive side effects nor immunosuppression nor myelosuppression were reported following BLM administration. In pre-clinical ECT regimens, BLM was first used with electroporation in 1988 to increase its *in vitro* uptake and thus increase its cytotoxic activity (Orlowski, 1988). Three years later, the internalisation of BLM mediated by electroporation was demonstrated to be dependent on the external concentration of the drug and that as few as 500 BLM molecules were sufficient to trigger cell death (Poddevin, 1991), highlighting the possibility of using doses that spare normal tissues thanks to electroporation, thus avoiding the side effects reported here above. The combination of BLM with EPs was tested on various cell lines and decreased the half-maximal inhibitory concentration (IC_{50}) by up to several thousand folds *(Jaroszeski et al.*, 1997; Larkin *et al.*, 2007; Poddevin, 1991). Similarly, *in vivo* investigations performed in several species (*i.e.*, mice, rats, rabbits, cats, dogs, horses) revealed that ECT regimens using BLM resulted in tumour regression in various types of both transplanted and spontaneous tumour models (Belehradek *et al.*, 1991; Čemažar, 2008; Gothelf, 2003; Larkin, 2007; Mir, 1991a). It is worth noting that the very low dose of BLM used in ECT protocols (*ca.* 0.5 mg/kg), along with the local delivery of EPs, enables the selective toxicity of the drug toward cancer cells. Indeed, in the treated region, both healthy and cancer cells are permeabilised and consequently will get their DNA cleaved.

However, the hundreds of BLM molecules internalised generate enough DNA breaks to drive cell death upon cell division (as is defined as mitotic cell death) but are not sufficient to cause metabolic cell death. Therefore, normal quiescent cells are spared.

3.2.2.2 *Cis*-platin

Cis-platin (*cis*-Pt or *cis*-diamminedichloridoplatinum (II) (CDDP)), another common antineoplastic agent, possesses a permeabilisation coefficient through the cell plasma membrane by passive diffusion of less than 50%. In contrast, the remainder is transported by carrier molecules (Eljack *et al.*, 2014). *Cis*-Pt has cytotoxic properties involving DNA transcription and replication interference. Nevertheless, many side effects are observed at the therapeutic dose, including neuronal, cardiac and renal toxicity and bone marrow suppression. Besides, *cis*-Pt resistance has been reported as associated with changes in cellular drug uptake, drug efflux, increased detoxification, inhibition of apoptosis and increased DNA repair. Consequently, electroporation represents a major advantage to avoid side effects and resistance, as much more molecules get access to the cell interior while decreasing the dose administered.

Indeed, in *in vitro*, the half-maximal inhibitory concentration (IC_{50}) of *cis*-Pt was decreased by up to 13-fold when using EPs (Gehl, 1998; Jaroszeski *et al.*, 2000). Interestingly, increased cytotoxicity to the drug was also observed in *cis*-platin-resistant cell lines (Čemažar *et al.*, 1998b). In *in vivo*, studies also showed an improvement of anticancer activity of ECT with *cis*-Pt as compared with *cis*-Pt alone (Serša *et al.*, 1995), in particular with an intratumoural administration of the drug (Čemažar *et al.*, 1998a). Other platinum (II) analogues have been tested in the context of ECT but *cis*-Pt appears to be the most efficient when combined with EPs (Čemažar *et al.*, 2006). *Cis*-Pt is only administrated intratumourally, otherwise, it will generate systemic toxicity (nephropathies, and others).

3.2.2.3 Other approaches

Other drugs which have been investigated for use in ECT protocols (but not used in the clinical practice of ECT) include:

- Daunorubicin, doxorubicin, etoposide, paclitaxel, fluorouracil, Taxotere, vincristine and methotrexate (Miklavčič, 2014; Orlowski, 1988). However, since they are lipophilic (thus already easily penetrating the cells) highly toxic drugs, no significant enhancement of cytotoxicity was observed when using electroporation.

Contrariwise, the application of EPs concomitant with mitomycin C administration showed a 30 % increase in the efficiency of intravesical chemotherapy in bladder cancer, in comparison to mitomycin C alone *(Vásquez et al.*, 2012).

- Calcium ions uptake: high concentrations of calcium are introduced into the cell cytosol by electroporation (calcium electroporation), inducing cell death *in vitro* and tumour necrosis *in vivo* with a difference in sensitivity between different tumour types (Frandsen *et al.*, 2012., Frandsen *et al.*, 2018). This novel anticancer strategy has recently entered a clinical trial to treat cutaneous metastases (Falk *et al.*, 2018). Results of this first clinical trial showed an apparent effect of calcium electroporation comparable to the effect of bleomycin-based ECT, results which were confirmed recently during another double-blinded randomised controlled phase II trial where no serious adverse events were registered and where the complete response was confirmed histologically in both arms (Ágoston *et al.*, 2020). Calcium, like *cis*-Pt, is administered intratumourally only and in small tumours.

3.2.3 Adjuvant effects of ECT

Together with the direct cytotoxicity of ECT toward cancer cells, other bystander effects have been reported and contribute to the ECT beneficial outcome. In particular, ECT induces anti-vascular effects at the level of neo-formed blood vessels and stimulates the immune system.

3.2.3.1 Anti-vascular effects

Serša and colleagues have shown that EPs application on a tumour induces immediately vasoconstriction lasting up to several hours rather than minutes, resulting in an 80 % drop in the tumour blood flow – a phenomenon called “vascular lock” (Jarm, 2010; Markelc *et al.*, 2013; Serša *et al.*, 1999). This “vascular lock”, by avoiding the drug clearance even after cell membrane resealing, enables a prolonged drug uptake by tumour cells (mainly proposed for low-permeant drugs, such as *cis*-Pt). This transient vascular lock in the tissues exposed to the EPs is followed by anti-vascular effects resulting from the death of the endothelial vascular cells (provide tumour cells are also killed and thus no longer secrete angiogenic factors…). The “vascular lock” associated with the destruction of the endothelium leads to tumour starvation (lack of oxygen and growth factors) and thus to cancer cell death. Moreover, these anti-vascular effects are of

significant interest for treating bleeding tumours as they enable to cease the haemorrhage immediately (*Figure **22***) (Snoj, 2009).

Figure 22| ECT induced vascular lock on a haemorrhagic melanoma metastasis immediately after delivery of the electric pulses

Follow-up of bleomycin-mediated ECT on bleeding melanoma metastasis on a leg of a patient treated at the Institute of Oncology Ljubljana. Immediately after delivery of the EPs, the bleeding ceased and did not recur. The lesion developed a crust during a week post-treatment, fell off within three weeks. The tumour reduced in size considerably and remained in partial response during 21 weeks of observation time. (Snoj, 2009).

3.2.3.2 Immune stimulation

There is evidence that the immune system contributes to ECT efficiency. Indeed, in comparison to immunocompetent mice, ECT-mediated tumour regression was dramatically decreased in animals exempt from functional T lymphocytes, either due to the pre-treatment injection of OKT3 mAb (Mir, 1992) or when treatments were performed in nude mice (Mir, 1991a; Serša *et al.*, 1997a). In other words, blocking the immune system would block the systemic effect of ECT. Moreover, *in vivo* studies from our group have shown synergistic effects of the combination of ECT and interleukin-2 (IL-2) not only in the enhancement of the local anti-tumour effect in the treated area but also in the induction of a memory effect (treated animals did not develop tumours of a given type when re-challenged at a later time) (Mir *et al.*, 1995). Local oedema was also observed in tumours treated by ECT after intramuscular administration of the drug, suggesting that the EPs delivered to the tumour were the sole responsible ones for the swelling observed (Mir, 1991a). The oedema was more severe in immunocompetent than in immunodeficient mice, consistent with EP-mediated effects that depend on the presence of an intact immune system. The increase of the vascular permeability by oedema probably paved the way for the local infiltrates of dendritic cells (DCs) (Roux *et al.*, 2008) and lymphocytes (Mekid *et al.*, 2003), which were found in treated tumours. ECT treatment of human melanoma led to the maturation of pre-existing tumour-resident Langerhans cells - an epidermal subset of DCs, and their subsequent migration to the tumour-draining lymph node as early as 24 hours after the treatment (Gerlini *et al.*, 2013). Similarly, an intratumoural recruitment of DCs

expressing CD80/CD86 maturation markers 48 hours after the ECT treatment was also detected in immunogenic murine tumours in immunocompetent mice (Roux, 2008).

In *in vivo* studies, our group have also shown that ECT had high efficiency as it stimulates the immune response, which can destroy the cells that escaped the direct anti-tumoural effect of ECT, either because they were not sufficiently permeabilised by the electric pulses or not surrounded by enough BLM molecules for generating cytotoxicity. ECT thus causes immunogenic cell death (ICD), a phenomenon that occurs partially due to the application of EPs that trigger on their own both an early and physiologically relevant ATP leakage (immune-attractant for DCs) and a calreticulin translocation to the cell surface (a protein activating the DCs). As a consequence, after the bona fide ICD of electroporated cells, cancer antigens can be captured and recognised by DCs and eventually increase antitumour response (Calvet, 2014b). ECT could be considered as the adjuvant immunogen electrotransfer to peritumoural tissue (Serša *et al.*, 2015). The process leads to the local effects and triggers the systematic response against distant metastases – the so-called abscopal effect (Postow *et al*., 2012).

3.2.4 Medical applications and current developments of ECT

3.2.4.1 Electrochemotherapy of superficial tumours

Solid tumours present several barriers to the targeted delivery of chemotherapies (Minchinton *et al.*, 2006). Treatment of superficial tumours with ECT has shown a steep rise for almost two decades, whose indications range from skin cancers to locally advanced or metastatic neoplasms. Since the release of the ESOPE and especially after its updated version in 2018, consolidated indications include superficial metastatic melanoma, breast cancer, head and neck skin tumours, nonmelanoma skin cancers, and Kaposi sarcoma (Campana *et al., 2019b)*. Moreover, ECT ensures appreciable symptom control in well-selected patients with oropharyngeal cancers.

Key aspects favouring the broad acceptance of ECT for the treatment of superficial tumours are the simplicity and versatility of its procedure. Indeed, based on flexible technology, standard ECT (*i.e.*, ECT applied through fixed-geometry electrodes, as shown in *Figure **8***) represents an easy-to-master procedure that allows treating various cancers. Emerging applications of ECT include treatments of skin metastases from visceral malignancies, cutaneous metastases from

hematologic cancers, vulvar carcinoma, and noncancerous skin lesions (Keloid scars). The application of ECT to treat visceral and deep-seated tumours will be discussed thereafter.

3.2.4.2 Palliative anti-cancer treatment for human patients

With a 5-year survival rate ranging from 98.4% for localised melanoma at diagnosis, over 62.4% for patients with regional lymph nodes being affected at diagnosis or treatment, to only 17.9% for widespread metastatic melanoma (Hachey *et al.*, 2016), effective palliation is ultimately necessary for malignant melanoma patients. For almost three decades since its application in clinics, electrochemotherapy (ECT) was introduced in palliative care to alleviate the burden imposed by tumours, such as cutaneous and subcutaneous malignant melanoma, breast cancer, head and neck cancer with relatively successful local response rates (Campana *et al.*, 2019c; Linnert *et al.*, 2012; Longo *et al.*, 2019; Matthiessen *et al.*, 2012; Pichi *et al.*, 2018). A recent meta-analysis of ECT in a palliative setting found a complete response (CR) rate of 46.6% and objective response rates (ORR) of 82.2% according to the RECIST, regardless of the tumour type (Morley *et al.*, 2019). Furthermore, this meta-analysis specified that small tumours were over twice as likely (2.25) to have a complete response than large, and highlighted the need for tailored ECT depending on individual cases.

It is worth reporting the latest use of ECT as palliative care of cancer metastasis in the spinal cord for two human patients (interventional radiology service at the Tenon Hospital, Paris, in collaboration with our group). Two patients received percutaneous image-guided ECT of blastic spine metastases. The first (whose results depicted in *Figure **23***) had metastatic breast carcinoma, and the second patient had metastatic lung carcinoma. Both patients had previously undergone chemotherapy and received radiation therapy on bone metastases due to severe back pain. Only 24 hours after ECT, enhancement of metastases decreased on contrast-enhanced MRI (*Figure **23F***). The tolerance was excellent, and the post-treatment period was uneventful without reported side effects. The pain was quantified on the visual analogue scale (VAS) which consists of a straight 10 cm line with the endpoints defining extreme limits such as “no pain at all” (0 mm) and “pain as bad as it could be” (100 mm). If before ECT, the VAS was at 65 mm for the first patient and 90 mm for the second, at discharge, the VAS was 0 mm for the first patient and 10 mm for the second.

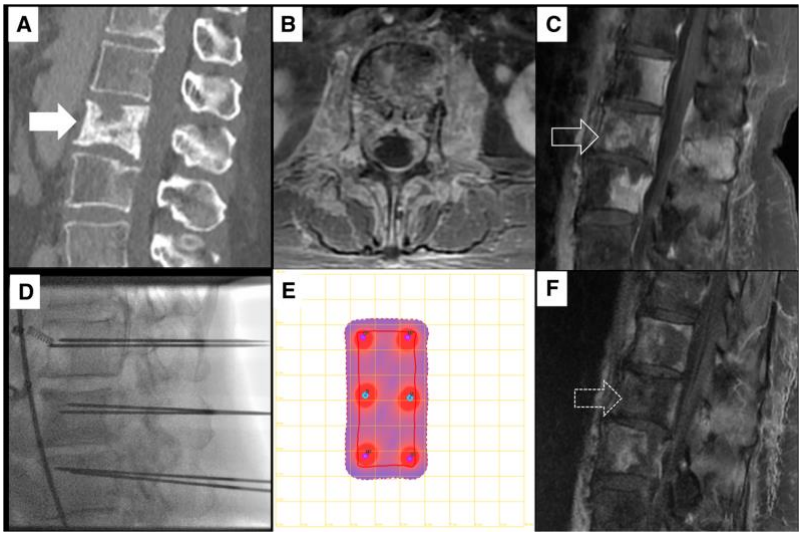

Figure 23| Percutaneous image-guided ECT of spine metastases as a local palliative care option

Study case of a 59-year-old woman with breast carcinoma who underwent percutaneous image-guided ECT of spine metastases. (**A**) A blastic tumour of the L2 vertebra (white arrow) was observed during pre-procedure CT tomography reconstructed in the sagittal plane. (**B**) Pre-procedural axial post-contrast T1-weighted MRI confirms the epidural extension of the tumour in the L2 vertebra. (**C**) Preprocedural sagittal post-contrast T1-weighted MRI shows the metastases located on L1, L2, and L3 vertebra (arrow). (**D**) Following the individualised treatment plan and under the imaging guidance under cone-beam CT, six needles were inserted to cover the whole tumour. (**E**) Coronal reconstruction of the individualised treatment plan, allowing the production of a sufficiently intensive electric field encompassing the tumours. (**F**) Enhancement decreased on the sagittal post-contrast T1- weighted MRI performed the day after ECT (dashed arrow). (Cornelis *et al.*, 2019).

3.2.4.3 Treatment of visceral or deep-seated tumours

ECT easily accesses superficial (cutaneous and subcutaneous) tumours. However, with the skin electrodes (fixed geometry, as shown in *Figure **8***), it is not simple to apply ECT protocols successfully on deep-seated tumours located in internal organs, such as the colon, liver, bone and brain, whose surfaces are often not regular (Miklavčič *et al.*, 2012; Miklavčič, 2014). Efforts are being put into the development of new electrodes to reach internal tumours with minimally invasive procedures while preserving the efficiency of the ECT (Edhemovic *et al.*, 2011; Linnert, 2012; Mahmood *et al.*, 2011):

- Variable geometry long single needle electrodes, mainly designed to treat liver and bone metastases and soft tissue sarcoma
- Endoluminal electrodes to treat colorectal cancers and oesophageal tumours
- Retractable electrodes for the treatment of brain and liver tumours

The insertion of electrodes is prepared by numerical modelling, proved to be feasible, and is done according to the treatment plan. Since the first reported clinical case of deep-seated tumour ECT (Miklavčič *et al.*, 2010), these new types of electrodes (*Figure **24***) have been widely

employed in both pre-clinical and clinical studies, primarily in the liver ECT (Edhemovic, 2011; Fiorentzis *et al.*, 2019; Simioni *et al.*, 2020; Zmuc *et al.*, 2019). These new configurations of electrodes and ECT procedures have paved the way for the approval of ECT treatment of visceral and deep-seated tumours.

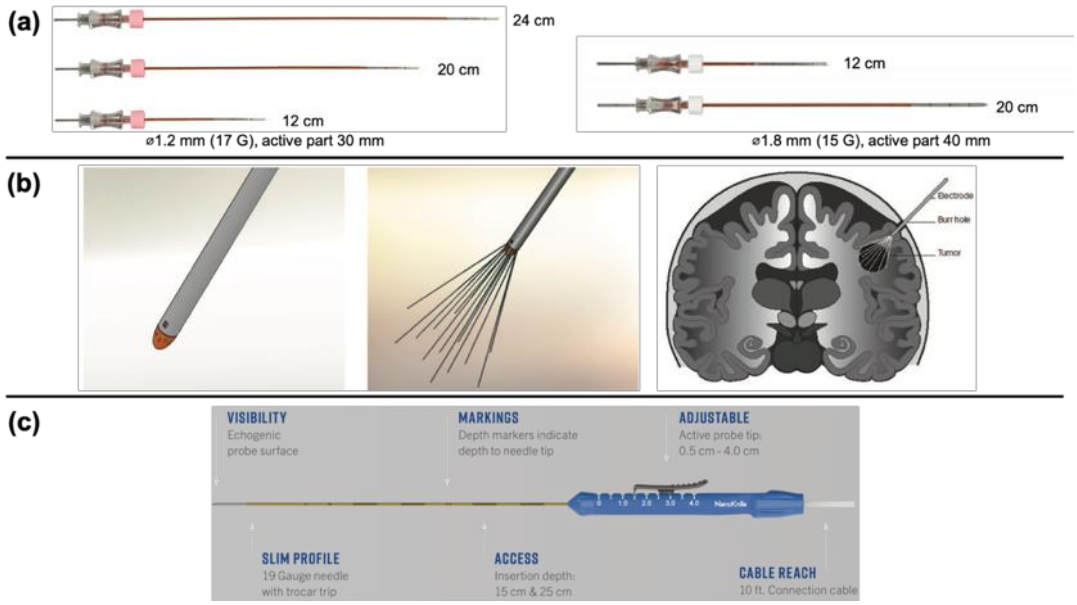

Figure 24| Invasive electrodes developed for the treatment of deep-seated tumours

(**a**) Individual needle electrodes for the treatment of bone or visceral lesions. (**b**) Retractable electrodes developed for the treatment of brain: Rendering of the electrode in the fully retracted state (left panel), electrode in the fully extended state. Recommended voltage is 1000 V for the fully extended electrodes (middle panel), diagram of the insertion into the brain (right panel). Figures **a** and **b** adapted from the "Electrodes and Accessories" of the IGEA® Clinical Biophysics (Carpi, Italy) and from (Linnert, 2012; Probst, 2018). (**c**) NanoKnife Single Electrode Activation Probe (15 or 25 cm insertion depth) from the NanoKnife 3.0 System (AngioDynamics, NY, USA).

3.2.4.4 Veterinary oncology

Besides clinical applications in human patients, ECT also finds success in the veterinary oncology (Čemažar, 2008; Mir, 1997; Tamzali *et al.*, 2012). An example of a successful ECT in an animal bearing carcinoma is shown in *Figure **25***.

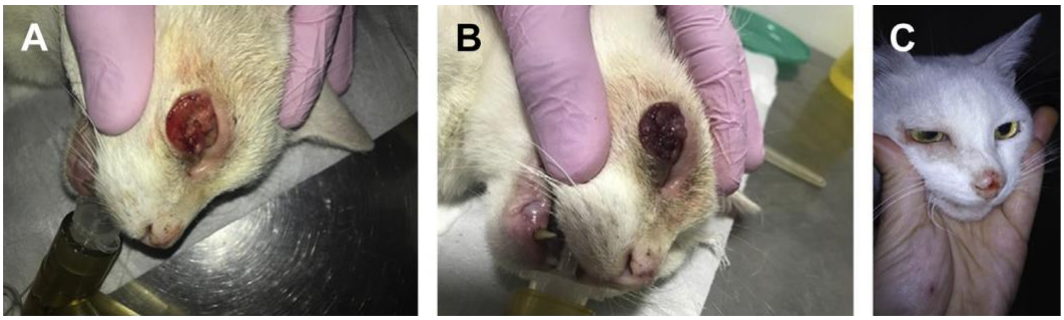

Figure 25| The outcome of a carcinoma in a cat treated with ECT

(**A**) White cat (whose race is highly prone to sun-induced malignancies) at presentation with a palpebral squamous cell carcinoma (SCC); (**B**) Patient after one session of ECT: the tumour mass is reduced and appears less vascularised; (**C**) Patient after two sessions of ECT, showing complete resolution of the palpebral neoplasm. Photos from (Spugnini *et al.*, 2019) cited the treatment performed by D. Santos dos Anjos, DVM, MSc, PhD student (Unesp-Jaboticabal), Brazil, Mexico.

Although ECT efficacy both in human and veterinary oncology was well demonstrated rapidly after the first clinical trial (Mir, 1991b), differences amongst the choice of electrodes, the lack of defined operating procedures, and the use of different pulse generators prevented the widespread adoption of ECT in the clinical setting until the mid-2000s (Serša, 2006), when the development of the first version of **standard operating procedure** (SOP) has been validated in the **European Standard Operating Procedures for ECT** (ESOPE) in **2006** (Gehl, 2006; Marty, 2006; Mir *et al.*, 2006). Provided with the SOP decision tree to help clinical staff make treatment decisions, this SOP reference describes the recommendations for indication of ECT, pre-treatment information, treatment choices, and follow-ups to safely and conveniently treat patients with cutaneous and subcutaneous nodules. As a result, the evaluation and confirmation of treatment response based on ESOPE showed an 85% objective response (OR) rate and a 74% complete response (CR) rate of ECT, regardless of tumour histology, the drug used and route of administration (Campana *et al.*, 2016). In 2018, a new version of SOP for ECT of cutaneous tumours and skin metastasis is updated by a Pan-European expert panel from dermatology, general surgery, head and neck surgery, plastic surgery, and oncology (Gehl *et al.*, 2018). This group concluded that **the best tumour control was achieved with i.v. BLM**, followed by i.t. *cis*-Pt and i.t. BLM. ECT procedure can be performed within 30 minutes both in local, loco-regional or general anaesthesia – a procedure decided by the treating surgeon. Standardisation of ECT procedure has allowed its implementation in over 150 European cancer centres and has contributed to its diffusion in the clinical practice (Campana, 2019a). In most clinical investigations that focused on the patient's response (in both human and veterinary medicine),

the Response Evaluation Criteria in Solid Tumors (RECIST) was applied *(Coletti et al., 2017; Eisenhauer et al., 2009; Milevoj et al.*, 2020).

The timeline of clinical ECT is illustrated in *Figure **26***.

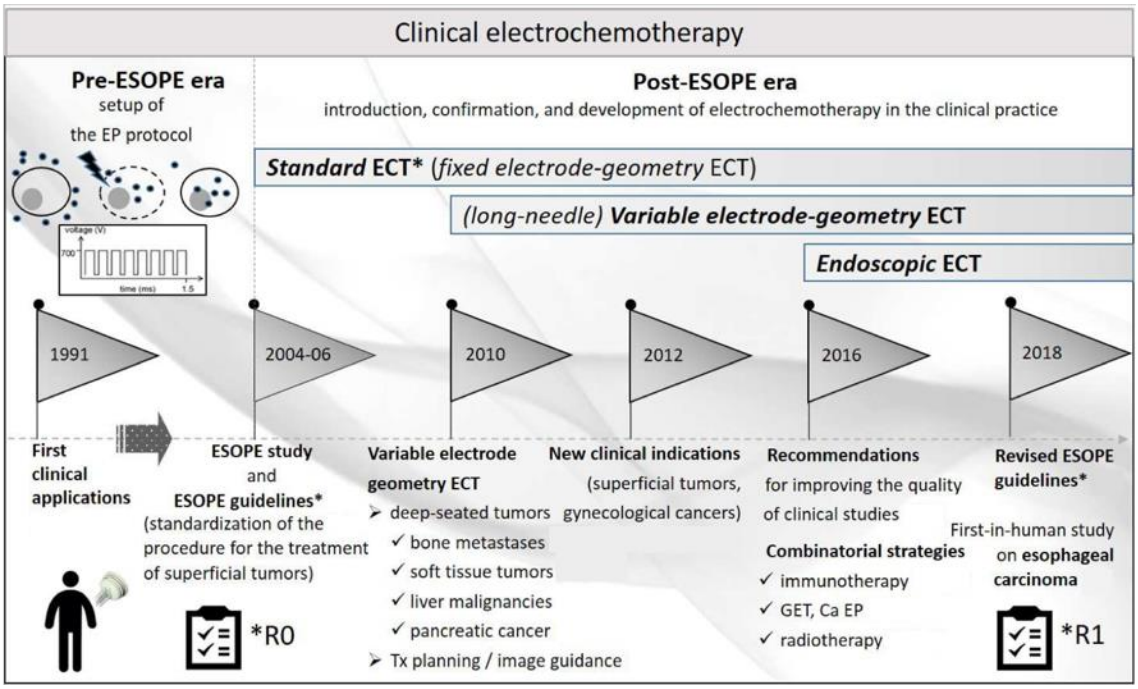

Figure 26| Timeline of clinical electrochemotherapy
Figure adapted from (Campana, 2019a).

3.3 Plasma oncology

3.3.1 The rise of a new physicochemical source for cancer therapy

In the past decade, the most important field of investigation of NTP for medicine is the application in cancer treatment. The anti-cancer potential of NTP was first reported by Fridman and colleagues in 2007 via their *in vitro* study demonstrating the selective induction of apoptotic in melanoma skin cell lines treated with FE-DBD, suggesting a local and tumour-specific up-regulation of the systemic immune response by NTP (Fridman *et al.*, 2007). Ten years later, the first clinical trial as proof of concept for NTP treatment of actinic keratoses (*in situ* squamous cell carcinomas of the skin), achieved encouraging results in five enrolled patients (Friedman *et al.*, 2017). NTP has open the door to palliative care of patients whose tumour ulcerations was infected. In some particular cases, also transient tumour remission occurred (Metelmann *et al.*, 2015., Metelmann *et al.*, 2018a; Schuster *et al.*, 2016). NTP is also used in human clinics in conjunction with surgery to treat the margins of the surgical site to destroy residual cells that

may not have been removed during surgical intervention (Metelmann *et al.*, 2018b). Plasma oncology could be considered as the newest application of NTP in biomedical research.

Along with fundamental research and pre-clinical investigations in plasma oncology, this recent field of applications of NTP has already found its place in clinics, mostly in Germany and garnered raising interest from investigators for oncology. An example of the very first clinical application of direct NTP treatment in a patient with a locally advanced tumour contaminated with bacteria is shown in *Figure **27*** (Metelmann, 2018a). This direct NTP treatment reduced microbial load and the resulting typical fetid odour from infected lesions.

Figure 27| Photograph of the progress of a palliative care employing NTP treatment

Plasma treatment with the kINPen® in a 56-year-old male patient having locally advanced squamous cell carcinoma of the oropharynx with tumour ulceration contaminated with bacteria. The kINPen® MED was used every 2 to 3 days with an exposure protocol of 1 minute/cm² treatment, with the jet moved across the tumour surface with a 1 cm separation between the jet and the surface. This NTP treatment, without reported plasma-induced side effects, induced tumour reduction and significantly improved the tumour decontamination, while no lasting remission nor cure could be expected by surgery, radiation or chemotherapy (Metelmann, 2018a).

To date, there are four scientifically based plasma medical devices available on the market for clinical utilisation, with European Conformity (CE) certification as medical devices class IIa according to the European Council Directive 93/42/EEC (Metelmann, 2018b; Privat-Maldonado, 2019):

- kINPen MED® (developed by the Institute of Plasma Physics (INP) and manufactured at Neoplas tools GmbH (Greifswald, DE)): the first CE-marked NTP jet for the treatment of chronic wounds as well as pathogen-induced diseases of the skin, skin appendages, extremities and body. This Argon plasma jet is generated by an RF powered (1 MHz) maximum power of 8 W (110/230 V, 50/60 Hz).
- PlasmaDerm® (CINOGY GmbH, Duderstadt, DE) and PlasmaCare® (terraplasma medical GmbH, Garching, Germany): atmospheric air-driven DBD based on NTP technology which received CE approval for (chronic) wound-healing disorders such as acute wounds, venous and arterial ulcers, pressure sores, and the diabetic foot

syndrome. The novel CE-marked PlasmaCare® is a hand-held, and battery-driven plasma device.

- SteriPlas®: a microwave (2.45 GHz) powered Ar-plasma torch designed and manufactured at ADTEC Europe Ltd., Hounslow, UK in compliance with internationally recognised ISO13485 quality management system

Ongoing clinical trials using those CE-marked plasma devices for dermatology are reported in the review of (Privat-Maldonado, 2019)

To date, NTP technology used in human oncology consists of the direct application of the plasma for palliative care with a few anti-cancer effects reported. This direct NTP treatment remains the strategy of NTP in plasma oncology. Thus, the following sections will **exclusively discuss** the mechanisms and applications of NTP technology in **pre-clinical investigations** (**plasma oncology**) for the potential clinical practice and current challenges.

3.3.2 Mechanisms of biological action of NTP on cancer cells

As mentioned above, from killing bacteria to destroying cancer cells, NTP has emerged in the last twenty-five years as a novel and promising therapy for wound and skin decontamination, promoting wound healing, and controlling wound-resident multi-drug resistant bacteria, dental and cosmetic applications and cancer remission. Many studies are underway worldwide with rapid progress in basic research and in developing useful plasma devices for clinical purposes. Mechanisms coupling the physics and chemistry of NTP to medically- relevant biochemistry and biology are beginning to be understood but much remains to be explored.

It is known that the NTP generated reactive species first interact with the cell membrane, chemically modifying (*e.g.*, oxidising) its lipids within the phospholipid bilayer. The implication of RONS generated by NTP treatment has long been demonstrated as potential anti-cancer agents. One of the first *in vitro* studies of NTP to generate abundant ROS that induced DNA damages in two human cancer cell lines was conducted at the GREMI (Orléans, France) (Vandamme *et al.*, 2012). The cytotoxic effect of RONS generated by NTP treatment, as mentioned in section 1.3.2, is in principle attributed by other recent studies to the **intracellular redox homeostasis** (Graves, 2012b; Privat-Maldonado, 2019; Von Woedtke, 2019; Wolff *et al.*, 2019). Indeed, redox adaptation in cancer development and drug resistance has been studied

(see the complete review of Trachootham *et al.*, 2009 describing the cancer redox biology, which includes cell proliferation and angiogenesis).

The vicious cycle of ROS stress in cancer development and progression is described in *Figure **28a***. Generated from extracellular or intracellular sources, these reactive species, especially ROS, function as a double-edged sword. A moderate increase of ROS may promote cell proliferation and survival, but when reaching the **toxic threshold** (dashed line in the figure), ROS may overwhelm the cell antioxidant capacity and thus trigger cell death. Under physiological conditions, non-cancerous cells maintain redox homeostasis with a low level of basal ROS by controlling the balance between ROS generation (pro-oxidants) and elimination (antioxidant capacity). This balance ensures tolerance of a certain level of exogenous ROS stress by non-cancerous cells, owing to their "reserve" antioxidant capacity, which can be mobilised to prevent the ROS level from reaching the cytotoxic (cell-death) threshold. On the contrary, the increase in ROS generated from metabolic abnormalities and oncogenic signalling in cancer cells may trigger a redox adaptation response, leading to an upregulation of cell antioxidant capacity and a shift of redox dynamics with high ROS generation and elimination. As a result, **cancer cells would be more dependent on the antioxidant system and more vulnerable to further oxidative stress induced by exogenous ROS. They could** lose their viability if the ROS level surpasses the cytotoxic threshold (*Figure **28b***, red bar) (Trachootham, 2009). Those exogenous ROS can be ROS-generating agents or compounds that inhibit the antioxidant system or **ROS generated by an NTP treatment**.

Some cellular pathways could explain those effects in response to ROS stress. ROS can cause DNA damage, activating wild-type p53 in normal cells and triggering stress responses and DNA repair to eliminate the ROS-mediated damage to genetic materials. Contrariwise, ROS-mediated DNA damage would accumulate in cancer cells with defective p53 due to a compromised DNA repair function. The malfunctioning p53 in cancer cells would promote genomic instability leading to activation of oncogenes, aberrant metabolic stress, mitochondrial dysfunction and a decrease in antioxidants. These events can further **increase ROS levels, promoting more DNA damage and genetic instability**.

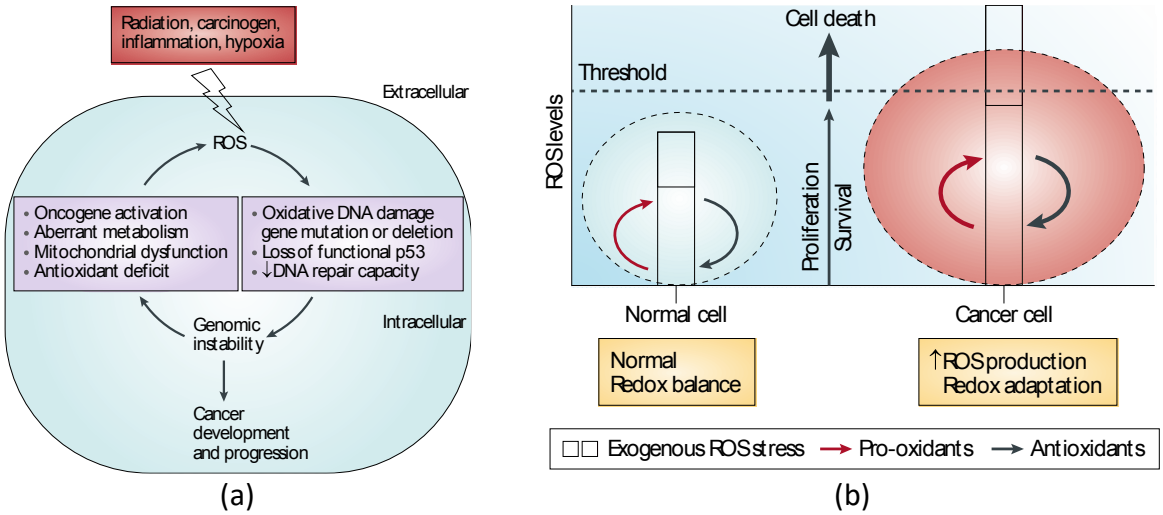

Figure 28| Cancer redox biology: a biological basis for therapeutic selectivity

(**a**) The vicious cycle of ROS stress in cancer development and progression. (**b**) The double-edged sword ROS. (Trachootham, 2009)

Almost all studies investigating the anti-cancer effects of NTP treatment attributed the observed effects as cell-line dependent. Alongside yet unknown mechanisms, the adaptative stress response of specific cancer cells under persistent ROS stress (*Figure **29***) may explain the different observed results of NTP within the other studies (or cell lines?).

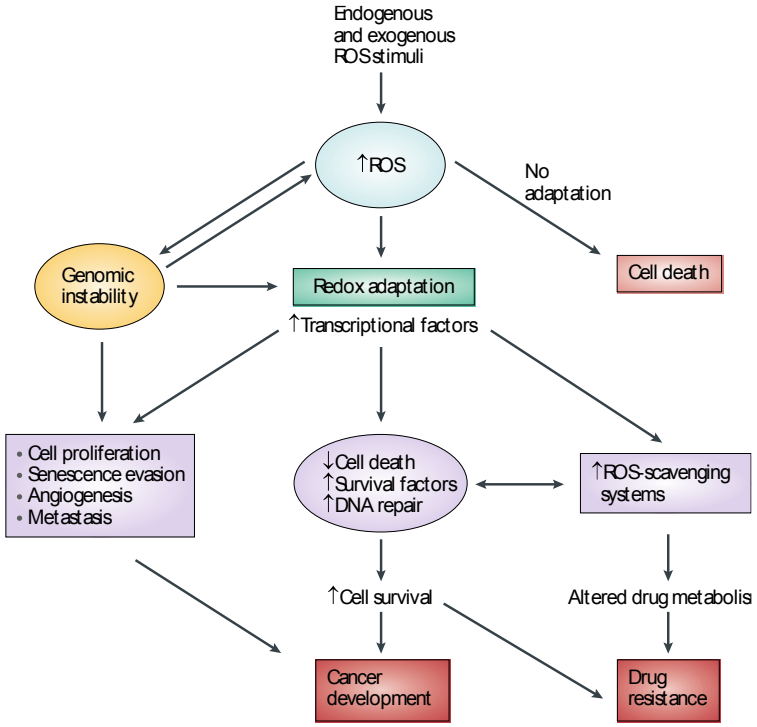

Figure 29| Redox adaptation in cancer development and drug resistance

Severe accumulation of cellular ROS under various endogenous and exogenous stress stimuli may induce lethal damage in cells with inadequate stress responses or adaptation. Furthermore, the increase in glutathione during adaptation can enhance the export of certain anticancer drugs and their inactivation. Together with enhanced cell survival, this altered drug metabolism may render cancer cells more resistant to chemotherapeutic agents (Trachootham, 2009).

The research group PLASMANT (Antwerp, Belgium), lead by Dr A. Bogaerts, has performed several **MD simulations** to understand and explain the effect of NTP treatment on cancer cells. Firstly, Yan *et al.* proposed a mechanism for the possible selectivity of ROS towards cancer cells based on aquaporins (AQPs), *i.e.*, the only *in vitro* verified H_2O_2 channels present at the cell membrane of cancer cells (Yan *et al.*, 2015). They found that after the NTP treatment, NTP-generated H_2O_2 species diffuse into cancer cells significantly faster than in normal homologous cells, resulting in a significant rise of ROS in cancer cells compared with normal cells. Indeed, with the diameter of the pore varied amongst different AQPs, these intrinsic membrane proteins are known to facilitate the transport of free RONS and other small molecules, including carbon dioxide, nitrogen monoxide, ammonia, urea, and glycerol (Kruse *et al.*, 2006). Besides, AQPs 1, 3, and 8 are demonstrated to be involved in the transport of H_2O_2 in mammalian cells (Bienert *et al.*, 2007; Wang *et al.*, 2020). Yet several AQPs have been reported as more abundant at the cell membrane in cancer cells than in non-cancerous cells (Verkman *et al.*, 2008), and the rise of intracellular RONS contributed to an increased sensitivity of these cells to NTP treatment.

Besides the expression of AQPs, the diffusion of free radicals is also dependent on the amount of cholesterol in the plasma membrane. Within the same research group, the MD simulation performed by Van der Paal *et al.* predicted that the lipid order in a phospholipid bilayer decreases upon the addition of lipid peroxidation products, *i.e.*, pore formation occurs when all phospholipids are oxidised (Van der Paal *et al.*, 2016) – what would explain the cell membrane permeabilisation observed during (and after) NTP treatment. They also found that **cholesterol** can protect oxidised membranes against pore formation. Cancer cells have a significantly lower concentration of cholesterol in their plasma membrane (*ca.* 2-fold lower) than that in the phospholipid bilayer of their non-tumorigenic counterparts (Shinitzky, 1984; van Blitterswijk *et al.*, 1982); they will be more vulnerable to the consequence of lipid peroxidation. These researchers also demonstrated the synergistic effect of electric field and lipid oxidation on the permeability of cell membranes (Yusupov, 2017) – effects that have also been observed by our group, employing MD simulations, for electroporating fields that target oxidatively damaged areas in the plasma membrane (Vernier, 2009), as mentioned above (see **section 1.2.2**). Therefore, this molecular-level insight is crucial for selectively treating tumours with NTP technology and electroporation-based technology.

The PLASMANT research group also recently investigated the permeabilisation of RONS across native and oxidised phospholipid bilayers. Their MD simulations revealed that the

assessed RNS (NO, NO_2, N_2O_4) and O_3 could permeate more easily through both native and oxidised membranes in comparison to hydrophilic ROS (OH, HO_2, H_2O_2) (Razzokov *et al.*, 2018). More *in vitro* and *in vivo* studies and investigations of the plasma chemistry are needed to have relevant concluding remarks with those previous MD simulations.

Amongst the RNS, it has been identified for at least a decade that nitrite anion (NO_2^-) can act therapeutically, most probably as a precursor source of nitric oxide (Vitturi *et al.*, 2011). A recent study assumes that whether RONS have a signal-transducing or damaging effect is primarily defined by their quality, being primary or secondary RONS, and only secondly by their quantity (Weidinger *et al.*, 2015). Girard and colleagues identified *in vitro* the three long-lived RONS, the **H_2O_2**, **NO_2^-** and **NO_3^-** as the main reactive species in plasma-treated PBS responsible for the *in vitro* anti-cancer effects (Girard *et al.*, 2016).

*Figure **30*** highlights recent understanding of molecular mechanisms involved in the effectiveness of NTP in cancer cells could be resumed in eight major steps (Semmler *et al.*, 2020): (**1**) While minimal amounts of RONS can diffuse through the cell plasma membrane (PM), an increase expression of different aquaporins (AQ) in cancer cells facilitates the intracellular transition of RONS; (**2**) In parallel, lipid peroxidation of the PM by free radicals leads to pore formation that further facilitates the diffusion of RONS into the cell. As discussed above, this effect may be enhanced in cancer cells due to reduced concentration of cholesterol in the PM; (**3**) Increased intracellular RONS interfere with calcium signalling (*e.g.*, through interaction with inositol trisphosphate receptor [IP3-RR] and ryanoid receptor [RR]) resulting in increased calcium influx into cytosol; (**4**) Besides, RONS induced endoplasmic reticulum (ER) stress leads to a calcium influx into mitochondria, reducing the membrane potential ($\Delta\psi_O$), thus inducing mitochondria-dependent apoptosis; (**5**) NTP induced DNA double-strand breaks (DSB) – an effect that may not directly due to NTP but rather as a consequence of NTP induced apoptosis. DNA damage response includes activation of ATM, H2AX, p53, and p73; (**6**) Increased intracellular levels of RONS overwhelm the cell antioxidant system, hence reduce its protective capacity against oxidative stress; (**7**) The reduction of cell adhesion, migration, and invasion after NTP treatment may be explained by the reduction of integrins expression; (**8**) Notwithstanding the reported necrosis, apoptosis, and senescence induced processes as consequences of NTP treatment, little is known about their underlying pathways triggered by NTP treatment.

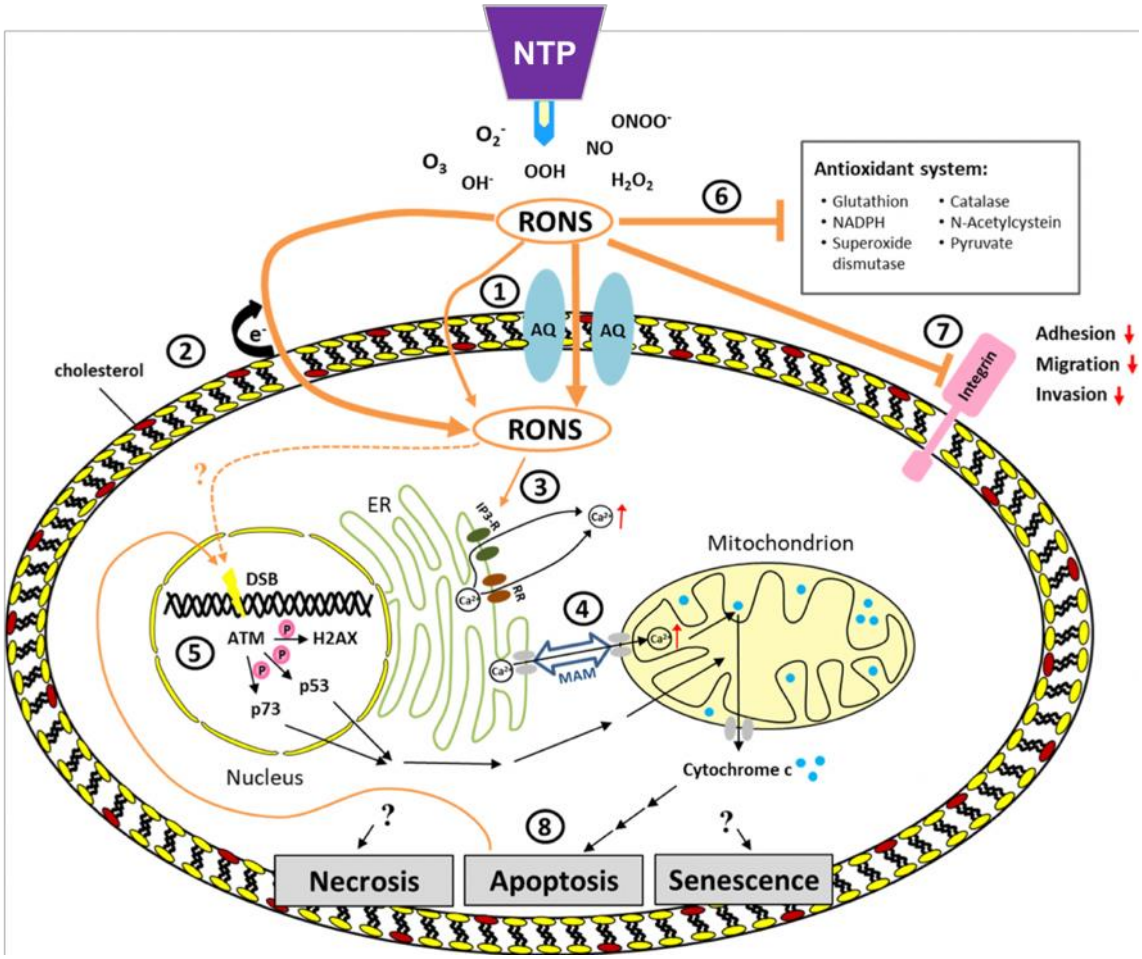

Figure 30| Overview of the current understanding of molecular mechanisms involved in the efficacy of non-thermal plasmas in cancer cells

ATM: Ataxia-telangiectasia-mutated protein, H2AX: a histone H2A variant, MAM: mitochondria-associated ER membranes, NTP: non-thermal plasma. Scheme adapted from (Semmler, 2020)

Nonetheless, to the best of my knowledge, the underlying mechanisms that decide which process of growth arrest or cell death will drive the fate of the cell as a consequence of NTP treatment, either by direct treatment or via the plasma-treated liquids, are not yet elucidated. Further details on the complexity of the cellular responses to NTP treatment can be found in recent review articles by (Bauer, 2016; Graves, 2014; Privat-Maldonado, 2019; Trachootham, 2009). Other exciting reviews such as (Lu, 2016), explain the generation, transport, and biological effects of RONS produced in NTP treatment. The review of (Semmler, 2020) reports the molecular mechanisms of NTP in oncology, as partially above discussed.

3.3.3 Strategies in pre-clinical NTP treatment

There are two basic strategies in plasma oncology research, schematically illustrated in *Figure **31***:

- **Direct treatment** on *in vitro* cells, *in vivo* subcutaneous tumours or human living tissues. Strong electric fields, radiation and RONS come into play in the direct plasma treatment strategy.
- **Indirect treatment** on liquids (**plasma-treated liquids**) will be used *in vitro* or administered in tumours for animal studies (*e.g.,* in the form of a subcutaneous injection or intraperitoneal injection, depending on the study's design and model).

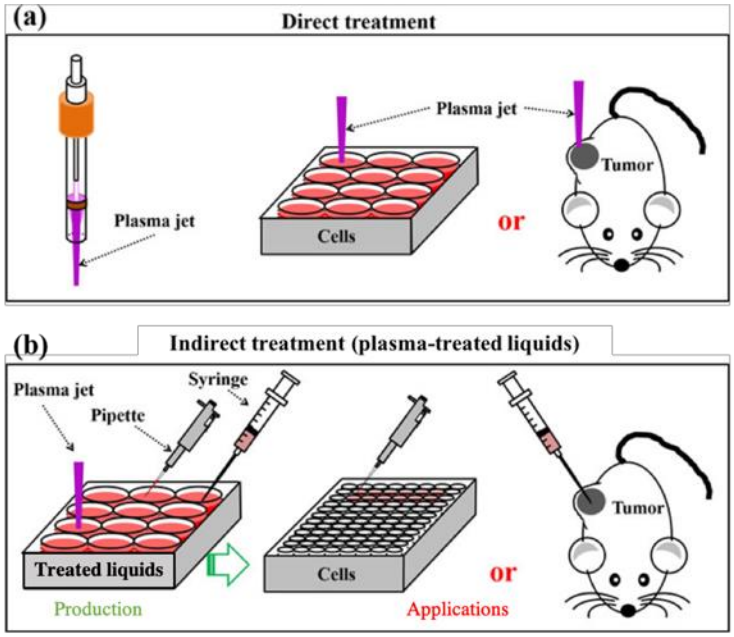

Figure 31| Two basic strategies in plasma oncology (using a plasma jet source)

(**a**) A direct NTP treatment of cancer cells *in vitro* or subcutaneous tumours *in vivo*. (**b**) An indirect NTP approach with the treatment of liquids will be used *in vitro* on cells or administered in tumours *in vivo*. Schematic illustration adapted from (Yan, 2017)

Being directly in the scope of this thesis, the indirect plasma treatment strategy will be emphasised in the following sections. The *in vitro* and *in vivo* effects resulting from different major studies of the last decade using indirect strategy will be specially summarised in *Table **3*** of **section 3.3.4** below.

3.3.3.1 Direct treatment

Yonson and colleagues were, in 2006, the first to investigate the promotion of cell adhesion and proliferation by modifying the surface with a miniature glow discharge plasma torch (Yonson *et al.*, 2006). They studied those effects on a human hepatocellular carcinoma (HepG2), then other adherent and non-adherent cells lines such as melanoma, glioblastoma, and leukaemia cells were used by other investigators (Arndt *et al.*, 2013a; Fridman, 2007; Keidar *et al.*, 2011; Vandamme *et al.*, 2010). As mentioned previously, Vandamme and colleagues from the GREMI not only investigated cancer cell lines but also in an *in vivo* tumour model (Vandamme, 2012). Their human glioblastoma U87MG bearing nude mice showed a reduction of bioluminescence and tumour volume after treatment with an FE-DBD, as compared to

untreated mice. Induction of apoptosis was observed together with an accumulation of cells in their S phase, suggesting an arrest of tumour proliferation. Especially, apoptosis was also observed in the tumour site not being directly exposed to the plasma.

Following those pioneering investigations, other *in vitro* studies demonstrated the cytotoxic effects of direct NTP treatment on cancer cells. It has been shown that DBD plasma exposed to melanoma cells at doses that did not induce necrosis, induced apoptosis via the production of intracellular ROS (Sensenig *et al.*, 2011). The GREMI group displayed *in vivo* effects of an NTP treatment, alone or in combination with the anti-cancer drug Gemcitabine, in an MIA PaCa2-luc human pancreatic carcinoma transplanted in nude mice (*Figure **32***) (Brullé *et al.*, 2012), being the first research group successfully obtaining *in vivo* anti-tumour effects of NTP.

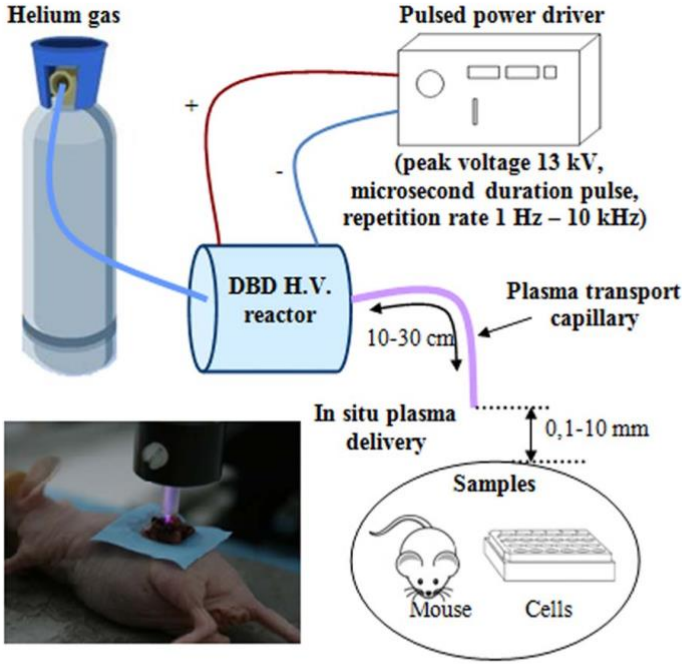

Figure 32| Example of an *in vivo* direct NTP treatment of a tumour

Schematics of a fibered plasma (Plasma Gun) setup (upper panel) used to treat human pancreatic carcinoma transplanted in nude mice (lower panel), in combination with gemcitabine, from the first published *in vivo* anti-cancer study using direct NTP combined with a chemotherapeutic agent (Brullé, 2012).

Another effect of NTP treatment, the induction of immunogenic cell death (ICD) has also been reported *in vitro* using direct plasma treatment strategy (Lin *et al.*, 2017., Lin *et al.*, 2018; Miller *et al.*, 2016) but also by the indirect strategy (see *Table **3***). Direct plasma treatment was also used to permeabilise the HeLa cell membrane *e.g.,* using a plasma torch (Leduc *et al.*, 2009) or the plasma jet (Vijayarangan *et al.*, 2020).

To date, *in vivo* studies on small animals with direct plasma treatments often employed plasma jets exposed directly to tumours. As this is not in the scope of this thesis, those studies will not be reported but overall, the induction of apoptosis in the tumour tissue and/or the

increase in the ratio of the apoptotic to anti-apoptotic proteins expression has usually been observed.

3.3.3.2 Indirect treatment

The most commonly used liquids for indirect NTP treatment are cell culture media saline solutions, buffered saline solutions (*e.g.,* phosphate buffered solution or PBS), Ringer's lactate solution or water. The resulting plasma-treated liquids (PTL) were adopted by NTP scientific community under different terms: plasma-irradiated medium, plasma-activated liquid (PAL), plasma-activated (PAM) or plasma-treated medium (PTM), plasma-activated PBS (P-A PBS) or plasma-treated PBS (P-T PBS or pPBS). Until now, no consensus has been reached yet. **Our group and collaborators employed the term "plasma-treated liquids" or PTL as referred to all types of liquids being used to be treated with NTP.**

As illustrated in *Figure **31b***, the properties or at least especially the long-lived RONS of the NTP can be transferred to a liquid which can be stored, transported and used in *in vitro* as well as *in vivo* studies (Jablonowski *et al.*, 2015; Yan *et al.*, 2014). Those plasma-treated liquids have been demonstrated as inducers of physiological outputs in cells and tissues. The anti-cancer potential of the PTLs has first been reported using cell culture media, such as DMEM or RPMI. However, the use of these complex cell culture media has raised some issues. Indeed, their composition, rich in amino acids, vitamins, sugars and inorganic salts, has a strong influence on the reactive species generated in the liquids and their stability. One of the standard components of cell culture media is the pyruvate, which is the output of the glycolysis, has been known as a potent antioxidant and has been demonstrated to be a ROS scavenger (Desagher *et al.*, 1997; Jagtap *et al.*, 2003; Tauffenberger *et al.*, 2019). Several studies highlighted that pyruvate mitigated the effectiveness of PTLs on cells by inducing oxidative stress resistance, thus reducing the cytotoxicity of PTLs treatment (Bergemann *et al.*, 2019; Tornin *et al.*, 2019). Some studies also demonstrated that culture media components such as cysteine, tryptophan, phenylalanine or tyrosine were the main targets of effective RONS present in the PTL, yet the degradation of those amino acids due to NTP would impact the stability of the RONS (Chauvin *et al.*, 2017; Yan, 2015).

Therefore, other liquids with a more straightforward composition (without RONS scavengers), such as saline solutions (isotonic NaCl or Ringer's lactate solution (RLS)), buffered saline solution (PBS) or water, were proposed in various studies as more relevant liquids to

generate PTL, promoting an easier transition to clinical practice. *Table **3*** depicts the studies, models, cellular mechanisms, and effects of plasma-treated liquids reported in some major *in vitro* and *in vivo* studies of the past ten years, either as monotherapy or in combination with molecules, cytotoxic drugs, or other therapies.

Study; models	Cell lines	Plasma device; Plasma-treated liquids	Cellular effects and molecular mechanisms	References
in vitro; adherent cells	U251SP human glioblastoma	Ar plasma jet; DMEM	Caspase-dependant apoptosis; Caspase 3/7 cleavage; ↘ phosphorylation kinases pathways PI3K/AKT/mTOR ↘ PDK1	(Tanaka *et al.*, 2011., Tanaka *et al.*, 2012)
in vitro; adherent cells ***in vivo***; i.t. PAM at 24h post-inoculation	NOS2 and NOS3 (chronic resistance to paclitaxel and cisplatin, respectively)	Ar plasma jet; RPMI-1640	↘ cell viability ↘ NOS2 cell - inoculated tumour by 66%	(Utsumi *et al.*, 2013)
in vitro; adherent cells	Human carcinoma (lung epithelial A549, liver HepG2 and breast MCF7), and neuroblastoma SH-SY5Y	Ar plasma jet; DMEM stored at -80°C	Caspase-dependent apoptosis; ↗ TRMP2 ↗ mitochondrial stress Zn^{2+}-dependant cell death ↗ Zn^{2+}, ↘ NAD^{+}, ↘ ATP	(Adachi *et al.*, 2015; Hara *et al.*, 2015., Hara *et al.*, 2017)
in vitro; adherent cells ***in vivo***; i.t. PAM at 24h post-xenograft	Human pancreatic cancer cell lines (PANC-1, Capan-2, BxPC-3 and MIA PaCa-2)	Ar plasma jet; RPMI-1640	Caspase-dependent apoptosis; Caspase 3/7 cleavage; ↘ cell proliferation ↘ tumour volume	(Hattori *et al.*, 2015)
in vitro; adherent cells	Human ovarian carcinomas (OVCAR-3 TOV21G, ES-2 and NOS2)	Ar plasma jet; RPMI-1640	Cell shrinking, blebbing, and detachment; ↘ cell proliferation TOV21G and ES-2 are more sensitive (mesenchymal phenotype)	(Utsumi *et al.*, 2016)
in vitro; adherent cells	human glioblastoma (U251SP) and mammary epithelial (MCF10A) cells	Ar plasma jet; DMEM w/ or w/o FBS and P/S	Apoptotic cell death for U251SP but not for MCF10A; Antitumour effect was not due solely to the synergism of H_2O_2 and NO_2^- (that was incubation-time dependent)	(Kurake *et al.*, 2016)

in vitro; spheroids	Human colorectal carcinoma cells HCT 116	He plasma jet; DMEM stored at -80°C & +4°C	↘ spheroid growth DNA damage (peripheral spheroid cells)	(Judée *et al.*, 2016)
in vitro; suspended cells	Human cervical carcinoma HeLa and Chinese hamster CHO-K1	HV DBD; DMEM (direct ttt) and PBS and FBS (indirect ttt)	↘ cell re-adhesion and cell growth; PBS more cytotoxic than DMEM ↗ mutagenic potential of FBS in long-term exposure	(Boehm *et al.*, 2016)
in vitro; adherent cells	Human melanoma (A375, A2058), lung adenocarcinoma epithelial (A549) and osteosarcoma (MG63, SAOS-2, HOS) cell lines	He plasma jet; DMEM stored at +4°C	Caspase-dependent apoptosis; Activate intracellular ROS generation and mitochondrial ROS accumulation; Excessive mitochondrial fragmentation and clustering; ↗ Drp1 ↘ cell viability	(Saito *et al.*, 2016)
in vitro; adherent cells	Human skin fibroblasts (NHSF), human colon cancer (HCT116) and human melanoma (Lu1205) cell lines	He plasma micro-jet; PBS (Ca^{2+}/Mg^{2+})	H_2O_2 was not toxic (effect cell-type dependent); Synergism of H_2O_2 and NO_2^- (but not NO_3^-): ↘ cell viability; He plasma jet interaction with ambient air was required to generate NO_2^- and NO_3^-	(Girard, 2016)
in vitro; adherent cells ***in vivo***; subcutaneous tumour (i.t. PAM at 24h post-inoculation, repeated ttt)	Human glioblastoma U251SP, mammary epithelial MCF10A, cervical cancer SiHa and ovarian cancer SK-OV-3 cells	Ar plasma jet; RLS	↘ tumour volume Only lactate exhibited anti-tumour effects through activation by NTP	(Tanaka *et al.*, 2016)
in vitro; suspended cells	Human lymphoplasmacytic lymphoma (LPL) MWCL-1 and RPCI-WM1	He plasma jet; IMDM	↗ cellular differentiation ↗ human PRDM1 α ↘ tumourigenic population	(Wada *et al.*, 2017)
in vitro; adherent cells	Human oral squamous cell line SCC15	Air plasma jet; DMEM	↘ cell viability Transcriptomic analysis p53 pathway, hypoxia pathway	(Shi *et al.*, 2017)
in vitro; adherent cells ***in vivo;*** i.p. PAM at D1 to 4, then D8 post post-xenografts	SC-2-NU, AGS, and enhanced GFP-tagged GCIY (GCIY-EGFP) human gastric cancer cells	Ar plasma jet; RPMI	↘ cell adhesion and migration ↘ tumour burden	(Takeda *et al.*, 2017)

in vitro; adherent cells ***in vivo;*** i.p. PAM 15min post-inoculation (repeat 3 days)	Human ovarian carcinomas (ES2 and SKOV-3) and foetal lung fibroblasts WI-38	Ar plasma jet; RPMI	↘ cancer cell motility ↘ MMP-9 ↘ tumour burden ↘ metastatic nodules by 60%	(Nakamura *et al.*, 2017)
in vitro; adherent cells	human GBM cell lines (U87, U251 and LN229)	kINPen®; PBS; catalase	Anti-cancer capacity of pPBS: H_2O_2 is a more important than NO_2^-; pPBS more stable than other PTL; not same anticancer effect w/ PBS supplemented with H_2O_2 and/or NO_2^- or w/ pPBS	(Van Boxem *et al.*, 2017)
In vitro; suspended cells; combined ttt w/ BLM, paclitaxel or dacarbazin	Mouse melanoma (B16), human melanoma (A375) and glioblastoma (A172)	DBD PlasmaDerm® PBS	↘ cell viability (most prominent with the combined plasma-treated PBS and BLM)	(Daeschlein *et al.*, 2018)
in vitro; spheroids	Human head and neck carcinomas (FaDu)	He plasma jet; DMEM	Detachment of peripheral spheroid cells since the first day after 1 ttt, followed by a rapid spheroids' regrowth (more than the Ctrl); ↘ cell growth after 4 successive ttt	(Chauvin *et al.*, 2018)
in vitro; adherent cells ***in vivo***; i.t. PAM at 24h post-xenograft	Human pancreatic cancer cell lines Capan-2 and BxPC-2	Ar plasma jet; RLS	Caspase-dependant apoptosis DNA fragmentation ↘ cell proliferation ↘ tumour burden ↘ metastatic nodules	(Sato *et al.*, 2018)
in vitro; adherent cells ***in vivo***; i.p. PAM at D0, 1, 2, 6, 7, 8 post-xenografts	Human endometrial carcinoma HEC-1 and gastric cancer GCIY cells	Ar plasma jet; DMEM	↘ cell viability (better with PAM + *cis*-Pt than only PAM or *cis*-Pt) Caspase 3 cleavage; ↘ ALDH Anticancer effects both *in vitro* and *in vivo*	(Ikeda *et al.*, 2018)
in vivo; subcutaneous tumour (at 7 days post inoculation: i.t. PAM w/ or w/o i.p. cyclo-phosphamide)	B16-F10 murine metastatic melanoma	He plasma jet; DMEM	↘ tumour growth ↗ BAX/BCL2, apoptosis Direct NTP treatment was more efficiency than indirect strategy; PAM + drug = ↗ cell death	(Saadati *et al.*, 2018)
in vitro; adherent cells	U251SP human glioblastoma	Ar plasma jet; DMEM	Metabolomic analysis ↗ glycolysis ↘ pentose phosphate pathway	(Kurake *et al.*, 2019)

in vitro; adherent cells & spheroids ***in vivo;*** i.p. PAM at 48h post-xenografts	*in vitro*: Murine MC38 colon and PDA6606 pancreatic cancer cells *in vivo*: CT26 colorectal cancer cells	kINPen® plasma jet; PBS	Cell cycle arrest; Actin network reorganisation; ↗ actin protrusion dynamics ↗ CRT, HSP70 and HMGB1 ↗ ICD ↘ tumour burden ↗ i.t. macrophages and T lymphocytes	(Freund *et al.*, 2019)
in vitro; spheroids	Green fluorescent protein (GFP) transduced human colorectal carcinoma cells HCT 116-GFP	He plasma jet; PBS; combined ttt with PEFs	Early DNA damage; Caspases 3/7 activation; Alteration of cell junctions and cytoskeleton; ↘ spheroid growth	(Griseti *et al.*, 2019)
in vitro; adherent cells	Human glioblastoma U251SP cells derived	Ar plasma jet; DMEM and RLS	↘ phosphorylation of AKT; DMEM induces more intracellular ROS than LRS	(Tanaka *et al.*, 2019)
in vitro; adherent cells	Human immune-suppressive PSC (hPSC21, hPSC128 and RLT-PSC) and pancreatic cancer PCC (MIA-Paca-2, PANC-1, BxPC3, Capan-2)	kINPen® plasma jet; PBS	↘ cell viability Co-culture with DC: ↗TNF-α and IFN-γ ↘ TGF-β PCCs: ↗ ICD (expressed and released damage-associated molecular patterns); PSCs: ↘ immunosuppressive tumour microenvironment.	(Van Loenhout *et al.*, 2019)
in vitro; adherent cells	Endometrial cancer cell lines AMEC, HEC50, ISHIKAWA, and RL95	Ar plasma jet; RPMI-1640	↗ autophagic cell death & late apoptotic cells (time and concentration-dependant); ↘ phosphorylation of mTOR and AKT	(Yoshikawa *et al.*, 2020)
in vitro; spheroids	Human colorectal HCT 116 and ovarian carcinoma SKOV-3 cells	He plasma jet; PBS, NaCl 0.9%	↗ cell death ↘ spheroid growth	(Griseti *et al.*, 2020)

Table 3*| Summary of the in vitro and in vivo cellular mechanisms and effects of plasma-treated liquids from studies of the past ten years*

Legend: ↗ activation or enhancement; ↘ inhibition or reduction; ***ALDH****: aldehyde dehydrogenase;* ***AKT/PI3K/mTOR pathway****: cell cycle progression, prevention of apoptosis pathway;* ***ATP****: adenosine triphosphate;* ***Ar****: argon;* ***BAX/BCL2****: apoptotic regulators;* ***CRT****: calreticulin;* ***DBD****: dielectric barrier discharge;* ***DCs****: dendritic cells ;* ***DMEM****: Dulbecco's Modified Eagle's Medium;* ***Drp1****: dynamin-related protein 1;* ***GFP****: green fluorescent protein;* ***He****: helium;* ***HMGB1****: high-mobility group protein 1 and amphoterin;* ***HSP70****: 70kDa heat shock proteins;* ***HV****: high voltage;* ***ICD****: immunogenic cell death;* ***IMDM****: Iscove's Modified Dulbecco's Medium;* ***i.p.****: intraperitoneal;* ***i.t****.: intratumoural;* ***MMP-9****: matrix metallopeptidase 9 (extracellular matrix degradation);* ***NAD⁺****: nicotinamide adenine dinucleotide;* ***PAM****: plasma-activated medium;* ***PEF****: pulsed electric field;* ***P/S****: penicillin/streptomycin;* ***RLS****: Ringer's lactate solution;* ***RPMI****: Roswell Park Memorial Institute medium;* ***PDK1****: 3-phosphoinositide-dependent protein kinase-1;* ***PRDM1 α****: PR domain zinc finger protein 1 (a repressor of beta-interferon (β-IFN) gene expression and a*

*tumour-suppressor); **PTL**: plasma-treated liquid; **TRPM2**: transient receptor potential cation channel, subfamily M, member 2; **ttt**: treatment; **w/ or w/o**: with or without.*

Those various aforementioned *in vitro* studies of plasma-treated liquids, together with a very few numbers of *in vivo* studies, presumed a common cytotoxicity mechanism mediated by RONS, and more specifically by hydrogen peroxide (H_2O_2), as H_2O_2 is the main component of long-lived RONS present in plasma-treated liquids with anti-cancer potential. As discussed in the previous section, very high concentrations of H_2O_2 in the cell induce exhaustion of its antioxidant mechanisms and, ultimately, its energy metabolism. However, the level of toxicity generated by the presence of H_2O_2 remains cell line-dependent. Most cancerous cell lines are affected by oxidative stress, yet some lines and study models show increased cell proliferation. The latter effect could be defended by the **redox adaptation** of cancer cells under persistent ROS stress, processes by which cancer cells maintain their redox homeostasis, as described above (see **section 3.3.2**). Henceforth, this stimulation of cancer development could eventually explain the lack of success *in vivo* investigations on the anti-cancer effectiveness of NTP treatment as **a single treatment** (especially those employing an indirect strategy).

Consequently, efforts have been allocated to combining NTP with other therapies, such as chemotherapy, to improve the treatment effectiveness, as presented by some studies in *Table **3***. Indeed, some studies claimed the efficacy of NTP treatment when an anti-cancer drug was combined. Also, since there is a synergistic effect between electric pulses and the lipid oxidation by ROS (see **section 3.3.2**), results of *in vitro* combining NTP and electric pulses have been reported (*Table **3***).

Nevertheless, there have been very few in vivo studies with positive antitumour effects for almost a decade of investigating anticancer therapy using NTP. Only nine *in vivo* studies (compared with about forty *in vitro* studies) reported anti-tumour results of plasma-treated liquids. Moreover, for all of those investigations, none to very few had similar treatment parameters, from the used plasma devices to the studied *in vivo* models and treatment protocols. As discussed in previous sections, besides the three CE marked plasma devices for clinical practice, all other plasma devices are in-lab-built. Despite their practical applications and reported anti-cancer effects, very inadequate to no physical, technical and biological description is fully detailed and reported.

Despite all the advantages above and limits of ECT and NTP in cancer treatment, there are, up to date, very few studies investigating the combination of those two therapies to outperform each monotherapy. At the beginning of this thesis, there was no *in vitro* study that examined the combination of ECT and indirect NTP, and only three years later, some studies investigating the combination of direct or indirect NTP with chemotherapy or PEFs or the combined chemotherapy + PEFs (thus ECT) have been published.

To the best of my knowledge, the only *in vivo* study undertaken to compare the anti-tumour effectiveness of ECT with direct NTP strategy was conducted by Daeschlein and colleagues in the B16 melanoma mouse model (Daeschlein *et al.*, 2013). By applying the plasma jet (APPJ) and DBD plasma sources directly to the tumour surface (when the tumour size reaches 8 mm Ø), they compare the effects of the NTP direct treatment with ECT alone or in combination with ECT. In both cases, NTP treatment was repeated daily for five days. ECT was performed with i.v. BLM at a field strength of 1000 V/cm using the Cliniporator® (IGEA, Carpi, Italy). When combined with ECT, a one-shot treatment, plasma treatment was subsequently applied until day 5. Their results showed that: both plasma sources as a single treatment displayed a significant delay of the tumour growth, which proved less effective than ECT alone; plasma jet combined with ECT significantly improved per cent mouse survival, with significant superiority compared with ECT.

3.3.4 Current challenges for research & development in plasma medicine

Plasma-treated liquids have broadened how NTP can be applied by providing a tool for cancer treatment, demonstrating their efficiency in various cancer cell lines eradication in different *in vitro* studies and in a few *in vivo* investigations. Unlike electrochemotherapy, an established anti-cancer treatment modality (established operating procedure, as described in **Chapter 1.2**), there are still current challenges for research and development in plasma medicine before achieving clinical practice.

The issues mentioned above regarding the reproducibility and relevance of *in vitro* and especially *in vivo* studies could be resolved, at least in a significant part, by establishing a better specification and systematisation of NTP devices for biomedical applications as regards clinical practice. Indeed, it might be convenient if plasma devices could be manufactured and used by considering the purpose of the application. Undeniably, the NTP devices used for treatment close to the medical target should be limited to a temperature below 40°C. In contrast, a

treatment that would require thermal damage should be performed with devices more comparable to the electrosurgical plasma devices, etc.

A further approach to improving plasma characterisation *in vitro* is identifying a technical target that is representative of the human body – the clinical target- and identifying plasma-target interactions and their effects on plasma characteristics. This issue was evoked last year by (Judée *et al.*, 2019), the same year of the publication of my first article, which in part deals with this issue, providing an excellent solution to experimentally deliver direct plasma treatment to models possessing the electrical characteristics of the human body. This article represents the first chapter of the results section.

RESEARCH HYPOTHESES AND OBJECTIVES

Although electrochemotherapy (**ECT**) is an established and standardised targeted anti-cancer treatment in human and veterinary medicine, given its nature, it still has some inherent drawbacks, including erythema, superficial epidermal erosion, muscle contraction and relative discomfort due to the application of intense pulsed electric fields (**PEFs**), thus the necessity of administrating myorelaxant and anaesthesia (local, loco-regional or general) (Yarmush, 2014). On the other hand, non-thermal plasma (**NTP**) and plasma-treated liquids give particular interest of their rich source of reactive oxygen and nitrogen species (**RONS**). The newest field of research and application of NTP in medicine, and one of the main foci of my thesis, is plasma oncology. Indeed, as introduced in state of the art, NTP being used either as direct therapy or as indirect therapy displays selective anti-cancer effects when allowing cell permeabilisation (Cramariuc *et al.*, 2008; Jinno *et al.*, 2016; Leduc, 2009; Sasaki *et al.*, 2016; Tanaka *et al.*, 2017a). One of the molecular mechanisms involved in the efficacy of NTP in oncology is lipid peroxidation by free radicals, which leads to pore formation in the cell membrane, hence facilitating the diffusion of RONS into the cell (***Figure 30***). Recent studies suggested possible synergy between PEFs and NTP on the permeability of cell membranes via lipid oxidation, an effect that has also been demonstrated using MD simulations (Yusupov, 2017). Since PEFs allow cell electropermeabilisation (Mir, 1988; Rols *et al.*, 2002; Vernier, 2009) and electric pulses (electroporating fields) target oxidatively damaged areas, if the plasma membranes are oxidised, they are more prone to become permeabilised when the cells are exposed to short and intense electric pulses.

To date, there are, to the best of our knowledge, only nine *in vivo* studies exploring the anti-tumour effects of plasma-treated liquids (see *Table **3***). Only recently, some pioneer studies are investigating the combination of NTP and µsPEFs in different *in vitro* cell models (Griseti, 2019; von Woedtke *et al.*, 2018; Wolff *et al.*, 2020) or for bacterial inactivation (Zhang *et al.*, 2014) or the combination of direct NTP with ECT *in vivo* (Daeschlein, 2013). Most of this knowledge was not yet published when this thesis was initiated. Because of the background of the team in the *in vitro* and *in vivo* cell electroporation, and because of the potential of

collaboration with two groups of experts in the NTP production and application, we sought to address hypothetical cumulative effects, maybe additive or synergistic responses of the combination of NTP and ECT via respective impact on the phospholipid bilayer of the cell membranes.

My thesis's objectives for three years of research were:

1) Study possible synergistic effects of µsPEFs (thus ECT) and NTP on the cell membrane permeabilisation (thus cytotoxicity)
2) Improve the outcome of ECT by:
    - Enhancing the electropermeabilisation level of the cell membrane
    - Reducing the dose of anti-cancer drugs (bleomycin)
    - or reducing the µsPEF amplitude without altering the electropermeabilisation effects
3) Develop quantitative and qualitative studies of the indirect plasma treatment via the studies of plasma-treated liquids (their pH and their stability over different storage conditions, the chemical analysis of long-lived RONS present in those plasma-treated liquids)
4) Enhance our understanding of the electroporation mechanisms

Thus, this thesis sought to improve electrochemotherapy (ECT) by employing non-thermal plasma (NTP) medicine. Antitumour ECT consists of the extraordinary sensitisation of the effect of certain anticancer drugs (in particular bleomycin, a typical example of molecules unable to enter the cell cytosol) by very short and local electrical pulses (8 pulses at a pulse length of 100 microseconds), delivered to the treated tumour nodules. These impulses transiently permeabilise the cells without killing them. ECT is particularly effective on treated tumour nodules and has very few side effects. Nevertheless, ECT is known to cause contractions and requires anaesthesia. It is essential to explore several methods (already demonstrated *in vitro*) to reduce these undesirable effects and make ECT more comfortable for the patient while always being effective. Therefore, we investigated *in vivo* the safety and efficiency of our NTP multijet device, then the *in vitro* enhancement of the cell membrane permeabilisation level when combining pPBS and µsPEFs at very low amplitude and finally, the *in vivo* anti-tumour effect of the combined treatment with pPBS and ECT on small animal, applying a field strength lower than that used in conventional ECT.

RESULTS

1 Characterisation of a novel NTP device for stable and reproducible applications in both pre-clinic and clinic

Some of the most critical problems in plasma medicine are plasma devices coupled electrically to targets, and different targets have different impedances (as termed "bio-impedances" of biological targets). Measurements of the biomedical effects of plasma on one type of system will partly depend on the different electrical properties of the targets, obscuring the differences in biological responses. Furthermore, results from various *in vitro* or *in vivo* tests will not be the same as applications on human targets.

To obtain a stable NTP system for reproducible applications in both pre-clinic and clinic, we first characterised our plasma devices to control the bio-impedances of different targets, ranging from *in vitro* to *in vivo* models and humans. We designed working conditions and conception of the NTP device for applications in both pre-clinical and clinical studies, using a Plasma Gun designed by the GREMI, which has a more stable reactor (than other plasma devices from the GREMI) with a grounded electrode.

This study is published in IEEE Transactions on Radiation and Plasma Medical Sciences (pre-print in August 2019 and published in May 2020), introduced below (**article #1**).

This study was also investigated *in vivo* using a newly developed NTP multijet device based on the Plasma Gun to explore the toxicity of the NTP multijet treatments on mice skin. Those results were presented in the second section of this chapter (see **section 1.2 of the Results**). They were used to establish clinical assay and treatments on human patients since there is no electrical difference between the animal models and the patient, thanks to our proposed method. The characteristics of this NTP multijet device are described in the second paper (**article #2**, see **section 2 of the Results**).

1.1 Mimicking of human body electrical characteristics for easier translation of plasma biomedical studies to clinical applications (article #1)

In this paper, we proposed to add a simple compensating circuit between targets and ground to make the electrical properties of all analysed systems (*in vitro*, *in vivo* and human patients) as similar as possible, at least from the electrical point of view. We then showed results for various *in vitro* and *in vivo* target exposures using a typical He plasma jet device. Measurements include voltage-current characteristics, optical emission spectra for key reactive species and the composition of liquid solutions exposed to the plasma.

The addition of the compensation circuit is shown to significantly reduce the differences observed between different targets (the differences between *in vitro* targets, mouse model targets and human targets).

My contribution to this paper, as the second co-author, consists of the *in vitro* and *in vivo* experiments performed at the Gustave Roussy Institute (conceptualisation, methodology, data acquisition and validation, data analysis and visualisation, data interpretation), and the writing (original draft preparation of the *in vitro* and *in vivo* experiments, review and editing of the whole paper).

Mimicking of Human Body Electrical Characteristic for Easier Translation of Plasma Biomedical Studies to Clinical Applications

A. Stancampiano, T.-H. Chung, S. Dozias, J.-M. Pouvesle, L. M. Mir, and E. Robert

***Abstract*—Nonthermal plasma (NTP) medical applications are now well established but the translation from *in vitro* plasma effects to *in vivo* effects remains far from being intuitive. Among various possible reasons, the translation may be disturbed by a loose control over the electrical characteristics of the different targets (e.g., cell culture dish, animal models) met during the development process, a parameter generally neglected and often unmentioned in papers. The aim of this article is to raise consciousness on how target electrical parameters (e.g., conductivity, electric potential...) play a major role in determining plasma treatment conditions. This effect is of particular relevance in plasma medicine where we move from treating small *in vitro* samples to humans, passing by animal models. The plasma conditions on targets with different electrical characteristics are compared by means of electrical measurements, optical emission spectroscopy, and basic liquid analysis. Commonly tested *in vitro* targets induce the generation of a plasma significantly different from that produced in contact with a human body. We demonstrate how by means of a basic and easy to implement electrical circuit it is possible to "compensate" the electrical differences between *in vitro* models, mice and human body and in such a way to reach more reproducible treatment conditions between *in vitro* and *in vivo* targets. The proposed method for the control of the target electrical parameters could greatly favor the transition from *in vitro* and *in vivo* models to patients for many plasma devices developed for biomedical applications.**

***Index Terms*—Atmospheric pressure plasma, compensation circuit, plasma medicine, potential, targets.**

I. Introduction

THE ANTITUMOUR effect of nonthermal plasmas (NTP) is now well established. The list of studies demonstrating plasma action on tumour cells *in vitro* is too long to be reported here, but we can estimate that more than 50 cell lines of most types of cancers have already been tested [1]–[3]. Similarly, the number of studies demonstrating other *in vitro* plasma medical applications, such as wound healing and decontamination, is nowadays significant and constantly increasing [4]. Nevertheless, studies involving patients are still limited and the exact plasma action mode is far from being fully understood [5], [6]. In general, the translation from *in vitro* plasma effects to *in vivo* effects remains far from being intuitive. This task is even more challenging due to the physical and chemical complexity of NTP interactions with liquids/cells/tissues, which depend on a number of variables, such as, for example, the applied voltage, pulse duration, pulse repetition frequency, gas mixture, distance to the target, time of exposure, protocols of application, and physical and chemical characteristics evolution of the target during the NTP delivery.

Amongst these parameters, the electrical characteristics of the target are often neglected and usually go unmentioned, especially in particles which are more focused on the biological effects of the plasma. Nevertheless, as already reported in the literature, the target nature can strongly influence the plasma characteristics [7]–[11]. Physically, during a direct NTP treatment, the target (e.g., the medium bathing the cells in culture or the living treated tissue) is part of a "transient electrical circuit" that is formed between the high voltage electrode and the ground (physical electrical connection to the earth). This means that target electrical parameters (e.g., conductivity, potential, total impedance...) play a major role in determining treatment results. Even with all the other parameters fixed, different targets can lead to very different plasma characteristics, and therefore, very different plasma effects. In this article, we demonstrate that even the same target (water solution in a multiwell plate) but under different electrical conditions [grounded potential (GR) or at floating potential (FP)] or set on different supports (dielectric plate *versus* metallic plate) can lead to very different treatment results.

The variation of the NTP treatment conditions due to target characteristics is of extreme relevance, especially in the plasma medicine field where we move from treating small *in vitro* samples to humans passing by various animal models.

The standard approach for medical validation that foresees the sequence *in vitro* model → *in vivo* model → patients may not be the best option if applied in a straightforward manner to plasma medical studies. The plasma generated on a small *in vitro* sample, characterized by a high conductivity

Manuscript received May 23, 2019; revised July 26, 2019; accepted August 14, 2019. Date of publication August 21, 2019; date of current version May 1, 2020. This work was supported in part by the GdR 2025 HAPPYBIO and in part by the PLASCANCER Project (INCa-PlanCancer-n°17CP087-00) aimed at investigating potential synergistic effects between plasma and pulsed electric field. *(Corresponding author: A. Stancampiano.)*

A. Stancampiano, S. Dozias, J.-M. Pouvesle, and E. Robert are with GREMI, UMR7344 CNRS/Université d'Orléans, 45067 Orléans, France (e-mail: augusto.stancampiano@univ-orleans.fr; sebastien.dozias@univ-orleans.fr; jean-michel.pouvesle@univ-orleans.fr; eric.robert@univ-orleans.fr).

T.-H. Chung and L. M. Mir are with VTA, CNRS, Univ. Paris-Sud, Gustave Roussy, Université Paris-Saclay, 94800 Villejuif, France (e-mail: thai-hoa.chung@gustaveroussy.fr; luis.mir@cnrs.fr).

Color versions of one or more of the figures in this article are available online at http://ieeexplore.ieee.org.

Digital Object Identifier 10.1109/TRPMS.2019.2936667

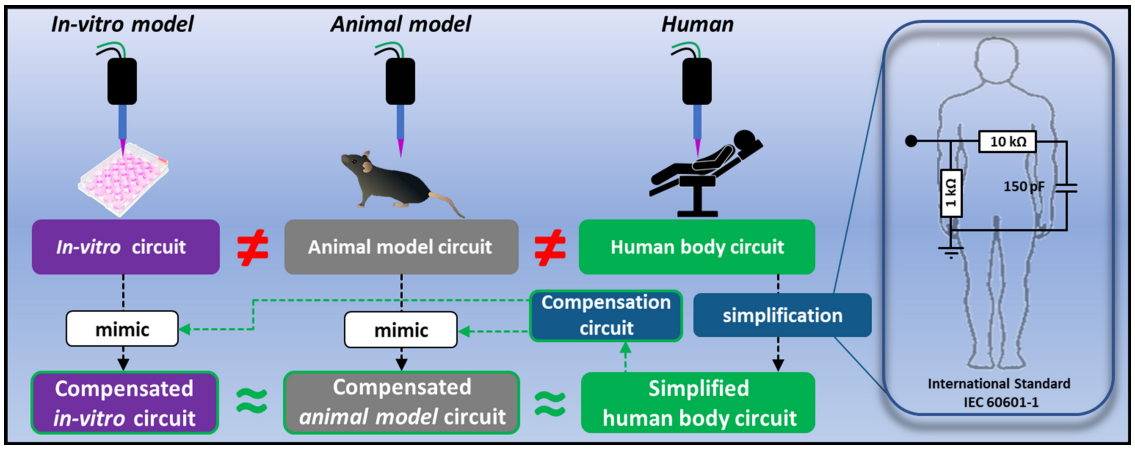

Fig. 1. Graphical representation of the proposed method to make *in vitro* and *in vivo* models look more similar to the reference substrate for plasma medical studies and the human body.

and a low capacitance, can definitively not be compared with the one produced on a human body, with typically a lower conductivity and a much higher capacitance. This in turn ends up potentially affecting the reliability of the results achieved on *in vitro* and even *in vivo* models and their possibility to be translated to patients beside plenty of biological reasons that already make the passage far from being trivial.

Very recently, the issue has been partially addressed by some studies proposing feedback control systems based on either the real time tuning of the thermal effect and the intensity of plasma jets [11] or on the dynamic response of cancer cells to NTP based on mathematical model developed starting from experimental results [12]. Another proposed approach is based on the development of a basic material target that mimics the same dielectric properties of the human body and that could be used for the study of the plasma properties in more realistic operating conditions [13].

An improved control over plasma treatment conditions will also help to better investigate the impact of physical and electrical stimuli possibly induced by plasma. Within the recent past, the importance of electrostimulation at weak currents and the impact of the plasma-associated electric field were being rediscovered and investigated [14], [15].

In this article, we propose and successfully test a simple and versatile solution to reduce the degree of variation encountered in NTP studies translating from *in vitro* and animal models to human body. The main idea is to compensate the electrical differences between the models and the human body by means of a small and affordable electrical circuit that can be applied on both animal and *in vitro* models (see Fig. 1). The approach is significantly different from those found in the literature as it is based on a noninvasive modification of the targets, with special attention to common biomedical models. Acting on the target electrical characteristics rather than on the plasma source control, the compensation method tackles the issue from a completely different angle and is potentially complementary to feedback-based control systems as those already proposed by Gidon *et al.* [11] and Lyu *et al.* [12]. Moreover, being based on a human body equivalent circuit derived from international standards for safety evaluation of electrical equipment, this approach could encourage the development of plasma sources complying with the requirements for basic safety and essential performance [16]. The same circuit may also be valuable for modeling studies trying to simulate targets close to those in actual plasma medical treatments.

II. Materials and Methods

A. Plasma Source

The atmospheric plasma jet used in this article is a Plasma gun (PG) already described in detail in [8]. Briefly, the PG is a coaxial DBD reactor with a quartz capillary flushed with helium and powered by a micropulsed high voltage generator. The 12 cm long capillary was tapered at the outlet ($Ø_{in} = 1.5$ mm, $Ø_{ext} = 3$ mm). The plasma source was operated in two sets of operating conditions. In the first part, concerning only *in vitro* experiments, the source was flushed with a helium flow of 1 slm, powered by 4 μs duration voltage pulses of +12 kV peak with a 1 kHz repetition rate and maintained at a distance of 10 mm from the target. In the second half of the work that included *in vitro*, animal targets and humans, the PG was operated at 0.5 slm of helium, +10 kV, 1 kHz, and at 15 mm from the target. The different sets of parameters were selected in order to on the one side emphasise reactive species production in *in vitro* liquid samples (so to ease their detection) and on the other side to limit the current crossing *in vivo* targets.

B. In Vitro Targets

To represent *in vitro* targets we used a common 24-multiwell plate (Nunclon Delta Surface, Thermo Fisher Scientific, DK) and a bigger custom-made well with a rectangular base (W 2 cm × L 5 cm × H 0.9 cm, material: PVC). The liquid adopted for the test was high purity water (distilled, conductivity < 1μS, by Chem-lab) with dissolved NaCl (Fisher Scientific, U.K.) to adjust its conductivity to the desired values of 10 and 20 mS/cm (reasonable values for common culture medium as those adopted in electroporation studies).

The conductivity of the solution was measured by means of a liquid conductivity probe (InLab Conductivity Probes

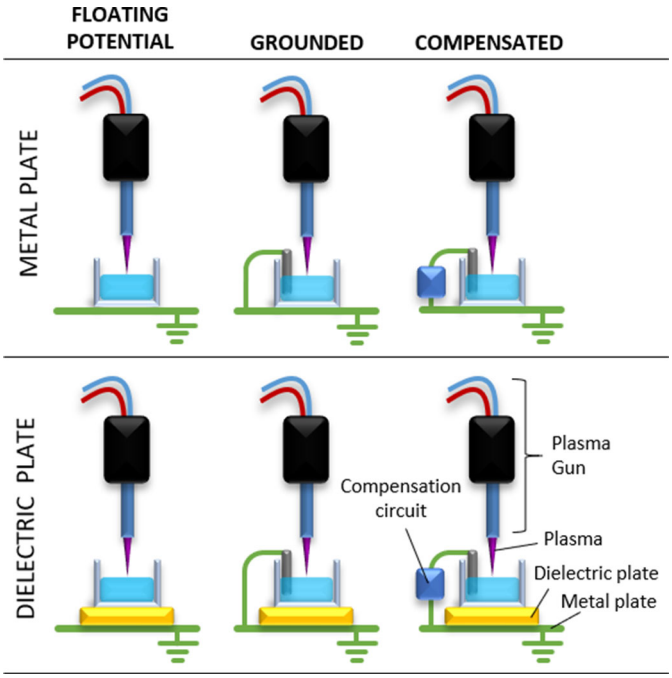

Fig. 2. Schematic summary of the investigated *in vitro* conditions for the PG impinging on a 24-multiwell plate filled with salted water.

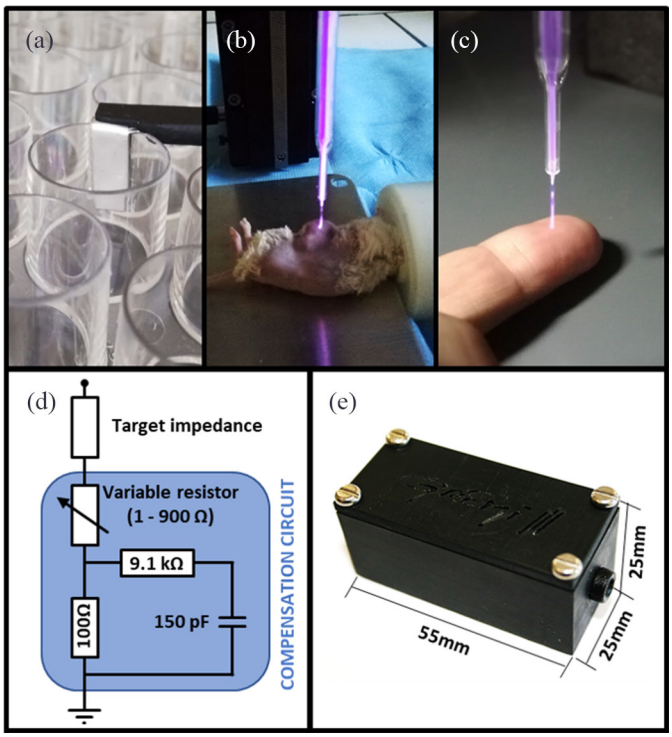

Fig. 3. (a) Ground connection for the 24-multiwell plate. (b) NTP treatment on animal model on a grounded plate. (c) NTP treatment on a human fingertip. (d) Compensation circuit electrical scheme. (e) Photograph of the compensation circuit with dimensions.

51344030, Mettler Toledo). A volume of 1–3 or 9 mL was introduced, respectively, in the multiwell plate and the custom well before each experiment. The multiwell plate was either positioned on a conductive plate (aluminium, 3 mm thick) electrically connected to ground or on a dielectric plate [low density polyethylene (LDPE), 15 cm thick] that was itself positioned on the conductive plate (Fig. 2). Both plates were chosen large enough to completely cover all the multiwell plate bottom.

Floating Potential (FP): The liquid at FP was not in contact with any conductive material.

Ground Potential (GR): The liquid in the multiwell plate was connected to ground by means of a small stainless-steel plate [3.6 × 7 × 0.5 mm; Fig. 3(a)] while in the custom-made well grounding was processed through a stainless-steel plate of bigger dimensions (19 × 8.1 × 1 mm). Both connection plates were positioned inside the liquid close to the wall of the well, so to be as far as possible from the plasma impinging point at the centre of the well. While possible, electrolysis was regarded as negligible in this configuration as no visible bubbling or erosion of the electrode was detected in any of the investigated conditions. Evaporation accounted for a liquid volume variation lower that 3% and was therefore considered negligible in this case.

C. In Vivo Targets

To represent *in vivo* targets we adopted mice (BALB/cJ) with or without tumour (CT26 murine colon carcinoma subcutaneously at 500.000 cells/100 μL on each flank, eight days before treatment). Treated flank of the mice was shaved and depilated the day before the treatment. Mice were anesthetised and positioned on a metal heating plate connected to the ground to maintain a constant body temperature of the mice during the treatment [Fig. 3(b)]. To represent the human body, the authors volunteered as samples. The chosen treated area was the fingertips of the index finger of the one hand [Fig. 3(c)]. Ground connection was realized by means of a hand-hold metal cylinder. No other grounded surfaces were in contact with the person during tests.

D. Electrical Measurements

Voltage measurements were performed by means of a high voltage passive probe (Tektronix P6015A) on the high voltage cable connecting the PG and the generator. Current measurements were made by a current passive probe (Pearson 6585). For tests comparing *in vitro* and *in vivo* targets with human body, the current probe was positioned on the cable connecting the target to the ground. For tests comparing *in vitro* targets in different electrical conditions, since no ground connection was available for the cases at FP, the current probe was positioned around the plasma source capillary (5 cm away from the outlet).

E. Reactive Species in Liquid Evaluation

Semi-quantitative chemical analyses of peroxide, nitrate, and nitrite concentrations produced in the plasma treated liquid were performed to support the understanding of the influence of the target electrical conditions. For these semi-quantitative measurements Quantofix test strips (Macherey-Nagel GmbH & Co. KG, DE) were used. Tests were repeated in triplicate.

F. Optical Emission Spectroscopy

Plasma spectra were acquired by means of a spectrometer (MayaPro2000, integration time 200 ms, 8 averaged spectra for each acquisition) connected to a 1 mm in diameter VIS and UV optical fibre (14° full angle aperture). The optical fibre inlet was positioned horizontally 2 mm away from the plasma jet axis. The fibre vertical position was varied by means of a millimetric manual displacement system in order to scan the emission along the jet axis. All acquisitions were done within 10 s from the start of the treatment on a new sample. The spectra were analyzed to extract the line intensity (a.u.) with no sensitivity correction for the chosen reference lines associated with species significant from a biological point of view: NO* (2363 nm), OH* (3088 nm), N_2* (B-A) (775 nm), and O* (777.2 nm).

G. Compensation Circuit

The human body is a very complex system and presents electrical characteristics that can greatly vary from one person to another due to various factors as, for example, age, size, sex, and health conditions. Moreover, the total body impedance is frequency dependent on and vary with the characteristics and position of the electrodes/contact points [17]–[19]. Even the same person may present very different total impedances if is connected to the ground through his bare feet, one hand or not at all. For safety reasons, in general in medical practice patient are unlikely to be completely insulated (at FP) and are more often connected to GP or to the return electrode of the electrical medical instrument in use (e.g., in electro-surgery) [20], [21]. In this article, we decided to adopt as a reference circuit for the human body the electrical model (see Fig. 1) reported in the International Standard IEC 60601-1 for medical electrical equipment [22]. This standard has been chosen as internationally recognized and widely adopted [16], [23]. In practice, the circuit is realized starting from the one proposed in the IEC 60601-1 (Fig. 1) and reducing both resistors (becoming 100 Ω and 9.1 kΩ) so to have some margin to take into account the target impedance [Fig. 3(d)]. In first approximation, due to the short duration of the current pulse (0.7 μs) with respect to the characteristic time of the circuit (RC time constant = 1.5 μs) we can assume the 150 pF capacitance to be as a closed circuit. In this way, we can calculate the equivalent impedance as the results of resistors in parallel. The equivalent impedance of the human body circuit (Fig. 1) after the simplification results in 909 Ω while that of the compensation circuit, without taking into account the variable resistor, is 99 Ω . The difference between the two circuits after the simplification is therefore of 810 Ω . If we position the compensation circuit in series between the target and the ground, we will ideally end up with three resistors connected in series: the target, the variable resistor, and the equivalent impedance of 99 Ω calculated above. In order to make the target-compensation circuit look similar to the human body circuit, it is sufficient to adjust the variable resistor so that summed with the target natural impedance (that can be measured or estimated), will give a 810 Ω impedance. The proposed method is certainly affected by strong approximations but on the other hand presents a very simple structure and is easy to implement. Moreover, being composed of widely available electrical components, the total cost of the circuit results very low and its dimension can be further reduced starting from this first prototype [Fig. 3(e)].

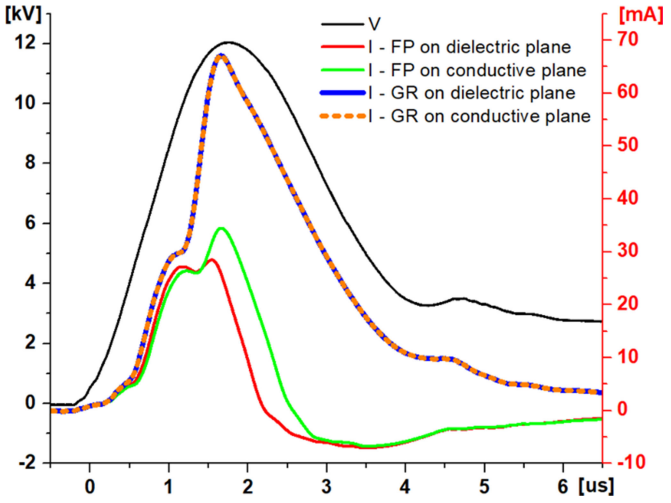

Fig. 4. Voltage (V) and current (I) waveforms during direct treatment of water in 24-multiwell plates at different electrical potentials (FP or GR) and on different supports (dielectric or conductive). Gap distance 10 mm.

TABLE I
CONCENTRATIONS OF H_2O_2, NO^-_3, AND NO^-_2 GENERATED IN 1 mL OF WATER IN 24-MULTIWELL PLATES FOR DIFFERENT TARGET ELECTRICAL CONDITIONS. TREATMENT TIME 5 MIN. GAP DISTANCE 10 mm

Target potential	Support	H_2O_2 [mg/l]	NO^-_3 [mg/l]	NO^-_2 [mg/l]
Floating	Dielectric	2 - 5	10	<1
	Conductive	10	10-25	<1
Grounded	Dielectric	25	100	20
	Conductive	25	100	20

III. RESULTS AND DISCUSSION

A. To Ground or Not to Ground

As already mentioned, the electrical characteristics of *in vitro* targets are often neglected or considered as marginal. In this first part of the study, we demonstrate how even by positioning the same liquid (1 mL salt water at 10 mS/cm), in the same 24-multiwell plate, but on a conductive grounded plate (e.g., biosafety cabinet) or on a dielectric plate (e.g., standard lab table) we can greatly influence the treatment conditions. Considering the cases with the liquid at FP, we see that moving the plate from a dielectric support to a conductive one significantly modify the current going through the plasma in the capillary (Fig. 4). For these FP cases, the current peak (28 mA on dielectric plate and 35 mA on conductive plate) that takes

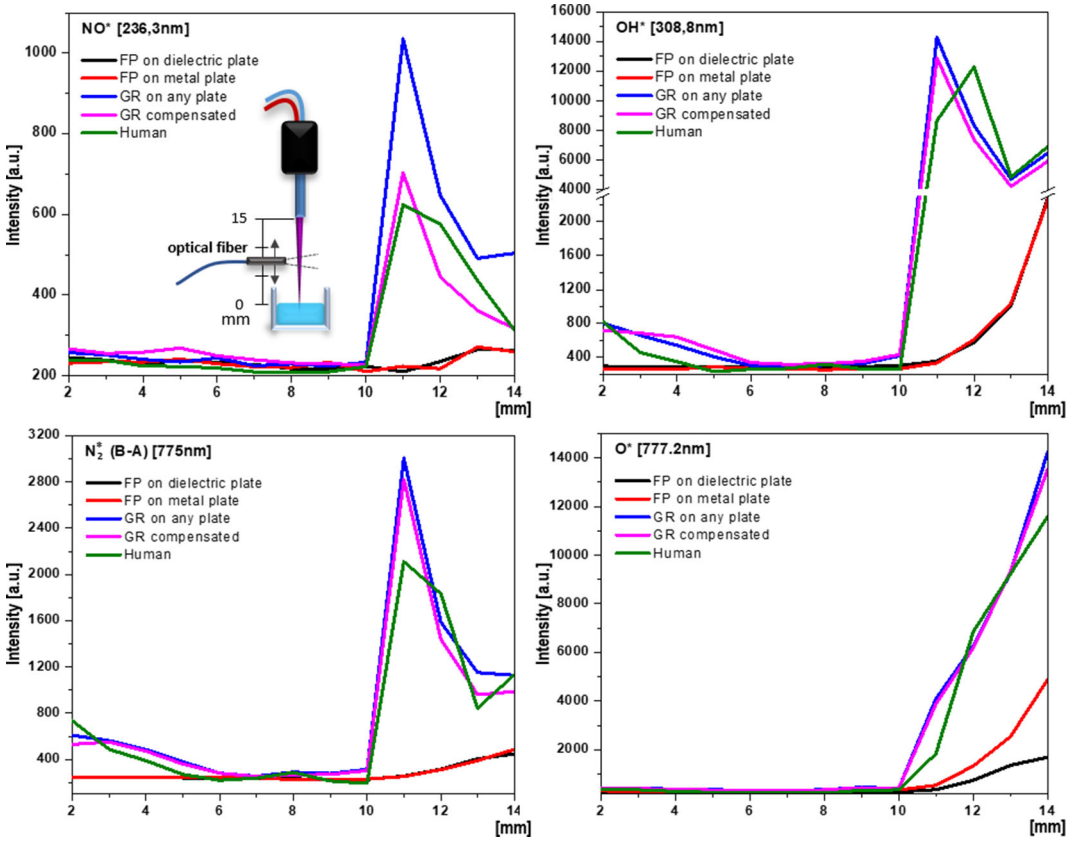

Fig. 5. PG (0.5 slm, 10 kV, 1 kHz, and 15 mm gap) emission intensity (expressed in arbitrary unit) for selected spectral lines and for different electrical conditions of an *in vitro* target (FP and GR) and a grounded human body. Acquisition were collected at different distances from the surface of the target.

place after the impact of the primary plasma front and the formation of a conductive channel between the high voltage electrode inside the capillary and the target [8] is limited by the capacitance associated to the *in vitro* target. Therefore, increasing this capacitance by moving the plate from a dielectric plate to a conductive grounded plate may increase the associated current.

A variation of the treatment conditions moving from one support to another is also testified by the analysis of the treated liquid (Table I) where we measure that a significantly greater amount of peroxides and nitrates are produced when the support is conductive. Therefore, we are led to believe that two biological *in vitro* assays, performed on the one inside a biosafety cabinet and the other on a dielectric table would supposedly produce different results.

The same test was repeated with the liquid set at GR. In this case, the recorded currents resulted virtually identical between the two supporting plates (Fig. 4). Grounding the liquid is like connecting a resistor in parallel to the capacitance as we already discussed above. Since the conductivity of the tested liquid (as well as that of the most common culture media) is relatively high, the equivalent resistance results small. This in turn favors the passage of a greater conduction current compared to the cases at FP (Fig. 4) and greatly reduces the impact of the capacitance associated with the plate underneath. These observations were confirmed by the liquid analysis where the shift from FP to GR induced the production of higher concentrations of reactive species (Table I) and hindered the influence of the supporting plate. In fact no significant difference could be detected between the two grounded cases.

The differences between the FP and the GR reactive species production in liquid can potentially be attributed also to different mechanism of charges accumulation on the liquid surface (reduced in GR cases) and the influence of induced current on the liquid chemistry.

Also optical emission spectroscopy (OES) acquisitions (Fig. 5) show a significant higher intensity emission for the GR cases (since they were identical, only one is reported for the simplicity) compared to the cases at FP. Emission of the NO* system and nitrogen first positive system N_2(B-A) almost only occur for the GR cases. This is in agreement with already published studies on the PG comparing free jet condition with those impinging on a grounded metallic target [8].

The differences between the FP and the GR cases are particularly emphasized in proximity of the plasma source outlet. While the FP cases exhibit a constant decrease of the emission intensity moving away from the outlet, the GR cases present a peak for the NO*, OH*, and N_2(B-A) at 11 mm from the liquid surface (4 mm from the capillary, see Fig. 5). This is probably due to fluid dynamic reasons related to the mixing of the helium flow with the surrounding air. Interestingly, for some species [OH* and N2 (B-A)] there is an evident difference between the FP and the GR cases also in close proximity of the target surface. While the FP present nearly no emission in close proximity to the target surface, the GR cases show some significant emission. This is probably the

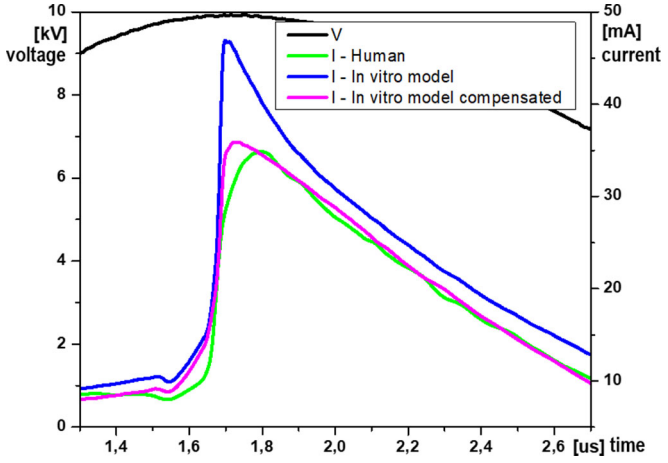

Fig. 6. Voltage (V) and current (I) waveforms during direct treatment on grounded human body and on grounded salt water (10 mS/cm) in 24-multiwell plate with and without compensation circuit. Gap distance 15 mm.

consequence of a secondary ionization front propagating from the target to the high voltage electrode as already reported in the previous studies [8] and that may be more energetic in the GR cases in virtue of a higher degree of ionization in the noticed plasma channel left by the primary ionization front. It must be recalled that while reactive species with relatively long lifetime (e.g., NO*, O_3, and H_2O_2) generated in the plasma channel can be transported to the liquid surface by the gas flow, other with submillisecond lifetime such as the OH* can reach the target only if generated in close proximity to the interface [24].

In this perspective, it is important to underline how the emission spectra of the *in vitro* GR case results significantly more similar to that of a human body than both *in vitro* FP cases. Several reactive species playing important roles in plasma medical applications such as in our case NO* for the promotion and regulation of wound healing [25], may not be produced on an *in vitro* FP target or are produced in significant lower amounts when compared to a human body target (Fig. 5).

These results suggest that grounding *in vitro* samples may be a good option to achieve more realistic operating conditions in plasma medical studies. Summing up this first part of results, we may conclude that grounding *in vitro* models may beneficially affect the plasma treatment making it more stable and independent of the supporting plate nature while increasing the amount of reactive species, especially the nitrogen ones, produced both in gas and in liquid phase.

B. Electrical Compensation of Models

In the second part of the study, the proposed compensation circuit described in the materials and methods was assessed. As mentioned, the goal of the circuit is to adjust the total impedance of the investigated models to match that of a human body. As a first step, the current on the ground connection of a human body treated by the PG (Fig. 6) was recorded. This measurement was adopted as a reference for later tests.

TABLE II
CONCENTRATIONS OF H_2O_2, NO^-_3, AND NO^-_2 GENERATED IN WATER IN A 24-MULTIWELL PLATE (3 mL) AND IN THE CUSTOM WELL (9 mL) WITH AND WITHOUT THE COMPENSATION CIRCUIT. GAP DISTANCE 10 mm

Compensation	Well	Treatment time [min]	H_2O_2 [mg/L]	NO^-_3 [mg/L]	NO^-_2 [mg/L]
no	24-multiwell	5	2	10-25	1
	Custom-made	15	5	25	1-5
yes	24-multiwell	5	2	10	1
	Custom-made	15	2	10	1

Then, the current going through 3 mL of salt water (10 mS/cm) in a 24-multiwell plate and connected to the ground was measured. The same was repeated for the same setup but after the connection of the compensation circuit between the liquid and the ground. As shown in Fig. 6, the current peak going through a liquid sample (not compensated) is significantly higher than that through a human body. This is due to the considerably lower resistance and capacitance characterizing the *in vitro* sample. The introduction of the compensation circuit greatly reduces these differences so that the current measured on compensated *in vitro* targets is much closer to that measured on a human body.

Since the recorded current depends on the characteristics of the plasma, we can assume that with the compensation circuit, the current generated on the *in vitro* sample being more similar to the one generated on a patient, the plasma effects would thus be more similar. This is partially confirmed by the OES results (Fig. 5) where it is observed that for the emission associated to NO* the compensation circuit helps the plasma generated on the *in vitro* sample to resemble that on the human body. The emissions associated to the other species are less affected but on the other hand no negative effect is observed due to the introduction of the compensation circuit. Especially, it is worth noting that if compared to the more common condition featuring an *in vitro* sample at FP, the proposed condition with a grounded and compensated sample significantly helps the generation of a plasma similar to the one found when treating a human body.

Only for the human body and GR cases, we observe a significant production of nitrogen reactive species, absent in the FP cases. The same holds for OH* that looks similar, as well as for the magnitude of the O* emission which is the same.

The same tests were repeated with similar results (data not shown) changing the geometry (use of the custom-made well) or the liquid conductivity (20 mS/cm instead of 10 mS/cm). Interestingly, the circuit, originally designed to make the *in vitro* samples to behave more similar to the human body, may also be used to homogenize the behavior of different *in vitro* samples (e.g., different well or liquid) from an electrical point of view. This is confirmed in Table II where the compensation leads to the production of similar amounts of

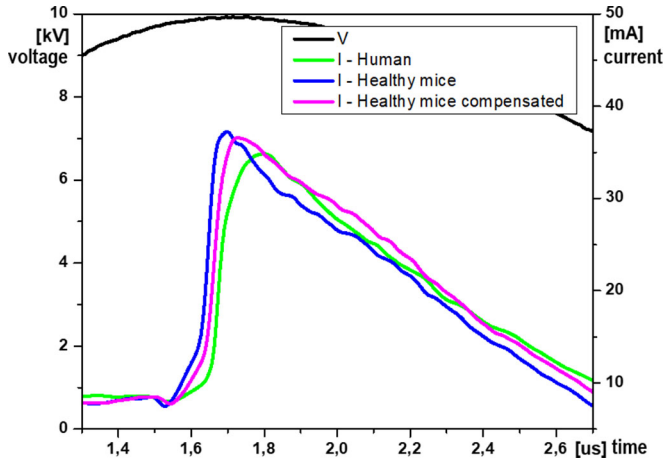

Fig. 7. Voltage (V) and current (I) waveforms during direct treatment of human body and healthy mice with or without compensation circuit. Gap distance 15 mm.

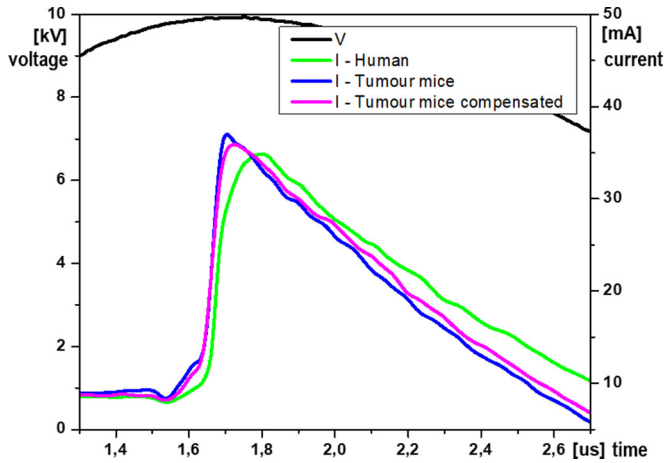

Fig. 8. Voltage (V) and current (I) waveforms during direct treatment of human body and mice with grafted tumour and with or without compensation circuit. Gap distance 15 mm.

reactive species for two different well geometries and liquid volumes. In this case, not only the compensation circuit was adapted but also the treatment time so to maintain a constant ratio of 5 min treatment every 3 mL of liquid. Such setting of the ratio between treatment duration and liquid volume to reach the same reactive species concentration is very often used but may not be accurate enough as expected without the compensation circuit. This was measured with our set up for the compensated cases for which moving from 5 to 15 min of treatment when increasing the liquid volume, resulted in a drastic change of the reactive species concentration (first two rows of Table II).

As a further validation of the compensation method, the same approach was repeated on animal targets. Due to a lack of supporting literature concerning equivalent electrical circuit for mice and the complexity of effectuating accurate measurements of the mice properties, in this case we approached the compensation through successive iterations. The best results in this case were achieved assuming a mouse equivalent impedance of 200 Ω. This is certainly an approximation that may be affected by several factors, such as skin condition and mouse to ground connection (in this case processed through the metal plate supporting the mouse). Preliminary results show that the electrical characteristics of a mouse are, as expected, already closer to those of a human body than those of an *in vitro* sample. Even if on a smaller scale, also in this case, the addition of the compensation circuit contributed to increase the similarity both in the rising and falling front of the current waveform (Fig. 7). The same experiment was repeated on mice with grafted tumours (Fig. 8). For this target, the compensation resulted less satisfactory probably in virtue of the different resistivity of the tissues exposed to the plasma (healthy skin and tissues *versus* a thinner skin and a more conductive tumour mass below the skin). Indeed, tumours present a conductivity that is usually higher than the healthy tissue [26], meaning that the equivalent circuit also will be different. Perhaps it should have to be compared to the reference circuit for a human body affected by the same pathology.

IV. Conclusion

In the first part of this article, the importance of taking into account and control the electrical characteristics of the *in vitro* samples commonly employed in plasma biomedical studies was demonstrated. When the target is at FP, even the nature of the plate supporting the sample can influence the treatment. For example, different concentrations of reactive species in the treated medium can be the result of treating the sample on a dielectric table rather than inside a biosafety metallic cabinet. For this reason, it may be advisable to impose the potential of the target to ground level in order to reduce the influence of the surroundings and increase the reproducibility of the experiments. Nevertheless, a well-controlled FP condition can still be more appropriate for specific cases where, for example, the risk of contamination does not allow the use of submerged electrodes into the liquid.

In the second part of the study, we proposed a new method aimed at the reduction of the degree of variation encountered in NTP studies moving from *in vitro*/animal models to human body. Keeping in mind that the final target of plasma medicine studies are human patients, we propose to adopt a small and affordable electrical circuit to compensate the electrical differences between models and human body and, as result, have the same NTP effects on very different targets including humans.

The use of the compensation method was proven to lead to not only closer current waveforms through different targets but also to a closer reactive species generation in liquid solutions. Also, emission spectra analysis confirmed that the plasma characteristics on a compensated *in vitro* sample are closer to that found on a human body if compared with those generated on a more common FP configuration.

Therefore, results confirm that the circuit helps maintaining the same treatment effects from one target to another.

Moreover, the mimicking circuit could also help to keep the same treatment conditions when there is a change from one *in vitro* support to another (e.g., from a well plate type to another).

In spite of the promising results, the compensation circuit alone is clearly not sufficient to transform *in vitro* samples into perfect replica of a human body. Other factors not related to the electrical properties such as surface evaporation and morphology inherently induce differences between models and human body. For these aspects, other studies have proposed other methods to mimic various human body properties [27]. Is not to be excluded that in the future these methods could be implemented with the electrical compensation method here described to provide even better results.

In the meantime, while being not perfect, the proposed compensation method could significantly improve the representativity of *in vitro* plasma experiments in a practical and simple manner that at present show no drawback that could prevent its use.

Therefore, we hope that this solution would help to optimize the transition from preclinical to clinical studies in the plasma medicine field.

REFERENCES

[1] J. Schlegel, J. Köritzer, and V. Boxhammer, "Plasma in cancer treatment," *Clin. Plasma Med.*, vol. 1, no. 2, pp. 2–7, 2013.

[2] K. Song, G. Li, and Y. Ma, "A review on the selective apoptotic effect of nonthermal atmospheric-pressure plasma on cancer cells," *Plasma Med.*, vol. 4, nos. 1–4, pp. 193–209, 2014.

[3] E. A. Ratovitski *et al.*, "Anti-cancer therapies of 21st century: Novel approach to treat human cancers using cold atmospheric plasma," *Plasma Process. Polym.*, vol. 11, no. 12, pp. 1128–1137, 2014.

[4] S. Bekeschus, P. Favia, E. Robert, and T. von Woedtke, "White paper on plasma for medicine and hygiene: Future in plasma health sciences," *Plasma Process. Polym.*, vol. 16, no. 1, pp. 1–12, 2018.

[5] O. Assadian *et al.*, "Effects and safety of atmospheric low-temperature plasma on bacterial reduction in chronic wounds and wound size reduction: A systematic review and meta-analysis," *Int. Wound J.*, vol. 16, no. 1, pp. 103–111, 2019.

[6] H.-R. Metelmann *et al.*, "Clinical experience with cold plasma in the treatment of locally advanced head and neck cancer," *Clin. Plasma Med.*, vol. 9, pp. 6–13, Mar. 2018.

[7] V. V. Kovačvić, G. B. Sretenović, E. Slikboer, O. Guaitella, A. Sobota, and M. M. Kuraica, "The effect of liquid target on a nonthermal plasma jet—Imaging, electric fields, visualization of gas flow and optical emission spectroscopy," *J. Phys. D Appl. Phys.*, vol. 51, no. 6, 2018, Art. no. 065202.

[8] T. Darny, J.-M. Pouvesle, V. Puech, C. Douat, S. Dozias, and E. Robert, "Analysis of conductive target influence in plasma jet experiments through helium metastable and electric field measurements," *Plasma Sources Sci. Technol.*, vol. 26, no. 4, 2017, Art. no. 045008.

[9] A. Stancampiano, E. Simoncelli, M. Boselli, V. Colombo, and M. Gherardi, "Experimental investigation on the interaction of a nanopulsed plasma jet with a liquid target," *Plasma Sources Sci. Technol.*, vol. 27, no. 12, 2018, Art. no. 125002.

[10] K. Gazeli *et al.*, "Effect of the gas flow rate on the spatiotemporal distribution of Ar($1s_5$) absolute densities in a ns pulsed plasma jet impinging on a glass surface," *Plasma Sources Sci. Technol.*, vol. 27, no. 6, 2018, Art. no. 065003.

[11] D. Gidon, B. Curtis, J. A. Paulson, D. B. Graves, and A. Mesbah, "Model-based feedback control of a kHz-excited atmospheric pressure plasma jet," *IEEE Trans. Radiat. Plasma Med. Sci.*, vol. 2, no. 2, pp. 129–137, Mar. 2018.

[12] Y. Lyu, L. Lin, E. Gjika, T. Lee, and M. Keidar, "Mathematical modeling and control for cancer treatment with cold atmospheric plasma jet," *J. Phys. D Appl. Phys.*, vol. 52, no. 18, 2019, Art. no. 185202.

[13] F. Judée and T. Dufour, "Plasma gun for medical applications: Engineering an equivalent electrical target of the human body and deciphering relevant electrical parameters," *J. Phys. D Appl. Phys.*, vol. 52, no. 16, 2019, Art. no. 16lt02.

[14] D. B. Graves, "Lessons from Tesla for plasma medicine," *IEEE Trans. Radiat. Plasma Med. Sci.*, vol. 2, no. 6, pp. 594–607, Nov. 2018.

[15] M. Jinno, Y. Ikeda, H. Motomura, Y. Isozaki, Y. Kido, and S. Satoh, "Synergistic effect of electrical and chemical factors on endocytosis in micro-discharge plasma gene transfection," *Plasma Sources Sci. Technol.*, vol. 26, no. 6, 2017, Art. no. 065016.

[16] M. Stella *et al.*, "Introduction to DIN-specification 91315 based on the characterization of the plasma jet kINPen® MED," *Clin. Plasma Med.*, vol. 4, no. 2, pp. 35–45, 2016.

[17] K. Chinen, I. Kinjo, A. Zamami, K. Irei, and K. Nagayama, "New equivalent-electrical circuit model and a practical measurement method for human body impedance," *Biomed. Mater. Eng.*, vol. 26, no. S1, pp. S779–S786, 2015.

[18] J. E. Bridges, M. Vainberg, and M. C. Wills, "Impact of recent developments in biological electrical shock safety criteria," *IEEE Power Eng. Rev.*, vol. PER-7, no. 1, pp. 55–56, Jan. 1987.

[19] R. M. Fish and L. A. Geddes, "Conduction of electrical current to and through the human body: A review," *Eplasty*, vol. 9, p. e44, Oct. 2009.

[20] N. N. Massarweh, N. Cosgriff, and D. P. Slakey, "Electrosurgery: History, principles, and current and future uses," *J. Amer. College Surgeons*, vol. 202, no. 3, pp. 520–530, 2006.

[21] A. T. Golpaygani, M. M. Movahedi, and M. Reza, "A study on performance and safety tests of electrosurgical equipment," *J. Biomed. Phys. Eng.*, vol. 6, no. 3, pp. 175–182, 2016.

[22] *Medical Electrical Equipment—Part 1: General Requirements for Basic Safety and Essential Performance*, International Standard IEC 60601–1, 2005.

[23] A. Lehmann, F. Pietag, and T. Arnold, "Human health risk evaluation of a microwave-driven atmospheric plasma jet as medical device," *Clin. Plasma Med.*, vols. 7–8, pp. 16–23, May 2017.

[24] R. Ono and T. Oda, "Dynamics of ozone and OH radicals generated by pulsed corona discharge in humid-air flow reactor measured by laser spectroscopy," *J. Appl. Phys.*, vol. 93, no. 10, pp. 5876–5882, 2003.

[25] A. B. Shekhter, V. A. Serezhenkov, T. G. Rudenko, A. V. Pekshev, and A. F. Vanin, "Beneficial effect of gaseous nitric oxide on the healing of skin wounds," *Nitric Oxide* vol. 12, no. 4, pp. 210–219, 2005.

[26] A. Županič, S. Čorović, and D. Miklavčič, "Optimization of electrode position and electric pulse amplitude in electrochemotherapy," *Radiol. Oncol.*, vol. 42, no. 2, pp. 93–101, 2008.

[27] E. J. Szili, J. W. Bradley, and R. D. Short, "A 'tissue model' to study the plasma delivery of reactive oxygen species," *J. Phys. D Appl. Phys.*, vol. 47, no. 15, 2014, Art. no. 152002.

1.2 *In vivo* toxicity of direct NTP multi-jet treatment on mice skin

All the *in vivo* experimentations respected the following animal models and protocol:

- Male Swiss nude mice and inbred female immunocompetent C57Bl/6J mice (7-week-old at an average weight of 19 g) were purchased at the animal facilities of our Institute Gustave Roussy (Villejuif, France) and Janvier laboratory (Saint-Berthevin, France), respectively. Animals were housed at specific pathogen-free animal housing facilities of the Institute Gustave Roussy for seven days before experimentation. All animal experiments were performed in strict compliance with the ethical guidelines issued by the European Committee (Directive 2010/63/EU). Animals were handled in strict accordance with good animal practice. The study and experimental protocol (#2017_061_11278), reviewed by the Comité d'Éthique pour l'Expérimentation Animale CEEA 26, were approved by the registered ethics committee in animal experimentation of the Ministry under the identification code APAFIS#13409-2018020711382163.
- Before experimentation, mice were permanently identified by single-colour toe tattooing using green paste (Ketchum Animal Tatto Ink Paste, Ketchum Manufacturing Inc., Canada).
- For the immunocompetent C57Bl/6J mice bearing subcutaneous (s.c.) tumours: To facilitate inoculation and avoid obstruction with treatments, the fur on the right flank was removed from mice by dry shaving.

1.2.1 Aim of the study

To the purpose mentioned in the Research Hypotheses and Objectives, an *in vivo* experimentation was proposed to investigate the safety of the NTP multijet designed by the GREMI for its potential in skincare and treatments. This project collaborated with the GREMI and the Service of Infectious Diseases of the Orléans Regional Hospital, which provides care for skin issues (primarily infection) patients.

1.2.2 Materials and methods

Treatment parameters

Two different modes of exposure to NTP multijet on the skin were studied: the "multi-jet" mode, where the distance between the NTP output and the target (mouse skin surface) was fixed at 5 mm ($d_{plasma\text{-}skin}$ = 5 mm) (upper panel of *Figure* ***33*** and ***Error! Reference source not found.***), and the "diffuse" mode where $d_{plasma\text{-}skin}$ = 2 mm (lower panel of *Figure* ***33*** and ***Error! Reference source not found.***). Those distances were controlled thanks to customised 3D-printed spacers (not shown on those figures). In the "diffuse" mode, due to the proximity of the plasma jets to the skin surface, the NTP treatment formed a homogeneous "cloud" (similar to what was observed with low-pressure glow discharge plasma) in comparison to the "multi-jet" mode of exposure where five distinguished single jets were seen on the skin.

The NTP device was set at 11 kV with a helium flow rate of one standard litre per minute (1 slm). Various plasma parameters and exposure times were studied: 500 Hz *versus* 1 kHz *versus* 2kHz, 1-minute plasma exposure *versus* three times of 1-minute exposure with at least a pause of 1 minute between each treatment *versus* 3 minutes of continuous plasma exposure.

Animal model and experimental protocol

- Male Swiss nude mice and female C57Bl/6J mice (see description above), three mice per group.
- A day before the experiment, mice were depilated with depilatory cream (Veet® hair removal cream) and identified as described above.
- On the experiment day, mice were anaesthetised with Isoflurane (Isoflurin® 1000 mg.g-1, Axience, FR) and were treated with NTP multijet under different treatment parameters described above.
- The potential skin effects due to thermal heating during plasma-surface interaction were monitored by thermal imaging using an IR camera (FLIR i7) during the treatment and up to a minute post-treatment, and by photographs of the treatment surface on mice skin immediately after the plasma treatment and by a follow-up of the treated zone of each mouse (as well as the weight and behaviour of each mouse, according to end-point criteria) up to two weeks post-treatment.

1.2.3 Results of *in vivo* toxicity of direct treatment with NTP multijet

The experimental protocol and selected results of this *in vivo* study on two mice strains are shown in *Figure* ***33*** and ***Error! Reference source not found.***. The results presented here were from the plasma treatment where the most damage effects on the skin were observed, *i.e.*, with the plasma treatment using HV pulses at 2 kHz for a treatment time of 3 minutes continuously or three times of 1-minute treatment. Other plasma parameters (500 Hz and 1 kHz) and treatment times showed no to very mild damage to the skin after the treatment.

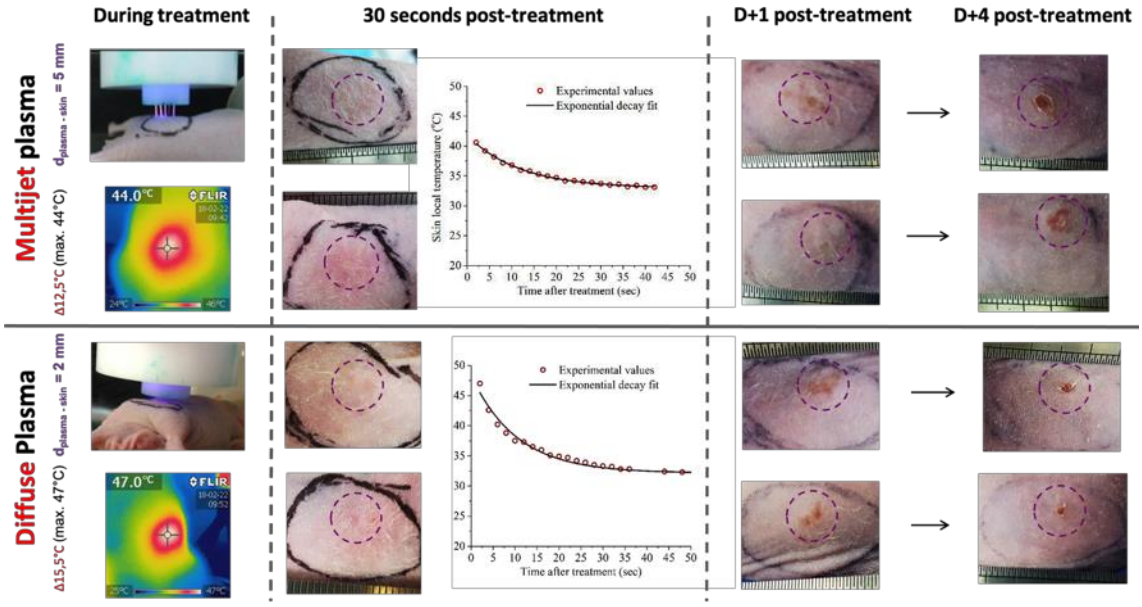

Figure 33| *In vivo* NTP direct treatments on nude mice at 2 kHz, 11 kV for 3 minutes continuously

Mice were treated with two different modes of plasma exposure: multijet mode ($d_{plasma\text{-}skin}$ = 5 mm, upper panel) and diffuse mode ($d_{plasma\text{-}skin}$ = 2 mm, lower panel), with at least two mice per condition. The potential skin effects due to thermal heating during plasma-surface interaction were monitored using an IR camera (FLIR i7) during the treatment and up to a minute post-treatment and by photographs of the treatment surface on mice skin at 30 seconds post-treatment and after one day and four days. The purple dashed circles indicate the skin zones exposed to the plasma.

When applying the most aggressive treatment protocol on mice skin, a continuous exposure of NTP set at 2 kHz for 3 minutes (*Figure* ***33***), the skin surface temperature during (and after) the plasma treatment (monitored with thermal imaging) showed a mean increase of 12,5°C for the multi-jet exposure mode and 15,5°C for the diffuse mode, with the highest surface temperature recorded during the treatment at 44°C for the multi-jet mode and at 47°C for the diffuse mode. However, as soon as the plasma treatment ceased, the temperature on the skin surface gradually dropped. After 30 seconds post-treatment, it was recorded at *ca.* 32-34°C for both plasma exposure modes of this treatment condition. The site exposed to the plasma was slightly red but dry with no blisters, except for one mouse in the group “multi-jet”

treatment where a pale colour spot was observed in the red zone, resembling a blister but without fluid (*Figure **33*** upper panel, second range of figures from the top). This pale colour spot was widened at D+1 post-treatment and formed a reddish scab a few days later.

Similar thermal skin damage effects were observed on mice of other groups of treatment (*Figure **33*** lower panel and ***Error! Reference source not found.***), in particular in four to five visible reddish spots on the skin of mice receiving the multijet plasma treatment (in a geometry reminiscent of the individual jets applied on the skin), as compared with the skin of mice receiving the "diffuse" mode where no trace of single jets was observed but a zone representing the plasma-treated area, with milder thermal effects. We also observed that nude mice skin was more affected under the same plasma treatment than C75Bl/6 mice skin. Moreover, the treatment with plasma being set at 500 Hz gave more muscle contraction in mice (muscle contraction of the leg was observed when plasma treatment was on the thigh) compared to other HV pulses (1 kHz or 2 kHz).

Given that the mouse thermal-neutral point (TNP) is *ca.* 29°C in the light phase and *ca.* 33°C in the dark phase (Škop *et al.*, 2020), the results of different treatment protocols indicated - besides the safety measurements of the temperature of the skin during and after the treatment – that direct NTP treatment was tolerable for those two mice strains with the maintenance of skin integrity - crucial to ensure mice physiology. Indeed, the red zone on the skin of all treatments described above was never bled, and it quickly formed dry red scabs the day following the treatment, which scabbed over the following week. All mice remained healthy all along with the experimentation (via monitoring mice's fur, behaviour, and weight).

As the outcome of those *in vivo* experimentations on the skin toxicity under NTP multijet treatments, we proposed optimal protocols to the Infectious Diseases Service of the Orléans Regional Hospital as:

1) **Use diffuse mode** while knowing that the appearance of individual jets is acceptable (they are almost obligatorily formed in case of skins or wounds with an irregular surface)
2) **Dose escalation**: 500 Hz then 1 kHz; if the tolerance is excellent and if the efficacy is insufficient, the 2 kHz should also be considered because the recommendations

(see point N°3) propose to start with shorter treatments than those tested in the preclinical study

3) **Exposure durations**:
    1) 1 minute, once a day
    2) Two times 1 minute (1 or 2 minutes apart), once a day
    3) Possibly 2 (or 3) minutes, once a day

The NTP multijet source will be used to develop a new medical device for advanced clinical studies.

2 Cell electropermeabilisation enhancement by plasma-treated PBS (article #2)

Before *in vivo* studies on animals, we established *in vitro* protocols of a combination treatment with indirect plasma medicine and pulsed electric fields (PEFs) on two different cell lines (DC-3F Chinese hamster lung fibroblasts and B16-F10 murine melanoma). These *in vitro* studies aimed at outperforming *in vitro* cell electropermeabilisation, the basis of ECT, at an amplitude lower than that employed in conventional ECT (*i.e.*, lower than 1300 V/cm).

We used a novel helium plasma setup based on a Plasma Gun device for the aforementioned purposes. With the set-up developed and described in **section 1 of the Results**, I prepared plasma-treated liquids using PBS 1X (Ca^{2+}, Mg^{2+}) for two different exposure times to the NTP multijet (so-called **plasma-treated PBS** or **pPBS**), which is used afterwards for *in vitro* and *in vivo* studies. A schematic illustration of the *in vitro* experimental set-ups and procedure of the combined treatment with pPBS and µsPEFs is displayed in *Figure **34***.

After preliminary results testing several conditions (data not shown), an established treatment protocol combining pPBS and µsPEFs was proposed. It significantly enhanced the cell permeabilisation level under very low electric pulse amplitudes. The design of these *in vitro* studies and their results with discussion and perspectives have been published in the journal Cancers *(Basel)* in January 2020, which is introduced below. A critical discussion of the paper with some hypotheses explaining the observed results is figured in the Discussion section. This paper paved the way for *in vivo* studies of plasma-treated liquids combined with ECT and new perspectives for their pre-clinical and clinical applications.

My contribution to this paper, as the first author, consists in the conceptualisation, the methodology, the data acquisition and validation, the data analysis and visualisation, the data interpretation, and the writing (original draft preparation, review and editing).

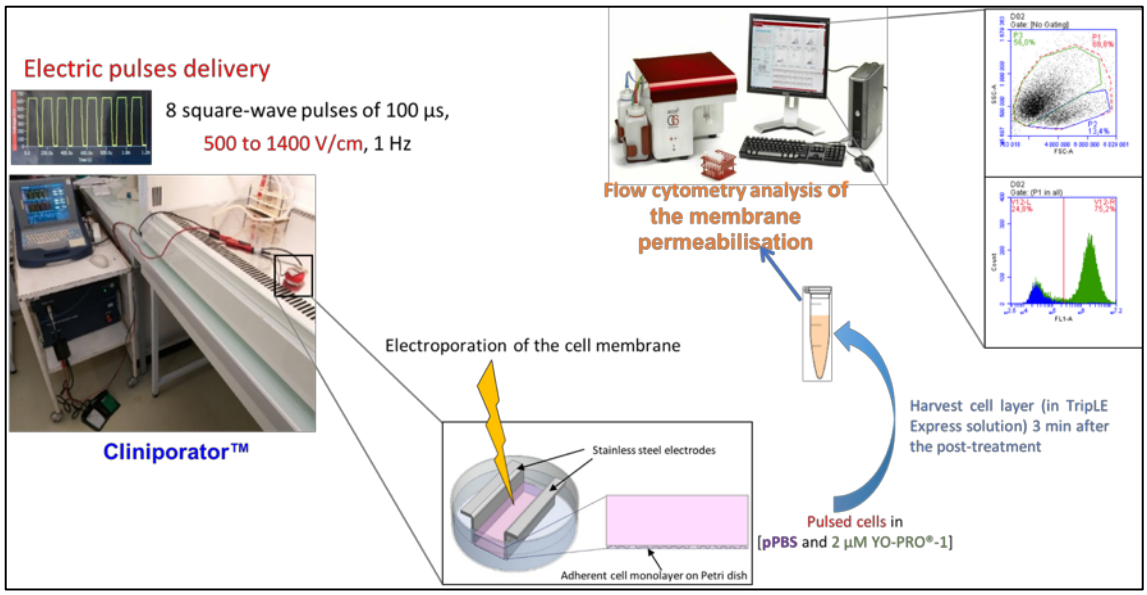

Figure 34| Schematic illustration of the *in vitro* experimental set-ups and procedure of the combined treatment with pPBS and µsPEFs

A day before the treatment, cells were seeded and cultured as a monolayer on a defined area of 2 cm^2 of Ø 35 mm Petri dishes. On the day of the treatment, after being gently washed twice with PBS 1X (Ca^{2+}, Mg^{2+}), cells were incubated at RT in pPBS in the presence of the YO-PRO®-1 Iodide (an indicator of membrane permeabilisation) and this pre-treatment time varied in different protocols. Afterwards, electric pulses were delivered to the cells (8 square-wave pulses of 100 µs, 1 Hz, amplitude ranging from 500 to 1400 V/cm) via two stainless steel parallel plate electrodes connected to the Cliniporator™. Cells were post-treated with a new treated liquid, always in the presence of YO-PRO®-1 Iodide, for a fixed incubation time of 10 minutes. After the post-treatment, the cell layer was harvested in TripLE Express solution, and the cell membrane permeabilisation was analysed by flow cytometry. Graphical abstract adapted from (Chung *et al.*, 2020).

cancers

MDPI

Article

Cell Electropermeabilisation Enhancement by Non-Thermal-Plasma-Treated PBS

Thai-Hoa Chung [1], Augusto Stancampiano [2], Kyriakos Sklias [3], Kristaq Gazeli [3], Franck M. André [1], Sébastien Dozias [2], Claire Douat [2], Jean-Michel Pouvesle [2], João Santos Sousa [3], Éric Robert [2] and Lluis M. Mir [1,*]

1 Université Paris-Saclay, CNRS, Institut Gustave Roussy, Metabolic and Systemic Aspects of Oncogenesis (METSY), 94805 Villejuif, France; Thai-Hoa.CHUNG@gustaveroussy.fr (T.-H.C.); Franck.ANDRE@cnrs.fr (F.M.A.)

2 GREMI, UMR 7344 CNRS/Université d'Orléans, 45067 Orléans, France; augusto.stancampiano@univ-orleans.fr (A.S.); sebastien.dozias@univ-orleans.fr (S.D.); claire.douat@univ-orleans.fr (C.D.); jean-michel.pouvesle@univ-orleans.fr (J.-M.P.); eric.robert@univ-orleans.fr (É.R.)

3 Université Paris-Saclay, CNRS, Laboratoire de Physique des Gaz et des Plasmas, 91405 Orsay, France; kyriakos.sklias@u-psud.fr (K.S.); kristaq.gazeli@u-psud.fr (K.G.); joao.santos-sousa@u-psud.fr (J.S.S.)

* Correspondence: Luis.MIR@cnrs.fr; Tel.: +33-(0)1421-14792

Received: 20 December 2019; Accepted: 13 January 2020; Published: 16 January 2020

Abstract: The effectiveness of electrochemotherapy (ECT) in local eradication of tumours in human and veterinary medicine has been proven. ECT consists of increasing the uptake of cytotoxic drugs by means of pulsed electric fields (PEFs) that transiently permeabilise the cell membrane. Still, this tumour treatment includes some drawbacks that are linked to the characteristics of the intense electric pulses (EPs) used. Meanwhile, the emerging field of cancer therapies that are based on the application of non-thermal plasmas (NTP) has recently garnered interest because of their potentialities as rich sources of reactive species. In this work, we investigated the potential capabilities of the combined application of indirect NTP treatment and microsecond PEFs (μsPEFs) to outperform in vitro cell electropermeabilisation, the basis of ECT. Thus, phosphate-buffered saline (PBS) was plasma-treated (pPBS) and used afterwards to explore the effects of its combination with μsPEFs. Analysis of two different cell lines (DC-3F Chinese hamster lung fibroblasts and malignant B16-F10 murine melanoma cells), by flow cytometry, revealed that this combination resulted in significant increases of the level of cell membrane electropermeabilisation, even at very low electric field amplitude. The B16-F10 cells were more sensitive to the combined treatment than DC-3F cells. Importantly, the percentage of permeabilised cells reached values similar to those of cells exposed to classical electroporation field amplitude (1100 V/cm) when the cells were treated with pPBS before and after being exposed only to very low PEF amplitude (600 V/cm). Although the level of permeabilisation of the cells that are treated by the pPBS and the PEFs at 600 V/cm is lower than the level reached after the exposure to μsPEFs alone at 1100 V/cm, the combined treatment opens the possibility to reduce the amplitude of the EPs used in ECT, potentially allowing for a novel ECT with reduced side-effects.

Keywords: cancer; non-thermal atmospheric pressure plasma (NTP); plasma medicine; indirect treatment; plasma-treated phosphate-buffered saline; electroporation; electric pulses; pulsed electric field amplitude; melanoma; long-lived reactive species

1. Introduction

Electrochemotherapy (ECT) is a non-thermal, safe, and efficient tumour treatment [1–4] that is currently used in more than 150 clinics in the European Union and abroad, together with its application

in veterinary oncology for treatment of metastases as well as primary tumours [5,6]. ECT is based on the combination of otherwise non- or low-permeant drugs possessing a high intrinsic cytotoxicity (*e.g.*, hydrophilic molecules such as bleomycin or cisplatin) with the local application of a train of eight short and intense monopolar electric pulses (EPs), yet nontoxic [7,8]. The applied EPs create a transient transmembrane potential difference that causes changes in the cell membrane structure and transiently permeabilise its phospholipid bilayer [7]. This biophysical process, which is named reversible electroporation or reversible electropermeabilisation, allows for the penetration of the chemotherapeutic agent inside the cell to generate irreversible DNA damages.

ECT selectively kills the tumour cells at the low doses of the chemotherapeutic agents used, since bleomycin (BLM, of 1415 Da) at low doses is only toxic for the cells dividing in the volume treated by the EPs. Overall, no serious negative effects that are related to the application of ECT on patients have ever been reported. Nevertheless, one of the main drawbacks of ECT application are muscles contraction with discomfort sensations associated with repeated electrical stimulation, mainly linked to the characteristics of the high-amplitude electric pulses used. Indeed, these EPs depolarise the neurons in the treated area and can, therefore, generate action potentials, either in the musculo-excitatory nerves or in the sensory nerves, imposing the use of at least a local anaesthesia during the treatment [9]. Recent clinical studies have reported that the painful sensation that is associated to ECT can last longer for locally advanced and metastatic soft tissue sarcomas [10] and large cutaneous recurrences of breast cancer [11].

The main objective of the present study was, therefore, to determine new conditions for ECT, devoid of these side effects. We were interested in reducing the electric field strength of the classical 100 microseconds pulses used in ECT, without reducing the permeabilisation of the cell membrane. We suggest a combined treatment of µsPEFs with non-thermal plasma (NTP) to outperform ECT since cell electropermeabilisation is characterised by lipids oxidation at the time of the electric pulses delivery [12]. Indeed, NTP can be a source of reactive species favouring the lipid oxidation reactions. Over the last decade, several studies in the plasma medicine field have pointed out the use of plasmas at atmospheric pressure in oncology, as plasmas offer the possibility to achieve cell membrane permeabilisation [13,14] as well as to selectively kill cancer cells without affecting normal cells [15–17]. Nowadays, NTP are broadly used not only in preclinical development of anticancer therapies, including malignant melanoma, ovarian, colorectal, liver, lung, hepatoma, breast, and brain cancers [18], but also in clinical studies [19]. The virtue of NTP relies on the abundant production of reactive species that were primarily generated upon plasma-air interactions: reactive oxygen species (ROS), such as superoxide ($O_2^{\bullet -}$), hydroxyl radicals (OH$\bullet$), atomic oxygen (O_2), singlet delta oxygen ($^1O_2$), ozone (O_3), and hydrogen peroxide (H_2O_2), as well as reactive nitrogen species (RNS), such as nitric oxide (NO), nitrogen dioxide (NO_2), nitrogen trioxide (NO_3), nitrous oxide (N_2O), dinitrogen tetroxide (N_2O_4), and also positive ions, such as dinitrogen (N_2^+) [20]. Two general NTP strategies are defined for cancer treatment: direct treatment and indirect treatment. The first approach consists of a direct treatment of cancer cells or tumours with the NTP source, where the gaseous plasma species and the plasma-induced electric field have direct actions on the surface of the targets. The second approach implicates an indirect treatment, where the plasma source is used to treat liquids (cell culture media, water, or physiological solutions) and the biological targets are subsequently exposed to the plasma-treated liquids [16,21–24]. Some of the long-lived ROS and RNS (also known as RONS) that are generated in the plasma-treated liquids (such as hydrogen peroxide, nitrite and nitrate) are known to play a major role in the oxidation of phospholipid bilayers of the cell membrane [25,26]. We speculate that the NTP caused oxidative stress might be an important factor in augmenting the efficacy of the electroporation-based therapies.

Thus, the improvement of cell membrane permeabilisation by the combination of indirect plasma treatment and µsPEFs was explored. Furthermore, we were interested in eventual different responses of two different cell lines to the proposed combined treatment. The study was especially focused on malignant melanoma cells, a very aggressive skin cancer, which is one of the main targets of ECT [8,27–29] and plasma medicine [17,30]. For this purpose, we used a novel NTP setup that was able

to create multiple plasma jets and, therefore, offer a larger and more homogeneous surface treatment. We also implemented a compensation circuit to change the electrical impedance of in vitro targets to that of a reference model for the human body based on our recent studies on the sample influence on plasma characteristics [31]. This setup was used for the plasma treatment of phosphate-buffered saline (PBS) with Ca^{2+}/Mg^{2+} ($PBS^{+}/_{+}$). The responses to the combined treatment of the plasma-treated $PBS^{+}/_{+}$ (or pPBS) with pulsed electric fields of different strengths were investigated while using adherent DC-3F Chinese hamster lung fibroblasts and adherent malignant B16-F10 murine melanoma cells. Cell membrane permeabilisation was monitored by flow cytometry. The obtained results demonstrate the great potential of the combination of indirect NTP application and µsPEF delivery for cancer treatment.

2. Results

We tested the cytotoxic effect of pPBS alone to define favourable initial conditions under which cells would not be excessively harmed by the pPBS prior to the assessment of the effect of the combined treatment (pPBS and EPs). The first assay combining pPBS produced at +7 kV and µsPEF with an amplitude of 1100 V/cm was performed in DC-3F fibroblasts. The results, as shown in Appendix A as a proof of concept, give an initial evaluation of the potential effect of indirect plasma treatment and external electric field pulses. Following these preliminary results, the combined effect of pPBS with PEF was investigated in more detail after the pPBS was further characterised and the experimental conditions were optimised and shown to be reproducible.

2.1. Evaluation of the Reactive Species in the Plasma-Treated $PBS^{+}/_{+}$

We explored the conditions where the NTP multi-jet source used for the preparation of pPBS would be stable, easy to apply, and its characteristics reproducible over all the treatments of the $PBS^{+}/_{+}$, as well as the chemical composition of the resulting pPBS reproducible.

2.1.1. Reactor Electrical Characteristics

3 mL of $PBS^{+}/_{+}$ were treated by the NTP that was produced with the multi-jet source. Different treatment times between 1 and 20 min. were studied. The reactor was driven by positive high voltage pulses of either +7 kV or +11 kV peak amplitudes. For both voltage amplitudes, the electrical current of the discharge was monitored continuously during the treatment. The electrical measurements (Figure 1) revealed that the treatment corresponding to +11 kV peak voltage was more stable than that of +7 kV peak voltage over the whole treatment duration. In the frame of this analysis, high-definition videos of the NTP multi-jet operated at +7 kV and at +11 kV (see Videos S1 and S2 in Supplementary Materials) were also recorded, furthermore supporting the higher stability of the NTP multi-jet at +11 kV. Thus, this value was chosen as the operating voltage to produce plasma-treated $PBS^{+}/_{+}$.

2.1.2. Characterisation of the Plasma-Treated $PBS^{+}/_{+}$

The concentration of hydrogen peroxide, which is a key player for the peroxidation of lipids [21,32], was first assessed in pPBS prepared while using the NTP setup 1 described in the Materials and Methods. The concentration of H_2O_2 increased almost linearly with the treatment time for both voltage amplitudes studied here, i.e., +7 and +11 kV. On top of that, at +11 kV, the concentration of H_2O_2 in the pPBS is up to three-fold higher than that in the pPBS that results from a treatment at +7kV (Figure 2a).

After the collection of the proof of concept (Appendix A) and the optimisation of the NTP setup 1, as described in the Materials and Methods (resulting in NTP setup 2), we performed a precise dosimetry of the predominantly stable secondary RONS generated in the pPBS (H_2O_2, NO_2^-, and NO_3^-) as a function of the plasma treatment time (Figure 2b). The reactive radicals accumulation in the pPBS was time-dependant, being the highest when the plasma treatment was the longest (20 min, see Figure 2).

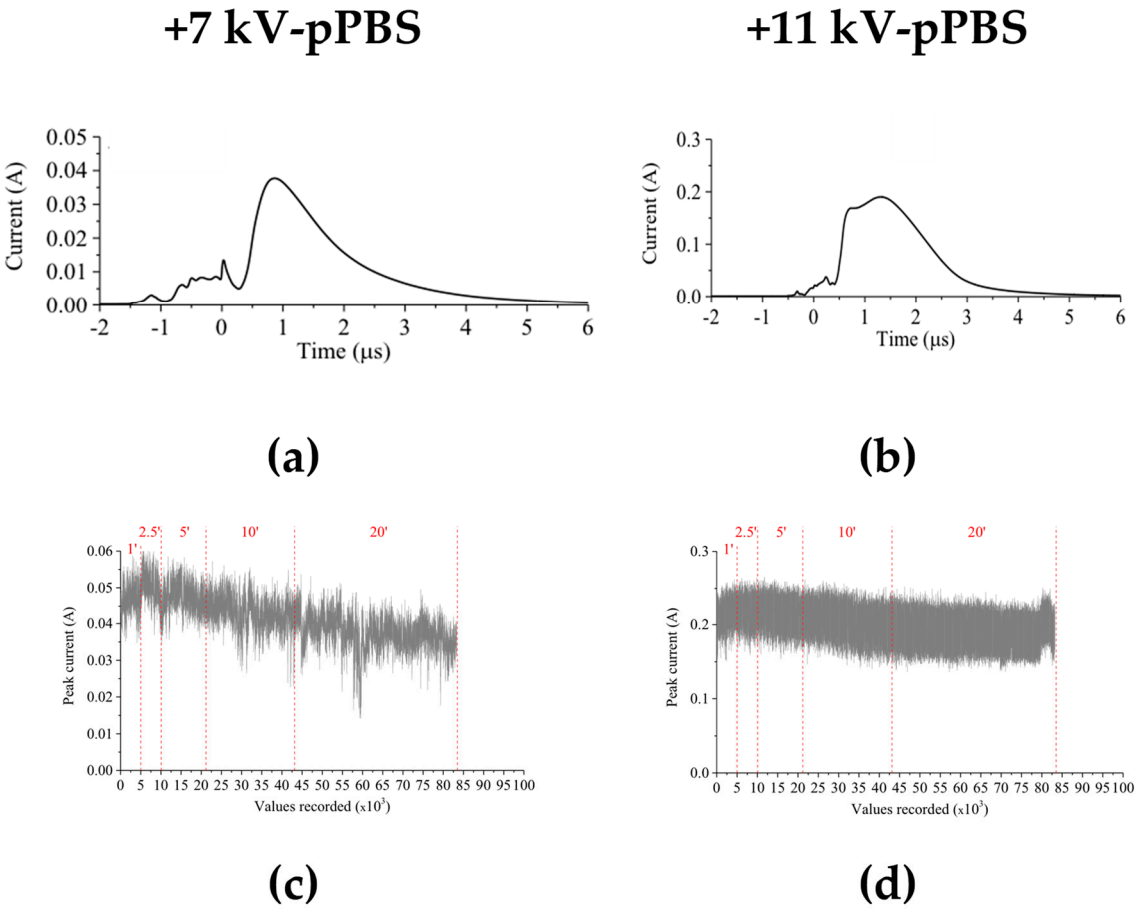

Figure 1. Assessment of the electrical characteristics of the non-thermal plasma (NTP) multi-jet source during 20 min. treatment of $PBS^{+}/_{+}$ at +7 kV (**a**,**c**) and + 11 kV (**b**,**d**) pulses peak values. Current signals, averaged from 128 single recordings (**a**,**b**) and the evolution of the maximum current (**c**,**d**) were measured during the treatment process.

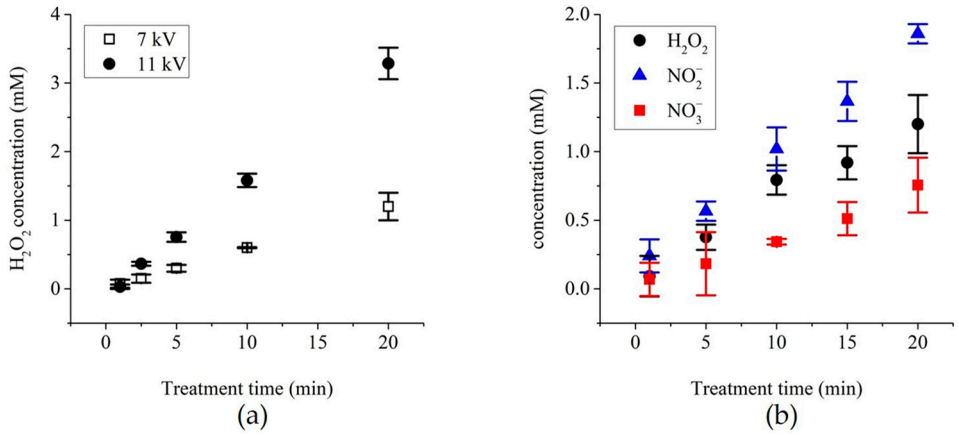

Figure 2. Chemical analysis of the plasma-treated PBS (pPBS) prepared with the NTP multi-jet source using (**a**) NTP setup 1 and (**b**) NTP setup 2. (**a**) The evolution of the concentration of H_2O_2 in +7 kV- and +11 kV-pPBS as a function of the treatment time with the plasma, (**b**) Dosimetry of H_2O_2, NO_2^-, and NO_3^- levels in $PBS^{+}/_{+}$ treated during 20 min. at +11 kV. Data are presented as mean values ± SD of independent duplicates ((**b**): 1, 5, and 15 min.) or triplicates (all other points).

Finally, the pH and the conductivity (σ) of the sham ($PBS^{+}/_{+}$ exposed to only the helium flow (no plasma) and compensated for the evaporation with distilled water) and the pPBS after 20 min.

of treatment at either +7 kV or +11 kV were also evaluated (Table 1). When compared to the sham, the pPBS displayed a slightly reduced pH and increased conductivity at both +7 kV and +11 kV. The pPBS produced with the plasma source at +11 kV displayed a lower pH and a higher conductivity than that generated at +7 kV.

Table 1. pH and conductivity (σ) of the control (sham) and the pPBS at +7 kV and +11 kV for a $PBS^{+}/_{+}$ treatment time of 20 min. Data are presented as mean values ± SD of independent quadruplicates.

	Control (sham)		+7 kV pPBS		+11 kV pPBS	
	Mean	**SD**	**Mean**	**SD**	**Mean**	**SD**
pH	7.18	0.05	6.68	0.02	6.24	0.10
σ (S/m)	10.7	0.08	11.27	0.21	13.08	0.27

The plasma treatment time of 20 min. was selected as the condition to use for the preparation of pPBS for all of the following experiments and pPBS was therefore further analysed. The storage temperature and stability overtime of pPBS were investigated (Figure 3). No significant degradation of the previously mentioned RONS was observed over 14 days for a storage temperature of +4 °C.

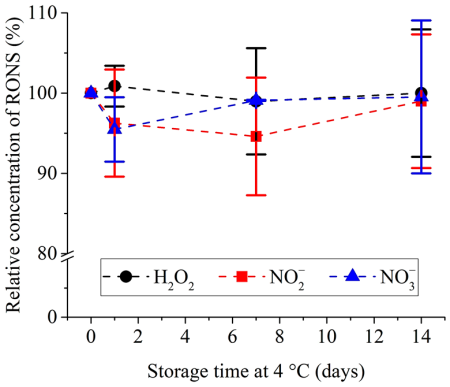

Figure 3. Relative concentration of H_2O_2, NO_2^- and NO_3^- in pPBS treated with NTP setup 2 at +11 kV during 20 min. and stored afterwards at +4 °C for up to 14 days. The reference (100%) is the concentration measured after plasma treatment at day 0. Data are presented as mean values ± SD of independent quadruplicates.

Altogether, the above results assist in the definition of the optimal NTP multi-jet parameters for the production of the pPBS used in our experiments with cells. Thus, the voltage amplitude of +11kV and the plasma treatment time of 20 min. were used for the chemical activation of the $PBS^{+}/_{+}$, which was subsequently stored at +4 °C for up to 14 days.

2.2. Investigation of the Effects of the Combined Treatment on DC-3F Chinese Hamster Lung Fibroblasts

Adherent DC-3F Chinese hamster lung fibroblasts were exposed to µsPEF of various amplitudes, 0 V/cm (i.e., no PEF), 600 V/cm, and 1100 V/cm. The µsPEFs were combined with different pre- and/or post-treatments either with sham or with pPBS, as described in Figure 4.

The permeabilisation of the cell membrane was analysed by flow cytometry while using YO-PRO®-1 iodide. This approach allows for the determination of the percentage of permeabilised cells (Figure 5a) and the intracellular fluorescence per cell (Figure 5b). In the conditions where no PEF was applied to the cell monolayer (0 V/cm), a slight increase of the YO-PRO®-1 uptake was observed in the cells treated while using protocols 2, 4, or 6, as compared to those that were treated with sham. The increase in the intracellular fluorescence intensity of the dye was significant in the case of protocols 2 and 6. When a µsPEF of 1100 V/cm was applied, the percentage of permeabilised cells increased in all of the groups and no significant increase in the percentage of electropermeabilised

DC-3F cells was caused by the pPBS treatment, regardless of the treatment protocol (Figure 5a). However, we remarked a significant increase of up to 2.4-fold of the intracellular fluorescence in cells that were treated while using protocol 5, when compared to all of the other protocols and, in particular, to the control (Figure 5b). At 600 V/cm, the results were just the opposite: with respect to the PEF alone, no significant enhancement of the intracellular fluorescence of YO-PRO®-1 iodide uptake was caused by the pPBS, regardless of the treatment protocol, but the percentage of electropermeabilised cells displayed a significant increase in the population of cells that were treated under protocols 3, 5, and 6 as compared to the control. Indeed, while only ca. 30 to 35% of cells treated while using sham were permeabilised at 600 V/cm, the population of permeabilised cells treated using protocol 6 was increased by almost 1.7-fold (+69%) and that of the cells treated using protocol 5 was the double (2-fold enhancement). There is no statistically significant difference between protocols 5 and 6. Remarkably, for protocol 5 at 600 V/cm, c.a. 60 to 70% of the treated cells were permeabilised, reaching the same percentage of permeabilised cells as that of the cells in the control that was only exposed to µsPEFs at 1100 V/cm.

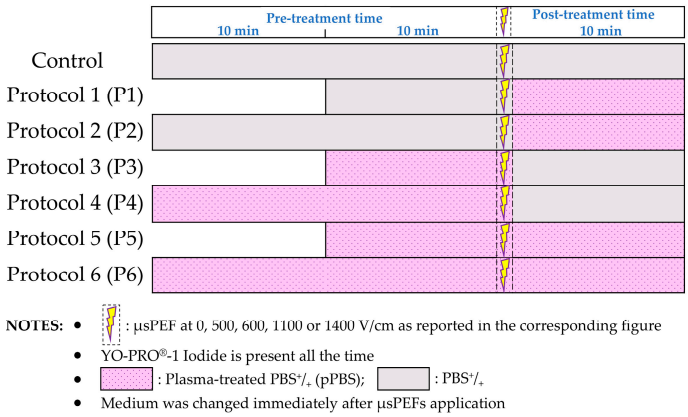

Figure 4. Schematic illustration of the protocols applied in the combined treatments, with µsPEF at 0, 500, 600, 1100 or 1400 V/cm.

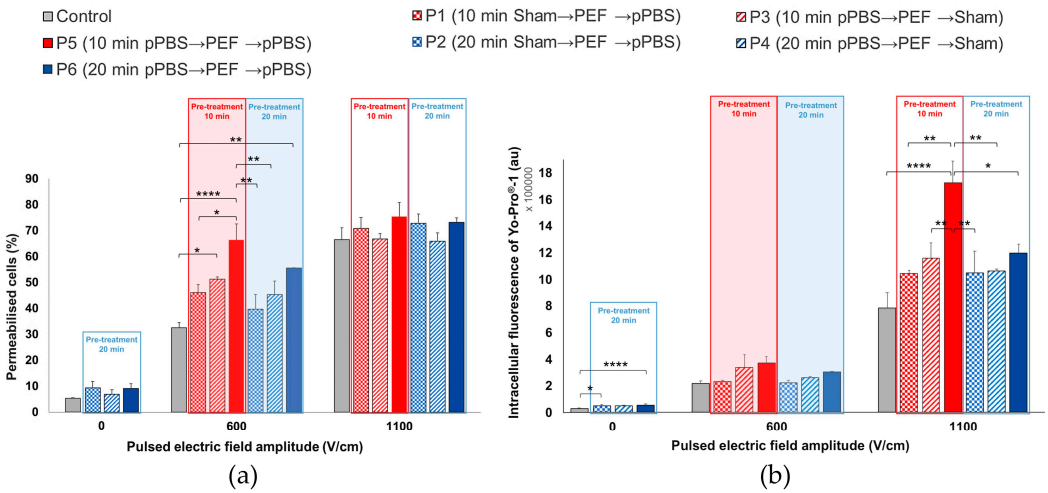

Figure 5. Effects of the combined treatment on DC-3F fibroblasts at 0, 600, and 1100 V/cm. (**a**) Percentage of electropermeabilised cells and (**b**) intracellular fluorescence of YO-PRO®-1 iodide entering the cells as a function of the 7 combined protocols applied. The data are presented as mean (for **a**) and median (for **b**) values ± SD of independent triplicates. Statistical differences were analysed while using One-way ANOVA followed by Bonferroni's multiple comparison test. * $p < 0.05$, ** $p < 0.01$, and **** $p < 0.0001$ significant differences.

2.3. Investigations of the Effects of the Combined Treatment on B16-F10 Murine Melanoma Cells

2.3.1. Comparison of the Effect of µsPEF at 600 V/cm versus 1100 V/cm on B16-F10 Cells

We investigated the effect of the combined treatment on B16-F10 melanoma cells while using the same seven protocols of the previous section (Figure 6). Even without any PEF applied, a significant increase of the intracellular fluorescence intensity of the dye was detected for protocols 2, 4, and especially protocol 6. For this protocol 6, even the percentage of permeabilised cells displayed a significant two-fold enhancement as compared to the control. Using PEFs at 1100 V/cm, the percentage of electropermeabilised cells was not statistically different from the control without pPBS, except for protocol 4, which was significantly lower. However, with protocols 5 and 6, a significant increase of up to 2.66-fold of the intracellular fluorescence of YO-PRO®-1 iodide was observed as compared to the control. When applying a 600 V/cm PEF, the pre- and post-treatment of cells with pPBS (protocols 5 and 6) induced a significant enhancement of the cell membrane electropermeabilisation, both in the percentage of electropermeabilised cells (up to a 1.8-fold enhancement) and in the fluorescence intensity per cell (up to a two-fold enhancement). There is no statistically significant difference between protocols 5 and 6, both inducing strong cell permeabilisation increase, reaching the same percentage of permeabilised cells as that of the cells that were exposed to 1100 V/cm in the absence of pPBS. We also observed a significant enhancement of the YO-PRO®-1 iodide intracellular fluorescence in the cells that were treated at 600 V/cm while using protocol 4, i.e., with only a pre-treatment with pPBS for 20 min.

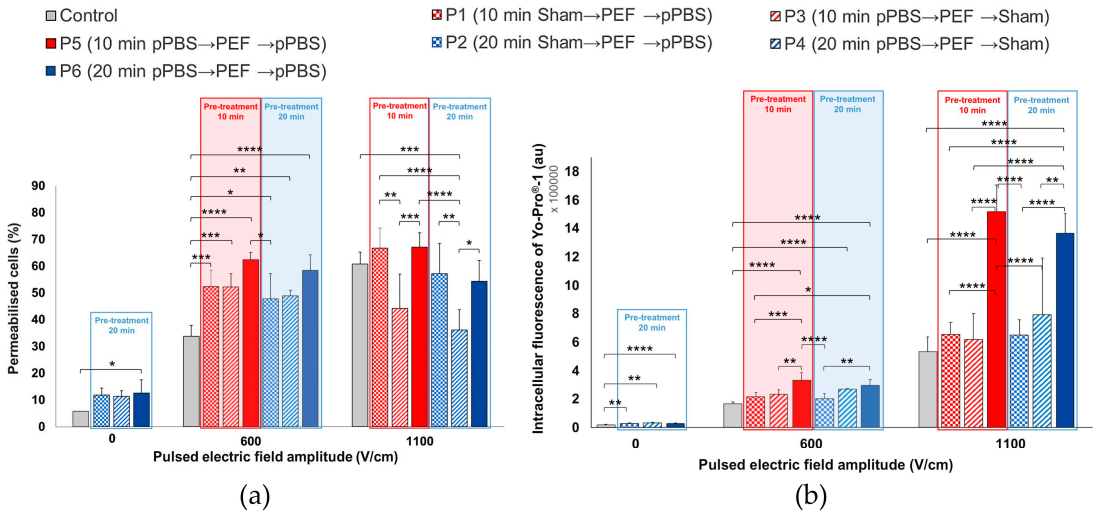

Figure 6. Effects of the combined treatment on malignant B16-F10 melanoma cells using µsPEF at 0, 600, and 1100 V/cm. (**a**) Percentage of electropermeabilised cells and (**b**) intracellular fluorescence of YO-PRO®-1 iodide entering the cells as a function of the seven combined protocols applied. Data are presented as mean (for **a**) and median (for **b**) values ± SD of independent triplicates. Statistical differences were analysed while using One-way ANOVA followed by Bonferroni's multiple comparison test. * $p < 0.05$, ** $p < 0.01$, *** $p < 0.001$, and **** $p < 0.0001$ significant differences.

2.3.2. Comparing the Effect of 500 V/cm versus 1400 V/cm µsPEF on B16-F10 Murine Melanoma Cells

The two previous sections show different behaviours of the two cell lines, particularly in the case of the median intracellular fluorescence while using pPBS and µsPEFs of 600 V/cm amplitude. With the B16-F10 cells being apparently more sensitive to the µsPEF than the DC-3F cells, we decided to investigate the consequences of the application of the seven protocols using µsPEF of only 500 V/cm amplitude. It was also of interest to explore the consequences of using µsPEFs of high field amplitude, as for instance 1400 V/cm, anticipating a larger cell permeability. In this last case, the YO-PRO®-1 iodide concentration was reduced to 1µM (instead of 2 µM) to avoid a saturation of the flow cytometer signals.

Once more, when no PEF was applied, simple treatment of the B16-F10 cells with pPBS induced a statistically significant increase, not only in the percentage of permeabilised cells but also in the intracellular fluorescence of YO-PRO®-1 iodide. Regarding the percentage of permeabilised cells that were treated with pPBS alone, we observed significant increases when compared to the control: two-fold using protocol 2, 2.2-fold using protocol 4, and 2.8-fold using protocol 6 (Figure 7a). Concerning the intracellular fluorescence of YO-PRO®-1 iodide (Figure 7b), we observed a significant 1.7-fold enhancement while using protocol 6, which also showed statistically significant differences with protocols 2 and 4 (there is no statistical difference between protocols 2 and 4 as compared to the control).

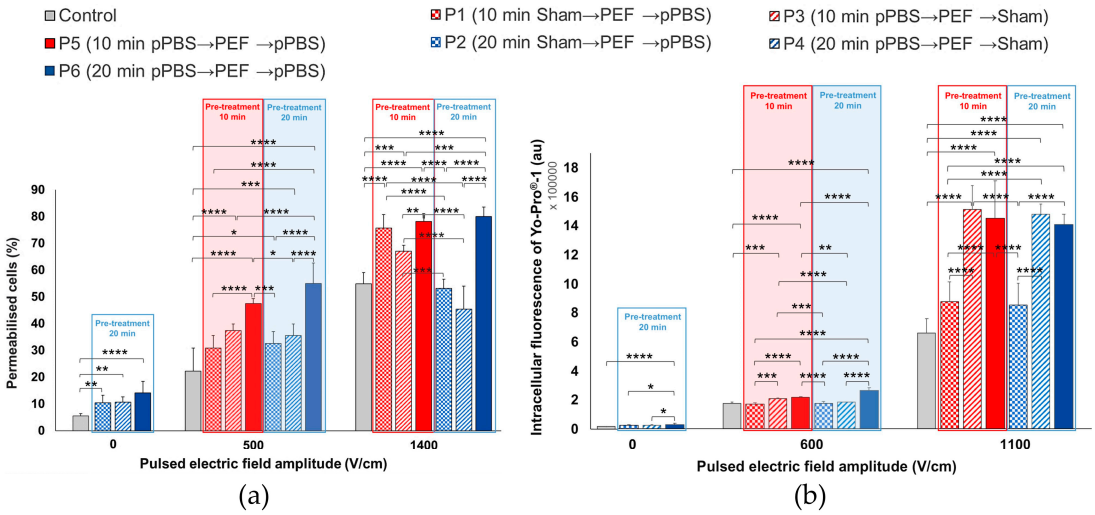

Figure 7. Effects of the combined treatment on adherent malignant B16-F10 melanoma cells using µsPEF at 0, 500, and 1400 V/cm. (**a**) Percentage of electropermeabilised cells and (**b**) intracellular fluorescence of YO-PRO®-1 iodide entering the cells as a function of the seven combined protocols applied. Data are presented as mean (for **a**) and median (for **b**) values ± SD of independent triplicates. Statistical differences were analysed using One-way ANOVA followed by Bonferroni's multiple comparison test. * $p < 0.05$, ** $p < 0.01$, ***, $p < 0.001$, and **** $p < 0.0001$ significant differences.

At 1400 V/cm, when compared to the control, a significant enhancement of the cell membrane permeabilisation level was observed in cells that were treated while using protocols 1, 3, 5, and 6 in what regards the number of permeabilised cells (up to a 1.5-fold enhancement) (Figure 7a) and while using protocols 3, 4, 5, and 6 in what concerns the intracellular fluorescence of YO-PRO®-1 iodide entering the cells (up to a 2.2-fold enhancement) (Figure 7b). No statistically significant difference between protocols 5 and 6 was found at 1400 V/cm. Concerning the PEFs at 500 V/cm, all of the combinations (except protocol 1) resulted in a significant enhancement of the percentage of electropermeabilised cells with respect to the control. The intracellular fluorescence intensity also significantly increased while using protocols 3, 5, and 6 as compared to the control. At this very low µsPEF amplitude and with these cells sensitive to the pPBS alone, a statistically significant difference between protocols 5 and 6 (i.e., between a total contact time of 20 and 30 min. between the cells and the pPBS) was found in the intracellular fluorescence intensity.

Figure 8 illustrates the observed differences in the membrane permeabilisation level of B16-F10 melanoma cells due to the combined treatment. The fluorescence threshold for permeabilised cells was determined from the cells that were treated with sham (the control cells exposed to untreated $PBS^{+}/_{+}$) and not exposed to PEF (Figure 8a). We noticed that, even though no PEF was applied (0 V/cm), a slight shift towards higher values of the fluorescence per cell (indicating an increase in membrane permeability) was already present in the population of cells that were treated while using protocol 6 (pre- and post-treatment with pPBS) (Figure 8e when compared to Figure 8a). This corresponds to the significant enhancement of membrane permeabilisation that was observed in Figures 6a and 7a

induced by pPBS alone. This shift was larger when low amplitude µsPEFs were applied to the cells using protocol 6 at 500 V/cm (Figure 8f) and 600 V/cm (Figure 8g). At 1100 V/cm (Figure 8h), this shift was much larger and actually the population of positive cells constituted a separate peak. The very high level of fluorescence brought by the PEFs at 1100V/cm indicates a high permeabilisation level, being in agreement with the statistically significant enhancement of the membrane electropermeabilisation levels that were observed in Figures 6 and 7.

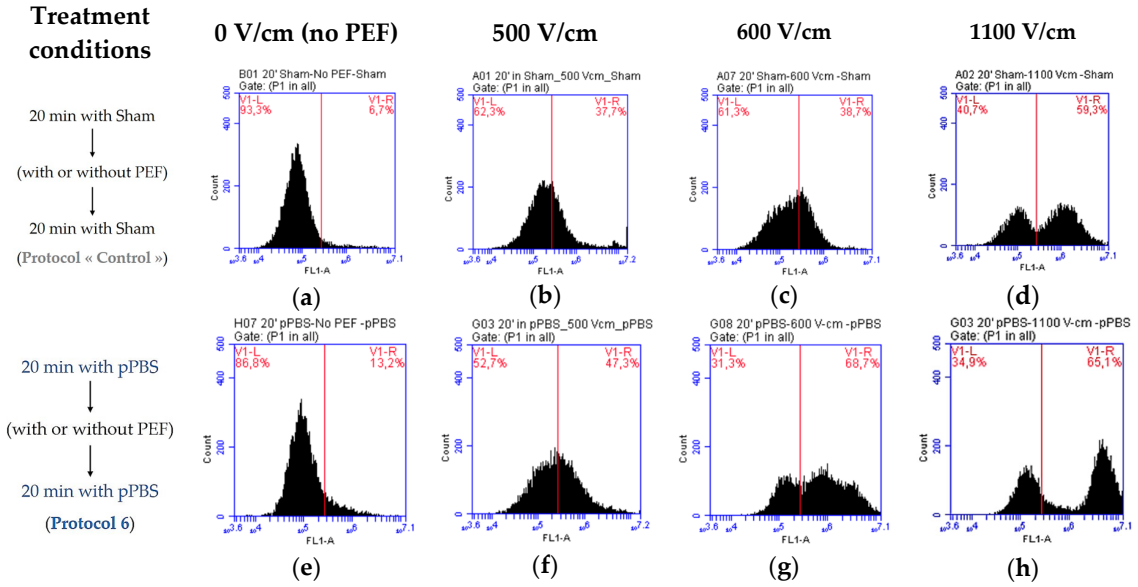

Figure 8. Flow cytometry analysis of a few interesting conditions of the combined treatment in adherent B16-F10 murine melanoma cells to compare effects of protocol 6 (**e**–**h**) versus the control (**a**–**d**) with µsPEFs of 0 (**a**,**e**), 500 (**b**,**f**), 600 (**c**,**g**), and 1100 (**d**,**h**) V/cm. The peak of count as a function of the green fluorescence (FL1-A) shifts towards higher values of the fluorescence per cell, indicating the enhancement of the permeabilisation of the cell membrane.

3. Discussion

In this study, the potential effects of a treatment combining plasma-treated $PBS^{+}/_{+}$ (pPBS) and monopolar microsecond pulsed electric fields (µsPEFs) on two different cell lines were investigated. The indirect use of the NTP, by means of the application of pPBS, allowed for us to treat the cells in a very homogenous way. The use of parallel plate electrodes encompassing the whole cell monolayer also brought very homogeneous conditions for the cells' treatment by the µsPEFs. Finally, great care was put on the cell culture conditions before the application of the pPBS and/or the µsPEFs in order to have homogeneous subconfluently (at ca. 80% density) monolayers. Therefore, all of the conditions were gathered to make possible comparisons between the various protocols that were used in our study.

The combination of the µsPEF and the pPBS aimed at the reduction of the applied electric field strength (without decreasing the cells electropermeabilisation) and/or the enhancement of the electropermeabilisation level of the cell membrane. The range of intensities of the µsPEF that was used in our study has already been demonstrated as non-cytotoxic [33,34]. The work reported in the results section was performed with a setup optimised, as described in the results section and in [31] (NTP setup 2), after establishing the proof of concept (Appendix A) with a new NTP multi-jet setup that was recently developed by our group to homogeneously treat large surfaces (NTP setup 1). The NTP setup 2 produced pPBS with reproducible characteristics due to well-controlled exposure of the $PBS^{+}/_{+}$ and allowed for us to examine possible differences in the pPBS effects on the two different cell lines used in this study. Our results indicate that the DC-3F cells are less sensitive than the B16-F10 cells to the pPBS alone. Nevertheless, a statistically significant increase in the intracellular concentration of the YO-PRO®-1 could be detected in DC-3F cells, even though the pPBS treatment did not suffice

for significantly increasing the percentage of permeabilised cells. A low µsPEF intensity (600 V/cm) combined with a pre- and post-treatment of cells with pPBS favours the permeabilisation of cell membrane and doubles the population of permeabilised cells (as compared to the exposure to only µsPEFs of the same intensity). Furthermore, this combined treatment allows for reaching the same percentage of permeabilised cells as a treatment with µsPEFs alone at 1100 V/cm. However, the level of the intracellular fluorescence is not comparable: this level is much lower at 600 V/cm (even in combination with the pPBS) than at 1100 V/cm. At 1100 V/cm, a further increase, significant (over two-fold enhancement), in the intensity of the fluorescence per cell was observed when the µsPEFs were combined with a pre- and post-treatment of the cells with pPBS. All of these increments reveal an increase of the level of electropermeabilisation by the pPBS.

For the comparison with the DC-3F cells, experiments were also performed with the "cancerous" B16-F10 melanoma cells whose size is larger than that of DC-3F cells. This cell size difference is known to play an important role in the cell membrane electropermeabilisation level [35,36]. Therefore, B16-F10 cells were expected to be more sensitive than the DC-3F cells when exposed to µsPEF of the same amplitude. This was indeed observed at 1100 V/cm, since the median intracellular fluorescence of the B16-F10 cells (about 1.8×10^6 a.u.) was higher than that of the DC-3F cells (0.8×10^6 a.u.), in the absence of pPBS application (Figures 5b and 6b, control conditions). When applying PEFs at low field amplitudes (600 V/cm), this consequence was also noticed (median intracellular fluorescence of 0.55×10^6 a.u. for the B16-F10 cells versus 0.22×10^6 a.u. for the DC-3F cells). These data also point out the increase of the median intracellular fluorescence of both cell lines with higher PEFs intensities. This trend is also observed when the individual flow cytometry diagrams are analysed (Figure 8c versus Figures 8d and 8g versus Figure 8h). The results on the percentage of permeabilised cells also show that B16-F10 cells seem to be more sensitive to both treatments. With a single treatment with pPBS (protocol 6, i.e., 30 min. of total contact time between cells and pPBS) without any PEF application, the percentage of permeabilised B16-F10 cells (Figures 6a and 7a) is significantly higher than the untreated cells (two-fold enhancement), while no statistical difference was found in the case of the DC-3F cells (Figure 5a). At 1100 V/cm for both cells, when the percentage of the µsPEF-permeabilised cells was already very high, this percentage was not increased by the pPBS, regardless of the treatment protocol. Interestingly, when the percentage of µsPEF-permeabilised cells was low (at 600 V/cm for the DC-3F cells and 500 V/cm for the B16-F10 cells—see below), the application of the pPBS resulted in an increase of the percentage of permeabilised cells. Moreover, in a first approximation, the longer the total treatment time with the pPBS, the higher that increase. In the case when the B16-F10 cells were exposed to 1400 V/cm, protocols 5 and 6 again revealed an increase in this percentage, as well as an increase in the intracellular fluorescence intensity, caused by the pPBS application. We can speculate that the increase by pPBS in the cells permeabilisation at 1400 V/cm could be related to the occurrence of longer or irreversible electroporation, which would cause a larger uptake of the YO-PRO®-1 iodide by the electroporated cells. To conclude, a pre- and post-treatment of cells with pPBS enhances the membrane electropermeabilisation level for most of the combined treatment protocols with PEFs of 600 to 1400 V/cm amplitude. The oxidative stress that was generated within the phospholipid bilayer of the cells by the radicals brought by the pPBS could mediate this effect. Moreover, a period of 10 min. of pre-treatment of cells with pPBS (protocol 5) is sufficient for starting to generate these effects.

Experiments were repeated at 500 V/cm with the malignant B16-F10 melanoma cells to be under the same extremely low permeabilisation levels by PEF alone as those of the DC-3F cells that were treated at 600 V/cm. Interestingly, even at this low µsPEF amplitude, 10 min. of pre-treatment with pPBS (protocol 3) could already achieve an increase in both the percentage of the µsPEF-permeabilised cells and the intracellular uptake of the dye. A combination of both pre- and post-treatment with pPBS (protocols 5 and 6) strongly induced these effects. Especially, 30 min. of total contact time between the cells and pPBS (protocol 6) resulted in the same percentage of µsPEF-permeabilised cells as the controls µsPEF only treated at 1100 V/cm or 1400 V/cm.

It is worth mentioning that pPBS should affect all of the cells, although slightly, because radicals are present throughout the whole volume of the pPBS in contact with the cells, while µsPEF, particularly at low field amplitudes, should only strongly affect part of the cells (those whose size and geometry allows for locally generating a sufficiently high transmembrane voltage difference). In this respect, we can underline that, regardless of the µsPEF strength applied, it was never observed an entire electropermeabilisation of the cell population for both cell lines studied (i.e., the percentage of electropermeabilised cells did not reach 100% in any of the cell lines that were tested at any treatment condition). This result agrees with most of the in vitro electroporation studies, where the viability of most of the cells is sought [34,35].

Multiple research groups discussed the critical influence of both cell type and cancer type on the cell sensitivity to indirect plasma treatment [16,17,37,38]. On the other hand, it has been documented that different cell types have different responses to oxidative stress [39] or PEFs/electrochemotherapy/electroporation-based therapies [35,36,40,41]. From the "electropermeabilisation" point of view, the most important factor is the size of the cells. Microscope images easily show that the B16-F10 cells are larger than the DC-3F cells. Therefore, it was expected that, in this study, for the B16-F10 cells, lower field amplitudes (500 V/cm) would be necessary to electropermeabilise them to the same extent as the DC-3F cells at 600 V/cm. What we could not anticipate was the increased sensitivity of the B16-F10 cells to the pPBS alone. While the various protocols with pPBS in the absence of PEFs only resulted in a higher intracellular uptake of the YO-PRO®-1 for the DC-3F cells, significant differences with respect to the controls were achieved in the case of the B16-F10 cells, concerning both the percentage of permeabilised cells and the intracellular YO-PRO®-1 concentration. There is no obvious reason for such a difference.

Importantly, the cell-dependant phenomena that were observed in this study have to be also discussed along with the "plasma-treated PBS" effects. We demonstrate here that the radicals of the pPBS contribute to the enhancement of the cell membrane permeabilisation level in the combined treatment. This observation is in agreement with the study of Vernier and colleagues, who, while using molecular dynamics (MD) simulations and experiments with living cells, demonstrated that electroporating fields target oxidatively damaged areas in the cell membrane [42]. Yusupov and colleagues also used MD simulations to demonstrate that oxidation of the lipids in a phospholipid bilayer lowers the permeation free energy barriers of the ROS, which can further enhance the action of the ROS and also result in a drop of the electric field threshold needed for pore formation (electroporation), with respect to the potential facilitation of the pPBS effects by the PEFs. Their study also highlights that the lipid oxidation by plasma generated ROS synergistically enhances this effect [43].

Regarding the NTP multi-jet that was used in the present study to produce pPBS, there is evidence that the efficacy of plasma-treated liquids depends on the generated RONS concentration, which depends on the operating conditions used for liquid treatment [18,24]. Consolidated data were achieved while using an optimised NTP setup that delivers a stable peak current under very precise geometrical conditions. It is interesting to note that the effects were similar to those that were achieved in the proof of concept (Appendix A) while using a non-optimised setup. In fact, with both setups, the accumulation of H_2O_2 in pPBS reached similar levels (ca. 1.4 mM, see Figure 2a,b), which might explain why the increase in the cell permeabilisation level was similar. This fact reinforces the implication of the pPBS radicals in the improvement of the cell membrane permeabilisation by the µsPEF. Moreover, the resulted pPBS can remain stable at +4 °C for later use over a long period (at least 14 days), which facilitates its application and stock production, offering extensive advantages for biomedical purposes as compared to recent studies [44–46] It is worth mentioning that there are contradicting observations as to whether the conductivity of an external medium impacts the efficiency of the reversible cell membrane permeabilisation that is caused by PEFs [33,47,48]. However, a study from our group investigating the same DC-3F cell line and µsPEFs, demonstrated that media of lower conductivity induced more efficient reversible permeabilisation [33]. Our results indicate that the observed effects are not linked to the conductivity of the liquids, but rather to the radicals presence,

since the pPBS has a higher conductivity than that of the sham (see Table 1) and yet induces more permeabilisation effects on the cell membrane.

As previously mentioned, when cells were treated with pPBS before and after low amplitude µsPEFs, the percentage of permeabilised cells reached values similar to those of cells that were exposed to a classical electroporation field amplitude (1100 V/cm). The combined treatment, thus, opens the possibility to reduce the amplitude of the EP used in ECT, one of the goals of the present study. However, formal proofs have to be brought. Indeed, as demonstrated by the low uptake of the YO-PRO®-1 iodide by the cells exposed to the combined treatment at 600 V/cm (DC-3F cells) or 500 V/cm (B16-F10 cells) when compared to the uptake by the cells electropermeabilised by the µsPEFs alone at 1100 V/cm, the intensity of the fluorescent dye in cells that were treated by the combined treatment is low. Nevertheless, because of the large efficacy of BLM once inside the cells (500 molecules are sufficient to kill the dividing cells [49]), the percentage of permeabilised cells is more important than the level of permeabilisation (as quantified by the median intracellular fluorescence). As a matter of fact, in 1988, we already published that the same DC-3F cells, which were exposed to pulses leading to the reversible permeabilisation of 98% of the cells according to Lucifer Yellow uptake (a permeabilisation marker of ca. 450 Da, slightly smaller than the YO-PRO®-1 Iodide) also lead to 98% of cell killing in the presence of BLM [7]. In any case, the combined treatment that is explored in this paper is interesting as the µsPEF amplitudes could be greatly reduced during ECT or other electroporation-based therapies (to mitigate their side effects), or the used anticancer drug concentration could be reduced if it is chosen to maintain a high µsPEF amplitude.

4. Materials and Methods

Unless specified otherwise, all of the reagents were purchased from Life Technologies, Courtabœuf, France.

4.1. Cell Culture

DC-3F Chinese hamster lung fibroblasts [50] and B16-F10 murine melanoma cells [51], all mycoplasma-free, were cultured in Minimum Essential Medium (MEM, 31095-029) and Dulbecco's Modified Eagle Medium (DMEM, High Glucose, GlutaMAX Supplement, pyruvate, 31966-021), respectively. All of the media were supplemented with 10% foetal bovine serum (FBS, F7524), 100 $U{\cdot}mL^{-1}$ penicillin and 100 $mg{\cdot}mL^{-1}$ streptomycin (15140-122). The adherent cells were propagated at 37 °C in a 95% humidity atmosphere containing 5% CO_2 (HERAcell 240i incubator CO_2, Thermo Fisher Scientific, Courtaboeuf, FR) and then passaged upon confluency (every two days at a 1:10 dilution or every three days at a 1:30 dilution) while using TrypLE™ Express (12604-013). The cells were routinely checked for mycoplasma contamination via polymerase chain reaction (PCR). Cell viability was assessed while using trypan blue exclusion dye method (Trypan Blue Solution, T8154) with the Countess™ II FL Automated Cell Counter (Invitrogen, Thermo Fisher Scientific, Courtaboeuf, FR) and only viable cells were considered.

4.2. Plasma-Treated $PBS^{+}/_{+}$ Preparation Using NTP Multi-Jet Setups

4.2.1. Specifications of the NTP Multi-Jet Setup

The NTP multi-jet used in this study is based on a Plasma Gun (PG) device, which was described previously [31]. Briefly, the PG is a coaxial dielectric barrier discharge (DBD) reactor that consists of a quartz capillary tube flushed with helium and a microsecond-pulses high voltage (µs-pulses HV) generator powers it. As compared to the classical configuration, this new version presents two reactor zones (Figure 9a). The first zone is located inside the µs-pulsed HV generator, where a high voltage electrode (hollow metallic tube) is placed into a glass tube. At the outlet of the glass tube, a flexible dielectric tube is mounted containing a floating-potential electrode (conductive wire of ca. 1 mm^2 section) inside it. The dielectric tube goes out from the first reactor zone by connecting it with the

second reactor zone. This zone of the plasma device (the applicator) is essentially a second coaxial DBD reactor that is made of a PTFE (Polytetrafluoroethylene) body (shown in white in Figure 9) with the floating electrode being placed in its centre and a grounded ring electrode on the outside. The outlet of the second reactor zone has five micro-orifices ($Ø_{int}$ = 800 µm) producing, thus, five distinct plasma jets and covering a larger liquid area during the treatment (Figure 9b). Four of the orifices are disposed at the corner of a 4.2 mm square with the fifth orifice located at the crossing of the square diagonals. For all of the experiments, helium (99.9999% pure, Air Liquide, FR) at a fixed flow rate of 1 slm (standard litre per minute) was used as the operating gas. The NTP source was powered by high voltage pulses with duration of 4 µs (measured at half height) and a peak value of either +7 or +11 kV at a repetition rate of 2 kHz. The applied voltage was measured while using a high-voltage passive probe (Tektronix P6015A), while the current was determined by measuring the voltage drop on the resistor in the compensation circuit with another high-voltage passive probe (Tektronix TPP1000, Beaverton, OR, USA).

A non-optimised setup 1 was used for cytotoxicity assessment and the proof of concept that is reported in Appendix A (NTP setup 1). It used a stainless steel plate as ground electrode with no compensation circuit and a three-dimensional (3D) printed spacer to fix the gap distance between the plasma output orifices and the surface of the PBS. Based on our concomitant recent work [31], the NTP multi-jet source was optimised (NTP setup 2). It consists of (i) a new and more stable reactor, (ii) a ring shaped wire electrode (stainless-steel wire Ø = 1mm) placed in the bottom of the well (instead of the plane electrode used in the setup 1), which allows for avoiding liquid leakage from the well and reducing the number of discharges that formed between the plasma jets and the grounded electrode, and (iii) a compensation circuit designed to impose the total target impedance to a reference model mimicking the human body impedance [31], which would ease the translation of the results to animal models or human body (Figure 9, note that to allow for better visualisation of the plasma multi-jets, the spacer is not represented in the simplified scheme of Figure 9a and not in use in Figure 9b).

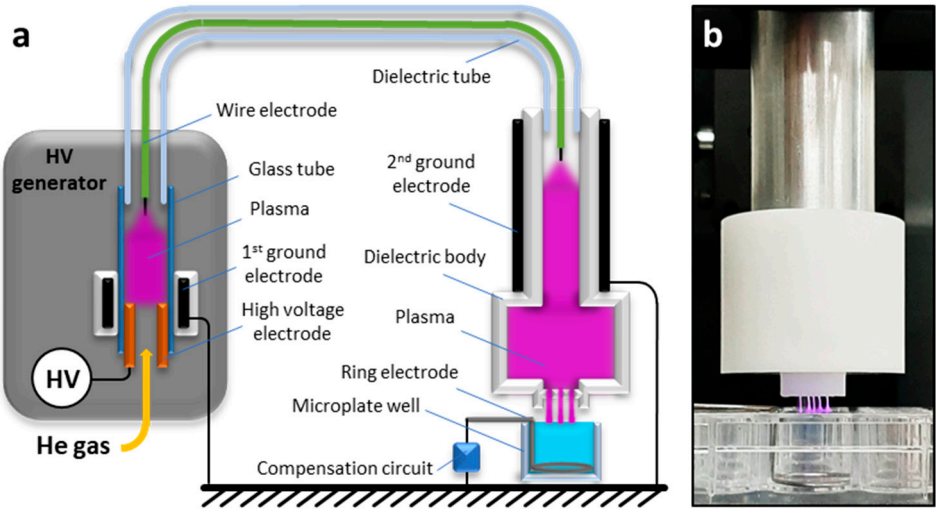

Figure 9. Schematic representation (**a**) and photo (**b**) of the NTP device with a multi-jet nozzle.

4.2.2. Preparation of the Plasma-Treated $PBS^{+}/_{+}$

For the preparation of the liquids used in the indirect plasma treatment with the NTP multi-jet device, Dulbecco's phosphate-buffered saline with Calcium and Magnesium (DPBS, Ca^{++}, Mg^{++}, 14040-133), termed $PBS^{+}/_{+}$, was chosen, as it is an appropriate buffer for adherent cells. Each well in 24-multiwell plates (Nunclon® Delta Surface, Thermo Fisher Scientific, DK, 142475) was filled with 3 mL of $PBS^{+}/_{+}$. The distance between the liquid surface and the plasma multi-jet output orifices was maintained at 4 mm thanks to a customised 3D-printed spacer. $PBS^{+}/_{+}$ was exposed to the NTP multi-jet for different times, varying between 1 and 20 min. A digital hygrometer/thermometer (Velleman®

Home, BE) was used to monitor the humidity and the room temperature in the working area. Water loss due to evaporation was compensated by distilled water addition in the pPBS at the end of the plasma treatment to maintain the osmolality of the plasma-treated $PBS^{+}/_{+}$ (pPBS). Depending on the room temperature, 600 to 700 µL of sterile water were added per well when $PBS^{+}/_{+}$ was plasma-treated for 20 min.

4.3. Plasma-treated $PBS^{+}/_{+}$ Characterisation

The concentration of peroxide (H_2O_2) in pPBS was determined while using titanium (IV) oxysulfate ($TiOSO_4$). H_2O_2 reacts with $TiOSO_4$ to produce pertitanic acid, which is yellow [22] and detectable by a spectrophotometer. The absorbance was measured at 407 nm while using a spectrophotometer multi-plate reader (Infinite® M200 PRO Tecan). The quantification of nitrite (NO_2^-) and nitrate (NO_3^-) in pPBS was performed within an hour after its treatment with the NTP multi-jet using nitrate/nitrite colorimetric assay kits (Cayman Chemical, Interchim, FR), according to the supplier's instructions and using the same spectrophotometric system was used. The pH and the conductivity of the treated-liquids were also measured while using specific probes for liquid analysis (InLab Micro Pro and Seven Compact Duo, by Mettler-Toledo). Semi-quantitative chemical analyses of peroxide, nitrate, and nitrite concentrations produced in pPBS were also assessed after each pPBS preparation while using Quantofix® test strips (Macherey-Nagel GmbH & Co. KG, Düren, DE) to ensure the quality of each preparation, which also revealed the reproducibility of the pPBS preparation.

For the evaluation of the RONS stability under storage at +4 °C, the initial pPBS volume (3 mL) was divided into four samples of equal volume. The concentration of the reactive species (H_2O_2, NO_2^-, and NO_3^-) in one of the samples was measured in the day of plasma treatment (day 0) and used as a reference (100%). The concentration in the other three samples was measured after 1, 7, and 14 days of storage at +4 °C. The relative concentration of the reactive species after storage at +4 °C is, thus, given in relation to the concentration measured at day 0.

4.4. Adherent Cells Electropulsation Setup

We used the system described in [34] for the electropulsation of the adherent cell monolayer. More precisely, as displayed in Figure 10, an in-house built mould of PDMS (polydimethylsiloxane, SYNGARD™ 184 Silicone Elastomer, DE) with an empty 2 cm^2 rectangle was inserted in a Ø 35 mm Petri dish (Nunclon® Delta Surface, Thermo Fisher Scientific, DK, 353001) to obtain a 2 cm^2 surface for cell growth. One day before the experiment, 600 µL of cell suspension were added to the defined area of each Petri dish at a density of 2.20×10^5 cells·mL^{-1} (i.e., 1.32×10^5 cells/600 µL) for DC-3F fibroblasts or 1.80×10^5 cells·mL^{-1} (i.e., 1.08×10^5 cells/600 µL) for B16-F10 melanoma cells, in respect to their growing speed and morphology (malignant B16-F10 murine melanoma cells grow much faster than DC-3F Chinese hamster lung fibroblasts). These seeding densities are based on our previous observation and experience, as they appear to be suitable for obtaining a homogenous cell layer at ca. 80% confluency (not entirely dense) after 24 h of cell culture. Different pre-treatment protocols were tested on the day of the experiment. Afterwards, the electric pulses were applied on the cell layer by means of an in-house built electrode configuration consisting of two parallel stainless-steel plates (2 mm thick), fixed in the PDMS mould, and distant of 6 mm (Figure 10). The electrodes and the custom moulding PDMS were designed to ensure the entire exposition of the cell monolayer to EPs. To generate microsecond pulsed electric fields (µsPEFs), the Cliniporator™ (IGEA, Carpi, IT) was used to deliver eight consecutive square-wave electric pulses of 100 µs duration, at a repetition frequency of 1 Hz, and different field strengths (500, 600, 1100, and 1400 V/cm).

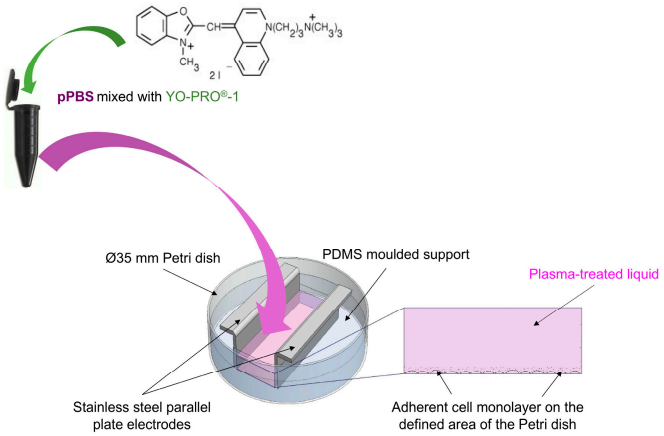

Figure 10. Schematic illustration of the electropulsation setup used in the combined treatment.

4.5. Combined Treatment

The combined treatment associated µsPEFs and pPBS to treat cells. Sham ($PBS^{+}/_{+}$ not treated with the plasma multi-jet) was used as a control for all of the experiments. Before exposing the cells to the sham or the pPBS, YO-PRO®-1 Iodide (629.04 Da) (Life Technologies, Y3603) was added to these media at a final working concentration of 2 µM (unless otherwise specified). In the day of experiment, the medium above the cells was removed and the cell layer was washed twice with $PBS^{+}/_{+}$. 500 µL of the YO-PRO®-1-containing pre-treatment liquid (sham or pPBS) was added on the cells for different incubation times (10 or 20 min.), and then µsPEFs were delivered (strengths ranging between 500 and 1400 V/cm). Afterwards, the electrodes were removed from the PDMS support and the pre-treatment liquid was then replaced by the YO-PRO®-1-containing post-treatment liquid (sham or pPBS) for 10 min.

In the absence of PEF (0 V/cm), the pre-treatment time was fixed at 20 min. In the presence of µsPEFs, the control condition (cells pre- and post-treated using Sham) was carried out with 20 min. of pre-treatment.

4.6. Evaluation of Cell Membrane Electropermeabilisation Induced by the Combined Treatment

The eventual permeabilisation of the cells that were treated by the combined treatment was investigated by fluorescent nucleic acids stain YO-PRO®-1 Iodide uptake. YO-PRO®-1 is a non-permeant dye that is frequently used as an indicator for permeabilisation. Indeed, when the cell membrane is permeabilised, YO-PRO®-1 can enter the cell and intercalates with nucleic acids, which results in a strong green fluorescence signal that can be detected by flow cytometry.

After the post treatment, the treated liquid above the cell monolayer was removed and the cells were harvested while using TrypLE™ Express Enzyme dissociation (400 µL per Petri dish). The cell suspension was then analysed by flow cytometry (C6 flow cytometer, BD Accuri, San Jose, California, US). 10 000 events were recorded, the YO-PRO®-1 uptake (cell permeabilisation) was evaluated while using green fluorescence channel (excitation 488 nm, emission 530/30 nm). More precisely, the percentage of fluorescent/permeabilised cells as well as the mean and median fluorescence intensity per cell (level of permeabilisation of each cell) were assessed. The cell membrane permeabilisation threshold was fixed for all of the samples based on that of cells treated with Sham and not exposed to PEF.

4.7. Statistical Analysis

The experiments were performed at least three times independently, i.e., at least over three different days. In addition, each parameter set was performed in triplicate, which resulted in a total of at least nine replicates for each parameter set. The outliers were identified and removed while using the Grubb's method (Alpha = 0.05). To study the significance of differences, one-way ANOVA,

followed by Bonferroni's multiple comparison tests, were performed while using Prism (GraphPad Software, La Jolla, CA, US). Statistical significance levels were associated with p-values of <0.05 (*), <0.01 (**), <0.001 (***) and <0.0001 (****).

5. Conclusions

The present study demonstrates that the application of plasma-treated $PBS^{+}/_{+}$ that is produced by the newly-developed NTP multi-jet source could effectively enhance the µsPEFs induced cell membrane permeabilisation, both in terms of the percentage of permeabilised cells and the intracellular content of a permeabilisation marker. These effects occur, even at very low µsPEF amplitudes, and the results are cell-dependant. The malignant B16-F10 murine melanoma cells are more sensitive to the effect of this combined treatment than the DC-3F Chinese hamster lung fibroblasts.

These very promising results underline the great potential of a combined ECT and indirect NTP treatment for anticancer therapies. Investigation and in-depth physical, chemical, and biological understanding of those effects will be fundamental for in vivo studies and clinical trials, which might open up new ways for the implementation of guided cancer therapies while using indirect NTP treatment and ECT in the future.

Supplementary Materials: The following are available online at http://www.mdpi.com/2072-6694/12/1/219/s1, Video S1: NTP multi-jet generated at +7 kV peak voltage; Video S2: NTP multi-jet generated at +11 kV peak voltage.

Author Contributions: Conceptualisation, T.-H.C., É.R. and L.M.M.; methodology, T.-H.C., A.S., F.M.A., C.D., J.S.S., K.G., S.D. and J.-M.P.; validation, T.-H.C., F.M.A. and L.M.M.; formal analysis, T.-H.C. and F.M.A.; investigation, T.-H.C., K.S., K.G. and A.S.; resources, J.S.S., É.R. and L.M.M.; writing—original draft preparation, T.-H.C.; writing—review and editing, T.-H.C., A.S., J.-M.P., J.S.S., K.S., K.G., F.M.A., É.R. and L.M.M.; visualisation, T.-H.C. and A.S.; supervision, J.S.S., É.R. and L.M.M.; project administration, L.M.M.; funding acquisition, J.S.S., É.R. and L.M.M. All authors have read and agreed to the published version of the manuscript.

Funding: We acknowledge the financial support from the PLASCANCER project (INCa-PlanCancer N°17CP087-00) and the GDR 2025 HAPPYBIO.

Acknowledgments: The authors thank T. García-Sánchez, J-R. Bertrand (Gustave Roussy) and G. Bauville (LPGP) for technical support.

Conflicts of Interest: The authors declare no conflict of interest.

Appendix A.

Treatment with $PBS^{+}/_{+}$ Increases Cell Electropermeabilisation without Affecting the Cell Viability: Proof of Concept.

Appendix A.1. Assessment of the Plasma-Treated $PBS^{+}/_{+}$ Cytotoxicity

Appendix A.1.1. Materials and Methods

The cytotoxicity of pPBS was determined via a clonogenic survival assay that overcomes some of the limitations of other in vitro assays, such as apoptosis measurements, by monitoring all types of cell death, even the mitotic cell death. This colony forming technique is a robust in vitro cell survival test based on the ability of each single viable cell to grow into a colony (defined to consist of at least 50 cells) after being treated by specific agents.

300 µL of adherent DC-3F cells at a density of 1.60×10^5 cells·mL^{-1} were seeded per well in the wells of a 48-well plate (Nunclon® Delta Surface, Thermo Fisher Scientific, DK, 150687) for an overnight cell culture at 37 °C in a humidified, 5% CO_2 incubator. In the day of experiment when the cell layer reached ca. 70 to 80% confluency, the medium above the cells was removed and the cell layer was washed twice with $PBS^{+}/_{+}$. After being prepared (plasma setup not grounded neither compensated, plasma parameters: +7 kV, 2 kHz, Helium 1 slm, distance 5 mm between the plasma outlet and the liquid layer in well), 300 µL of fresh pPBS was added to the cell layer. After different incubation times in pPBS, pPBS was removed from the cell layer; cells were dissociated by 100 µL

TrypLE™ Express Enzyme solution and suspended in their culture medium. Cells were counted without Trypan Blue Stain and seeded out, in appropriate dilutions, 250 cells per well of a 6-multiwell plate (Nunclon® Delta Surface, Thermo Fisher Scientific, DK, 140675). After 5 days of cell culture, the medium above the cells was discarded, cells were washed carefully twice with PBS. To each well, 2 mL of colony fixation-staining solution (crystal violet 0.2% (wt/vol), formaldehyde 3.7% (vol/vol) and ethanol 20% (vol/vol) in H_2O) was added and left for 2 to 5 min. before being removed carefully. Stained cells were rinsed by immersing the plates in a sink filled with tap water. The plates were dried at room temperature, then the resulting clones were counted for each treatment condition. The viability, reported as a percentage of survived and proliferated adherent cells, was referred to the number of clones in the sham condition.

Appendix A.1.2. Results and Discussion

In order to ensure that the pPBS alone does not significantly affect cell growth and death within a "sublethal" contact time with the cells, cells were incubated with pPBS for a large incubation time and the cell viability after the treatment was assessed via a cytotoxicity assay. The survival curves of cells in percentage of viable colonies with respect to the sham condition (Figure A1) show that the viability of DC-3F cells was preserved when being in contact with pPBS for 1 to 15 min. When the cells were incubated in pPBS for longer, up to 30 min., the long-term cytotoxic effect was limited, with a maximal loss of viability of 40%. For even longer durations, cytotoxicity was larger. These results demonstrate that the long-term cytotoxicity of pPBS depends on time of contact with the cells, as reported in other works [52]. As up to 30 min. of exposure to the pPBS resulted in a tolerable range of cytotoxic, in the remaining work of our study, the maximal duration of treatment of the cells to the pPBS was fixed to 30 min. We thus considered this incubation time window as the most appropriate to combine with µsPEFs for a sublethal and efficient cell reversible electropermeabilisation.

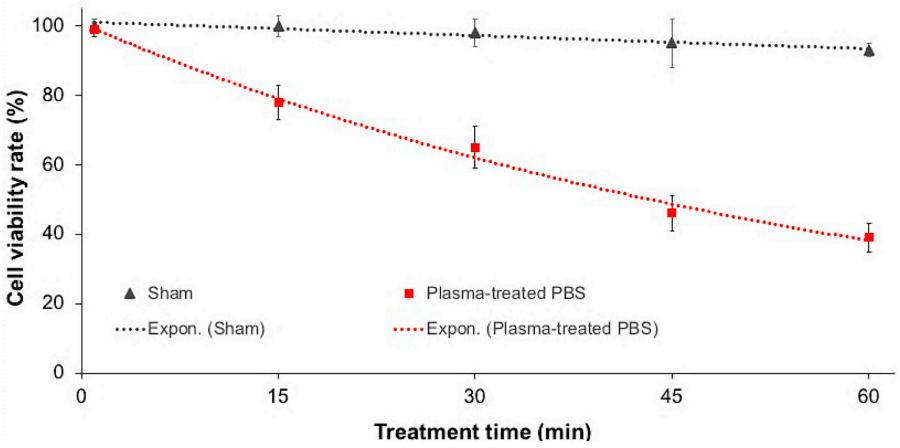

Figure A1. Cytotoxicity of pPBS to adherent DC-3F cells. Survival curves of DC-3F cells that were plated immediately after being incubated with pPBS between 1 and 60 min. are presented as the number of viable colonies formed five days after the treatment. Results from three independent experiments (each in triplicate) are shown as mean values ± SD for each parameter set.

Appendix A.2. Enhancement of Electropermeabilisation by Combination of Plasma-Treated PBS$^{+}/_{+}$ with PEFs: First Assay

Adherent DC-3F cells were pre-treated with either sham or pPBS for 10 min., before being exposed to a pulsed electric field (8 pulses, 100 µs, 1100 V/cm, 1 Hz) and post-treated for 10 min. with sham. Cell permeabilisation was evaluated by flow cytometry immediately after the treatments (Figure A2). In the condition where no PEF was applied (0 V/cm), a slight though not significant increase of YO-PRO®-1 uptake was observed in cells pre-treated with pPBS compared to those pre-treated with Sham. The exposure of the cells to the EPs increases the intracellular fluorescence intensity

of YO-PRO®-1 Iodide (present in all the treatment liquids), indicating membrane permeabilisation (Figure A2). This effect is significantly greater in cells pre-treated with pPBS than in control cells pre-treated with sham (1.68-fold enhancement).

The treatment of DC-3F cells with pPBS combined with an EP at 1100 V/cm intensity has thus given a proof of concept that pPBS favoured the membrane electropermeabilisation.

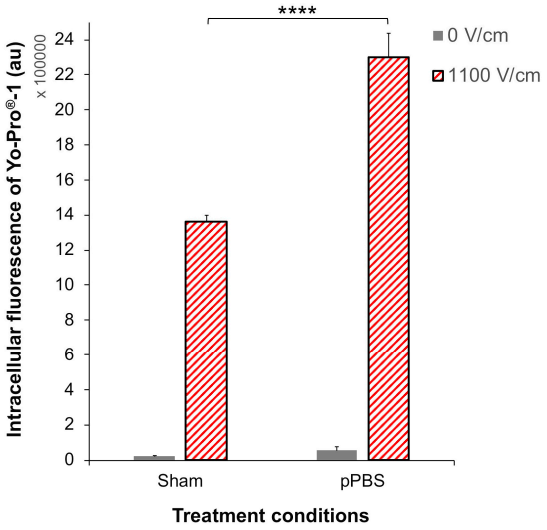

Figure A2. Enhanced electropermeabilisation of adherent DC-3F cells with pPBS treatment. Cells were pre-treated with pPBS for 10 min. and exposed to 8 pulses of 100 µs and 1100 V/cm at a 1 Hz repetition rate. The cell membrane permeabilisation was monitored by the fluorescence of the YO-PRO®-1 iodide taken up by the cells. Data are presented as median values ± SD of independent triplicates. Statistical analysis used the One-way ANOVA followed by Bonferroni's multiple comparison test. **** $p < 0.0001$.

References

1. Mir, L.M.; Belehradek, M.; Domenge, C.; Orlowski, S.; Poddevin, B.; Belehradek, J.; Schwaab, G.; Luboinski, B.; Paoletti, C. Electrochemotherapy, a new antitumor treatment: First clinical trial. *C. R. Acad. Sci. III* **1991**, *313*, 613–618. [PubMed]
2. Mir, L.M.; Gehl, J.; Serša, G.; Collins, C.G.; Garbay, J.R.; Billard, V.; Geertsen, P.F.; Rudolf, Z.; O'Sullivan, G.C.; Marty, M. Standard operating procedures of the electrochemotherapy: Instructions for the use of bleomycin or cisplatin administered either systemically or locally and electric pulses delivered by the CliniporatorTM by means of invasive or non-invasive electrodes. *Eur. J. Cancersuppl.* **2006**, *4*, 14–25. [CrossRef]
3. Campana, L.G.; Testori, A.; Curatolo, P.; Quaglino, P.; Mocellin, S.; Framarini, M.; Borgognoni, L.; Ascierto, P.A.; Mozzillo, N.; Guida, M.; et al. Treatment efficacy with electrochemotherapy: A multi-institutional prospective observational study on 376 patients with superficial tumors. *Eur. J. Surg. Oncol.* **2016**, *42*, 1914–1923. [CrossRef] [PubMed]
4. Campana, L.G.; Kis, E.; Bottyán, K.; Orlando, A.; de Terlizzi, F.; Mitsala, G.; Careri, R.; Curatolo, P.; Snoj, M.; Serša, G.; et al. Electrochemotherapy for advanced cutaneous angiosarcoma: A European register-based cohort study from the International Network for Sharing Practices of electrochemotherapy (InspECT). *Int. J. Surg.* **2019**, *72*, 34–42. [CrossRef]
5. Mir, L.M.; Devauchelle, P.; Quintin-Colonna, F.; Delisle, F.; Doliger, S.; Fradelizi, D.; Belehradek, J.; Orlowski, S. First clinical trial of cat soft tissue sarcomas treatment by electrochemotherapy. *Br. J. Cancer* **1997**, *76*, 1617–1622. [CrossRef]
6. Cemazar, M.; Tamzali, Y.; Serša, G.; Tozon, N.; Mir, L.M.; Miklavčič, D.; Lowe, R.; Teissié, J. Electrochemotherapy in Veterinary Oncology. *J. Vet. Intern. Med.* **2008**, *22*, 826–831. [CrossRef]
7. Orlowski, S.; Belehradek, J.; Paoletti, C.; Mir, L.M. Transient electropermeabilization of cells in culture. Increase of the cytotoxicity of anticancer drugs. *Biochem. Pharmacol.* **1988**, *37*, 4727–4733. [CrossRef]

8. Marty, M.; Sersa, G.; Garbay, J.R.; Gehl, J.; Collins, C.G.; Snoj, M.; Billard, V.; Geertsen, P.F.; Larkin, J.O.; Miklavčič, D.; et al. Electrochemotherapy—An easy, highly effective and safe treatment of cutaneous and subcutaneous metastases: Results of ESOPE (European Standard Operating Procedures of Electrochemotherapy) study. *Eur. J. Cancersuppl.* **2006**, *4*, 3–13. [CrossRef]
9. Gehl, J.; Serša, G.; Matthiessen, L.W.; Muir, T.; Soden, D.; Occhini, A.; Quaglino, P.; Curatolo, P.; Campana, L.G.; Kunte, C.; et al. Updated standard operating procedures for electrochemotherapy of cutaneous tumours and skin metastases. *Acta Oncol. (Madr).* **2018**, *57*, 874–882. [CrossRef]
10. Campana, L.G.; Bianchi, G.; Mocellin, S.; Valpione, S.; Campanacci, L.; Brunello, A.; Donati, D.; Sieni, E.; Rossi, C.R. Electrochemotherapy treatment of locally advanced and metastatic soft tissue sarcomas: Results of a non-comparative phase II study. *World J. Surg.* **2014**, *38*, 813–822. [CrossRef]
11. Matthiessen, L.W.; Johannesen, H.H.; Hendel, H.W.; Moss, T.; Kamby, C.; Gehl, J. Electrochemotherapy for large cutaneous recurrence of breast cancer: A phase II clinical trial. *Acta Oncol. (Madr).* **2012**, *51*, 713–721. [CrossRef] [PubMed]
12. Breton, M.; Mir, L.M. Investigation of the chemical mechanisms involved in the electropulsation of membranes at the molecular level. *Bioelectrochemistry* **2018**, *119*, 76–83. [CrossRef] [PubMed]
13. Leduc, M.; Guay, D.; Leask, R.L.; Coulombe, S. Cell permeabilization using a non-thermal plasma. *New J. Phys.* **2009**, *11*, 115021. [CrossRef]
14. Sasaki, S.; Honda, R.; Hokari, Y.; Takashima, K.; Kanzaki, M.; Kaneko, T. Characterization of plasma-induced cell membrane permeabilization: Focus on OH radical distribution. *J. Phys. D. Appl. Phys.* **2016**, *49*, 334002. [CrossRef]
15. Keidar, M.; Walk, R.M.; Shashurin, A.; Srinivasan, P.; Sandler, A.D.; Dasgupta, S.; Ravi, R.; Guerrero-Preston, R.; Trink, B. Cold plasma selectivity and the possibility of a paradigm shift in cancer therapy. *Br. J. Cancer* **2011**, *105*, 1295–1301. [CrossRef]
16. Tanaka, H.; Mizuno, M.; Ishikawa, K.; Nakamura, K.; Kajiyama, H.; Kano, H.; Kikkawa, F.; Hori, M. Plasma-activated medium selectively kills glioblastoma brain tumor cells by down-regulating a survival signaling molecule, AKT kinase. *Plasma Med.* **2011**, *1*, 265–277. [CrossRef]
17. Zucker, S.N.; Zirnheld, J.; Bagati, A.; DiSanto, T.M.; Des Soye, B.; Wawrzyniak, J.A.; Etemadi, K.; Nikiforov, M.; Berezney, R. Preferential induction of apoptotic cell death in melanoma cells as compared with normal keratinocytes using a non-thermal plasma torch. *Cancer Biol. Ther.* **2012**, *13*, 1299–1306. [CrossRef]
18. Yan, D.; Sherman, J.H.; Keidar, M. Cold atmospheric plasma, a novel promising anti-cancer treatment modality. *Oncotarget* **2017**, *8*, 15977–15995. [CrossRef]
19. Metelmann, H.-R.; Nedrelow, D.S.; Seebauer, C.; Schuster, M.; von Woedtke, T.; Weltmann, K.-D.; Kindler, S.; Metelmann, P.H.; Finkelstein, S.E.; Von Hoff, D.D.; et al. Head and neck cancer treatment and physical plasma. *Clin. Plasma Med.* **2015**, *3*, 17–23. [CrossRef]
20. Graves, D.B. Reactive species from cold atmospheric plasma: Implications for cancer therapy. *Plasma Process. Polym.* **2014**, *11*, 1120–1127. [CrossRef]
21. Bruggeman, P.J.; Kushner, M.J.; Locke, B.R.; Gardeniers, J.G.E.; Graham, W.G.; Graves, D.B.; Hofman-Caris, R.C.H.M.; Maric, D.; Reid, J.P.; Ceriani, E.; et al. Plasma-liquid interactions: A review and roadmap. *Plasma Sources Sci. Technol.* **2016**, *25*, 053002. [CrossRef]
22. Girard, P.-M.; Arbabian, A.; Fleury, M.; Bauville, G.; Puech, V.; Dutreix, M.; Sousa, J.S. Synergistic Effect of H_2O_2 and NO_2 in Cell Death Induced by Cold Atmospheric He Plasma. *Sci. Rep.* **2016**, *6*, 29098. [CrossRef] [PubMed]
23. Yan, D.; Cui, H.; Zhu, W.; Nourmohammadi, N.; Milberg, J.; Zhang, L.G.; Sherman, J.H.; Keidar, M. The Specific Vulnerabilities of Cancer Cells to the Cold Atmospheric Plasma-Stimulated Solutions. *Sci. Rep.* **2017**, *7*, 1–12. [CrossRef] [PubMed]
24. Van Boxem, W.; Van Der Paal, J.; Gorbanev, Y.; Vanuytsel, S.; Smits, E.; Dewilde, S.; Bogaerts, A. Anti-cancer capacity of plasma-treated PBS: Effect of chemical composition on cancer cell cytotoxicity. *Sci. Rep.* **2017**, *7*, 1–9. [CrossRef] [PubMed]
25. Radi, R.; Beckman, J.S.; Bush, K.M.; Freeman, B.A. Peroxynitrite-induced membrane lipid peroxidation: The cytotoxic potential of superoxide and nitric oxide. *Arch. Biochem. Biophys.* **1991**, *288*, 481–487. [CrossRef]
26. Pacher, P.; Beckman, J.S.; Liaudet, L. Nitric Oxide and Peroxynitrite in Health and Disease. *Physiol. Rev.* **2007**, *87*, 315–424. [CrossRef] [PubMed]

27. Roux, S.; Bernat, C.; Al-Sakere, B.; Ghiringhelli, F.; Opolon, P.; Carpentier, A.F.; Zitvogel, L.; Mir, L.M.; Robert, C. Tumor destruction using electrochemotherapy followed by CpG oligodeoxynucleotide injection induces distant tumor responses. *Cancer Immunol. Immunother.* **2008**, *57*, 1291–1300. [CrossRef] [PubMed]
28. Serša, G.; Čemažar, M.; Miklavčič, D.; Mir, L.M. Electrochemotherapy: Variable anti-tumor effect on different tumor models. *Bioelectrochemistry Bioenerg.* **1994**, *35*, 23–27. [CrossRef]
29. Heller, R.; Jaroszeski, M.; Perrott, R.; Messina, J.; Gilbert, R. Effective treatment of B16 melanoma by direct delivery of bleomycin using electro-chemotherapy. *Melanoma Res.* **1997**, *7*, 10–18. [CrossRef]
30. Pasqual-Melo, G.; Gandhirajan, R.K.; Stoffels, I.; Bekeschus, S. Targeting malignant melanoma with physical plasmas. *Clin. Plasma Med.* **2018**, *10*, 1–8. [CrossRef]
31. Stancampiano, A.; Chung, T.-H.; Dozias, S.; Pouvesle, J.-M.; Mir, L.M.; Robert, É. Mimicking of human body electrical characteristic for easier translation of plasma biomedical studies to clinical applications. *IEEE Trans. Radiat. Plasma Med. Sci.* **2019**. [CrossRef]
32. Chance, B.; Sies, H.; Boveris, A. Hydroperoxide metabolism in mammalian organs. *Physiol. Rev.* **1979**, *59*, 527–605. [CrossRef] [PubMed]
33. Silve, A.; Leray, I.; Poignard, C.; Mir, L.M. Impact of external medium conductivity on cell membrane electropermeabilization by microsecond and nanosecond electric pulses. *Sci. Rep.* **2016**, *6*, 19957. [CrossRef]
34. Ghorbel, A.; Mir, L.M.; García-Sánchez, T. Conductive nanoparticles improve cell electropermeabilization. *Nanotechnology* **2019**, *30*, 495101. [CrossRef] [PubMed]
35. Čemažar, M.; Jarm, T.; Miklavčič, D.; Lebar, A.M.; Ihan, A.; Kopitar, N.A.; Serša, G. Effect of electric-field intensity on electropermeabilization and electrosensitivity of various tumor-cell lines in vitro. *Electromagn. Biol. Med.* **1998**, *17*, 263–272.
36. Rols, M.-P.; Golzio, M.; Gabriel, B.; Teissié, J. Factors Controlling Electropermeabilisation of Cell Membranes. *Technol. Cancer Res. Treat.* **2002**, *1*, 319–327. [CrossRef]
37. Kim, S.J.; Chung, T.H. Cold atmospheric plasma jet-generated RONS and their selective effects on normal and carcinoma cells. *Sci. Rep.* **2016**, *6*, 1–14. [CrossRef]
38. Biscop, E.; Lin, A.G.; Van Boxem, W.; Van Loenhout, J.; De Backer, J.; Deben, C.; Dewilde, S.; Smits, E.; Bogaerts, A. Influence of Cell Type and Culture Medium on Determining Cancer Selectivity of Cold Atmospheric Plasma Treatment. *Cancers* **2019**, *11*, 1287. [CrossRef]
39. Cooper, G.M. The Development and Causes of Cancer. In *The Cell: A Molecular Approach*; Sinauer Associates: Sunderland, MA, USA, 2000; pp. 725–766.
40. Landström, F.J.; Ivarsson, M.; Koskela Von Sydow, A.; Magnuson, A.; Von Beckerath, M.; Möller, C. Electrochemotherapy-Evidence for Cell-type Selectivity In Vitro. *Anticancer Res.* **2015**, *35*, 5813–5820.
41. Frandsen, S.K.; Gibot, L.; Madi, M.; Gehl, J.; Rols, M.-P. Calcium electroporation: Evidence for differential effects in normal and malignant cell lines, evaluated in a 3D spheroid model. *PLoS ONE* **2015**, *10*, 1–11. [CrossRef]
42. Vernier, P.T.; Levine, Z.A.; Wu, Y.H.; Joubert, V.; Ziegler, M.J.; Mir, L.M.; Tieleman, D.P. Electroporating fields target oxidatively damaged areas in the cell membrane. *PLoS ONE* **2009**, *4*, e7966. [CrossRef] [PubMed]
43. Yusupov, M.; Van Der Paal, J.; Neyts, E.C.; Bogaerts, A. Synergistic effect of electric field and lipid oxidation on the permeability of cell membranes. *Biochim. Biophys. Acta Gen. Subj.* **2017**, *1861*, 839–847. [CrossRef]
44. Adachi, T.; Tanaka, H.; Nonomura, S.; Hara, H.; Kondo, S.I.; Hori, M. Plasma-activated medium induces A549 cell injury via a spiral apoptotic cascade involving the mitochondrial-nuclear network. *Free Radic. Biol. Med.* **2015**, *79*, 28–44. [CrossRef] [PubMed]
45. Yan, D.; Nourmohammadi, N.; Bian, K.; Murad, F.; Sherman, J.H.; Keidar, M. Stabilizing the cold plasma-stimulated medium by regulating medium's composition. *Sci. Rep.* **2016**, *6*, 1–11. [CrossRef] [PubMed]
46. Judée, F.; Fongia, C.; Ducommun, B.; Yousfi, M.; Lobjois, V.; Merbahi, N. Short and long time effects of low temperature Plasma Activated Media on 3D multicellular tumor spheroids. *Sci. Rep.* **2016**, *6*, 1–12. [CrossRef] [PubMed]
47. Neumann, E. Membrane electroporation and direct gene transfer. *Bioelectrochemistry Bioenerg.* **1992**, *28*, 247–267. [CrossRef]
48. Pucihar, G.; Kotnik, T.; Kandušer, M.; Miklavčič, D. The influence of medium conductivity on electropermeabilization and survival of cells in vitro. *Bioelectrochemistry* **2001**, *54*, 107–115. [CrossRef]

49. Poddevin, B.; Orlowski, S.; Belehradek, J.; Mir, L.M. Very high cytotoxicity of bleomycin introduced into the cytosol of cells in culture. *Biochem. Pharmacol.* **1991**, *42*, 67–75. [CrossRef]
50. Biedler, J.L.; Riehm, H. Cellular resistance to actinomycin D in Chinese hamster cells in vitro: Cross-resistance, radioautographic, and cytogenetic studies. *Cancer Res.* **1970**, *30*, 1174–1184.
51. Mir, L.M.; Orlowski, S.; Belehradek, J.; Paoletti, C. Electrochemotherapy potentiation of antitumour effect of bleomycin by local electric pulses. *Eur. J. Cancer Clin. Oncol.* **1991**, *27*, 68–72. [CrossRef]
52. Boehm, D.; Heslin, C.; Cullen, P.J.; Bourke, P. Cytotoxic and mutagenic potential of solutions exposed to cold atmospheric plasma. *Sci. Rep.* **2016**, *6*, 21464. [CrossRef] [PubMed]

3 Preserving the anti-cancer efficacy of plasma-treated liquids over time: a prerequisite for their clinical application (manuscript to be submitted)

Over the last decade, there has been an increasing interest in non-thermal plasma (NTP) uses in medical studies and applications, especially plasma-treated liquids in oncology, in combining treatment to enhance the efficacy of established procedures monotherapies. To develop new anti-cancer modalities or treatments, there was a primordial need to understand the stability, components, and pH over different storage conditions of those plasma-treated liquids.

After the characterisation of the abovementioned NTP multijet device for stable and reproducible applications in both pre-clinic and clinic (see **section 1 of the Results**), and after preliminary assay demonstrating the stability of the plasma-treated **PBS** (or **pPBS**), under certain conditions, to use for *in vitro* experiments (see **section 2 of the Results** and Annexe of the second paper), we here addressed a thorough study of chemical stability of **different pPBS** for optimal production and uses. This study, presented in a manuscript hereunder, is under final review by authors before its submission.

My contribution to this study, as the second co-author, consists in the coordination of the experiments between the LPGP and the Gustave Roussy Institute (including the planning and the management of materials) in the *in vitro* experiments performed at the Gustave Roussy Institute (conceptualisation, methodology, data acquisition and validation, data analysis and visualisation, data interpretation), and in writing (original draft preparation, review and editing of the whole paper).

Preserving the anti-cancer efficacy of plasma-treated solutions over time: a prerequisite for their clinical application

K. Sklias[1], T.-H. Chung[2], A. Stancampiano[3], K. Gazeli[1], T. Darny[1], G. Bauville[1], F.M. André[2], S. Dozias[3], C. Douat[3], J.-M. Pouvesle[3], E. Robert[3], L.M. Mir[2] and J. Santos Sousa[1]

[1] Université Paris-Saclay, CNRS, Laboratoire de Physique des Gaz et des Plasmas, 91405 Orsay, France
[2] Université Paris-Saclay, CNRS, Institut Gustave Roussy, Metabolic and Systemic Aspects of Oncogenesis (METSY), 94805 Villejuif, France
[3] GREMI, UMR 7344 CNRS/Université d'Orléans, 45067 Orléans, France
* Correspondence: joao.santos-sousa@universite-paris-saclay.fr

Abstract

To be considered as efficient anti-cancer agents, plasma-treated solutions (PTS) should maintain their anti-cancer efficacy over long periods. This study investigates the chemical stability of plasma-treated PBS(Ca^{2+}/Mg^{2+}), or pPBS, as a function of storage time and temperature, in terms of the evolution of the concentration of H_2O_2, NO_2^- and NO_3^-, the main drivers of the PTS anti-cancer effects, as well as the pPBS cytotoxic and cytostatic effects, and its cell membrane permeabilization capability, on two different cell lines (non-malignant DC-3F and tumorigenic fibrosarcoma LPB). pPBS was stored for up to 75 days at 4 different temperatures: +20, +4, –20 and –80 °C. The aforementioned long-lived reactive species remained stable for 21 days of storage at +20 or +4 °C. Contrariwise, significant degradation of H_2O_2 and NO_2^- was observed at –20 and –80 °C, even after only 1 day of storage. It is shown that the considerable acidification occurring during freezing (from pH 6 to 2–3) favors the conversion of NO_2^- into NO_3^- through peroxidation by H_2O_2. However, the freezing rate is inconsequential. In good agreement with the chemical dosimetry of pPBS, the cytotoxic and cytostatic capacities of pPBS were also preserved when stored at +4 °C (for at least 21 days) but not at –20 °C. The cell membrane permeabilization was cell-dependent and linked to the H_2O_2 content of the pPBS, thus also dependent on the pPBS storage conditions. In conclusion, the simple and stable storage at room temperature makes the practical application of pPBS in cancer therapy easy and accessible to all people.

1. Introduction

Over the last decades, plasma pharmacy has been an emerging research field within plasma medicine, especially when it comes to cancer treatment[1–3]. Numerous publications show that plasma-treated solutions (PTS) can be an effective anti-cancer agent against different types of tumor cells, including ovarian cancer, cervical cancer, pancreatic cancer, glioblastoma, colon cancer and melanoma, both *in vitro* and *in vivo*[4–9].

Several cold atmospheric pressure plasma (CAPP) sources have been used for the treatment of liquids, including radiofrequency discharges, dielectric barrier discharges (DBD) and atmospheric pressure plasma jets (APPJs)[9–1213]. Furthermore, a variety of solutions have been subjected to plasma treatment aiming their transformation into efficient anti-cancer agents, namely water, phosphate-buffered saline (PBS), ringer lactate and cell culture media[12,14–19] The anti-cancer properties of such PTS

are mainly due to the delivery of long-lived reactive oxygen and nitrogen species (RONS) that can be generated in or transferred into the liquid phase[17]. Despite their complex chemical composition, it is now widely accepted that hydrogen peroxide (H_2O_2) is the main species responsible for their cytotoxic effects. However, synergistic effects with nitrite (NO_2^-), nitrate (NO_3^-) and the pH of the PTS have also been reported[14,20,21]. Furthermore, some RONS (such as peroxynitrite ($ONOO^-$), nitric oxide (NO), nitrogen dioxide (NO_2) and hydroxyl radical ($^{\bullet}OH$)) have been identified as responsible for the oxidation of phospholipid bilayers of the cell membrane upon contact with PTS, which could lead to cell membrane permeabilization[22,23].

To be considered as effective anti-cancer agents, it is essential that these PTS maintain their anti-cancer properties over time. One key parameter for the conservation of PTS, as well as of any other agent, is the storage temperature. Shen *et al.* investigated the evolution of plasma-treated water when stored at 4 different temperatures (+25, +4, −20 and −80 °C) over 30 days in terms of H_2O_2, NO_2^- and NO_3^- concentrations as well as its bactericidal activity[24]. They found that the bactericidal ability of plasma-treated water increased with decreasing storage temperature. Besides, they also found that the concentrations of H_2O_2, NO_2^- and NO_3^- decreased over time for all storage temperatures except for –80 °C. Contrariwise, Judée *et al.*, who used plasma-activated medium (PAM) to treat colon adenocarcinoma multicellular tumor spheroid (MCTS), found that, when the PAM was stored at +4 °C or –80 °C, it retained its genotoxic activity, which was not the case for the PAM stored at +37 °C or –20 °C[16]. Thus, they suggested that H_2O_2 concentration in PAM remained stable during at least 7 days of storage at +4 °C and −80 °C, while storage at +37 °C and −20 °C certainly decomposed H_2O_2. Yan *et al.* showed that while the H_2O_2 was stable in plasma-treated PBS stored at +8 °C and –25 °C for up to 3 days, its concentration was reduced as a function of storage time (and for the same storage conditions) when the PTS was cell culture medium[25]. These discrepancies between reports can be attributed to both the different types of plasmas used for the treatment of the solutions and to the different treated solutions. Indeed, different working conditions such as gas flow rate, gas composition, treatment distance, room conditions (e.g. humidity and temperature) and high voltage amplitude result in the production/transfer of different reactive species in/into the liquid, the composition of which also plays a major role in its final complex chemistry[9,26,27]. Besides the fluctuation of the RONS concentration, the chemical reactivity of PTS is also highly dependent on the final pH of the solution after plasma treatment. The pH of the PTS could be one of the crucial parameters that may explain the choice of the different storage temperatures proposed by the aforementioned authors. Indeed, not only the acidic pH of PTS may contribute alongside RONS to their cytotoxic capacity, but it is also an important parameter for the stability of RONS[21,28].

The present work is devoted to the determination of pertinent storage conditions to preserve the cytotoxic effects of plasma-treated PBS(Ca^{2+}/Mg^{2+}) (pPBS). Thus, the chemical stability of pPBS was assessed here, in terms of the H_2O_2, NO_2^- and NO_3^- concentrations as a function of storage time and temperature for up to 75 days after production by plasma treatment. The chemical mechanisms leading to the degradation of these RONS in certain storage conditions of the PTS and the catalytic role of the acidic pH were also investigated. Finally, the impact of the appropriate conservation of PTS on their anti-cancer efficacy on two different cell lines was also assessed *in vitro*, by quantifying the viability and the membrane permeabilization of the cells following treatment with those pPBS. Indeed, understanding the physicochemical properties and the anti-tumor activity of PTS before and after the storage is crucial for their practical application as anti-cancer agents.

2. Materials and Methods

Unless otherwise specified, all the reagents for biological experiments were purchased from Life Technologies (Courtabœuf, France) and all the reagents for the dosimetry investigations of RONS were purchased from Sigma-Aldrich (France).

2.1 Experimental setup

The conceptual view of the plasma reactor used in this study is depicted in **Figure 1a**. It is based on the Plasma Gun (PG) device, which was described previously in detail[29–31] Briefly, it consists of a high voltage electrode inserted inside a quartz dielectric tube, and driven by high voltage pulses with an amplitude of 11 kV (FWHM of ~2.3 μs) at a repetition rate of 2 kHz provided by a custom-made power supply. A second electrode is placed outside the dielectric tube and is connected to the ground. Thus, a coaxial dielectric barrier discharge (DBD) is formed. The working gas used was pure helium (Alphagaz 1 He, >99.9999%, type S11, Air Liquide, France) at a flow rate of 1 standard litre per minute (SLM), regulated by a digital flowmeter (Vögtlin Instruments, ALTO Instruments, France). The main plasma reactor, where the plasma is produced, is located inside the power supply. At the reactor's orifice, a flexible dielectric tube is mounted, containing a floating-potential electrode (conductive wire of ca. 1 mm^2 section). The dielectric tube connects the main reactor with a second plasma reactor. This second part of the plasma device, the applicator, is essentially a second coaxial DBD reactor that is made of a PTFE (polytetrafluoroethylene) body with the floating electrode placed in its centre and a grounded electrode on the outside. The outlet of the second plasma reactor has five micro-orifices ($Ø_{int}$ = 800 μm), producing, thus, five distinct plasma jets covering a larger liquid surface area during the plasma treatment. Four of the orifices are disposed at the corner of a 4.2 mm square, with the fifth orifice located at the crossing of the square diagonals. The liquid treated by the plasma, here PBS(Ca^{2+}/Mg^{2+}), is placed in wells of an x24 well plate and is connected to the ground thanks to a ring-shaped wire electrode (stainless-steel wire Ø = 1 mm) located at the bottom of the wells. The distance between the applicator orifices and the surface of the liquid was maintained at 4 mm thanks to a customized 3D-printed spacer. Between the electrode and the ground, it was placed a compensation circuit designed to impose a total target impedance equal to that of a human body standard model, as presented in our previous work[31]. This grants additional control of the process parameters (which always include the target impedance) and eases the possible future translation of the results to a direct plasma application on animal models and human patients.

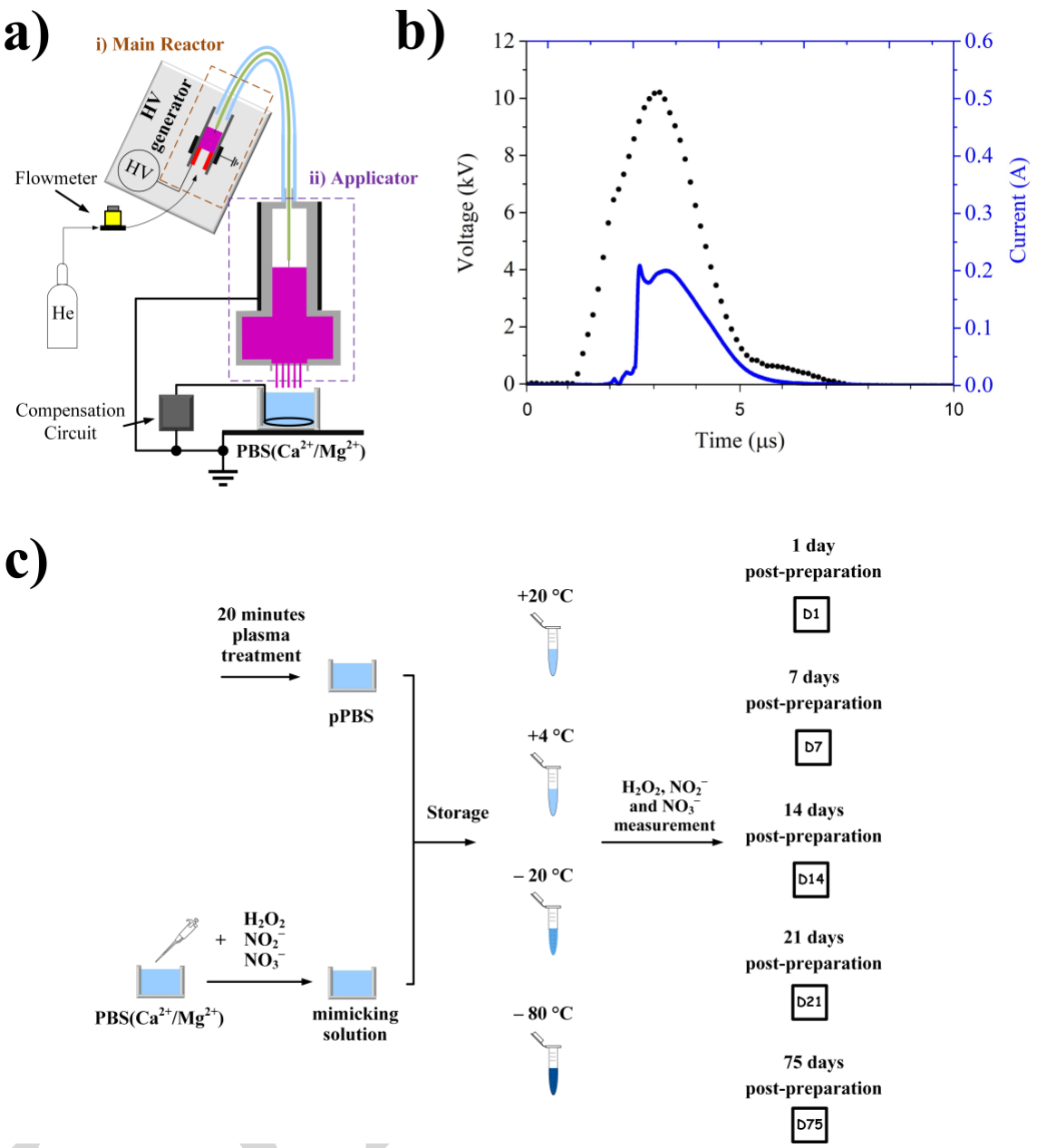

Figure 1. a) Conceptual view of the experimental setup and the two reactors used in this study **i)** for the plasma production and **ii)** for the liquid treatment. **b)** Electrical characteristics of the non-thermal plasma multi-jet source: high voltage measured on the power supply (black dots) and current measured on the compensation circuit (blue line). **c)** Conceptual view of the experimental procedure employed for the treatment, storage and analysis of the pPBS samples.

2.2 Electrical characteristics

The applied voltage was measured with a high-voltage passive probe (Lecroy, PPE 20 kV, France), while the current passing through the solution and reaching the ring electrode was determined by measuring the voltage drop on the resistor in the compensation circuit with another high-voltage passive probe (Lecroy, PPE 6 kV, France). As shown in **Figure 1b)**, the current pulse has an amplitude of 0.2 A and a width at half a maximum of ~1.5 μs. The current waveform exhibits a sharp current spike generated by the contact of the plasma plume with the liquid, followed by a broader component typically measured in the presence of conductive targets, but that is absent in the free jet operation[32]. Here, the compensation circuit is useful to monitor the real power delivered to the liquid solution.

2.3 pPBS production, mimicking solutions preparation and their storage procedure

The procedure followed to produce plasma-treated PBS(Ca^{2+}/Mg^{2+}), or pPBS, is depicted schematically in **Figure 1c**. More precisely, 3 mL of Dulbecco's phosphate-buffered saline (PBS) containing Ca^{2+} and Mg^{2+} (DPBS, Ca^{++}, Mg^{++}, 14040-133), named PBS(Ca^{2+}/Mg^{2+}), were placed in individual wells of 24-multiwell plates (Nunclon® Delta Surface, Thermo Fisher Scientific, DK, 142475, France) and treated by the plasma for 20 minutes (except if stated differently). Afterwards, the amount of water evaporated during the plasma treatment (ca. 700 µL) was compensated by adding 700 µL of sterile water. Subsequently, the pPBS was divided and placed into several Eppendorf tubes (0.5 mL each). On the day of the plasma treatment (D0), and within 2 hours after the PBS treatment, the absolute concentrations of H_2O_2, NO_2^- and NO_3^- (see **Figure 2**), as well as the pH value of the pPBS, were measured. Note that it has been verified that the RONS concentrations remain the same between immediately after () and a few hours after the plasma treatment, if the pPBS is kept at +4 °C or + 20 °C. The remaining Eppendorf tubes were stored at different storage temperatures considered in this study: +20 °C, +4 °C, –20 °C and –80 °C. For the preparation of mimicking solutions, we used untreated PBS(Ca^{2+}/Mg^{2+}), or uPBS, into which we added pure concentrations of H_2O_2, NO_2^- and NO_3^- as those measured in pPBS ([H_2O_2] = 3 mM, [NO_2^-] = 1.5 mM and [NO_3^-] = 0.75 mM). The pH of the mimicking solutions was adjusted to the same value as that measured in pPBS. The concentration of the reactive species (H_2O_2, NO_2^- and NO_3^-) and the value of the pH were measured, both in pPBS and in mimicking solutions, after 1 (24 hours after the treatment at D0), 7, 14, 21 and 75 days of storage (**Figure 1c**). Finally, the degradation of the RONS and the modification of the pH due to the storage time or/and temperature were quantified with the initial values measured on the day of the plasma treatment (for pPBS) or the day of preparation (for the mimicking solutions), within 2 hours after it (D0).

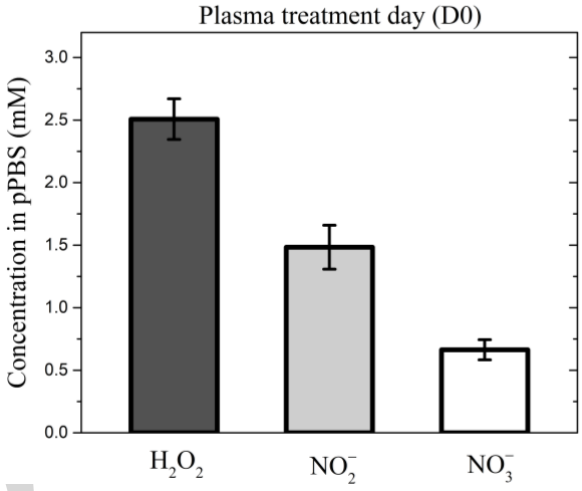

Figure 2. The concentration of H_2O_2, NO_2^- and NO_3^- in pPBS measured on the day of the plasma treatment (D0), within 2 hours after it. The data shown are the mean ± SEM of 34 independent experiments for H_2O_2 and 30 independent experiments for NO_2^- and NO_3^-.

2.4 Quantification of hydrogen peroxide (H_2O_2), nitrite (NO_2^-) and nitrate (NO_3^-)

The concentration of hydrogen peroxide in pPBS was determined using titanium oxysulfate, as previously described[9]. The absorbance was measured at 407 nm using a well plate reader (Infinite 627® M200 PRO Tecan, France). The quantification of nitrite and nitrate was performed using the nitrate/nitrite colorimetric assay kit (Cayman) according to the supplier's instructions, and the absorbance was measured at 540 nm using the same spectrophotometric system.

2.5 pH detection

The pH was measured in the pPBS using a SevenEasy™ pH meter S20 fitted with an InLab® 639 Microelectrode (Mettler Toledo, France). For monitoring the pH during the freezing process (slow (by

using isopropanol-filled containers) towards –80 °C, or fast (by liquid nitrogen) and then stored at –20 °C), two different electrophoretic color markers were used as pH indicators: bromophenol blue and thymol blue. While the first color marker changes from blue at pH 4.6 to yellow at pH 3.0, the second transitions from yellow at pH 2.8 to red at pH 1.2. Thymol blue was provided by Sigma-Aldrich, while Bromophenol blue was purchased from Bertin (France). The pH of the mimicking solutions (Figures 8 and 13) was modified using hydrochloric acid.

2.6 Dismutation of H_2O_2 by pyruvate

The contribution of H_2O_2 to the degradation of NO_2^- was quantified by using 5 mM and 50 mM of sodium pyruvate, a known H_2O_2 scavenger (Thermo-Fischer Scientific, France). The pyruvate was added to pPBS after the plasma treatment.

2.7 Cell culture

DC-3F Chinese hamster lung fibroblasts[33] and highly tumorigenic murine fibrosarcoma LPB cells[34], all mycoplasma-free, were cultured as adherent cells in Minimum Essential Medium (MEM, 31095-029) and Roswell Park Memorial Institute 1640 Medium (RPMI Medium, 21875-034), respectively. All media were supplemented with 10% fetal bovine serum (FBS, F7524), 100 $U.mL^{-1}$ penicillin and 100 $mg.mL^{-1}$ streptomycin (15140-122). Adherent cells were spread at 37 °C in a 95% humidity atmosphere containing 5% CO_2 (HERAcell 240i incubator CO_2, Thermo Scientific, France) and passaged upon confluency (every two days at a 1:10 dilution or every three days at a 1:30 dilution) using TrypLE™ Express Enzyme solution (12604-013). Short-term cell viability for routine sub-culturing was assessed by the trypan blue exclusion dye method (Trypan Blue Solution, T8154) with a Countess™ II FL Automated Cell Counter (Invitrogen, France), considering only viable cells. Cells were regularly checked for mycoplasma contamination *via* polymerase chain reaction (PCR) (not detailed).

For all assays on those cell lines (cytotoxicity and cell membrane permeabilization), 300 µL of cell suspension at a density of 1.80×10^5 $cells.mL^{-1}$ were used to seed each well of 48-well plates (Nunclon® Delta Surface, Thermo Fisher Scientific, DK, 150687, France), 24 hours before the experiment (*i.e.* at D–1), allowing to reach *c.a.* 80 to 90% confluence of the cell layer on the day of the experiment (D0). Just before any assay, the medium above the cells was gently removed by aspiration and the cell layer was washed twice with PBS(Ca^{2+}/Mg^{2+}). For sham conditions, all procedures remained identical to pPBS conditions, but untreated PBS(Ca^{2+}/Mg^{2+}) (non-exposed to the plasma), or uPBS, previously stored under the same storage conditions as the pPBS, was used instead.

2.8 Cell viability assessment by clonogenic assay

The cytotoxicity of pPBS, previously stored under different storage conditions, was determined employing the clonogenic assay for DC-3F cells. LPB cells do not form colonies and, therefore, the assessment of their viability could not be performed using this precise test. Adherent DC-3F cells were incubated with 200 µL of pPBS per well for 10 minutes (note that the pPBS put in contact with the cells was always at room temperature, and had just been unfrozen or warmed up a few minutes before, if applicable). Afterwards, pPBS was gently removed from the cell layer and cells in each well were detached by 100 µL TrypLE™ Express and suspended in its culture medium. A serial dilution of the single-cell suspensions was performed for cell cloning as previously reported[31]. Concretely, based on the total number of cells counted in the single-cell suspension in sham (for D0) or sham previously-stored at +4 °C (for D1 and D21), the single-cell suspension of every sample was diluted in complete medium at a final concentration of 125 $cells.mL^{-1}$ in a final volume of 8 mL. Cells were then distributed in 3 wells of a 6-multiwell plate (Nunclon® Delta Surface, Thermo Fisher Scientific, DK, 140675, France) by pouring 250 cells in 2 mL per well. This seeding allows individual (and surviving) cells to form discrete colonies over 5 days of cell culture at 37 °C in a 5% CO_2 humidified cell incubator. After 5 days of cell culture, colonies were fixed and stained with a solution of formaldehyde (3.7% vol/vol)

containing crystal violet (0.2% wt/vol) in H_2O. The number of clones for each condition was counted. Colonies containing more than 50 cells were counted as "normal size colonies", and those containing from *c.a.* 20 to fewer than 50 cells were counted as "small colonies". The viability was then normalized to the number of clones in the corresponding sham sample.

2.9 Cell membrane permeability assessment by flow cytometry analysis

The eventual permeabilization of the cells treated by the pPBS was investigated using the fluorescent nucleic acids stain YO-PRO®-1 Iodide uptake (629.04 Da). The non-permeant YO-PRO®-1 dye is commonly used as an indicator for cell membrane permeabilization. Indeed, YO-PRO®-1 can enter the cell only when the cell membrane is permeabilized, and, once in the cells, it intercalates with nucleic acids, resulting in a strong green fluorescence signal which is detectable by flow cytometry. On the day of the experiment, the medium above the cells was removed and the cell layer was washed twice with PBS(Ca^{2+}/Mg^{2+}). The two cell lines were then incubated for 1 hour with the mixture of pPBS (previously-stored under different storage conditions) and YO-PRO®-1 Iodide at 2 µM (200 µL per well). After the treatment, the liquid above the cell monolayer was gently removed and the cells were harvested using TrypLE™ Express Enzyme dissociation (200 µL per well). The cell suspension was immediately analyzed by flow cytometry (C6 flow cytometer, BD Accuri, San Jose, California, US) with 10 000 events recorded per sample within a selected gate that excludes cellular debris. The YO-PRO®-1 uptake (cell permeabilization) was evaluated using green fluorescence channels (excitation 488 nm, emission 530/30 nm). More precisely, we assessed the median of the fluorescence intensity per cell (an indication of the average level of permeabilization of the cells).

2.10 Statistical analysis

Unless otherwise specified, all the results corresponding to the chemical composition of the pPBS are expressed as mean values ± standard deviation (SD) of three independent experiments. All the results corresponding to the effect of the pPBS on the cancer cells are expressed as mean values ± SD of three independent experiments, with each time point in at least four independent samples (quadruplicate). The significance level, or p-value, was calculated using the Student's t-test. Statistical significance levels found between the values of different groups were associated with p-values of > 0.05 (NS), < 0.05 (*), < 0.01 (**), < 0.001 (***) and < 0.0001 (****).

3. Results

3.1 RONS (H_2O_2, NO_2^- and NO_3^-) degradation as a function of storage time and temperature

As previously observed[9], the anti-cancer properties of PTS are mainly due to the combined action of H_2O_2, NO_2^- and NO_3^-, and in some cases also with the acidic pH[21]. Thus, the chemical stability of these RONS in the plasma-treated PBS(Ca^{2+}/Mg^{2+}), hereafter termed pPBS, was assessed as a function of the storage time and temperature. The concentration of these reactive species in pPBS within 2h from plasma treatment (D0) is depicted in **Figure 2**. At first, the degradation of H_2O_2 in the pPBS was investigated (see **Figure 3**). When the pPBS was stored at room temperature (around +20 °C) or +4 °C, no significant degradation of H_2O_2 was observed for up to 75 days of storage concerning the initial concentration obtained just after the plasma treatment (at D0, **Figure 2**). Also, no significant difference was observed between these two storage temperatures, in terms of H_2O_2 stability over time. On the contrary, when the pPBS was stored at –20 °C or –80 °C, the concentration of H_2O_2 decreased over time, even after just 1 day of storage (24 hours after the treatment at D0). The maximum degradation was measured after 7 days of storage, when the concentration of H_2O_2 was found to be ~20% and ~30% lower than its initial concentration when stored at –80 °C and –20 °C, respectively. No further significant degradation was observed after this period of storage (>D7). However, it must be stressed that the

difference (~10% points) between these two storage temperatures (–20 °C and –80 °C) is statistically significant.

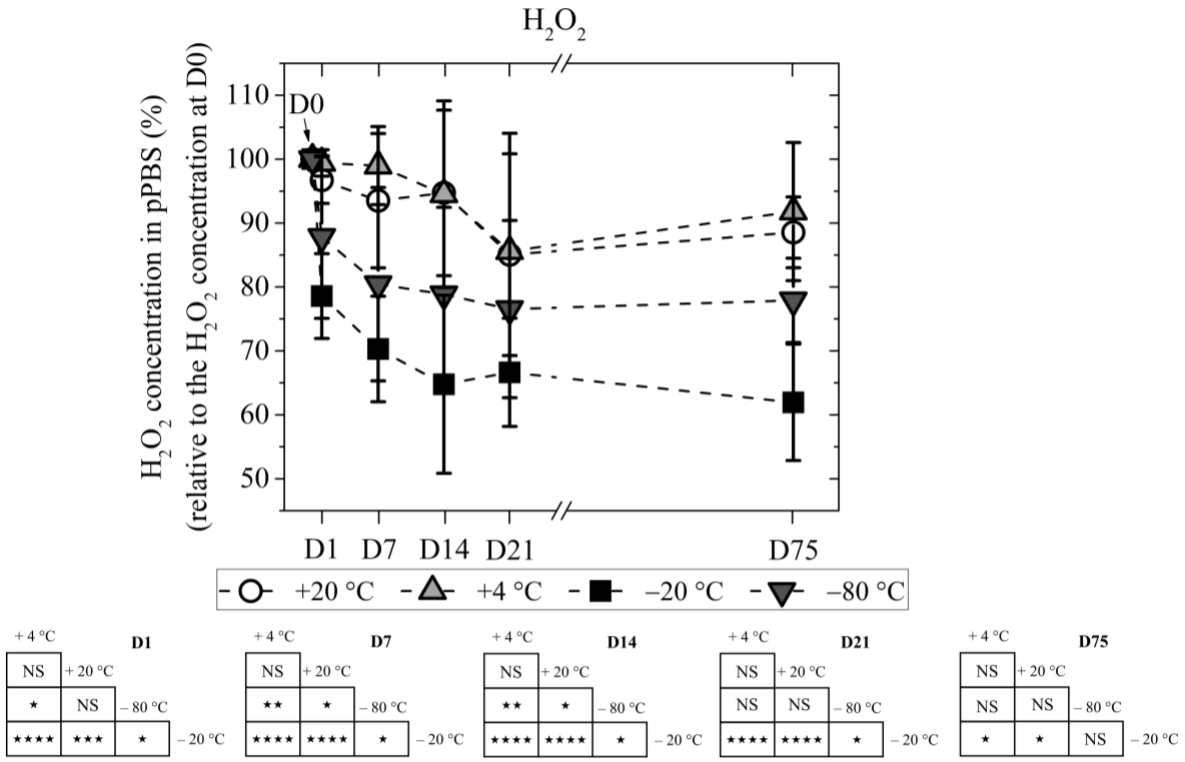

Figure 3. The concentration of H_2O_2 in the pPBS as a function of the storage time, when stored at four different temperatures: +20, +4, –20 and –80 °C. The concentration of H_2O_2 in % is calculated concerning the initial concentration measured on the day of plasma treatment (D0), within 2 hours from it. For up to 21 days of storage (D21), the data are the mean ± SD of 9, 9, 18 and 9 independent experiments for +20, +4, –20 and –80 °C, respectively. For 75 days of storage (D75), the data are the mean ± SD of 3 independent experiments for all the storage temperatures.

As previously reported[31], also in the present experimental conditions, the concentration of RONS (H_2O_2, NO_2^- and NO_3^-) in the pPBS increases almost linearly with the plasma treatment time (see **Figure 4**). To evaluate the effect of the total concentration of these reactive species on the degradation of H_2O_2, PBS(Ca^{2+}/Mg^{2+}) was plasma-treated for 1, 2.5, 5, 10 and 20 minutes and then stored at +4 °C and –20 °C (see **Figure 5**). These two storage temperatures were chosen because they induce the lowest and the highest degradation of H_2O_2 over storage time, respectively (see **Figure 3**). The ratio of the concentrations of H_2O_2 and NO_2^- varies between 0.5 and 2 for the plasma treatment times considered here (see **Figure SF1**). Our results unveil, on the one hand, that, independently of the plasma treatment time, and, thus, of the initial concentrations of the RONS studied here, H_2O_2 is always significantly degraded when the pPBS is stored at –20 °C (~20-35% degradation, as compared to the initial concentration of H_2O_2 measured at D0), except in some cases for only one day of storage (D1) where there is no degradation. This degradation is more pronounced after 7 days (D7) than on the first day (D1) of storage. On the other hand, the concentration of H_2O_2 is stable (>85% concerning the H_2O_2 concentration at D0) over 21 days (D21), when the pPBS is stored at +4 °C.

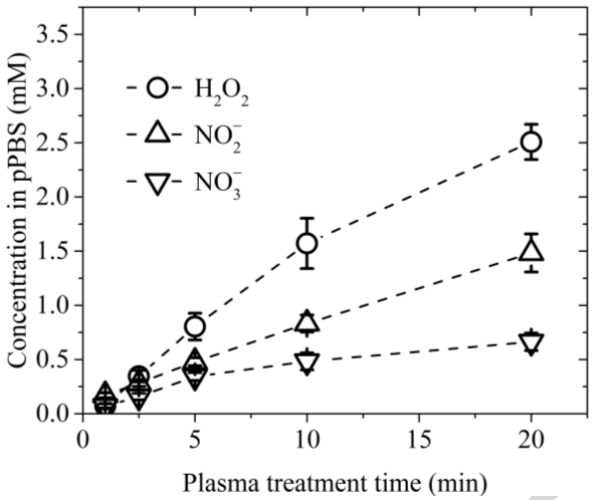

Figure 4. H_2O_2, NO_2^- and NO_3^- absolute concentrations as a function of the plasma treatment time, measured on the day of the plasma treatment (D0), within 2 hours from it. The data for the H_2O_2 is the mean ± SEM of 18 or 10 or 5 independent experiments for 20 or 10 or 5, 2.5 and 1 minutes of plasma treatment, respectively. For NO_2^- and NO_3^-, the data are the mean ± SEM of 6 independent experiments.

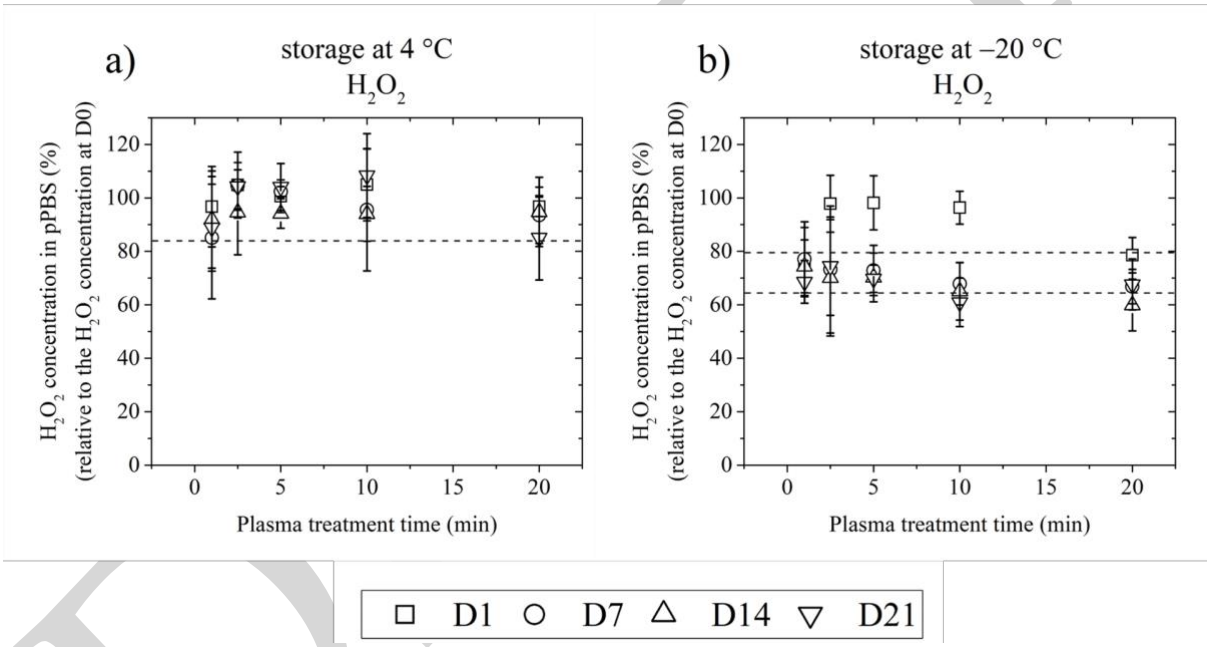

Figure 5. The concentration of H_2O_2 in the pPBS as a function of the plasma treatment time, when stored at **a)** +4 °C and **b)** –20 °C for 1 day (D1), 7 days (D7), 14 days (D14) and 21 days (D21). The concentration of H_2O_2 in % is calculated concerning the initial concentration of H_2O_2 measured on the day of the plasma treatment (D0), within 2 hours from it. For the 20 minutes plasma treatment time, the data are the mean ± SD of 9 (for +4 °C) and 17 to 18 independent experiments (for –20 °C), while for 10 minutes plasma treatment time, of 7 to 10 independent experiments (for both storage temperatures). For all the other plasma treatment times (1, 2.5 and 5 minutes), the data are the mean ± SD of 2 to 5 independent experiments (for both storage temperatures).

Although H_2O_2 has been described as a key player in pPBS-induced reduction of cancer cells viability[20], its synergistic effect with reactive nitrogen species such as NO_2^- has also been reported[9,21]. To conclude on the overall degradation of the pPBS as a function of the storage time and temperature, the concentration of these reactive nitrogen species was also monitored (see **Figure 6**). We found that both NO_2^- and NO_3^- are stable for up to 21 days when the pPBS is stored at +4 °C or +20 °C. For longer storage times (75 days), the concentration of NO_2^- decreases by ~35-40% at these storage temperatures. As for H_2O_2, there is no significant difference between storing at room temperature (around +20 °C) or in the fridge (+4 °C). When the pPBS is stored at –20 °C, we observe a massive degradation of NO_2^-, over ~90%, occurring even from the first day of storage. The degradation at –80 °C is also significant

(~70%). On the contrary, the concentration of NO_3^- increases when the pPBS is stored at –20 °C or –80 °C, showing an inversely proportional behavior to that of NO_2^-.

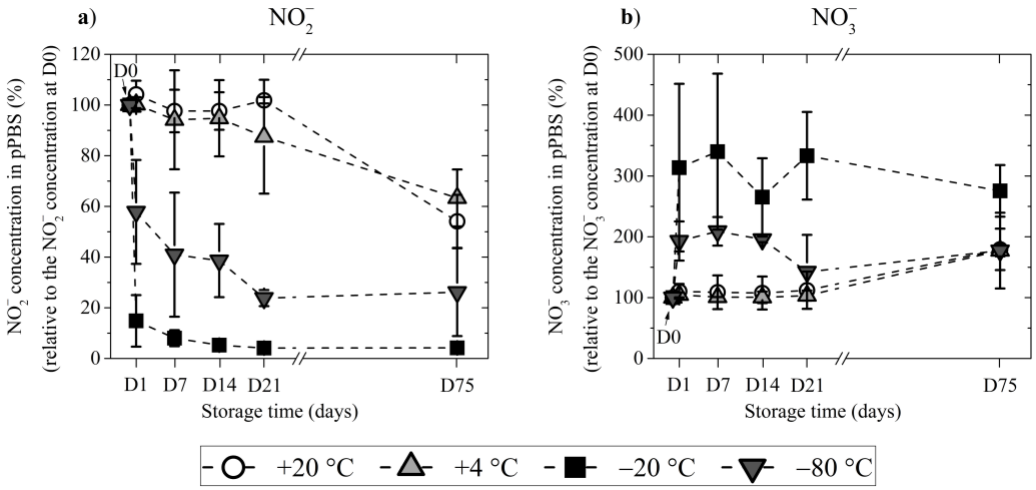

Figure 6. The concentration of **a)** NO_2^- and **b)** NO_3^- in the pPBS as a function of the storage time, when stored at four different temperatures: +20, +4, –20 and –80 °C. The concentration in % is calculated with the initial concentration of **a)** NO_2^- or **b)** NO_3^- measured on the day of the plasma treatment (D0), within 2 hours from it. For NO_2^-, the data are the mean +- SD of 8 and 3 independent experiments for up to 21 (D21) and 75 days of storage (D75), respectively. For NO_3^-, the data are the mean +- SD of 6 and 2 independent experiments for up to 21 (D21) and 75 days of storage (D75), respectively.

3.2 Impact on the degradation of RONS of their initial concentration and the pH of the solution

To understand the mechanisms of the pPBS degradation due to storage time or/and temperature, we first isolated the reactive species considered in this work (H_2O_2, NO_2^- and NO_3^-) by preparing mimicking solutions of those species in PBS(Ca^{2+}/Mg^{2+}) with concentrations equivalent to those produced by a 20 minutes plasma treatment ([H_2O_2] = 3 mM, [NO_2^-] = 1.5 mM and [NO_3^-] = 0.75 mM). Two different mimicking solutions were prepared: the first contained these reactive species concentrations in PBS(Ca^{2+}/Mg^{2+}) of pH = 7.1, while the second contained the same reactive species concentrations in PBS(Ca^{2+}/Mg^{2+}) of pH = 6.1 (equal to that of pPBS). For the following cases, there was no degradation over 21 days of storage at any of the storage temperatures studied here: 1) H_2O_2 alone, 2) NO_2^- alone, 3) NO_3^- alone, 4) NO_2^- + NO_3^-, 5) H_2O_2 + NO_3^- in mimicking solutions of both pH = 7.1 and pH = 6.1 (see **Figures SF2** (for 1), 2) and 3)), **SF3** (for 4)) and **SF4** (for 5))). In the case of H_2O_2 + NO_2^- in mimicking solutions of pH = 7.1, presented in **Figure SF5**, the evolution over storage time at different storage temperatures of the reactive species is similar to the case of H_2O_2 + NO_2^- + NO_3^- also at pH = 7.1 (see **Figure 7**). For these cases, the degradation over storage time of H_2O_2 in the mimicking solutions simulates its degradation in pPBS with a slightly delayed evolution, i.e., about –30% after 21 days instead of only 7 days of storage (see **Figure 3**). This time-shift is even more pronounced for the NO_2^- degradation, as the effect of the storage temperature observed after the first day of storage for the pPBS is only observed after 75 days of storage for the mimicking solutions (compare **Figures 6a** and **7**). As so, the degradation of both H_2O_2 and NO_2^- is similar in pPBS or mimicking solutions after 75 days of storage. Contrariwise, the degradation of the solutions containing H_2O_2 + NO_2^- or H_2O_2 + NO_2^- + NO_3^-, but at a pH = 6.1, simulates closely the degradation of the plasma-treated solution, as shown in **Figures SF5** and **8**, respectively. Finally, mimicking PBS(Ca^{2+}/Mg^{2+}) solutions with different concentrations of H_2O_2 or NO_2^- and pH = 7.1 were also investigated (see blue and red points in **Figure 7**), to study the effect of these RONS initial concentrations on their degradation. On the one hand, we observe that for a doubled concentration of H_2O_2, the degradation of H_2O_2 is slightly smaller and the degradation of NO_2^- slightly higher. On the other hand, with twice the concentration of NO_2^-, the degradation of H_2O_2 is significantly higher and that of NO_2^- significantly lower, especially when the solution is stored at –80 °C. This means that the stoichiometry of the reaction between H_2O_2 and NO_2^- inducing their

degradation should be of 1:1, as, after a 20 min plasma treatment, the concentration of H_2O_2 in pPBS is about double of that of NO_2^- (see **Figures 2** and **SF1**). As a whole, these experiments highlight the great importance of both the reactive species concentration and the pH of the solution on the degradation over time of these RONS concentration in pPBS.

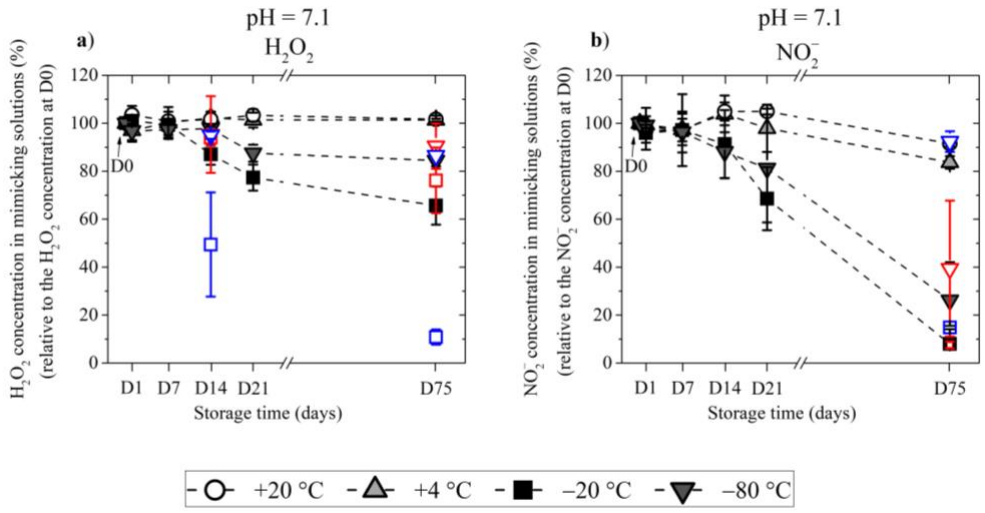

Figure 7. The concentration of **a)** H_2O_2 and **b)** NO_2^- in mimicking solutions of H_2O_2, NO_2^- and NO_3^- in PBS(Ca^{2+}/Mg^{2+}) of pH 7 .1, as a function of the storage time, when stored at four different temperatures: +20, +4, –20 and –80 °C. The blue and red points correspond to mimicking solutions containing 2*[NO_2^-] and 2*[H_2O_2], respectively, stored at –20 °C (squares) or –80 °C (down triangles). The concentration in % is calculated with the initial concentration of **a)** H_2O_2 or **b)** NO_2^- measured on the day of preparation of the solutions (D0). The data are the mean ± SD of 4 independent experiments for all experimental conditions, except for mimicking solutions containing 2*[NO_2^-] and 2*[H_2O_2] (2 independent experiments) and mimicking solutions containing 1*[NO_2^-] and 1*[H_2O_2] and stored for 75 days (D75) (3 independent experiments).

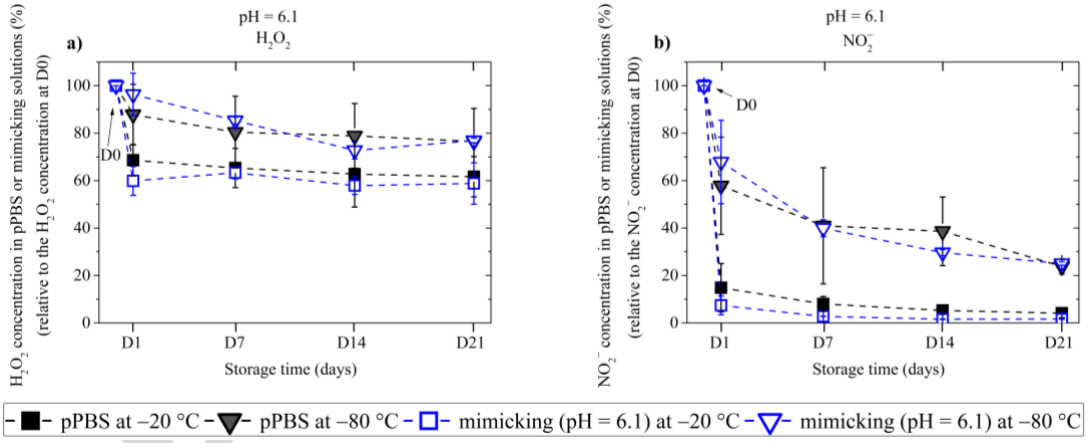

Figure 8. The concentration of **a)** H_2O_2 and **b)** NO_2^- in pPBS (black symbols; same data as in Figures 3 and 6) and in mimicking solutions of H_2O_2, NO_2^- and NO_3^- in PBS(Ca^{2+}/Mg^{2+}) of pH = 6.1 (blue symbols), as a function of the storage time, when stored at –20 °C (squares) and –80 °C (down triangles). The concentration in % is calculated with the initial concentration of **a)** H_2O_2 or **b)** NO_2^- measured on the day of preparation of the solutions (D0). For the mimicking solutions stored at –20 °C and –80 °C, the data are the mean ± SD of 3 and 2 independent experiments, respectively.

To underline the essential role of H_2O_2 on the NO_2^- oxidation in pPBS, due to storage time and/or storage temperature, pyruvate, a known H_2O_2 scavenger, was used. PTS containing or not 5 mM or 50 mM of sodium pyruvate (added after the plasma treatment) were stored at –20 °C and the concentration of H_2O_2, NO_2^- and NO_3^- was measured after 1, 7, 14 and 21 days of storage (see **Figures 9** for NO_2^- and NO_3^- and **SF6** for H_2O_2). By adding pyruvate, we were able to scavenge most (5 mM, 90% reduction) or virtually all (50 mM, below the detection limit) of the H_2O_2 in pPBS and, thus, to reduce its concentration

by at least 90% (**Figure SF6**). As depicted in **Figure 9**, the addition of pyruvate partially prevents the degradation of NO_2^-. More specifically, the quenching of 90% of the H_2O_2 present in pPBS resulting from the addition of 5 mM pyruvate led to a decrease of the degradation of NO_2^- from ~85-95% (without pyruvate) to ~35-50% (with 5 mM pyruvate) upon storage at –20 °C. This NO_2^- degradation that is still observed when pPBS with 5 mM pyruvate is stored at –20 °C is due to the remaining concentration of H_2O_2. Indeed, according to **Figure SF7**, even such small concentrations of H_2O_2 can oxidize ~20-30% of the NO_2^-. From **Figure SF7**, it can also be concluded that the reaction between H_2O_2 and NO_2^- is not catalytic and, again, that its stoichiometry is 1:1. Collectively, the results with the mimicking solutions at pH = 6.1 (**Figure 8**) and those with the addition of sodium pyruvate (**Figure 9**) suggest that H_2O_2 is by far the main oxidizer of NO_2^- in our experimental conditions of very low pH (~2-3), confirming previously published results on the nitrous acid oxidation in aqueous aerosols[35]. Finally, as shown in **Figure 9**, the concentration of NO_3^- increases inversely proportional to the decrease of the concentration of NO_2^-, both with and without pyruvate, highlighting that NO_3^- is a product of the peroxidation of NO_2^-.

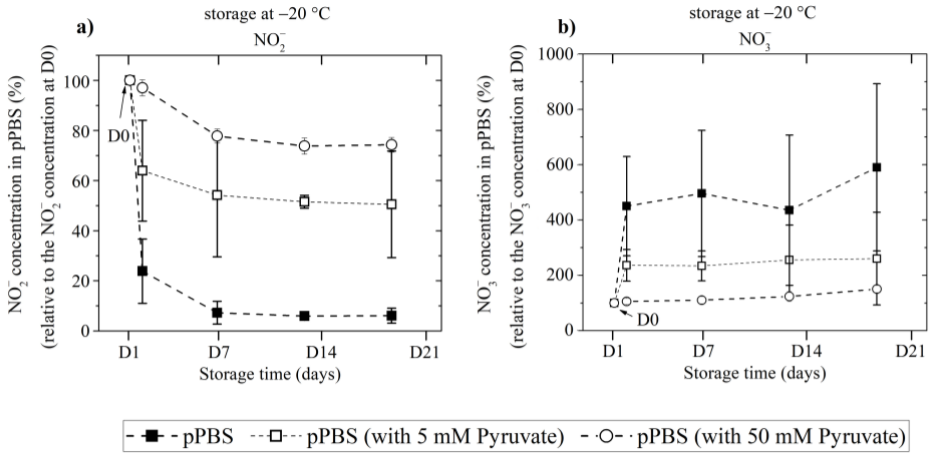

Figure 9. The concentration of a) NO_2^- and b) NO_3^- in pPBS containing or not 5 mM or 50 mM of pyruvate, as a function of the storage time, when stored at –20 °C. The concentration in % is calculated with the initial concentrations of NO_2^- and NO_3^-, measured on the day of the plasma treatment (D0), within 2 hours from it. The data are the mean ± SD of 2, 3 and 8 independent experiments for the pPBS + 50 mM Pyruvate, pPBS + 5 mM Pyruvate and the pPBS alone, respectively.

3.3 Impact of the freezing rate on the degradation of RONS

As stated before, the degradation of the RONS studied here (H_2O_2, NO_2^- and NO_3^-) occurs mainly for storage temperatures requiring the freezing of the pPBS solution (–20 °C and –80 °C). To better understand the impact of the freezing process, the degradation of the chemical components of the solution as a function of its freezing rate was studied. As so, pPBS solutions were fast frozen by liquid nitrogen and then stored at –20 °C (see open squares in **Figure 10**), or slowly frozen in isopropanol-filled containers when stored at –80 °C (see full circles **Figure 11**), or normally frozen when just stored at –20 °C (see full circles in **Figure 10**) or –80 °C (see open squares in **Figure 11**). As depicted in **Figures 10** and **11**, the freezing rate of the solution has almost no impact on the degradation of H_2O_2 and NO_2^-. It seems that the evolution over the storage time of the reactive species concentration at –20 °C and –80 °C depends only on the final storage temperature of the solution.

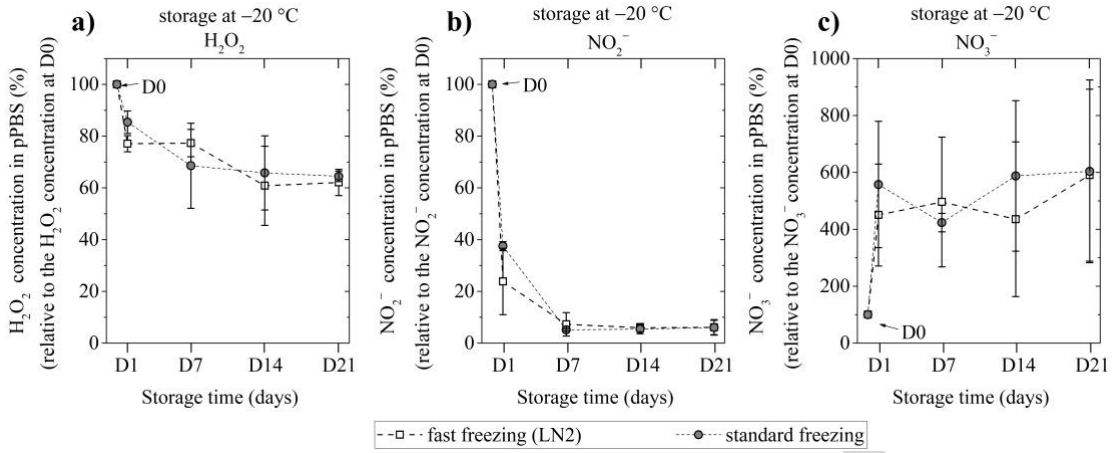

Figure 10. The concentration of **a)** H_2O_2, **b)** NO_2^- and **c)** NO_3^- in pPBS as a function of the storage time, when stored at –20 °C, but frozen at two different freezing rates: standard as a consequence of storage at –20 °C or fast by liquid nitrogen (LN2) before immediate storage at –20 °C. The concentration in % is calculated with the initial concentration of **a)** H_2O_2, **b)** NO_2^- and **c)** NO_3^- measured on the day of the plasma treatment (D0), within 2 hours from it. The data are the mean ± SD of 5 independent experiments.

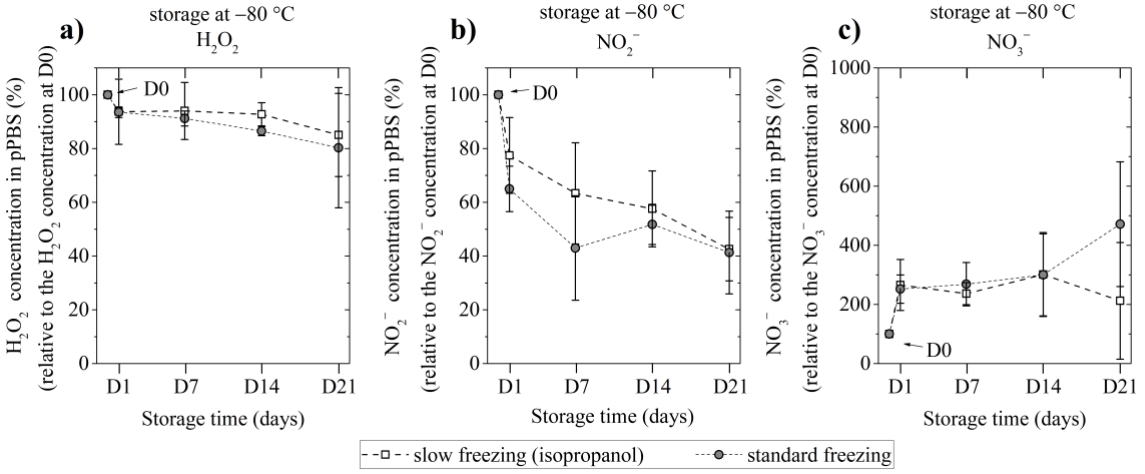

Figure 11. The concentration of **a)** H_2O_2, **b)** NO_2^- and **c)** NO_3^- in pPBS as a function of the storage time, when stored at –80 °C, but frozen at two different freezing rates: standard as a consequence of storage at –80 °C or slow by using isopropanol-filled containers when storing at –80 °C. The concentration in % is calculated with the initial concentration of **a)** H_2O_2, **b)** NO_2^- and **c)** NO_3^- measured on the day of the plasma treatment (D0), within 2 hours from it. The data are the mean ± SD of 5 independent experiments.

3.4 Acidification of the solution during its freezing

The pH of pPBS was monitored as a function of the storage time and temperature. We found that the plasma treatment results in an acidification of the PBS(Ca^{2+}/Mg^{2+}), from an initial pH of 7.1 (± 0.1) to a pH of 6.2 (± 0.5). This pH value stays relatively stable (± 0.3, see **Table 1**) independently of the storage time or temperature (note that for the cases of storage at –20 °C and –80 °C, the pH was measured after unfreezing the solutions of pPBS). Nevertheless, as previously reported[36], the pH value of the solutions is affected during the freezing process. Thus, the variation of the pH of the pPBS during the freezing towards –20 °C and –80 °C was monitored. As depicted in **Figures 12** and **SF8**, the pH of the still unfrozen solution changes throughout the first hour of freezing. Using two different pH indicators (bromophenol blue and thymol blue), the final pH value of the frozen pPBS is estimated to be around 2.5 and 0.75 for storage at –20 °C and –80 °C, respectively. The pH reaches values lower than 3 in less than 1 hour. **Figure SF9** shows the acidification of untreated PBS(Ca^{2+}/Mg^{2+}), uPBS, with different initial pH values (from 1 to 7), as a result of the freezing of the solutions. Both pH color markers indicate that freezing of uPBS, when its initial pH is around 6 or less, results in substantial acidification

of the solution. Moreover, the acidification, due to freezing, is rather similar for the uPBS with an initial pH of 6 than the pPBS (compare **Figures SF8** and **SF9**). Finally, the acidification of both uPBS for all the initial pH values considered here and pPBS is similar when stored at –20 °C or –80 °C. It is interesting to note that, after unfreezing the solutions, both pH color markers indicate that the initial pH is retrieved (**Figure SF8**), confirming the pH values measured with the pH meter (**Table 1**).

pH at D0 = 6.15 ± 0.52

pH	D1	D7	D14	D21	D75
+20 °C	6.29 ± 0.23	6.27 ± 0.32	6.31 ± 0.25	6.44 ± 0.23	6.23 ± 0.21
+4 °C	6.39 ± 0.16	6.44 ± 0.17	6.44 ± 0.13	6.31 ± 0.14	6.29 ± 0.10
–20 °C	6.44 ± 0.31	6.42 ± 0.11	6.44 ± 0.19	6.39 ± 0.19	6.35 ± 0.17
–80 °C	6.41 ± 0.32	6.19 ± 0.41	6.47 ± 0.21	6.35 ± 0.20	6.33 ± 0.25

Table 1. pH of the pPBS measured on the day of the plasma treatment (D0), within 2 hours from it, and after storage at different temperatures (+20, +4, –20 and –80 °C) for different periods (1, 7, 14, 21 and 75 days). The data are the mean ± SD of 3 (for D1, D7, D14 and D21) or 2 (for D75) independent experiments.

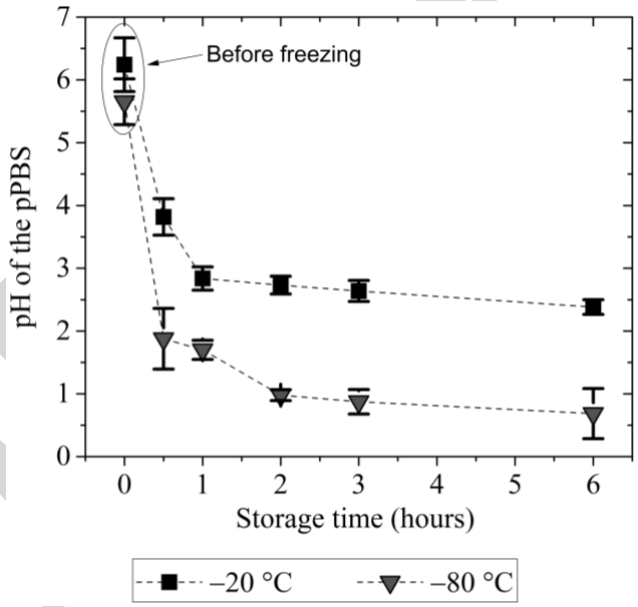

Figure 12. pH values of pPBS as a function of the storage time at –20 °C and –80 °C. The pH was evaluated by using bromophenol blue as a pH indicator and the polynomial function relating the sum of R+G–B values and the pH value determined in **Figure SF10 b)**. The RGB values used are the mean values of a large area of the photographs of the Eppendorf tubes containing pPBS and bromophenol blue after storage for 30 minutes, 1, 3 and 6 hours at –20 °C and –80 °C (**Figure SF8**). The data are the mean ± SD of 5 and 3 independent experiments for storage at –20 °C and at –80 °C, respectively.

Having established that the freezing of the solution decreases its pH, regardless if it is uPBS or pPBS, we then studied the effect of this acidification on the concentration of the three RONS considered here. **Figure 13** shows the concentration of H_2O_2, NO_2^- and NO_3^- 6 hours after the preparation of mimicking solutions of PBS(Ca^{2+}/Mg^{2+}) with different pH values and maintained at room temperature. As it can be seen in **Figure 13**, we should consider a pH value of 5 as a lower threshold for the stability of these reactive species. For pH values lower than 5, the acidic environment of the solution results in the degradation of H_2O_2 and favors the oxidation of NO_2^- and its partial transformation into NO_3^-. These data are coherent with both the calculated pH values of the frozen pPBS solutions determined with the

help of the pH indicators (~2-3) and our measurements of the concentration of the reactive species in pPBS stored at –20 °C or –80 °C. Indeed, similarly to after storage at –20 °C or –80 °C, at a pH of ~2-3, we observe a massive degradation of the NO_2^- and a modest degradation for the H_2O_2. The degradation of NO_2^- presented in **Figure 13** is even greater than after storing at –20 °C or –80 °C. This might be due to the higher temperature of the solutions considered in **Figure 13**(room temperature), which could favor the reactions of degradation of H_2O_2 and NO_2^-.

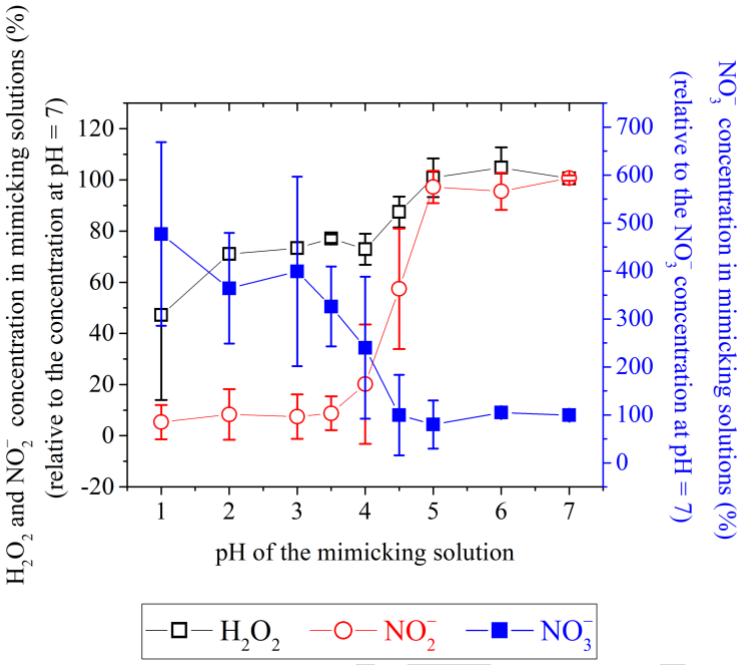

Figure 13. The concentration of H_2O_2, NO_2^- and NO_3^- 6 hours after the preparation of mimicking solutions of PBS(Ca^{2+}/Mg^{2+}) with different pH values, maintained at room temperature. The concentration in % is calculated with the concentration of H_2O_2, NO_2^- or NO_3^- measured in the solution with pH = 7 6 hours after preparation. The data are the mean ± SD of 6 independent experiments.

3.5 Application on cancer cells

3.5.1 Cell viability post pPBS treatment

The cytotoxicity of the pPBS stored in different conditions was studied on adherent DC-3F cells for a treatment time (time of incubation in pPBS) of 10 minutes, using the clonogenic assay. The results are presented in **Figure 14** and summarised in **Table 2**. Firstly, we observed that the pPBS is highly effective in reducing the viability of the cancer cells, even after only 10 minutes of treatment. Considering a total colonies count (normal and small colonies), the treatment of DC-3F cancer cells with pPBS at D0 (freshly produced and maintained at room temperature for a few hours) reduced their viability by 60 % (see **Figure 14** and **Table 2**). Regarding the normal size colonies, there is only 15% of cell viability (or 85% of cytotoxicity) after treatment with freshly prepared pPBS (D0). Subsequently, the ability of pPBS to preserve its anti-cancer capability was evaluated when stored for up to 21 days at +4 °C and –20 °C. Our results show that, even after 21 days of storage at +4 °C, the pPBS fully retained its cytotoxic capacity (only *ca.* 14.0 to 16.6% and *ca.* 40 to 50% of normal and total colonies are formed, respectively). Contrariwise, when the pPBS is stored at –20 °C, it is much less effective in inducing cancer cell death (even after only 1 day of storage). This loss of efficacy is more pronounced regarding the normal colonies than the small colonies and for longer storage periods. When using pPBS stored for 21 days at –20 °C, the cells retained their viability and formed 3-fold more colonies in normal size, as compared with those being treated with pPBS stored at +4 °C for 21 days or at –20 °C for 1 day. However, the reduction of the viability of small colonies does not exhibit a significant difference between the different storage conditions. It is interesting to note, though, that there is a 30-75% increase in the number of small colonies when using pPBS stored for 1 day at –20 °C compared to all the other treatment conditions, unveiling a transient cytostatic effect. As previously discussed, while the

degradation of NO_2^- is already massive after only 1 day of storage (85%), the decrease of the H_2O_2 concentration at D1 is not as significant (20-25%) and it is lower than after 21 days of storage (30-35%). Considering a total colony count, the cancer cells are highly resistant to the treatment with pPBS stored for 21 days at –20 °C (an increase of ca. 1.4 to 2.2-fold of total colonies, as compared with all the other treatment conditions). Collectively, these results show both a cytostatic and a cytotoxic effect of the pPBS, and are in full agreement with our observations regarding the concentration of the reactive species as a function of storage time and temperature. Indeed, at the storage conditions where H_2O_2 and NO_2^- are stable (+4 °C), the pPBS preserves its cytotoxic capacity over time, while at the storage conditions where these reactive species are degraded (–20 °C), the pPBS becomes less effective against tumor cells, especially over time of storage.

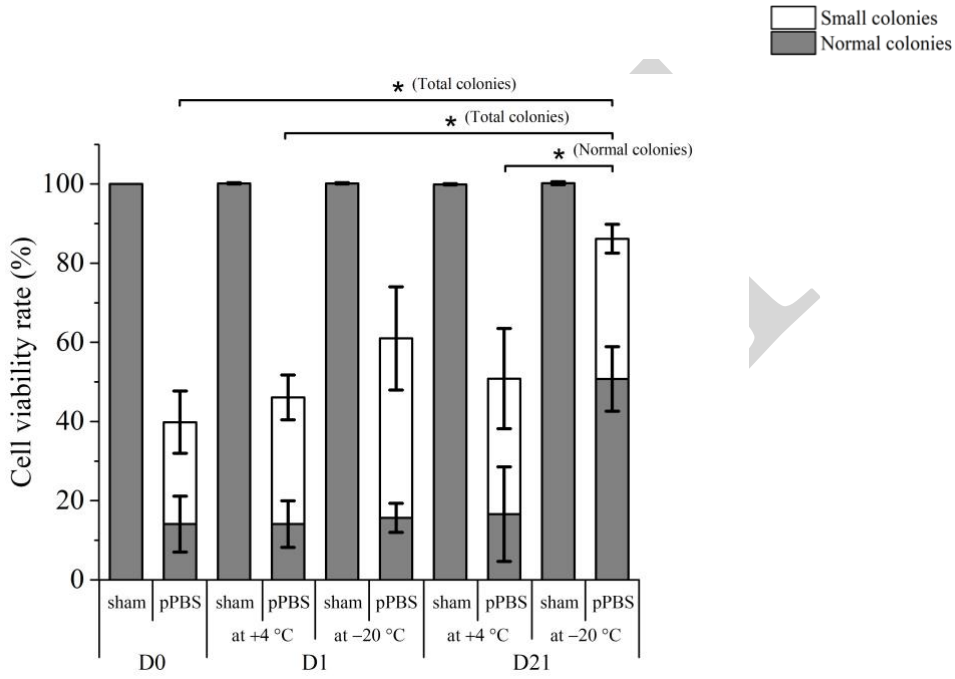

Figure 14. Cytotoxicity of pPBS previously-stored under different storage conditions to adherent DC-3F cells. After being incubated in pPBS for 10 min, DC-3F cells were plated immediately. The cell viability rate is presented as the number of colonies formed from viable cells five days after the treatment. Results from three independent experiments (each in quadruplicate) are shown as mean values ± SD for each parameter set. Statistical significance levels are presented as p-values of < 0.05 (*), < 0.01 (**), < 0.001 (***) and < 0.0001 (****). If no statistical significance is indicated, then p-values > 0.05 (NS).

Storage conditions		Normal colonies (%)	Small colonies (%)	Total colonies (%)
Day 0	RT	14.0 ± 7.0	25.8 ± 7.9	39.8 ± 14.9
Day 1	+4°C	14.0 ± 5.9	32.0 ± 5.7	46.0 ± 11.6
	–20°C	15.7 ± 3.7	45.3 ± 13.1	61.0 ± 16.8
Day 21	+4°C	16.6 ± 11.9	34.2 ± 12.7	50.8 ± 24.6
	–20°C	50.8 ± 8.1	35.4 ± 3.7	86.2 ± 11.8

Table 2. Cytotoxicity of pPBS stored at different storage conditions as a function of colonies formed after being treated with pPBS for 10 minutes and immediately cultured for 5 days at 37 °C in a 5% CO_2 humidified cell incubator. Visible colonies were stained, counted and normalized to the number of clones in the corresponding sham, expressed as 100%. Colonies containing more than 50 cells were counted as "normal size colonies", and those containing from *c.a.* 20 to fewer than 50 cells were counted as "small colonies". The data are the mean ± SD of 3 independent experiments (each in quadruplicate).

3.5.2 Cell membrane permeabilization post pPBS treatment

The effect of pPBS stored in different conditions on the cell membrane permeabilization was also studied on two different types of cancer cell lines: DC-3F and LPB cells. The results are presented in

Figure 15. First of all, we observed that the cellular membrane of both cancer cell lines is significantly permeabilized after 1 hour of contact with pPBS. This effect is in agreement with what our group has previously reported[31]. Contrary to the effect of the storage time and temperature on the viability of the cancer cells, here the pPBS stored at –20 °C is equally capable of permeabilizing the cells as those stored at +4 °C, for both cell lines and for all the different storage times studied. Interestingly, when the pPBS is stored for 21 days (both at +4 °C and –20 °C), it is still able to permeabilize the DC-3F cells but not the LPB cells. Indeed, even in conditions where the concentration of the RONS studied here is preserved (+4 °C), the pPBS is no longer effective in permeabilizing LPB cells after 21 days of storage. Collectively, these results unveil that the NO_2^-, that is massively degraded upon storage at –20 °C but not at +4 °C, does not play an important role in the permeabilization of these cancer cell lines. This could mean that H_2O_2 is the main driver of the cellular membrane permeabilization due to pPBS. As the H_2O_2 in the pPBS is further degraded from 1 to 21 days of storage (+10 percentage points), its concentration at D21 might be under the threshold required for permeabilizing LPB cells. However, the presence of another reactive species in pPBS (that is not studied here), responsible for the permeabilization of LPB cells, which is degraded over 21 days of storage, cannot be excluded.

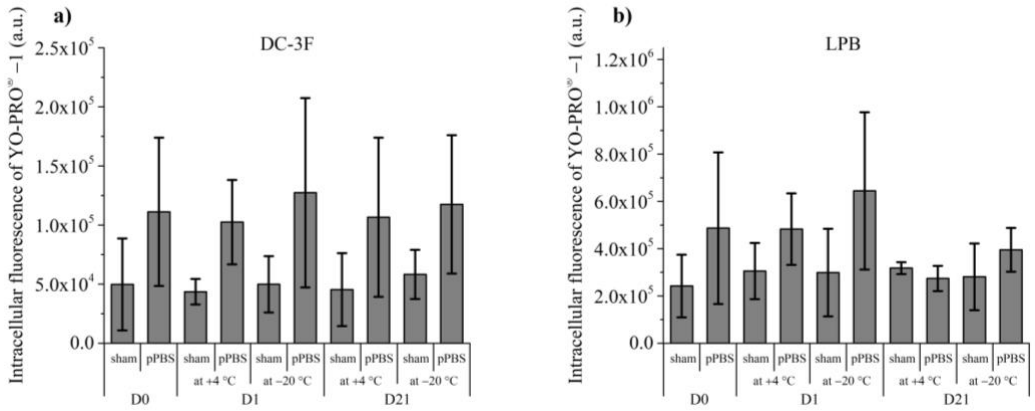

Figure 15. Effect of pPBS, previously stored at different storage conditions, on cell membrane permeabilization of adherent DC-3F and LPB cells. The ability of pPBS to permeabilize the cell membrane after 1 hour of treatment (incubation in pPBS) was analyzed by flow cytometry and expressed as an increase of the intracellular fluorescence of YO-PRO®-1 iodide in permeabilized cells. The data from 3 independent experiments (each in at least 4 independent replicates) are shown as mean values ± SD for each parameter set. If no statistical significance is indicated, then p-values > 0.05 (NS).

4. Discussion

The application of cold atmospheric-pressure plasmas (CAPPs) in cancer therapy has been lately one of the central research topics in the domain of plasma medicine. Two methods of plasma cancer treatment have mainly been used: direct and indirect plasma treatments[9,37], each one with its advantages and drawbacks[21]. One of the main advantages of indirect plasma treatment is the possibility of production and storage of extensive quantities of plasma-treated solutions (PTS), minimizing the time and equipment constraints that direct plasma treatment requires. However, to be considered as efficient anti-cancer agents, these PTS should retain their anti-cancer effects over time. This study aimed to bring new insights on the chemical stability of plasma-treated PBS(Ca^{2+}/Mg^{2+}), pPBS, when stored for a considerable time at different temperatures, and to determine whether the pPBS can preserve its anti-cancer properties over storage.

At first, the reactive oxygen and nitrogen species (RONS) that are mainly responsible for the anti-cancer effects of pPBS, i.e. H_2O_2, NO_2^- and NO_3^{-9}, were monitored as a function of storage time and temperature. On one hand, we found that these three reactive species are relatively stable both at around +20 °C (room temperature) and +4 °C (fridge) for a significant period of storage (up to 75 days). Contrariwise, when stored at –20 °C and –80 °C, the absolute concentration of both H_2O_2 and NO_2^- decreases significantly. This degradation is much more pronounced for NO_2^-, and at –20 °C for both

reactive species. On the other hand, we witnessed an increase in the concentration of NO_3^- when the pPBS was stored at –20 °C or –80 °C. Regardless of the storage conditions, the total concentration of the reactive nitrogen species studied here, *i.e.* [NO_2^- + NO_3^-], remains nearly constant. Thus, when the concentration of NO_2^- decreases, that of NO_3^- increases almost inversely proportionally. Similar behavior of the concentration of each of these three reactive species was also observed when, instead of pPBS, untreated PBS(Ca^{2+}/Mg^{2+}), uPBS, containing the same concentrations of H_2O_2, NO_2^- and NO_3^- and the same pH as in pPBS (named mimicking solution) was stored at –20 °C and –80 °C (**Figure 8**). Interestingly, when the initial pH of the mimicking solution was not altered (pH of uPBS = 7.1, while pH of pPBS = 6.1), the degradation of H_2O_2 and NO_2^- and the increase of NO_3^- was much less profound (**Figure 7**). Additionally, excessive concentrations of H_2O_2 or NO_2^- in the mimicking solution further degraded the NO_2^- or H_2O_2, respectively. Finally, the addition of 5 mM or 50 mM of pyruvate, a known H_2O_2 scavenger, in pPBS after the plasma treatment partially prevented the degradation of NO_2^- (**Figure 9**). Collectively, these results show that the main driver of the NO_2^- degradation when the pPBS is stored at –20 °C or –80 °C is the H_2O_2 (which is also degraded), while a key role in that degradation is also played by the pH of the solution before its storage.

To investigate the role of the pH on the chemical stability of the pPBS, mimicking solutions were prepared containing the same concentrations of reactive species as in pPBS, but with different pH values, from highly acidic (pH = 1) to neutral (pH = 7). We found that the three reactive species studied here are stable for 6 hours for a pH greater than 5, while in more acidic environments, their concentration either decreases (strongly for NO_2^- and moderately for H_2O_2) or increases (strongly for NO_3^-). Similarly, Lukes *et al.* showed that, under acidic conditions (pH = 3.3), the concentration of H_2O_2 and NO_2^- decreases during the post-treatment period (300 minutes), while the concentration of NO_3^- increases[38,39]. As reported by Anbar in 1954[28], the oxidation of nitrite (NO_2^-) to nitrate (NO_3^-), in the presence of H_2O_2, takes place rapidly when the pH of the solution is highly acidic (see **equation 1**). Another chemical reaction that could degrade NO_2^- is its oxidation by dissolved oxygen that takes place also in acidic environments[40]. Nevertheless, we can consider that dissolved oxygen is not playing an important role in our experimental conditions as uPBS containing only NO_2^- (without H_2O_2) did not exhibit any degradation upon storage at –20 °C or –80 °C, and uPBS containing both species and an adequate initial pH (6.1) simulate well the chemical evolution of pPBS. Interestingly, the pH of our PTS, pPBS, is much higher than that required for the NO_2^- oxidation to take place. On top of that, as reported in other works, also in our case the pH appears to remain stable regardless of the storage period or temperature of the solution (**Table 1**)[41]. Given that the degradation of H_2O_2 and NO_2^- is only observed, in our case, at the storage temperatures of –20 °C or –80 °C, one can wonder what are the mechanisms that are triggered by the freezing of the solution.

$$H_2O_2 + NO_2^- + H^+ \rightarrow NO_3^- + H^+ + H_2O \qquad (1)$$

As it was previously reported, freezing of phosphate buffer solutions can result in the gradual decrease of the pH of the part of the solution that remains in the liquid state during the freezing process[42–44]. These pH variations in partially frozen solutions are dependent upon the eutectic temperatures and the concentration and solubility of its various components. Thus, as water is removed from the liquid phase (during freezing), the concentration of the various salts increases in the remaining solution. To verify these observations in our experimental conditions, two pH indicators (bromophenol blue and thymol blue) were added to uPBS of different pH values. Subsequently, these solutions (uPBS + pH indicators) were stored at –20 °C or –80 °C. Photographs of the Eppendorf tubes containing these solutions unveiled the gradual acidification of the uPBS when stored at both –20 °C and –80 °C (**Figure SF9**). The final pH value of the frozen solutions was estimated to be around 2-3 for solutions of initial pH of 6 or less. When mimicking solutions of initial pH = 7 were frozen, their acidification was less significant (**Figures SF8** and **SF9**). Similar results were obtained when pPBS containing the pH indicators were frozen (**Figures 12** and **SF8**). Additionally, it is interesting to notice that no significant difference was observed regarding the solution acidification between storage at –20 °C and –80 °C, even if the acidification is more pronounced at –80 °C. Collectively, our results confirm that, when frozen, even uPBS becomes highly acidic. This acidification, which is related only to uPBS composition and to the storage temperature, and is likely not affected by the enriched chemistry of pPBS due to plasma

treatment, favors, as previously discussed, the subsequent oxidation of NO_2^- by H_2O_2 into NO_3^- (see **equation 1**).

Having established that the storage of the solutions (uPBS or pPBS) at –20 °C or –80 °C leads to the degradation of H_2O_2 and NO_2^- due to their acidification during freezing, we tried to explain the difference in this degradation observed between these two storage temperatures. Indeed, our results showed that, for all the cases studied here (both pPBS and mimicking solutions), the degradation of the solution is less significant when the freezing temperature is lower (–80 °C). It was previously reported that an important factor of the pPBS freezing that affects the concentration of the reactive species studied here (H_2O_2, NO_2^- and NO_3^-) is the freezing rate of the solution[40,45]. However, in our case, that degradation is not affected by the freezing rate (**Figures 10** and **11**). Recently, though, Alpana *et al.*[42] reported that the eutectic temperature of Dulbecco's PBS is −23.7 ± 0.3 °C (similar values were also found by Han *et al.*[46]). This means that when stored at –20 °C, the storage temperature at which the most considerable degradation of H_2O_2 and NO_2^- is observed, the temperature of the solutions is above the eutectic point of the saline buffer solutions used in this work. Contrariwise, when the solutions are stored at –80 °C, their temperature is far below this point. Taking this into consideration and that the freezing of the solution results in an acidic pH (either at –20 °C or –80 °C), we propose that the oxidation of NO_2^- by H_2O_2, and, thus, their mutual degradation, is favored at –20 °C compared to –80 °C because these reactive species co-exist for a longer time in an acidic pH in a solution partially frozen when stored at –20 °C than at –80 °C. Besides that, it has been determined that the rate constant of the reaction described in **equation 2** decreases with decreasing temperature at low pH (around 2)[47]. **Equation 2** also highlights that, as discussed before, the conversion of NO_2^- into NO_3^- by oxidation by H_2O_2 increases with the increase of the concentration of the reactants and the decrease of the pH. It is worth noting that both occur during the freezing of the pPBS.

$$-d[H_2O_2]/dt = -d[NO_2^-]/dt = +d[NO_3^-]/dt = k[H^+][H_2O_2][NO_2^-] \quad \textbf{(2)}$$

Two of the reactive oxygen and nitrogen species studied here (H_2O_2 and NO_2^-) are reported as the main drivers of the anti-cancer properties of pPBS[9,21]. Thus, the impact of the pPBS storage time and temperature on its cytotoxic capacity was also studied. As a functional assay, clonogenicity or colony formation assay is a complete characterisation of the ability of a single cell to grow into a colony, hence mandatory to determine not only the cell reproductive death after treatment with pPBS, but also the effectiveness of the cytotoxic pPBS at the defined treatment time. Indeed, the assay detects all cells that have retained the capacity for producing a large number of progenies after treatment, which can cause cell reproductive death as a result of damage to chromosomes, apoptosis, etc.[31,48]. Moreover, the cytostatic effect of pPBS stored at different temperatures over different periods has also been considered by analysing small size colonies. Our results revealed that the pPBS retains its cytotoxic capacity on DC-3F adherent cells for at least up to 21 days when it is stored at +4 °C. Contrariwise, its efficacy is drastically reduced over storage time when it is stored at –20 °C. This difference between the two storage temperatures is more profound when considering normal colonies rather than small colonies. Collectively, these results are in good agreement with the data obtained with the chemical analysis of the solutions for the same storage conditions, as degradation of H_2O_2 and NO_2^- is observed at –20 °C but not at +4 °C. Thus, for the pPBS to preserve its cytotoxicity over time, we propose it be stored at +4 °C and, most importantly, storage temperatures below 0 °C should be avoided.

Finally, direct plasma treatment of cells has been reported as being able to permeabilize the cell membrane[49–51] or, controversially, not being able to permeabilize the cell membrane[52], highlighting the dependence on the cell line. On the other hand, as demonstrated in our previous study[31], indirect plasma treatment leads to cell membrane permeabilization due to its potential oxidation of the lipids of the cell phospholipid bilayer by the RONS present in the plasma-treated solutions (here pPBS). A key player for the peroxidation of lipids is the concentration of H_2O_2[39,53], and for their oxidation is RNS generated in the pPBS (here NO_2^- and NO_3^-)[22,54]. Also reported in our previous study and documented in the literature[55–57], different cell types have different responses to oxidative stress, especially cancerous cells and non-malignant cells, undoubtedly resulting in their different behaviors against pPBS treatment. Our results on the cancer cells (DC-3F and LPB) permeabilization did not show any

difference between the pPBS stored at +4 °C and –20 °C. For both cell lines, pPBS stored at both temperatures was able to permeabilize the cellular membrane at D0 and after 1 day of storage. On the contrary, after 21 days of storage, only DC-3F cells were permeabilized by pPBS stored at +4 °C or –20 °C. When stored for 21 days, the pPBS was not able to permeabilize LPB cells, even in conditions where the concentration of the RONS studied here is preserved (+4 °C). As discussed before, when pPBS is stored at –20 °C, we observe, on the one hand, massive degradation of NO_2^- from the first day of storage (> –85%), while the degradation of H_2O_2 is, on the other hand, moderate but increasing with storage time (*ca.* –20-25% at D1 vs *ca.* –30-35% at D21). As so, while we can state NO_2^- does not play an important role in the permeabilization of these cancer cell lines, we also propose that H_2O_2 could be the main driver of the cellular membrane permeabilization due to pPBS. Indeed, after 21 days of storage, the H_2O_2 concentration in the pPBS might not be enough anymore for permeabilizing LPB cells. Another explanation could be the presence of another reactive species in pPBS (that is not studied here), which is responsible for the permeabilization of LPB cells and is considerably degraded after 21 days of storage. Different reactive species might be responsible for the cellular membrane permeabilization due to lipid oxidation.

5. Conclusions

In this study, the efficacy of plasma-treated PBS(Ca^{2+}/Mg^{2+}), pPBS, as an anti-cancer agent was investigated in terms of its chemical stability and preserved cytotoxic capacity, when stored at different temperatures over long periods. We found that when pPBS is stored at +4 °C, the concentration of the main reactive species responsible for its anti-cancer capacity, i.e., H_2O_2 and NO_2^-, remains stable for up to 21 days of storage. In parallel, the cytotoxic activity of pPBS is also preserved for the same storage time if stored at +4 °C. On the other hand, we showed that when pPBS is stored at temperatures below 0 °C (–20 °C and –80 °C here) both the concentration of the aforementioned reactive species and the efficacy of pPBS in inducing cancer cells death is degraded rapidly. The freezing of pPBS results in the acidification of the solution, enabling the pH-dependent NO_2^- oxidation by H_2O_2, which results in the degradation of both reactive species. However, it has been found that the freezing rate does not play a role in the acidification process. We conclude that pPBS can preserve their cytotoxic activity, at least for 21 days, if stored at 20 °C or 4 °C, providing a basis for practical application of plasma-treated PBS in cancer therapy. In the future, other storage conditions, such as light exposure and packaging, should be appraised. Finally, we also confirmed that pPBS can permeabilize the cellular membrane, and showed that it retains this ability regardless of the storage temperature. We exclude the role of NO_2^- and propose H_2O_2 to be the main driver of the cellular membrane permeabilization due to pPBS.

Author Contributions: conceptualization: K.S., T.-H.C, A.S., E.R., L.M.M., J.S.S.; methodology: K.S., T.-H.C., A.S., J.-M.P., E.R., L.M.M., J.S.S.; data acquisition: K.S., T.-H.C.; data validation: K.S., T.-H.C., F.M.A., L.M.M., J.S.S.; data analysis and visualization: K.S., T.-H.C., J.S.S.; data interpretation: K.S., T.-H.C., A.S., J.-M.P., E.R., L.M.M., J.S.S.; resources: E.R., L.M.M., J.S.S.; supervision: L.M.M., J.S.S.; funding acquisition: C.D., J.-M.P., E.R., L.M.M., J.S.S.; writing—original draft preparation: K.S., J.S.S.; writing—review and editing: K.S., T.-H.C., L.M.M., J.S.S.. All authors discussed the results, reviewed the manuscript, and have read and agreed to the published version of the manuscript.

Funding: We acknowledge the financial support from the PLASCANCER project (INCa-PlanCancer N°17CP087-00), the LabEx LaSIPS project PHeCell3D, the GDR 2025 HAPPYBIO, the CNRS, the Université Paris-Saclay and the Institut Gustave Roussy.

Acknowledgements: The authors thank P. Jeanney and M. Fleury (LPGP) for technical support, and P.-M. Girard (Institut Curie) for technical support and valuable discussions.

References

1. Joslin, J. *et al.* Aqueous Plasma Pharmacy: Preparation Methods, Chemistry, and Therapeutic Applications HHS Public Access. *Physiol. Behav.* **176**, 139–148 (2017).

2. Von Woedtke, T., Haertel, B., Weltmann, K. D. & Lindequist, U. Plasma pharmacy - Physical plasma in pharmaceutical applications. *Pharmazie* **68**, 492–498 (2013).

3. Oehmigen, K. *et al.* The role of acidification for antimicrobial activity of atmospheric pressure plasma in liquids. *Plasma Process. Polym.* **7**, 250–257 (2010).

4. Nakamura, K. *et al.* Novel Intraperitoneal Treatment With Non-Thermal Plasma-Activated Medium Inhibits Metastatic Potential of Ovarian Cancer Cells. *Sci. Rep.* **7**, 1–14 (2017).

5. Liedtke, K. R. *et al.* Non-thermal plasma-treated solution demonstrates antitumor activity against pancreatic cancer cells in vitro and in vivo. *Sci. Rep.* **7**, 1–12 (2017).

6. Utsumi, F. *et al.* Effect of indirect nonequilibrium atmospheric pressure plasma on anti-proliferative activity against chronic chemo-resistant ovarian cancer cells in vitro and in vivo. *PLoS One* **8**, 1–10 (2013).

7. Li, Y. *et al.* Effects of atmospheric-pressure non-thermal bio-compatible plasma and plasma-activated nitric oxide water on cervical cancer cells. *Sci. Rep.* **7**, 1–9 (2017).

8. Tanaka, H. *et al.* Plasma-activated medium selectively kills glioblastoma brain tumor cells by down-regulating a survival signalling molecule, AKT kinase. *Plasma Med.* **1**, 265–277 (2011).

9. Girard, P. M. *et al.* Synergistic Effect of H2O2 and NO2 in Cell Death Induced by Cold Atmospheric He Plasma. *Sci. Rep.* **6**, 1–17 (2016).

10. Papadopoulos, P. K. *et al.* Generic residual charge based model for the interpretation of the electrohydrodynamic effects in cold atmospheric pressure plasmas. *Plasma Sources Sci. Technol.* **28**, (2019).

11. Wende, K. *et al.* Identification of the biologically active liquid chemistry induced by a nonthermal atmospheric pressure plasma jet. *Biointerphases* **10**, 029518 (2015).

12. Azzariti, A. *et al.* Plasma-activated medium triggers cell death and the presentation of immune-activating danger signals in melanoma and pancreatic cancer cells. *Sci. Rep.* 1–13 (2019). doi:10.1038/s41598-019-40637-z

13. Girard, P. M. *et al.* Synergistic Effect of H2O2and NO2in Cell Death Induced by Cold Atmospheric He Plasma. *Sci. Rep.* (2016). doi:10.1038/srep29098

14. Adachi, T. *et al.* Plasma-activated medium induces A549 cell injury via a spiral apoptotic cascade involving the mitochondrial-nuclear network. *Free Radic. Biol. Med.* **79**, 28–44 (2015).

15. Shen, J. *et al.* Bactericidal Effects against S . aureus and Physicochemical Properties of Plasma Activated Water stored at different temperatures. *Nat. Publ. Gr.* (2016). doi:10.1038/srep28505

16. Judée, F., Fongia, C., Ducommun, B. & Yousfi, M. Short and long time effects of low-temperature Plasma Activated Media on 3D multicellular tumor spheroids. 1–12 (2016). doi:10.1038/srep21421

17. Graves, D. B. The emerging role of reactive oxygen and nitrogen species in redox biology and some implications for plasma applications to medicine and biology. *J. Phys. D. Appl. Phys.* **45**, (2012).

18. Bisag, A. *et al.* Plasma-activated ringer's lactate solution displays a selective cytotoxic effect on ovarian cancer cells. *Cancers (Basel).* **12**, 1–16 (2020).

19. Tanaka, H. *et al.* Non-thermal atmospheric pressure plasma activates lactate in Ringer's solution for anti-tumor effects. *Sci. Rep.* **6**, 1–11 (2016).

20. Bekeschus, S. *et al.* Hydrogen peroxide: A central player in physical plasma-induced oxidative stress in human blood cells. *Free Radic. Res.* **48**, 542–549 (2014).

21. Sklias, K., Sousa, J. S. & Girard, P. Role of short- and long-lived reactive species on the selectivity and anti-cancer action of plasma treatment in vitro. 1–29 (2020).

22. Pacher, P., Beckman, J. S. & Liaudet, L. Nitric oxide and peroxynitrite in health and disease. *Physiol. Rev.* **87**, 315–424 (2007).

23. Radi, R. *et al.* Peroxynitrite-induced membrane lipid peroxidation: The cytotoxic potential of superoxide and nitric oxide. *Arch Biochem Biophys* (1991). https://doi.org/10.1016/0003-9861(91)90224-7

24. Shen, J. *et al.* Bactericidal Effects against S. aureus and Physicochemical Properties of Plasma Activated Water stored at different temperatures. *Sci. Rep.* **6**, (2016).

25. Yan, D. *et al.* Stabilizing the cold plasma- stimulated medium by regulating medium ' s composition. *Nat. Publ. Gr.* 1–11 (2016). doi:10.1038/srep26016

26. Kaushik, N. K. *et al.* Biological and medical applications of plasma-activated media, water and solutions. *Biol. Chem.* **400**, 39–62 (2018).

27. Ghimire, B. *et al.* The effect of the gap distance between an atmospheric-pressure plasma jet nozzle and liquid surface on OH and N2 species concentrations. *Phys. Plasmas* **24**, (2017).

28. Anbar, M. & Taube, H. Interaction of Nitrous Acid with Hydrogen Peroxide and with Water. *J. Am. Chem. Soc.* **76**, 6243–6247 (1954).

29. Stancampiano, A. *et al.* Mimicking of human body electrical characteristic for easier translation of plasma biomedical studies to clinical applications. *IEEE Trans. Radiat. Plasma Med. Sci.* **PP**, 1–1 (2019).

30. Robert, E. *et al.* Characterization of pulsed atmospheric-pressure plasma streams (PAPS) generated by a plasma gun. *Plasma Sources Sci. Technol.* **21**, (2012).

31. Chung, T. H. *et al.* Cell electropermeabilisation enhancement by non-thermal-plasma-treated PBS. *Cancers (Basel).* **12**, (2020).

32. Sergii Golovynskyi, Oleksandr I. Datsenko, Luca Seravalli, Giovanna Trevisi, PaolaFrigeri, Ivan S. Babichuk, Iuliia Golovynska, Baikui Li, J. Q. ce d M us pt. *Nanotechnology* 0–22 (2019).

33. Biedler, J. L. & Riehm, H. Cellular resistance to actinomycin D in Chinese hamster cells in vitro: cross-resistance, radioautographic, and cytogenetic studies. *Cancer Res.* **30**, 1174–1184 (1970).

34. Belehradek, J., Barski, G. & Thonier, M. Evolution of cell-mediated antitumor immunity in mice bearing a syngeneic chemically induced tumor. Influence of tumor growth, surgical removal and treatment with irradiated tumor cells. *Int. J. Cancer* **9**, 461–469 (1972).

35. Damschen, D. E. & Martin, L. R. Aqueous aerosol oxidation of nitrous acid by O2, O3 AND H2O2. *Atmos. Environ.* **17**, 2005–2011 (1983).

36. Kolhe, P., Amend, E. & Singh, S. K. Impact of freezing on pH of buffered solutions and consequences for monoclonal antibody aggregation. *Biotechnol. Prog.* **26**, 727–733 (2010).

37. Tanaka, H. *et al.* New Hopes for Plasma-Based Cancer Treatment. *Plasma* **1**, 150–155 (2018).

38. Lukes, P., Dolezalova, E., Sisrova, I. & Clupek, M. Aqueous-phase chemistry and bactericidal effects from an air discharge plasma in contact with water: Evidence for the formation of peroxynitrite through a pseudo-second-order post-discharge reaction of H2O 2 and HNO2. *Plasma Sources Sci. Technol.* **23**, (2014).

39. Bruggeman, P. J. *et al.* Plasma-liquid interactions: A review and roadmap. *Plasma Sources Sci. Technol.* **25**, (2016).

40. Takenaka, N. *et al.* Fast oxidation reaction of nitrite by dissolved oxygen in the freezing process in the tropospheric aqueous phase. *J. Atmos. Chem.* **29**, 135–150 (1998).

41. Tsoukou, E., Bourke, P. & Boehm, D. Temperature Stability and Effectiveness of Plasma-Activated Liquids over an 18 Months Period. *Water* **12**, 3021 (2020).

42. Gómez, G., Pikal, M. J. & Rodríguez-Hornedo, N. Effect of initial buffer composition on pH changes during far-from-equilibrium freezing of sodium phosphate buffer solutions. *Pharm. Res.* **18**, 90–97 (2001).

43. Thorat, A. A. & Suryanarayanan, R. Characterization of Phosphate Buffered Saline (PBS) in Frozen State and after Freeze-Drying. *Pharm. Res.* **36**, (2019).

44. Van Den Berg, L. pH changes in buffers and foods during freezing and subsequent storage. *Cryobiology* **3**, 236–242 (1966).

45. Elwell, C. Acceleration of the Gifted. *Gift. Child Q.* **2**, 21–23 (1958).

46. Han, B., Devireddy, R. V. & Bischof, J. C. Phase change behavior of biomedically relevant solutions. *ASME Int. Mech. Eng. Congr. Expo. Proc.* 67–75 (2002). doi:10.1115/IMECE2002-32549

47. Lee, Y.-N. & Lind, J. A. Kinetics of aqueous-phase oxidation of nitrogen(III) by hydrogen peroxide. *J. Geophys. Res.* **91**, 2793 (1986).

48. Brown, J. M. & Attardi, L. D. The role of apoptosis in cancer development and treatment response. *Nat. Rev. Cancer* **5**, 231–237 (2005).

49. Yan, D. *et al.* The Cell Activation Phenomena in the Cold Atmospheric Plasma Cancer Treatment. *Sci. Rep.* **8**, 1–10 (2018).

50. Vijayarangan, V. *et al.* Cold Atmospheric Plasma Parameters Investigation for Efficient Drug Delivery in HeLa Cells. *IEEE Trans. Radiat. Plasma Med. Sci.* **2**, 109–115 (2017).

51. Vijayarangan, V. *et al.* New insights on molecular internalization and drug delivery following plasma jet exposures. *Int. J. Pharm.* **589**, 119874 (2020).

52. Wolff, C. M., Kolb, J. F., Weltmann, K. D., von Woedtke, T. & Bekeschus, S. Combination treatment with cold physical plasma and pulsed electric fields augments ros production and cytotoxicity in lymphoma. *Cancers (Basel).* **12**, (2020).

53. Chance, B., Sies, H. & Boveris, A. Hydroperoxide metabolism in mammalian organs. *Physiol. Rev.* **59**, 527–605 (1979).

54. Kumar, V., Khare, T., Sharma, M. & Wani, S. H. ROS-induced signaling and gene expression in crops under salinity stress. *React. Oxyg. Species Antioxid. Syst. Plants Role Regul. under Abiotic Stress* **288**, 159–184 (2017).

55. Cooper, G.M. The Development and Causes of Cancer. In *The Cell: A Molecular Approach*; Sinauer Associates: Sunderland, MA, USA, pp. 725–766 (2000).

56. Biscop, E. *et al.* Influence of cell type and culture medium on determining cancer selectivity of cold atmospheric plasma treatment. *Cancers (Basel).* **11**, 1–14 (2019).

57. Andreyev, A.Y.; Kushnareva, Y.E.; Starkov, A.A. Mitochondrial metabolism of reactive oxygen species. *Biochemistry (Mosc.)* **70**, 200–214 (2005).

Supplementary Information

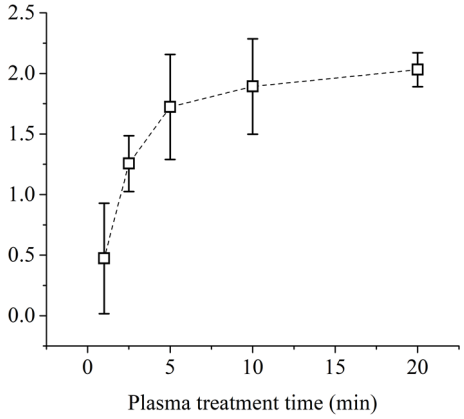

Figure SF1. The $[H_2O_2]/[NO_2^-]$ ratio was calculated for every independent experiment of **Figure 6** and the mean value ± SD of 5 independent experiments is presented as a function of the plasma treatment time.

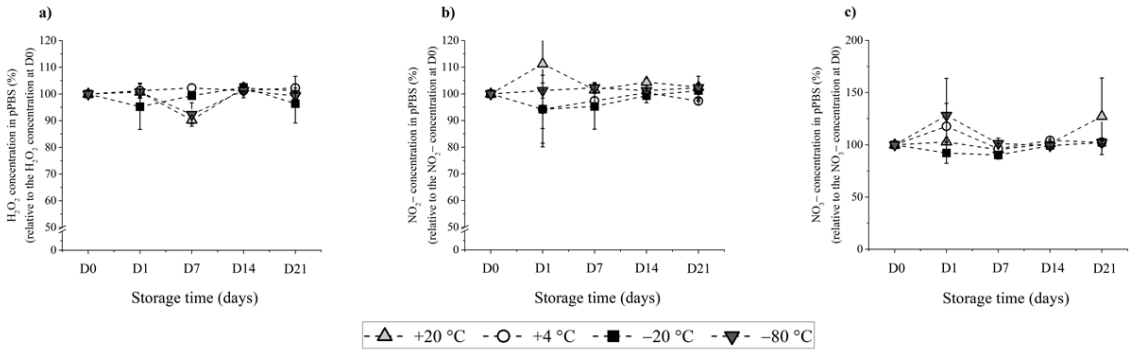

Figure SF2. RONS alone pH = 7.1 Concentration over storage time of a) H_2O_2, b) NO_2^- and c) NO_3^- in ad-hoc solutions at pH = 7.1 stored at +4, +20, –20 and –80 °C. Pure ad-hoc solutions were prepared containing only a) H_2O_2 or b) NO_2^- or c) NO_3^-. The data are the mean ± SD of 2 independent experiments.

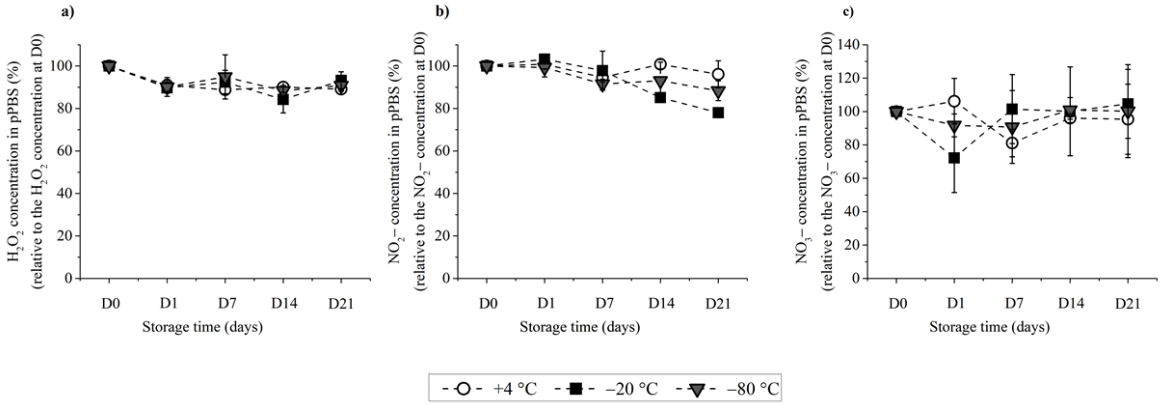

Figure SF3. RONS alone pH = 6.1 Concentration over storage time of a) H_2O_2 , b) NO_2^- and c) NO_3^- in ad-hoc solutions of pH = 6.1 stored at +4, +20, –20 and –80 °C. Pure ad-hoc solutions were prepared containing only a) H_2O_2 or b) NO_2^- or c) NO_3^-. The data are the mean ± SD of 2 independent experiments.

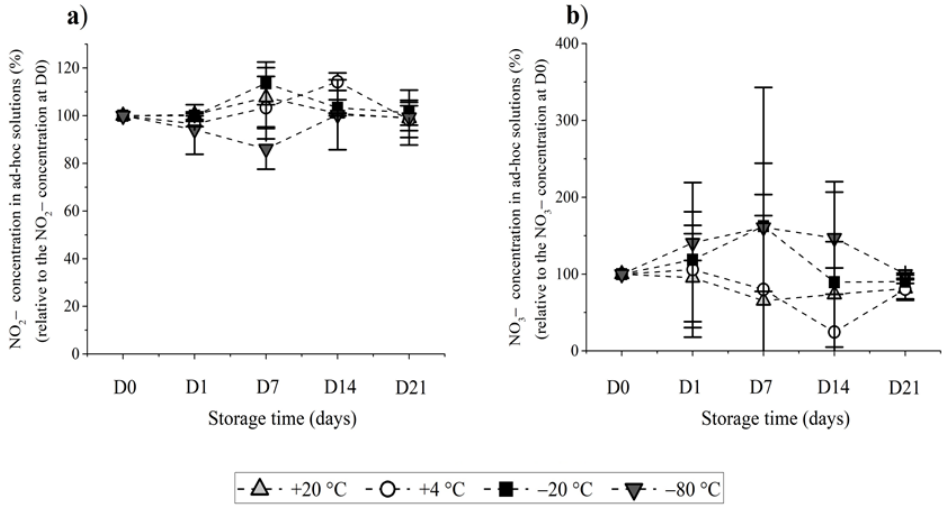

Figure SF4. NO_2^- + NO_3^- pH = 7.1 Concentration over storage time of a) NO_2^- and b) NO_3^- in ad-hoc solutions of pH = 7.1 stored at +4, +20, –20 and –80 °C. Pure ad-hoc solutions were prepared containing only NO_2^- and NO_3^-. The data are the mean ± SD of 2 independent experiments.

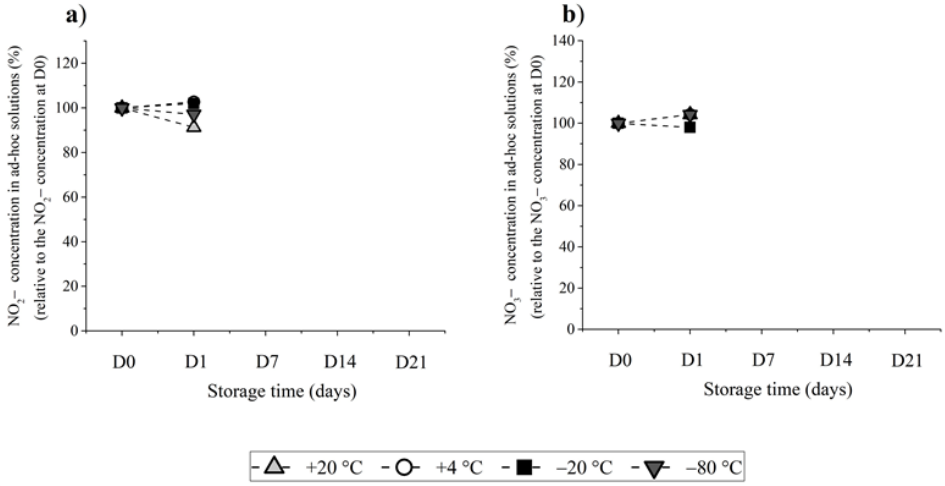

Figure SF5. NO_2^- + NO_3^- pH = 6.1 Concentration over storage time of a) NO_2^- and b) NO_3^- in ad-hoc solutions of pH = 6.1 stored at +4, +20, –20 and –80 °C. Pure ad-hoc solutions were prepared containing only NO_2^- and NO_3^-. The data are the mean ± SD of 2 independent experiments.

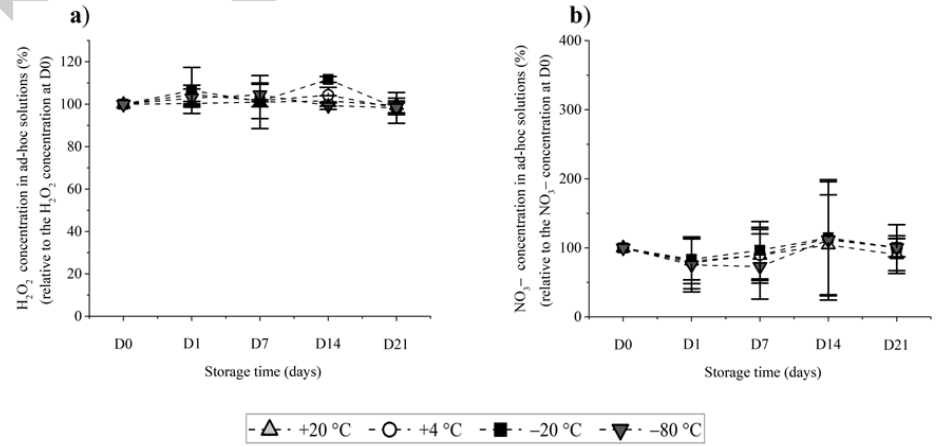

Figure SF6. H_2O_2 + NO_3^- pH = 7.1 Concentration over storage time of a) H_2O_2 and b) NO_3^- in ad-hoc solutions of pH = 7.1 stored at +4, +20, –20 and –80 °C. Pure ad-hoc solutions were prepared containing only H_2O_2 and NO_3^-. The data are the mean ± SD of 2 independent experiments.

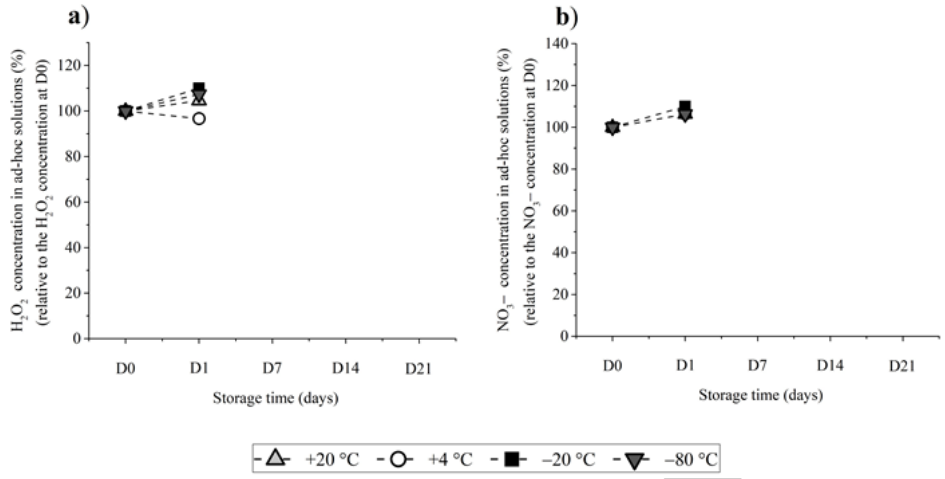

Figure SF7. H_2O_2 + NO_3^- pH = 6.1 Concentration over storage time of a) H_2O_2 and b) NO_3^- in ad-hoc solutions of pH = 6.1 stored at +4, +20, –20 and –80 °C. Pure ad-hoc solutions were prepared containing only H_2O_2 and NO_3^-. The data are the mean ± SD of 2 independent experiments.

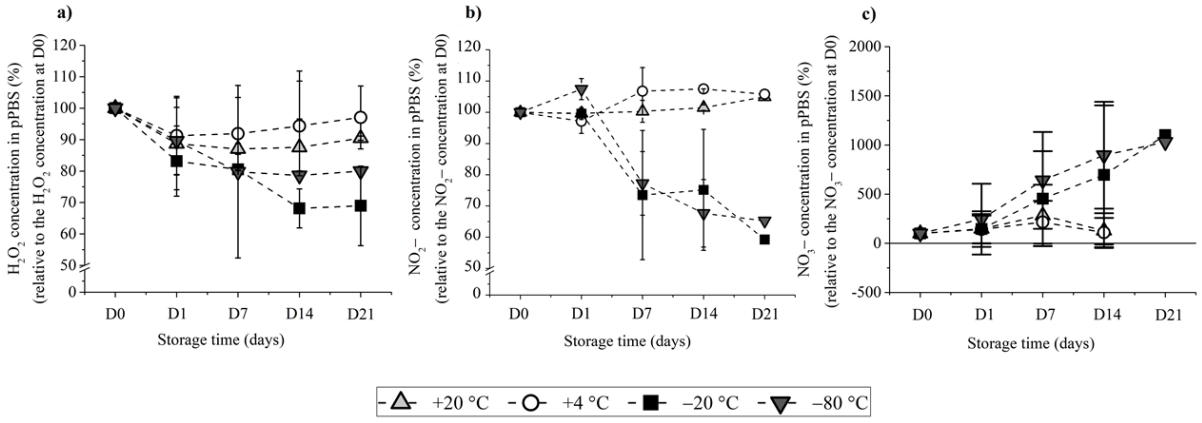

Figure SF8. H_2O_2 + NO_2^- pH = 7.1 Concentration over storage time of a) H_2O_2, b) NO_2^- and c) NO_3^- in ad-hoc solutions of pH = 7.1 stored at +4, +20, –20 and –80 °C. Pure ad-hoc solutions were prepared containing only H_2O_2 and NO_2^-. The data are the mean ± SD of 2 independent experiments, except for D21 for NO_2^- and NO_3^- (only 1 experiment).

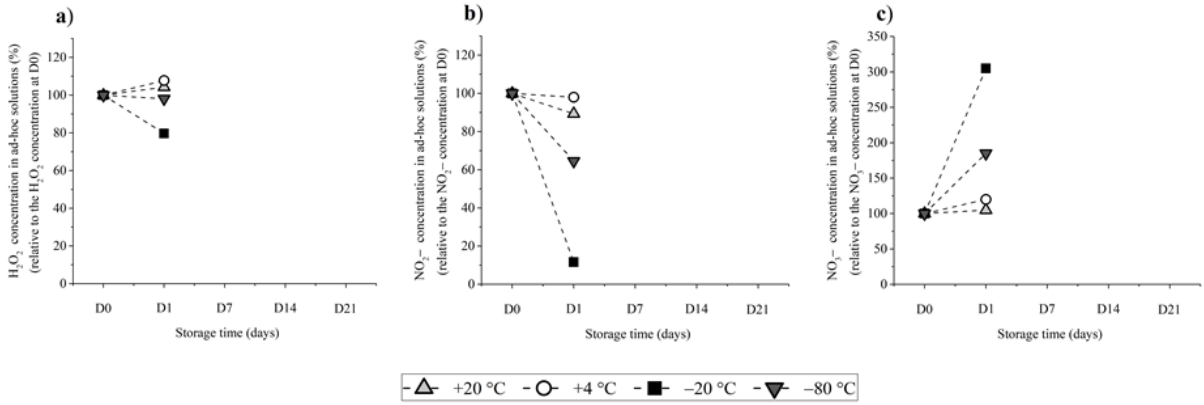

Figure SF9. H_2O_2 + NO_2^- pH = 6.1 Concentration over storage time of a) H_2O_2, b) NO_2^- and c) NO_3^- in ad-hoc solutions of pH = 6.1 stored at +4, +20, –20 and –80 °C. Pure ad-hoc solutions were prepared containing only H_2O_2 and NO_2^-. The data are the mean ± SD of 2 independent experiments.

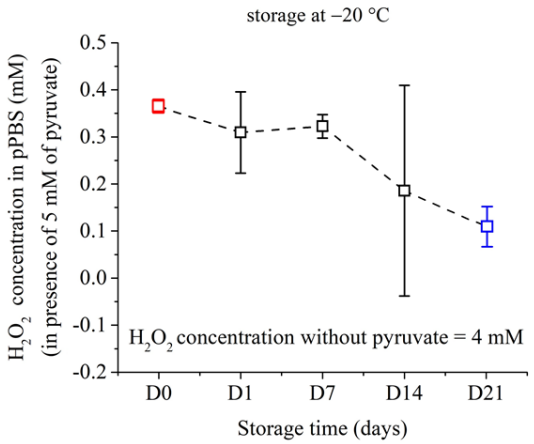

Figure SF10. Concentration over storage time at –20 °C of H_2O_2 in pPBS containing 5 mM of sodium pyruvate. The H_2O_2 initial concentration, before the addition of pyruvate, was 4 mM (>90% reduction of H_2O_2 due to pyruvate). The data are the mean ± SD of 3 independent experiments.

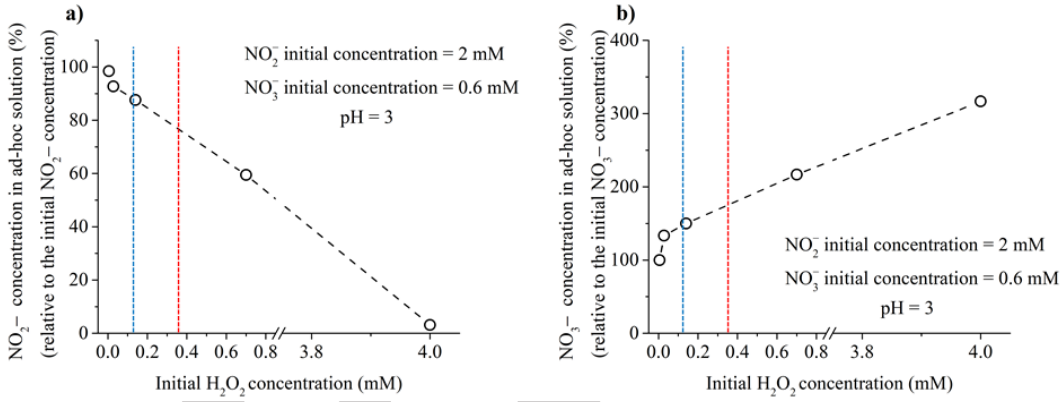

Figure SF11. Concentration of a) NO_2^- and b) NO_3^- in ad-hoc solutions of pH = 3 in the presence of different H_2O_2 concentrations. The blue and red vertical lines correspond to the minimum and maximum values of H_2O_2 concentration measured in pPBS in the presence of 5 mM pyruvate (Figue SF7). Only one experiment was performed.

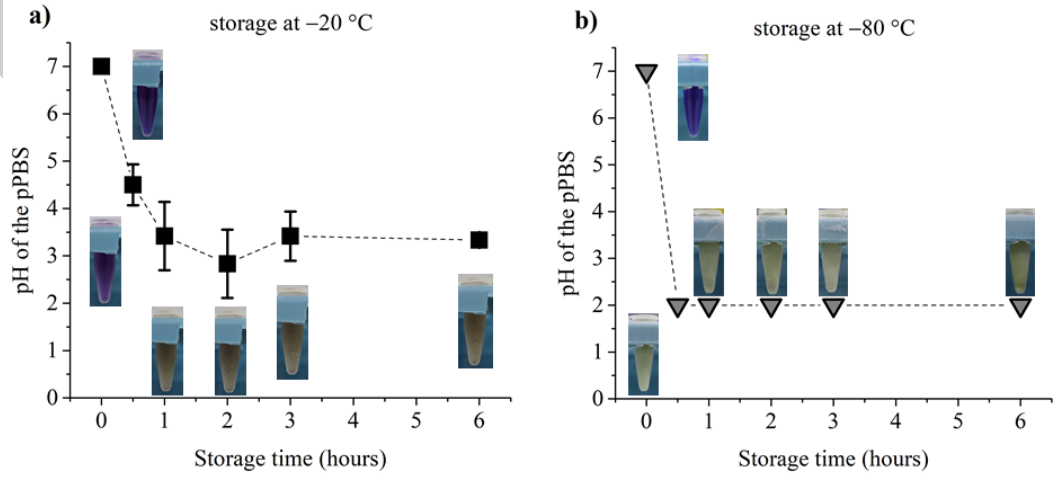

Figure SF12. pH values and photos of Eppendorf tubes as a function of the storage time at a) –20 °C and b) –80 °C. The pH was evaluated by using bromophenol blue as a pH marker and by comparing the RGB values of the tubes containing pPBS with the RGB values of tubes containing uPBS of well-known pH (Figure 13). The RGB values are the mean value of 3 independent points of the photos of each Eppendorf tube. The data are the mean ± SD of 3 independent experiments for storage at –20 °C. For storage at –80 °C, only one experiment was performed.

4 *In vivo* studies of NTP and its combination with ECT

Those ongoing studies will be presented below in two separate sections (*manuscript in preparation*).

Animal models of all the *in vivo* experimentations respected the models and protocol described in **section 1.2 of the Results** (details will be presented in each experiment).

4.1 *In vivo* investigation into indirect plasma treatment on subcutaneous tumours

4.1.1 Aim of the study

This first *in vivo* study aimed at exploring the anti-tumour effectiveness of plasma-treated liquids as mono-therapy in mice bearing s.c. tumours, via intratumoural (i.t.) administration of the plasma-treated liquids.

4.1.2 Materials and methods

Unless otherwise specified, all the reagents for biological experiments were purchased from Life Technologies (Courtabœuf, France).

Animal model

Inbred female immunocompetent C57Bl/6J mice were used in this experimentation. See the description above (section 4.1.) for details of this model and protocol.

Cancer cells culture for sub-cutaneous inoculation

Tumourigenic murine fibrosarcoma LPB cells, a methylcholanthrene-induced C57Bl/6 mouse sarcoma cell line (Belehradek Jr *et al.*, 1972), were employed to establish subcutaneous tumours in our animal model. LPB cells were sub-cultured for at least two weeks before inoculation. The culture of LBP cells was described previously (Sklias *et al.,* to be submitted - see **chapter 3 of the Results**) except for some specifications for cells used for inoculation in the animal. Cells were cultured as an adherent monolayer in RPMI 1640 Medium (21875-034) supplemented with 10% heat-inactivated foetal bovine serum (FBS, F7524), 100 $U.mL^{-1}$ penicillin and 100 $mg.mL^{-1}$ streptomycin (15140-122). Adherent cells were spread in this complete RPMI medium at 37°C in a 95% humidity atmosphere containing 5% CO_2 (HERAcell

240i incubator CO_2, Thermo Scientific, France) and passaged upon confluency (every two days at a 1:10 dilution or every three days at a 1:30 dilution) using TrypLE™ Express Enzyme solution (12604-013), considering only viable cells. The trypan blue exclusion dye method assessed short-term cell viability for routine sub-culturing (Trypan Blue Solution, T8154) with a Countess™ II FL Automated Cell Counter (Invitrogen, FR). Cells were regularly checked for the absence of mycoplasma contamination via polymerase chain reaction (PCR) (data not shown).

On the day of inoculation, LPB cells were detached using TrypLE™ Express Enzyme solution and resuspended in sterile PBS 1X (14190-094) at a final density of 5 $\times 10^6$ lived cells/mL. Soon after that, and under general anaesthesia, each mouse was inoculated with 5 $\times 10^5$ cells/100 µL on the right flank. When the LPB tumour volume of mice reached a defined average volume (detailed below in each experiment), mice were randomised and included in the different experimental groups.

Preparation of plasma-treated medium (or plasma-activated medium, termed PAM)

Minimum Essential Medium (MEM) 1X was used to produce plasma-activated medium (PAM). MEM 1X was exposed to helium NTP at two different modes, the multijet mode ($d_{plasma\text{-}liquid\ surface}$ = 5 mm) or the diffuse mode ($d_{plasma\text{-}liquid\ surface}$ = 2 mm), with the amplitude of HV pulses being set at 20 kV, 2 kHz, He flow rate at one standard litre per minute, for 10-minutes plasma treatment continuously. Similar to the controlled distance of the plasma exposure on mice skin, the distance between the NTP multijet output and the liquid surface was maintained thanks to customised 3D-printed spacers (data not shown).

Treatment protocol

When the mean tumour volume of all mice reached *ca.* 100 mm^3, mice were randomised into four groups (*Table **4***) with eight to ten mice per group, depending on the experiments. Intratumoural administration of PAM (*Figure **35***) was performed once a day for four days consecutively, at the same moment in the day, through an automatic syringe (controlled flow speed at 50 µL.min^{-1}). All the PAM for treatment were freshly prepared on the day of injection. The volume of administration of PAM was half of the tumour's volume measured before each treatment. Follow-up by tumour size monitoring with a digital calliper was performed three times per week for two weeks after the last treatment. The follow-up was performed until the endpoints.

The treatment parameters of each group are shown in *Table **4***.

Groups	Treatment parameters
1	Control (i.t. administration of PBS 1X)
2	i.t. administration of MEM 1X
3	i.t. administration of “multijet PAM”
4	i.t. administration of “diffuse PAM”

Table 4| *In vivo parameters of the mono-therapy using PAM in female C57Bl/6 bearing s.c. LPB tumours (n = 10)*

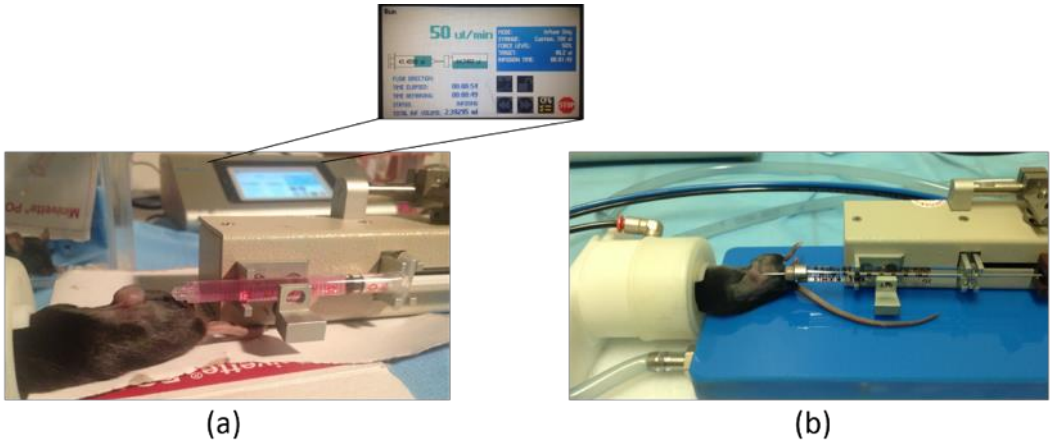

Figure 35| Illustration of the *in vivo* procedure for indirect plasma treatment using PAM

Female C57Bl/6J mice bearing s.c. LPB tumours were treated with (**a**) PAM or (**b**) PBS as a negative control. The i.t. administration of the treatment was monitored through an automatic syringe with a controlled flow speed (50 µL.min^{-1}). The administered volume was half of the tumour volume, measured just before the i.t. injection.

In vivo follow-up and end-point analysis

Tumour volume was assessed every second day or every three days by measuring the longest (a) and the orthogonal second largest (b) diameters with a precision calliper. Subcutaneous tumours were approximated as ellipsoids, and their volume was calculated following the formula: $V = a \times b^2 \times \frac{\pi}{6}$. The animal body weight was monitored once per week, and mice well-being (changes in behaviour, fur or skin condition) was also observed during the tumour volume assessment as indicators of potential systemic toxicity of the combined treatment. The same person did the measurements all along with the study to maintain consistency. If tumour growth impeded mobility, was ulcerated or exceeded the maximum growth limit of 1800 mm^{3,} or if mice lost over 20% of their body weight (end-points), mice have euthanised via Carbon dioxide (CO_2) inhalation, in agreement with the Guidelines for the

welfare and use of animals in cancer research and as has been approved by the ethical committee for our project (APAFIS#13409-2018020711382163).

The group tumour evolution is reported until the first animal of each treated group reached an end-point and was thus euthanised.

4.1.3 Results of *in vivo* monotherapy with plasma-treated liquids

The results of this *in vivo* pilot experiment studying PAM as mono-therapy are shown in *Figure **36***. We, unfortunately, did not observe differences such as tumour growth delays between the treated groups and the control. Those results raise the question of RONS scavengers present in cell culture media, such as pyruvate (Kaushik *et al.*, 2015; Sensenig, 2011; Turrini *et al.*, 2020).

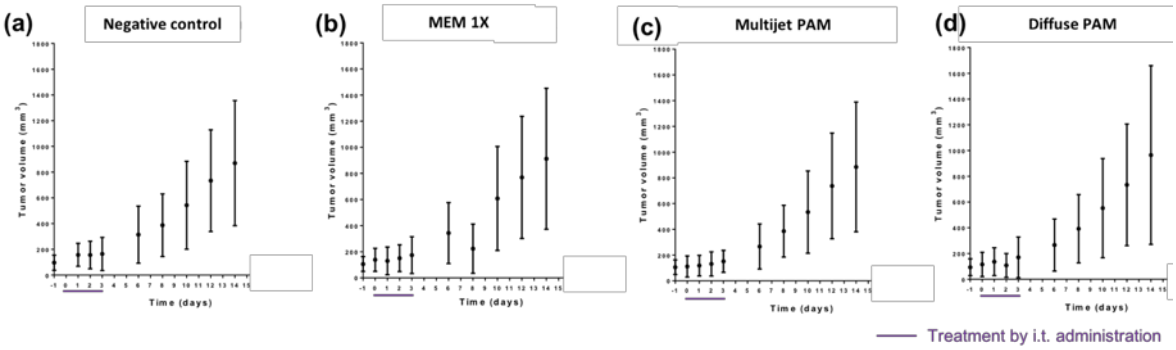

Figure 36| The tumour growth delay in C57Bl/6J mice treated with multijet PAM or diffuse PAM

The number of mice was n = 10 in each experimental group. Data represents as mean ± SD values. Mice were treated with i.t. administration of treated liquids (multijet PAM or diffuse PAM) or with MEM 1X, compared with the negative control being treated with PBS). The treatment was performed once a day for four days consecutively (D0 to D3). The tumour evolution is shown until day 14 after the first treatment.

To investigate this question, we decided to **replace MEM 1X with PBS 1X (Ca^{2+}, Mg^{2+})** which was studied previously in *in vitro* tests (see **chapters 1 and 2 of the Results**). Indeed, as a buffered and isotonic biological solution (pH 7.20), PBS 1X (Ca^{2+}, Mg^{2+}) is suitable for almost all living biological targets. Again, experiments were performed with female C57Bl/6J mice bearing s.c. LPB tumours, respecting the protocol established previously. The protocol of preparation of pPBS remained the same as that of PAM, either with a “multijet mode” (being group 2 “multijet pPBS”) or with a “diffuse mode” (being group 3 “diffuse pPBS”). The parameters of the NTP device used to treat PBS remained unchanged, except the amplitude of the high voltage pulses being set at **11 kV** (parameter at which our plasma generator was the more stable – data and observation not shown). Untreated PBS 1X (Ca^{2+}, Mg^{2+}) was used

as vehicle control (group 1). When the s.c. LPB tumour volume of mice reached an average of 80 mm^3, mice were randomised and included in 3 different groups with 8 mice per group. The treatments were daily i.t. administrated to mice for fourteen days consecutively (except D7). The follow-up was performed until the endpoints.

Results of tumour growth delay are displayed in *Figure **37***.

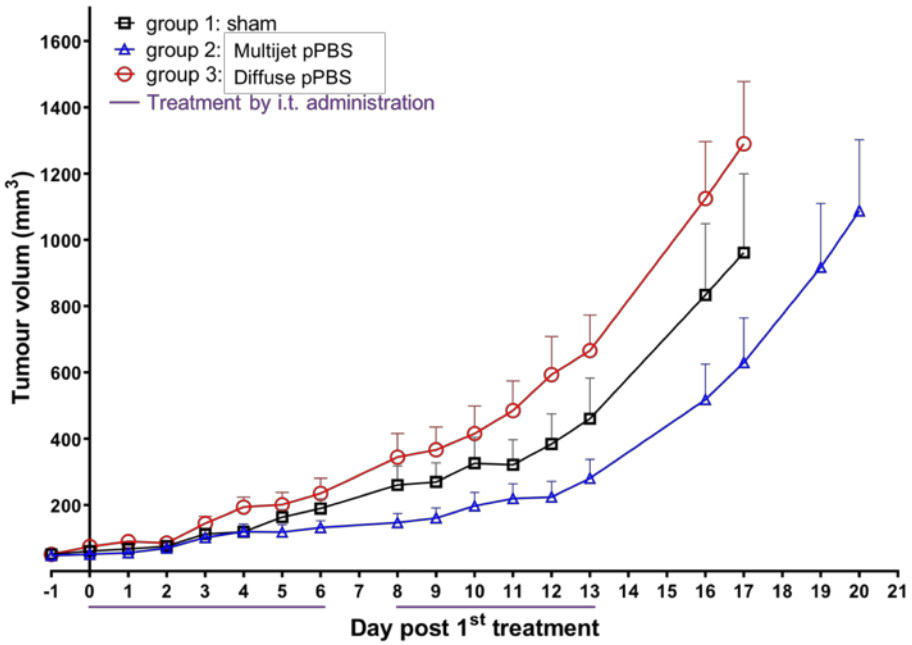

Figure 37| The tumour growth delay in C57Bl/6 mice treated with multijet pPBS or diffuse pPBS by i.t. administration

The number of mice was n = 8 in each experimental group. Data represented as mean ± SEM values. Mice were daily i.t. injected with pPBS (or with PBS 1X for group 1) for fourteen days consecutively (except D7 without treatment). The tumour evolution is shown until the first animal of each group reached an end-point.

Once again, as reported in the previous *in vivo* experiment with PAM, no noticeable slowdown of tumour growth delay was observed with mice treated with pPBS compared with sham. There is a slight tumour growth delay of two days with multijet pPBS (group 2) in comparison to sham (group 1). On the contrary, with the "diffuse pPBS" (group 3), there could be a tendency to accelerate the tumour growth, as compared with sham.

Key questions remain on whether PAM and pPBS are not an efficient anti-tumour treatment modality and on the reliability of other *in vivo* (published) studies showing the anticancer efficiency of those plasma-treated liquids being used alone as monotherapy, even if we are aware that each *in vivo* experiment has its experimental models and design, thus it is not obvious to compare results between different studies.

4.2 *In vivo* investigation into the combined treatment with pPBS and ECT

4.2.1 Aim of the study

This study aims at achieving the same level of permeabilisation of tumour cells (and, therefore, the same efficacy of ECT) with less intense and, hence, more "comfortable" electrical pulses.

For this purpose, immunocompetent C57Bl/6J mice bearing s.c. LPB tumours were treated with the combination of pPBS and ECT under conditions that did not cause any toxicity and were already used in clinics (see **section 4.1**). These are the pPBS and the murine LPB fibrosarcoma cells utilised previously for *in vitro* studies, as described in our second article (Chung *et al.*, 2020) and in our third article (Sklias *et al.,* to be submitted) (see **chapter 2 and 3 of Results**).

Treatment parameters

Subcutaneous LPB sarcoma tumours were treated either with i.v. BLM (group 1 Control) or with ECT (group 2, which received i.v. administration of BLM in the retro-orbital sinus followed by eight square-wave EPs of 100 µs, at 1000 V/cm and 1 Hz) or with pPBS combined with ECT (group 4 and group 5) or with 1-hour-pPBS or 20-minutes-pPBS followed by i.v. BLM (no electric pulse, groups 3 and 6, respectively). The tested parameters in the six different treatment groups are described in *Table **5***. Note that there were five experimental groups in the first in vivo experimentation (group 1 to group 5), and in the second *in vivo* experiment, there were six experimental groups.

Groups	Treatment parameters
1	Control (i.v. administration of BLM)
2	ECT (i.v. BLM followed by 8 square-wave EPs of 100 µs, at 1000 V/cm and 1 Hz)
3	i.t. 1-hour-pPBS followed by i.v. BLM
4	i.t. 1-hour-pPBS followed by ECT
5	i.t. 20-minutes -pPBS followed by ECT
6	i.t. 20-minutes-pPBS followed by i.v. BLM

***Table 5**| In vivo studied parameters of the combined treatment with pPBS and ECT in female C57Bl/6J mice bearing s.c. murine LPB fibrosarcoma*

4.2.2 Materials and methods

Animal model

Again, experiments were performed with female C57Bl/6J mice bearing s.c. LPB tumours, respecting the protocol established previously (see **section 4.2.2.**).

Cancer cells culture for sub-cutaneous inoculation

The LPB cell culture for sub-cutaneous inoculation and the inoculation were performed with respect to established protocol, as described in **section 4.2.2.** above. At around 12 days post-inoculation, when the average tumour volume reached *ca.* 70 mm^3 mice were randomised and included in the different experimental groups, with nine mice per group (except for the second *in vivo* experimentation where the Control group contained eight mice).

Preparation of different pPBS

Sterile PBS (Ca^{2+}, Mg^{2+}) 1X was treated continuously with NTP multijet either for twenty minutes (resulting in the "**20-minutes-pPBS**") or for one hour (resulting in "**1-hour-pPBS**"), using the protocol established in our previous study (Chung, 2020) (see **chapter 2 of the Results**). The pPBS were prepared a day before the treatment and stored at +4°C, as described in our previous study (Sklias *et al.,* to be submitted - see **chapter 3 of the Results**). Note that for the preparation of the 1-hour-pPBS, the compensation of water evaporation (and thus the maintenance of the original osmolarity of the liquid) was performed during the production of the pPBS, *i.e.*, 700 µL of water were added to the plasma-treated PBS every twenty minutes.

EP generator and electrodes

Electroporation was performed using the electric pulse generator Cliniporator™ (IGEA, Carpi, Italy), delivering HV pulses and LV pulses. Eight square-wave EPs of amplitude over a distance ratio of **1000 V/ cm**, a duration of 100 µs at 1 Hz, were used. Non-invasive stainless-steel plate electrodes (P30-8B, IGEA, Carpi, Italy) consisting of two metallic plates 1 mm thick and 4.7 mm apart were employed. Voltage was set up according to the distance between the two plates of the electrodes. Thus 470 V for the plate electrodes, distant 4.7 mm, was used in this study.

Experimental procedure

Before treatment, mice were anaesthetised with Isoflurane (Isoflurin® 1000 $mg.g^{-1}$, Axience, FR) in an induction chamber. For all groups receiving pPBS, an i.t. administration of pPBS, either the 20-minutes-pPBS or the 1-hour-pPBS, was performed **6 minutes before** the administration of bleomycin. The administered volume was half of the tumour volume, individually measured during the randomisation. Bleomycin (Roger Bellon SA, Neuilly-Sur-Seine, France) was i.v. administered in the retro-orbital sinus **4 minutes before** the delivery of the EPs, at a dose of 10 µg per 100 µL per animal. For mice receiving EPs (groups 2, 4 and 5), their tumour was placed between the electrodes. To ensure a correct electric field distribution around the tumour volume, conductive gel (Asept Uni'Gel US, Aspet Inmed, France) was used to fill the space between electrodes and the tumours (Ivorra *et al.*, 2008).

The *in vivo* treatment protocol of the combined approach is displayed in ***Figure 38***.

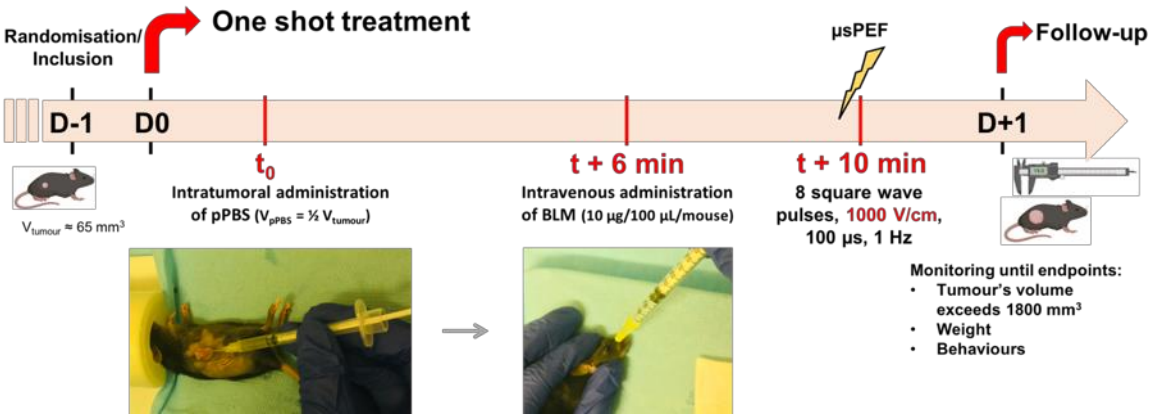

Figure 38| Illustration of the protocol and experimental strategy of the combined treatment with pPBS and ECT in C57Bl/6J mice bearing s.c. LPB tumour

In vivo follow-up and end-point analysis

See section 4.2.2. above.

Statistical analysis and data handling

Data represents as mean ± SEM values. GraphPad Prism software (version 8.4.0, La Jolla, CA, US) was used for data handling, analysis and graphic representations *(ongoing analysis)*.

4.2.3 Results of *in vivo* combined treatment with pPBS and ECT

Differences observed in anti-tumour effectiveness were evaluated by tumour growth delay and the probability of tumour cures achievement. The tumour growth delay of the first

in vivo experiment is shown in *Figure **39***. The efficacy of the single- and combined treatments was compared with ECT as the gold standard. We did not observe a delay of tumour growth in groups receiving treatment either with pPBS alone (group 3) or with pPBS followed by ECT (group 5), as compared with the ECT (group 2). On the contrary, with the 1-hour-pPBS alone, there could be a tendency to accelerate the tumour growth, as compared with the Control (group 1). If compared to the Control group, the combined treatment employing 1-hour-pPBS followed by ECT (group 4) **delayed the tumour growth for six days**, and ECT alone decelerated the tumour growth by **four days**.

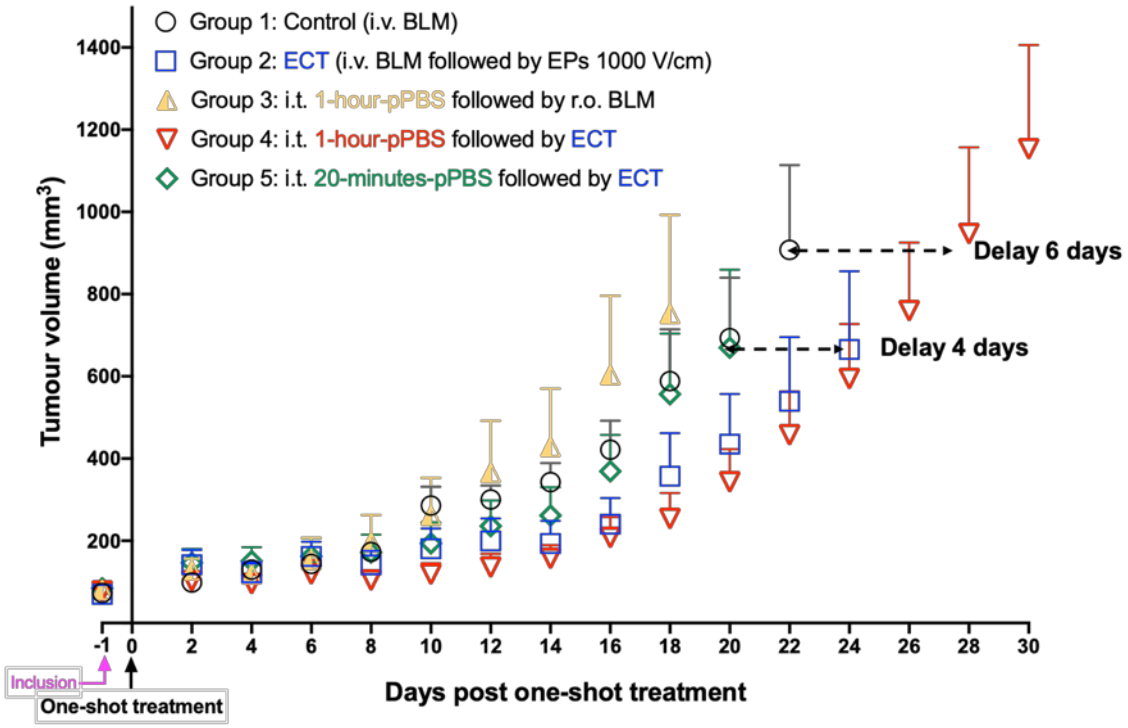

Figure 39| The tumour growth delay in female C57Bl/6J mice treated with pPBS combined with ECT in the first experiment

The number of mice was n = 9 in each experimental group. Data represents as mean ± SEM values. The tumour evolution is shown until the first animal of each group reached an end-point.

The per cent survival rates of the first *in vivo* experiment, given as Kaplan–Meier estimator plots, are shown in *Figure **40***. Survival times measure the time interval from a starting point until the occurrence of a given event, here from the one-shot treatment at D0 until the tumour size reaches the ethical limit (1800 mm^3). We observed a prolonged survival for mice in groups receiving combined treatments with pPBS and ECT, especially the one treated with the 1-hour-pPBS and ECT, compared with mice receiving single treatment with either pPBS or ECT. However, there is no significant difference between those two groups on day 34 (group 4) and

day 35 (group 2) post-treatment. Contrariwise, one mouse in group 4 (combination of 1-hour-pPBS and ECT) had a complete tumour regression after 60 days (thus considered a tumour cure). This mouse was monitored until day 100 post-treatment with no sign of tumour recurrence, *i.e.*, we obtained 11.11% complete regression for this group N°4. All other treatments showed the life span of the last surviving mouse of 53 days (for group 3: combined 1-hour-pPBS with BLM), 67 days (for group 2: ECT) and 78 days (for group 5: combined 20-min-pPBS with BLM) after treatment.

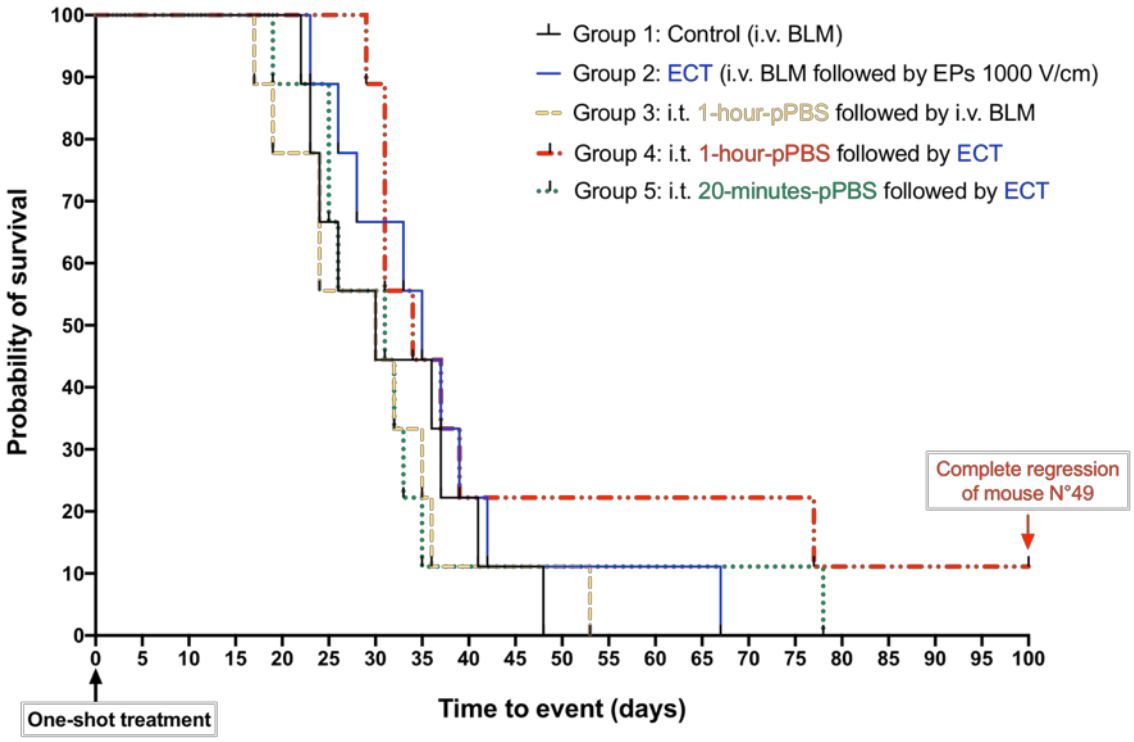

Figure 40| The probability of survival (Kaplan-Meier estimator) of female C57Bl/6J mice treated with pPBS combined with ECT in the first experiment

The number of mice was n = 9 in each experimental group. Survival times were measured from the one-shot treatment until the occurrence of an end-point. The observation time ended at day 100 post-treatment for mice with complete tumour regression (here, the mouse N°49 of group 4), considered a tumour cure.

Following this first *in vivo* experimentation, we repeated the experiment with six groups (the group 6, i.t. administration of 20-minutes-pPBS followed by i.v. administration of BLM, is the control of group 5).

The tumour growth delay of the second *in vivo* experiment is shown in *Figure **41***. There are two types of responses to the treatments: a group of curves presenting all the treatments without µsPEF (groups 1, 3 and 6) and a group presenting the treatments with µsPEFs (groups 2, 4 and 5). We observed that monotherapy with pPBS (*i.e.*, without ECT), either the 20-

minutes-pPBS (group 6) or the 1-hour-pPBS (group 3), decelerated the tumour growth for only two days, as compared with the control (group 1), thus no noticeable anti-cancer effect. Interestingly, with the combined treatment employing pPBS followed by ECT, better anti-tumour effects were observed, tumour growth delay being four days in group 4 (1-hour-pPBS followed by ECT) and seven days in group 5 (20-minutes-pPBS followed by ECT). This displacement of tumour growth curves also reveals the differences in the eventual synergy of ECT and the two pPBS: anti-tumour synergy effectiveness was much more pronounced with the 20-minutes-pPBS combined with ECT than with the 1-hour-pPBS combined with ECT.

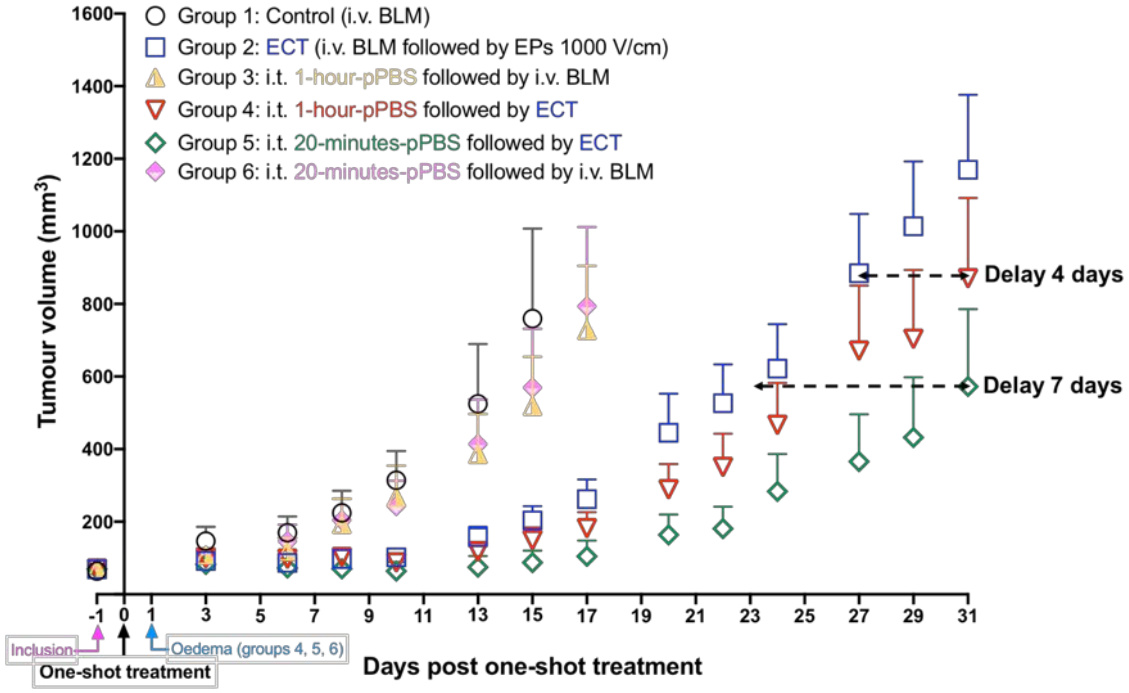

Figure 41| The tumour growth delay in female C57Bl/6J mice treated with pPBS combined with ECT in the second experiment

The number of mice was n = 9 in each experimental group except for the control group (n = 8). Data represents as mean ± SEM values. The tumour evolution is shown until the first animal of each group reached an end-point.

The per cent survival rates of the second *in vivo* experimentation given as Kaplan–Meier estimator plots are shown in *Figure **42***. Both ECT or combined treatments with pPBS and ECT have a 100% survival up to 31 days post-treatment, as compared with the same probability of survival in other groups (15 days for group 1 (Control) and 17 days for groups 3 and 6 receiving only pPBS and BLM without µsPEFs). In general, a prolonged survival was observed for mice receiving combined treatments with pPBS (the two types of pPBS) and ECT, compared with mice receiving single treatment without µsPEFs.

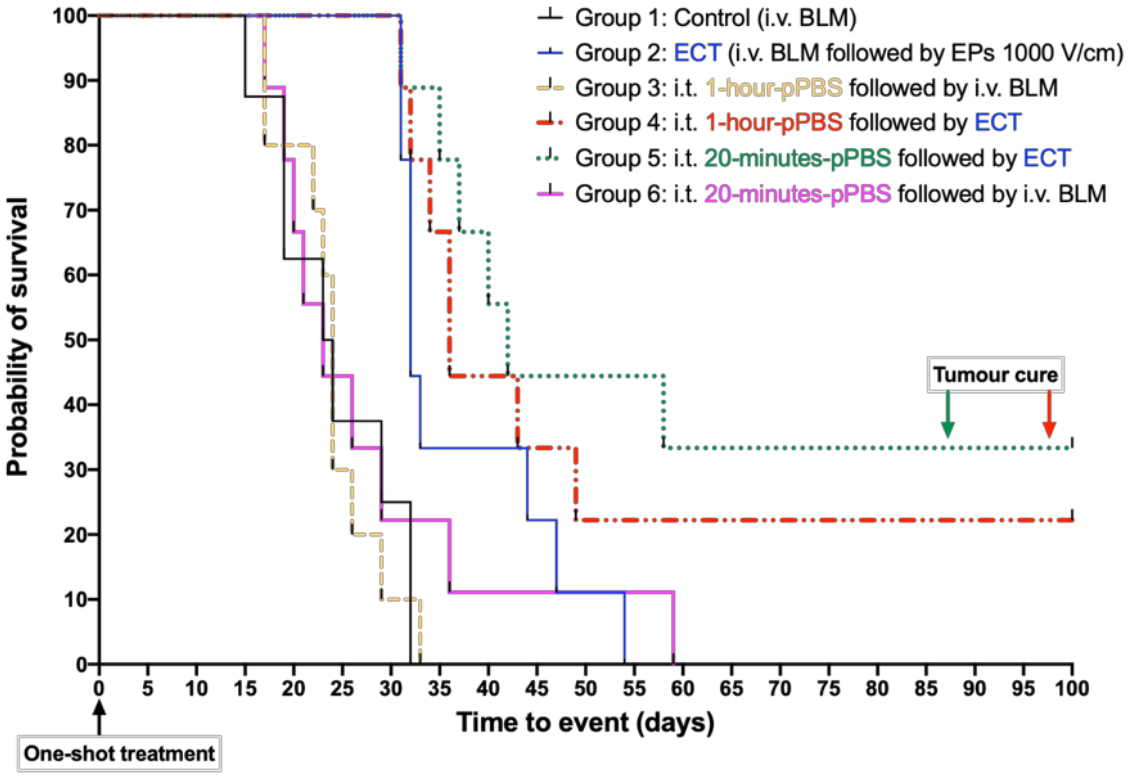

Figure 42| The probability of survival (Kaplan-Meier estimator) of female C57Bl/6J mice treated with pPBS combined with ECT in the first experiment

The number of mice was n = 9 in each experimental group except for the control group (n = 8). Survival times were measured from the one-shot treatment until the occurrence of an end-point. The observation time was ended at day 100 post-treatment for mice with complete tumour regression (here, two mice in group 4 and three mice in group 5), considered a tumour cure.

The efficiency of the combined treatments can be observed for example, at 35 days post-treatment, where 88.9% survival was found in the group receiving the "20-min-pPBS + ECT" (group 5), followed by the group 4 that received "1-hour-pPBS + ECT" with 77.2% survival, as compared with 33% survival in mice receiving ECT (group 2). Interestingly, there are two mice in group 4 (combination of 1-hour-pPBS and ECT) with complete tumour regression since day three post-treatment and three mice in group 5 (combination of 20-min-pPBS and ECT) with complete tumour regression since day nine post-treatment. After a hundred days of follow-up, their tumour volume remained zero (complete regression); those mice were thus considered cured (tumour cure). Indeed, when a mouse has a complete tumour regression (tumour volume is zero) for more than sixty days, the tumour is considered cured.

The cure rate was 22.22% for group 4 and 33.33% for group 5, at a field amplitude for the ECT lower than usual (which results in no cure if applied in the absence of the pPBS). In conclusion, with combined treatments employing pPBS followed by ECT at a µsPEF amplitude

of 1000 V/cm, a longer tumour growth delay and a higher curability rate of the tumours were obtained compared with ECT alone.

The survival rate based on the individual curve of tumour growth of each mouse is depicted in *Figure **43***.

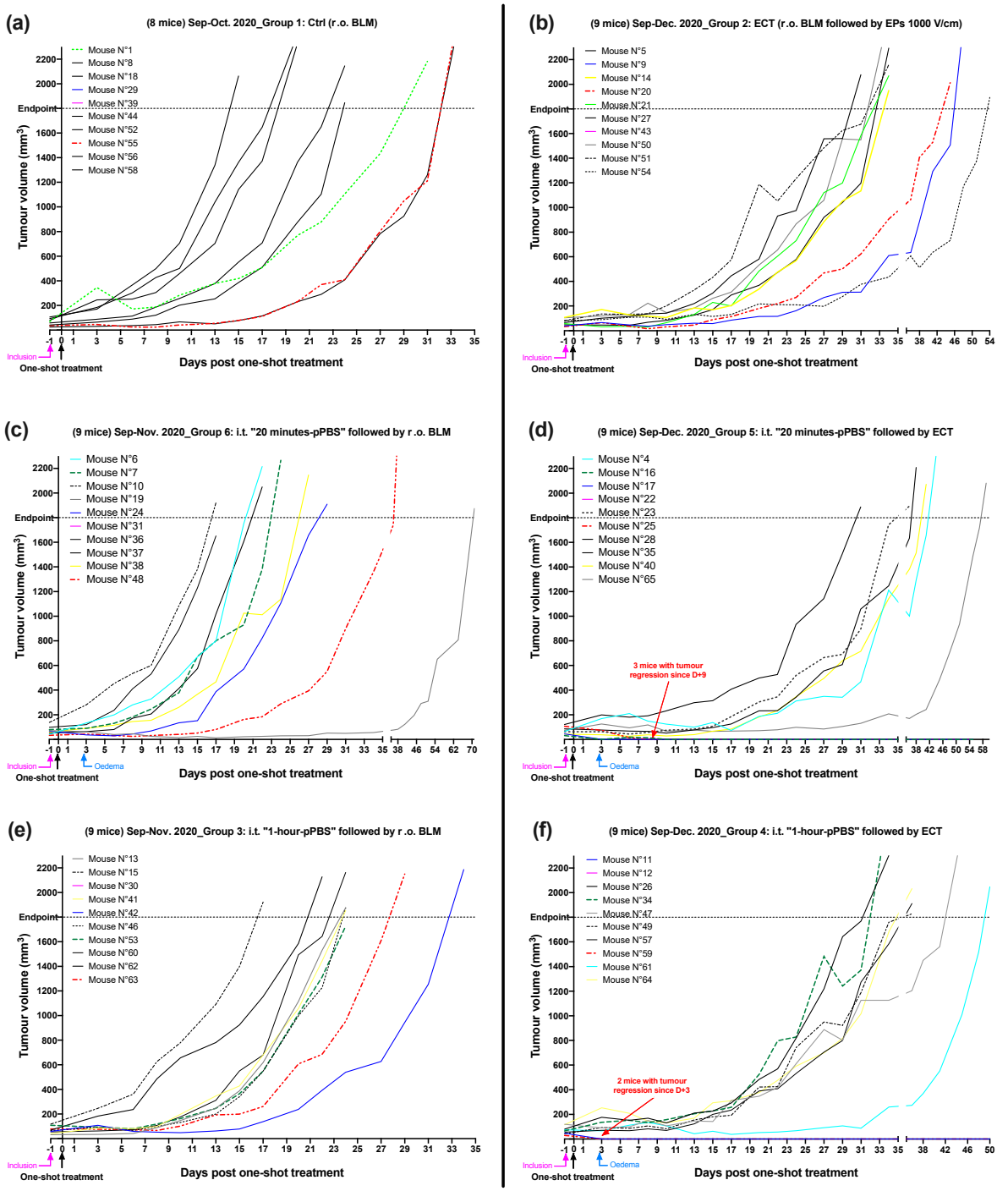

Figure 43| The tumour growth delay of each female C57Bl/6J mouse treated with pPBS combined with ECT in the second *in vivo* experimentation

The number of mice was n = 9 in each experimental group except for the control group (n = 8). Treatments without application of µsPEFs are shown in left panel (graphs **a**, **c** and **e** corresponding to the groups 1 (control), 6 (i.t. 20-minutes-pPBS + BLM) and 3 (i.t. 1-hour-pPBS + BLM), respectively), being the control of treatments with application of µsPEFs shown in the right panel (graphs **b**, **d** and **e** corresponding to the groups 2 (ECT), 5((i.t. 20-minutes-pPBS + ECT)) and 4 ((i.t. 1-hour-pPBS + ECT)), respectively). The individual tumour evolution was shown until the animal reached an end-point.

DISCUSSION

This thesis sought to improve electrochemotherapy (ECT) through non-thermal plasma (NTP) medicine, *i.e.*, to explore the combination of electric pulses and NTP.

In the first assessment, we attempted to obtain a stable helium NTP multijet device that could offer not only a large and homogeneous treatment surface, as compared with other NTP devices with single-jet, but also an easier translation from pre-clinical to clinical studies*, i.e.*, an NTP system suitable for fundamental research as well as for medical uses. The second assessment consisted of two parallel investigations: ***(i)*** the dosimetry of plasma-treated PBS (pPBS) and the study of its different storage conditions for optimal *in vitro* and *in vivo* uses, and ***(ii)*** the *in vitro* study on combined treatment with pPBS and µsPEFs on two different cell lines. Finally, we investigated a combination of pPBS and ECT on small animals to elucidate the anti-tumour effect of the combined treatment and the underlying mechanisms of the effects observed. The treatment employed two different pPBS and ECT at low PEF amplitude (lower than that used in conventional ECT in clinics).

In the first article, I contributed by performing the first biological assays of the newly introduced multijet plasma device, both in direct NTP applications and in indirect applications (thus through the preparation of plasma-treated liquids). To get **stable and reproducible plasma**, a dialogue had to be raised with the engineers that developed the device to ameliorate some issues. Connexion to ground and introduction of a compensating circuit was created, and I tested them. It is perhaps worth noting that these developments had some similarities with impedance matching circuits used for higher frequency (RF) power supplies to minimise reflected power. We highlight that for the examples used in this paper, the compensating course was not used its primary purpose (use in direct NTP applications) but rather for maintaining consistent results between targets with different impedances. We proposed to use the International Standard IEC 60601-1 electrical equivalent circuit for the human body. This circuit is applicable at frequencies below 10 MHz, where electrostatic effects dominate. The compensation circuit was designed to match the model of the human equivalent circuit when placed in series with the chosen target. This work has contributed to plasma medicine research to obtain more directly relevant results to human targets. Besides,

a compensation circuit should help minimise purely electrical differences between non-human targets.

In the second article, we attempted to **determine new conditions for ECT**, devoid of its side effects mainly due to intense electric pulses. We were interested in reducing the pulsed electric fields (PEFs) of the classical 100 microseconds pulses used in ECT without reducing the permeabilisation of the cell membrane. We investigated a **combined treatment of µsPEFs with pPBS to outperform ECT** in two different cell lines. We succeeded to enhance the cell membrane permeabilisation, both in terms of the percentage of permeabilised cells and the intracellular content of the used permeabilisation marker YO-PRO-1® Iodide, with reduced µsPEFs (500 V/cm instead of 1100 V/cm if combined with pPBS. This enhancement of the cell membrane permeabilisation level was cell-line dependent. Indeed, multiple research groups discussed the critical influence of both cell type and cancer type on the cell sensitivity to indirect plasma treatment (Biscop Eline *et al.*, 2019; Kim *et al.*, 2016; Tanaka, 2011; Wang *et al.*, 2013; Zucker *et al.*, 2012). Compared to their non-cancerous counterparts, many cancer cell types seem to function with higher levels of endogenous oxidative stress (higher intracellular levels of ROS) *in vitro* and *in vivo*, making them more vulnerable to damage by further ROS encroachments produced by exogenous agents (Trachootham, 2009). Besides, we have to consider the most common lipid component in animal cell membranes, cholesterol, which is fundamental for determining many structural properties of the plasma membrane and whose content ranges depending on the cell type. Indeed, as cholesterol is mainly responsible for the ordering of the lipids in the phospholipid membrane hence the membrane permeability (Meyer *et al.*, 2009; Raffy *et al.*, 1999), a lower ratio of cholesterol to phospholipids increases the fluidity of the plasma membrane (van Blitterswijk, 1982), making the phospholipid bilayer more susceptible to the oxidative stress which arises from the impinging RONS. These observations have also been predicted by molecular dynamic simulation (Delemotte, 2012; Tarek, 2005), especially for NTP treatment of cancer cells (Van der Paal, 2016; Yusupov, 2017). Interestingly, cancer cells have a significantly lower cholesterol concentration in their plasma membrane (*ca.* 2-fold lower) than in the phospholipid bilayer of their non-tumourigenic counterparts (Shinitzky, 1984; van Blitterswijk, 1982). Even though to our knowledge, a precise characterisation of the cholesterol level in the membranes of the two studied cell lines has never been investigated, this could, at least in part, explain the different behaviour of the two cell lines to the combined therapy in our

investigation. Indeed, the origin of the B16 cells is a melanoma explanted from mice, while the DC-3F are spontaneously transformed Chinese hamster lung fibroblasts, the latter being perhaps closer to the normal cells than the former. This could explain the situation where the single pre-and post-treatment of the two studied cell lines with pPBS without any PEF applied has enhanced the percentage of permeabilised cells. This effect is significantly more pronounced in the case of the B16-F10 melanoma cells (significant 2-fold enhancement) than within DC-3F fibroblasts bearing the same treatment condition. Moreover, the increased penetration of RONS in cancer cells explained by the decreased cholesterol fraction of their cell membrane was also observed three years ago by the group PLASMANT in Belgium (Van Der Paal *et al.*, 2017).

In the third article, we investigated the **pH and chemical stability of pPBS** in terms of the evolution of the concentration of H_2O_2, NO_2^- and NO_3^-, the main anti-cancer drivers of the pPBS effects, as well as the cytotoxic and cytostatic effects of the pPBS, and its capability to permeabilise the cell membrane. Two different cell lines were investigated, and the different studied pPBS were stored at different temperatures (ranging from -80°C to +21°C) for different storage times (up to 75 days). One of the most important differences between using plasma-treated liquids and direct plasma application is that any direct effect of UV radiation or electric fields on the biological target can be avoided using plasma-treated liquids. We could thus focus on the generated ROS and RNS in the pPBS used for our *in vitro* and *in vivo* investigations, which were precisely analysed in this third article. Understanding the chemical essence of the reactions between RONS and the intracellular molecules would help understand the underlying mechanisms of NTP treatment in cancer therapy. pPBS stored at +20°C (room temperature) or +4°C was revealed to preserve their cytotoxic activity, at least for 21 days. Also, pPBS can permeabilise the cellular membrane and showed that it retains this ability regardless of the storage temperature. We excluded the role of NO_2^- and proposed H_2O_2 to be the main driver of the cellular membrane permeabilisation due to pPBS.

With those encouraging *in vitro* results, an eventual **combination of pPBS with electrochemotherapy (ECT)** as a novel anti-cancer approach appeared to have significant potential and was therefore investigated in small animals. We firstly performed a pilot experiment investigating the anti-cancer efficiency of plasma-treated liquids as single anticancer therapy.

The mono-therapy with PAM or pPBS intratumourally administered in the LPB tumour model was unsuccessful regarding the tumour growth delay. We firstly suspected the presence of an eventual RONS scavenger in the MEM 1X used to produce the PAM, as reported in the literature (Chance *et al.*, 1979; Kaushik, 2015; Kondeti *et al.*, 2018; Tornin, 2019; Utsumi, 2013; Wang *et al.*, 2007). However, there is no pyruvate present in MEM 1X, according to the medium formulation from the producer's datasheet. There is no scavenger of RONS present in PBS (Ca^{2+}/Mg^{2+}) used to produce the pPBS. There could be, on the contrary, other RONS scavengers present in MEM 1X that are not to our knowledge. Therefore, we were very curious about the potential efficiency of the pPBS (instead of the PAM) as anti-tumour mono-therapy and, in addition, about the reliability of other published *in vivo* studies showing the anticancer efficiency of those plasma-treated liquids. The same lack of efficacy was found with the pPBS. Another possibility to explain the inefficiency of the i.t. PAM treatment alone in our experiments is the large size of the tumours that we treated (the mean tumour volume of mice in each experimentation was *ca.* 100 mm^3), *i.e.*, tumours that may be considered advanced, hence not easy to be treated, even incurable. The response to treatment could also depend on the tumour type, as demonstrated by various studies. Groselj and colleagues, in their research entitled "Vascularization of the tumours affects the pharmacokinetics of bleomycin and the effectiveness of electrochemotherapy", showed *in vitro* and *in vivo* results of intrinsic effectiveness of ECT (conventional one) with BLM in two different cell lines (and thus two different types of tumours), and concluded that carcinoma was significantly more responsive to ECT than melanoma due to differences in tumour vascularisation, as carcinoma tumours had numerous well-distributed, small blood vessels, while melanomas were less vascularised, exhibiting predominantly larger vessels (Groselj *et al.*, 2018). Nevertheless, ECT is used in the clinics to treat almost all the types of tumour nodules, as all cells are permeabilised by electric pulses of appropriate electric field amplitude and bleomycin is effective on all dividing cells, whatever their origin. In our *in vivo* experiments combining pPBS and ECT, since we only used one type of tumour, the LPB tumour, we could not compare the treatment effectiveness regarding the tumour microenvironment.

Thus, for investigating the effectiveness of the combined treatment with pPBS and ECT, we modified the protocol and treatment design: (**i**) Double the treatment time of PBS 1X by the NTP multijet, being 20 minutes of treatment (20-minutes-pPBS) instead of 10 minutes of exposure to the plasma multijet, to augment the RONS concentration present in the pPBS as

demonstrated in chapter 3 of Results section (article #3 of Sklias *et al.*, to be submitted); (**ii**) the LPB tumours volume for treatment was reduced, being smaller than that of the initial *in vivo* experiments (*ca.* 65-71 mm^3 *versus ca.* 100 mm^3). This was also for a homogenous tumour size amongst animals and a better observation of the combined treatment effects. For the second *in vivo* combined treatment, the control group (administration of BLM only) was constituted with one animal less than the other groups for two reasons: **1**) under the experimental conditions followed during the present study, there was repeatedly no anti-tumour effect of the BLM administered alone (García-Sánchez *et al.*, 2020; Miklavčič *et al.*, 1998; Mir, 1991a); **2**) to reduce the number of animals used according to the ethics 3Rs' rule (replacement, reduction and refinement) (Workman *et al.*, 2010).

For *in vivo* investigations, often, the effect is not so noticeable. Besides, it is usually obscured by notorious variations of animals' responses. Moreover, in vivo experiments are typically carried out with no more than ten animals per group due to limited resources. In our investigations, all groups possessed from 8 to 10 mice per group, which is considered the correct group size to analyse an eventually relevant effect of the treatment. The estimation for statistically significant identification of the treatment effect was based on the tumour-volume measurements, and the probability of survival was employed.

In our preliminary *in vivo* studies of PAM and pPBS (section 4.2), we treated tumours from two cancer cell lines (B16-F10 melanoma and LPB fibrosarcoma) syngeneic in C57Bl/6J mice (the treatment was therefore carried out in the same genetic background). The first tumour is characterised by irregular vascularisation and heterogeneous cell organisation, and the second by organised vascularisation and homogeneously arranged cells. This might explain rapid tumour growth in melanoma B16-F10 tumours. Indeed, melanoma exhibits notorious resistance to standard therapies, and the results of adjuvant and especially the palliative treatment of melanoma are more than unsatisfactory.

It is worth mentioning the efficiency of ECT (alone) and the choice of the *in vivo* models. Studies on immunocompetent and immunodeficient nude mice demonstrated that the host immune response is crucial for effective ECT with BLM (Mir, 1991a) and *cis*-Pt (Serša *et al.*, 1997b). The growth delay induced by ECT in tumours was more significant in immunocompetent than in immunodeficient mice. The most important observation was that a tumour could be eradicated by ECT exclusively in animals with a normal immune response. The importance of the immune system was also demonstrated by other studies in which

combined use of ECT with various types of immunotherapy resulted in potentiation of ECT effectiveness (Calvet *et al.*, 2016; Mir, 1992; Serša, 1997a).

In this *in vivo* study, we investigated the anticancer effect of two preparations of pPBS, the 20 minutes-pPBS and the one hour-pPBS, in combination with ECT at 1000 V/cm. This amplitude is 300 to 350 V/cm below the classical PEF amplitude in this kind of preclinical trial, and pulses at 1000 V/cm (+ bleomycin) are insufficient to obtain good anti-tumour effects (*e.g.*, no cure). As discussed in state of the art, the electropermeabilisation of cells (the basis of ECT) involves rearrangements of the cell membrane structure by partial oxidation of membrane lipids. Radical reactions cause the oxidation of lipids, and NTP produces radicals (RONS), which are known to pass from the gas phase of the NTP to biological targets exposed to the plasma, here the PBS. A pre-treatment of the tumour with pPBS helped create radicals inside the tumour and in the tumour micro-environment, aimed to favour the electropermeabilisation of the tumour cells at a less intense electric field amplitude (therefore more “comfortable” for the patients in clinics). To respect the 3R rule (Replacement, Reduction and Refinement), the combination of pPBS and µsPEFs at different amplitudes was previously studied in cultured cells in **chapters 2 and 3 of the Results** (see the second article (Chung, 2020) and the third article (Sklias *et al.,* to be submitted). We increase the rate of wholly cured animals by combining plasma-treated PBS with ECT at low electric field strength.

FURTHER PROSPECTS AND CHALLENGES

My thesis aimed to reduce the µsPEFs amplitudes using NTP as a complementary tool. We succeeded in obtaining exciting results with low µsPEFs amplitudes, promising results for ECT. The *in vivo* combined treatment with a pre-treatment with pPBS followed by ECT at low µsPEFs has a significant delay in tumour growth and a considerable lifespan of animals compared with those treated with mono-therapy pPBS or ECT.

Theory somehow works, up to now, for *in vitro* studies investigating indirect NTP (pPBS) with µsPEFs, with or without chemotherapeutic agents (bleomycin, paclitaxel, dacarbazine) (Daeschlein, 2018; Wolff, 2020) but those *in vitro* results show variable anti-cancer responses with still unclear mechanisms of the effects observed. Moreover, the *in vitro* and *in vivo* protocols and strategies of the NTP approach, being as monotherapy or in combination with PEFs (or with ECT), are often study-dependant; thus, results are usually not easy to compare (different radicals, different concentrations of the radicals, depending on the NTP production system - also potential caveats with the thickness of the liquid treated by the NTP, in the time between exposure to NTP and application to the cells or animals, not speaking about the conditions for storage if the application is delayed, etc.).

To the best of my knowledge, our *in vivo* study combining indirect NTP strategy with ECT represents the first *in vivo* combined therapy in the field and successfully demonstrates a synergistic effect of plasma-treated liquids (here, the plasma-treated PBS) and ECT *in vitro* and even *in vivo* (even though, our experiments with mice require further confirmation). In particular, our approach allowed a decrease of the pulsed electric field amplitude used in ECT, *i.e.*, 300 to 350 V/cm lower than that used for practical ECT in clinics, while offering a better treatment result than with the ECT alone. This novel combined approach would pave the way for promising targeted anti-cancer therapies.

In perspective, further confirmation of the last *in vivo* experimentation will be necessary. It would also be essential to scrutinise **the mechanisms** (what is not yet understood) **and applications** of pPBS and pPBS combined with ECT at different parameters. It would be worth investigating the proposed combined treatment with pPBS and ECT in other tumours (*e.g.,*

B16-F10 melanoma, which are less “rigid” than the studied fibrosarcoma LPB tumours, hence probably favour a more homogeneous distribution of pPBS or in other *in vitro* models such as spheroids.

The challenges are still ahead for better control of the RONS delivery, understanding the process chain leading to the antitumoural effects, or optimising the combined plasma/(electro)chemotherapy approach.

Indeed, debate still goes on within the plasma science community whether a definition of “dose” should be applicable to perform NTP treatment, as it is available for other physical-based therapies such as radiation treatment, phototherapy or laser therapy. Moreover, there still is no demonstration on which specific plasma component or plasma parameter would be responsible for a given specific reactive species, thus for a specific biomedical effect or therapeutic outcome. Subsequently, plasma impact on biological experiments and therapeutic applications is usually controlled via treatment time and energy supplied to the device. Because of the different technical setups of NTP devices under investigation or in medical applications, this has to be defined for every device specifically, and a generalisation is not possible. Identifying and defining such a parameter or set of parameters for device-independent control of biological plasma effectivity is possibly the biggest challenge in preclinical research in the plasma medicine (Adamovich *et al.*, 2017).

Unlike electrochemotherapy, there is, to date, no standard operating procedure for plasma medicine, as it is the newest field of non-thermal plasma technology.

REFERENCES

Ackroyd, R., Kelty, C., Brown, N. & Reed, M. (**2001**). The History of Photodetection and Photodynamic Therapy. *Photochem. Photobiol.* **74**, 656–69.

Adachi, T., Tanaka, H., Nonomura, S., Hara, H., Kondo, S. I. & Hori, M. (**2015**). Plasma-activated medium induces A549 cell injury via a spiral apoptotic cascade involving the mitochondrial-nuclear network. *Free Radic. Biol. Med.* **79**, 28–44.

Adamovich, I. *et al.* (**2017**). The 2017 Plasma Roadmap: Low temperature plasma science and technology. *J. Phys. D. Appl. Phys.* **50**, 323001.

Adhikari, B., Pangomm, K., Veerana, M., Mitra, S. & Park, G. (**2020a**). Plant Disease Control by Non-Thermal Atmospheric-Pressure Plasma. *Front. Plant Sci* **11**, pp 1-15.

Adhikari, B., Adhikari, M. & Park, G. (**2020b**). The Effects of Plasma on Plant Growth, Development, and Sustainability. *Appl. Sci.* **10**, 6045.

Adloff, J. P. (**1999**). THE LABORATORY NOTEBOOKS OF PIERRE AND MARIE CURIE AND THE DISCOVERY OF POLONIUM AND RADIUM. *CzechosJovak J. Phys.* **49**, Suppl. S1.

Ágoston, D. *et al.* (**2020**). Evaluation of calcium electroporation for the treatment of cutaneous metastases: A double blinded randomised controlled phase II trial. *Cancers (Basel).* **12**, 179.

Ahlfeld, B., Li, Y., Boulaaba, A., Binder, A., Schotte, U., Zimmermann, J. L., Morfill, G. E. & Klein, G. (**2015**). Inactivation of a foodborne norovirus outbreak strain with nonthermal atmospheric pressure plasma. *MBio* **6**, e02300-14.

Al-Sakere, B., André, F. M., Bernat, C., Connault, E., Opolon, P., Davalos, R. V., Rubinsky, B. & Mir, L. M. (**2007**). Tumor Ablation with Irreversible Electroporation. *PLoS One* **11**, e1135.

American Cancer Society® (**2009**). Cancer Facts & Figures 2009. *Am. Cancer Soc.*

André, F. M. & Mir, L. M. (**2004**). DNA electrotransfer: Its principles and an updated review of its therapeutic applications. *Gene Ther.* **11**, S33–S42.

André, F. M. *et al.* (**2008**). Efficiency of high and low voltage pulse combinations for gene electrotransfer in muscle, liver, tumor and skin. *Hum. Gene Ther.* **11**, 1261–71.

Andtbacka, R. H. I. *et al.* (**2015**). Talimogene laherparepvec improves durable response rate in patients with advanced melanoma. *J. Clin. Oncol.* **33**, 2780–8.

Aras, K. K. & Efimov, I. R. (**2018**). Irreversible electroporation: Proceed with caution. *Hear. Rhythm* **15**, 1880–1.

Arena, C. B., Sano, M. B., Rylander, M. N. & Davalos, R. V. (**2011**). Theoretical Considerations of Tissue Electroporation With High-Frequency Bipolar Pulses. *IEEE Trans. Biomed. Eng.* **58**, 1474.

Arena, C. B., Garcia, P. A., Sano, M. B., Olson, J. D., Rogers-Cotrone, T., Rossmeisl, J. H. & Davalos, R. V. (**2014**). Focal blood-brain-barrier disruption with high-frequency pulsed electric fields. *TECHNOLOGY* **02**, 206–213.

Arndt, S., Wacker, E., Li, Y. F., Shimizu, T., Thomas, H. M., Morfill, G. E., Karrer, S., Zimmermann, J. L. & Bosserhoff, A. K. (**2013a**). Cold atmospheric plasma, a new strategy to induce senescence in melanoma cells. *Exp. Dermatol.* **22**, 284–9.

Arndt, S. *et al.* (**2013b**). Cold atmospheric plasma (CAP) changes gene expression of key molecules of the wound healing machinery and improves wound healing in vitro and in vivo. *PLoS One* **8**, e79325.

Arndt, S., Unger, P., Berneburg, M., Bosserhoff, A. K. & Karrer, S. (**2018**). Cold atmospheric plasma (CAP) activates angiogenesis-related molecules in skin keratinocytes, fibroblasts and endothelial cells and improves wound angiogenesis in an autocrine and paracrine mode. *J. Dermatol. Sci.* **89**, 181–90.

Arnott, N. (**1827**). *Elements of physics, or natural philosophy, general and medical: explained independently of technical mathematics*. London: Underwood.

Arora, V. (**2013**). Cold Atmospheric Plasma (CAP) in Dentistry. *Dentistry* **4**, 189.

Atkins, M. B. *et al.* (**1997**). Phase I evaluation of intravenous recombinant human interleukin 12 in patients with advanced malignancies. *Clin. Cancer Res.* **3**, 409–17.

Awwad, S. & Angkawinitwong, U. (**2018**). Overview of Antibody Drug Delivery. *Pharmaceutics* **10**, 24 pages.

Aycock, K. N. & Davalos, R. V. (**2019**). Irreversible Electroporation: Background, Theory, and Review of Recent Developments in Clinical Oncology. *Bioelectricity* **1**, 214–34.

Azan, A., Gailliègue, F., Mir, L. M. & Breton, M. (**2017**). Cell membrane electropulsation: Chemical analysis of cell membrane modifications and associated transport mechanisms. In *Advances in Anatomy Embryology and Cell Biology*, pp. 59–71. Springer Verlag.

Bashraheel, S. S., Domling, A. & Goda, S. K. (**2020**). Update on targeted cancer therapies, single or in combination, and their fine tuning for precision medicine. *Biomed. Pharmacother.* **125**, 110009.

Bauer, G. & Graves, D. B. (**2016**). Mechanisms of Selective Antitumor Action of Cold Atmospheric Plasma-Derived Reactive Oxygen and Nitrogen Species. *Plasma Process. Polym.* **13**, 1157–78.

Beatson, G. (**1896**). On the Treatment of Inoperable Cases of Carcinoma of the Mamma: Suggestions for a New Method of Treatment, with Illustrative Cases. *Trans Med Chir Soc Edinb.* **15**, 153–79.

Bekeschus, S., Brüggemeier, J., Hackbarth, C., Partecke, L.-I., von Woedtke, T. & van der Linde, J. (**2017**). Platelets are key in cold physical plasma-facilitated blood coagulation in mice. *Clin. Plasma Med.* **7**–**8**, 58–65.

Bekeschus, S., Favia, P., Robert, É. & von Woedtke, T. (**2018a**). White paper on plasma for medicine and hygiene: Future in plasma health sciences. *Plasma Process. Polym.* **16**, e1800033.

Bekeschus, S., Clemen, R. & Metelmann, H.-R. (**2018b**). Potentiating anti-tumor immunity with physical plasma. *Clin. Plasma Med.* **12**, 17–22.

Belehradek, J., Orlowski, S., Poddevin, B., Paoletti, C. & Mir, L. M. (**1991**). Electrochemotherapy of spontaneous mammary tumours in mice. *Eur. J. Cancer Clin. Oncol.* **27**, 73–76.

Belehradek Jr., J., Barski, G. & Thonier, M. (**1972**). Evolution of cell-mediated antitumor immunity in mice bearing a syngeneic chemically induced tumor. Influence of tumor growth, surgical removal and treatment with irradiated tumor cells. *Int. J. Cancer* **9**, 461–9.

Benz, R., Beckers, F. & Zimmermann, U. (**1979**). Reversible electrical breakdown of lipid bilayer membranes: A charge-pulse relaxation study. *J. Membr. Biol.* **48**, 181–204.

Bergemann, C., Rebl, H., Otto, A., Matschke, S. & Nebe, B. (**2019**). Pyruvate as a cell-protective agent during cold atmospheric plasma treatment in vitro: Impact on basic research for selective killing of tumor cells. *Plasma Process Polym.* **16**, e1900088.

Bergler, W. F. (**2003**). Argon plasma coagulation (APC) surgery in otorhinolaryngology. *Surg. Technol. Int.* **11**, 79–84.

Bergonié, J. & Tribondeau, L. (**2003**). Interpretation of Some Results from Radiotherapy and an Attempt to Determine a Rational Treatment Technique. 1906. *YALE J. Biol. Med.* **76**, 181–2.

Bernhardt, J. & Pauly, H. (**1973**). On the generation of potential differences across the membranes of ellipsoidal cells in an alternating electrical field. *Biophysik* **10**, 89–98.

Bertholon, M. l'abbé (Pierre) (**1783**). *De l'électricité des végétaux*. Paris: Paris: Didot Jeune.

Beyer, T., Townsend, D. W., Brun, T., Kinahan, P. E., Charron, M., Roddy, R., Jerin, J., Young, J., Byars, L. & Nutt, R. (**2000**). A combined PET/CT scanner for clinical oncology. *J. Nucl. Med.* **41**, 1369–79.

Bienert, G. P., Møller, A. L. B., Kristiansen, K. A., Schulz, A., Møller, I. M., Schjoerring, J. K. & Jahn, T. P. (**2007**). Specific aquaporins facilitate the diffusion of hydrogen peroxide across membranes. *J. Biol. Chem.* **282**, 1183–92.

Biscop Eline, Lin, A. G., Van Boxem, W., Van Loenhout, J., De Backer, J., Deben, C., Dewilde, S., Smits, E. & Bogaerts, A. (**2019**). Influence of Cell Type and Culture Medium on Determining Cancer Selectivity of Cold Atmospheric Plasma Treatment. *Cancers (Basel).* **11**, 1287.

Blackadar, C. B. (**2016**). Historical review of the causes of cancer. *World J. Clin. Oncol.* **7**, 54–86.

Blahovec, J., Vorobiev, E. & Lebovka, N. (**2017**). Pulsed Electric Fields Pretreatments for the Cooking of Foods. *Food Eng. Rev.* **9**, 71–81.

Boehm, D., Heslin, C., Cullen, P. J. & Bourke, P. (**2016**). Cytotoxic and mutagenic potential of solutions exposed to cold atmospheric plasma. *Sci. Rep.* **6**, 21464.

Bol'shakov, A. A., Cruden, B. A., Mogul, R., Rao, M. V. V. S., Sharma, S. P., Khare, ¶ B N & Meyyappan, M. (**2004**). Radio-Frequency Oxygen Plasma as a Sterilization Source. *AIAA J.* **42**, 823–32.

Bourke, P., Ziuzina, D., Han, L., Cullen, P. J. & Gilmore, B. F. (**2017**). Microbiological interactions with cold plasma. *J. Appl. Microbiol.* **123**, 308–24.

Bower, M., Sherwood, L., Li, Y. & Martin, R. (**2011**). Irreversible electroporation of the pancreas: Definitive local therapy without systemic effects. *J. Surg. Oncol.* **104**, 22–28.

Braný, D., Dvorská, D., Halašová, E. & Škovierová, H. (**2020**). Cold Atmospheric Plasma: A

Powerful Tool for Modern Medicine. *Int. J. Mol. Sci.* **21**, 2932.

Breton, M. & Mir, L. M. (**2012a**). Microsecond and nanosecond electric pulses in cancer treatments. *Bioelectromagnetics* **33**, 106–23.

Breton, M., Delemotte, L., Silve, A., Mir, L. M. & Tarek, M. (**2012b**). Transport of siRNA through lipid membranes driven by nanosecond electric pulses: An experimental and computational study. *J. Am. Chem. Soc.* **134**, 13938–41.

Brömme, D., Rossi, A. B., Smeekens, S. P., Anderson, D. C. & Payan, D. G. (**1996**). Human bleomycin hydrolase: Molecular cloning, sequencing, functional expression, and enzymatic characterization. *Biochemistry* **35**, 6706–14.

Brullé, L., Vandamme, M., Riès, D., Martel, E., Robert, É., Lerondel, S., Trichet, V., Richard, S., Pouvesle, J.-M. & Le Pape, A. (**2012**). Effects of a Non Thermal Plasma Treatment Alone or in Combination with Gemcitabine in a MIA PaCa2-luc Orthotopic Pancreatic Carcinoma Model. *PLoS One* **7**, e52653.

Buchmann, L., Frey, W., Gusbeth, C., Ravaynia, P. S. & Mathys, A. (**2019**). Effect of nanosecond pulsed electric field treatment on cell proliferation of microalgae. *Bioresour. Technol.* **271**, 402–8.

Calvet, C. Y. & Mir, L. M. (**2016**). The promising alliance of anti-cancer electrochemotherapy with immunotherapy. *Cancer Metastasis Rev.* **35**, 165–77.

Calvet, C. Y., André, F. M. & Mir, L. M. (**2014a**). Dual therapeutic benefit of electroporation-mediated DNA vaccination in vivo: Enhanced gene transfer and adjuvant activity. *Oncoimmunology* **3**, e28540.

Calvet, C. Y., Famin, D., André, F. M. & Mir, L. M. (**2014b**). Electrochemotherapy with bleomycin induces hallmarks of immunogenic cell death in murine colon cancer cells. *Oncoimmunology* **3**, e28131-7.

Campana, L. G. *et al.* (**2016**). Treatment efficacy with electrochemotherapy: A multi-institutional prospective observational study on 376 patients with superficial tumors. *Eur. J. Surg. Oncol.* **42**, 1914–23.

Campana, L. G. *et al.* (**2019a**). Electrochemotherapy - Emerging applications technical advances, new indications, combined approaches, and multi-institutional collaboration. *Eur. J. Surg. Oncol.* **45**, 92–102.

Campana, L. G. *et al.* (**2019b**). Electrochemotherapy of superficial tumors – Current status: Basic principles, operating procedures, shared indications, and emerging applications. *Semin. Oncol.* **46**, 173–91.

Campana, L. G. *et al.* (**2019c**). Electrochemotherapy for advanced cutaneous angiosarcoma: A European register-based cohort study from the International Network for Sharing Practices of electrochemotherapy (InspECT). *Int. J. Surg.* **72**, 34–42.

Cao, G., He, X., Sun, Q., Chen, S., Wan, K., Xu, X., Feng, X., Li, P., Chen, B. & Xiong, M. (**2020**). The Oncolytic Virus in Cancer Diagnosis and Treatment. *Front. Oncol* **10**, 1786.

Carneiro, B. A. & El-Deiry, W. S. (**2020**). Targeting apoptosis in cancer therapy. *Nat. Rev. Clin. Oncol.* **17**, 395–417.

Carter, N. J. & Plosker, G. L. (**2013**). Rivaroxaban: A review of its use in the prevention of stroke

and systemic embolism in patients with atrial fibrillation. *Drugs* **73**, 715–39.

Čemažar, M., Milačič, R., Miklavčič, D., Dolžan, V. & Serša, G. (**1998a**). Intratumoral cisplatin administration in electrochemotherapy: antitumor effectiveness, sequence dependence and platinum content. *Anti-Cancer D* **9**, 525–30.

Čemažar, M., Serša, G. & Miklavčič, D. (**1998b**). Electrochemotherapy with cisplatin in the treatment of tumor cells resistant to cisplatin. *Anticancer Res.* **18**, 4463–6.

Čemažar, M., Pipan, Z., Grabner, S., Bukovec, N. & Serša, G. (**2006**). Cytotoxicity of different platinum (II) analogues to human tumour cell lines in vitro and murine tumour in vivo alone or combined with electroporation. *Anticancer Res.* **26**, 1997–2002.

Čemažar, M., Tamzali, Y., Serša, G., Tozon, N., Mir, L. M., Miklavčič, D., Lowe, R. & Teissié, J. (**2008**). Electrochemotherapy in Veterinary Oncology. *J. Vet Intern Med* **22**, 826–31.

Čemažar, M., Golzio, M., Serša, G., Hojman, P., Kranjc, S., Mesojednik, S., Rols, M.-P. & Teissie, J. (**2009**). Control by pulse parameters of DNA electrotransfer into solid tumors in mice. *Gene Ther.* **16**, 635–44.

Cha, E. & Daud, A. (**2012**). Human Vaccines & Immunotherapeutics Plasmid IL-12 electroporation in melanoma.

Chance, B., Sies, H. & Boveris, A. (**1979**). Hydroperoxide metabolism in mammalian organs. *Physiol. Rev.* **59**, 527–605.

Chauvin, J., Judée, F., Yousfi, M., Vicendo, P. & Merbahi, N. (**2017**). Analysis of reactive oxygen and nitrogen species generated in three liquid media by low temperature helium plasma jet. *Sci. Rep.* **7**,.

Chauvin, J., Judée, F., Merbahi, N. & Vicendo, P. (**2018**). Effects of Plasma Activated Medium on Head and Neck FaDu Cancerous Cells: Comparison of 3D and 2D Response. *Anticancer. Agents Med. Chem.* **18**, 776–83.

Chen, D. S. & Mellman, I. (**2013**). OncologyMeetsImmunology: TheCancer-ImmunityCycle. *Immunity* **39**, 10pp.

Chen, J. & Stubbe, J. A. (**2005**). Bleomycins: Towards better therapeutics. *Nat. Rev. Cancer* **5**, 102–12.

Choi, J. H., Lee, H. W., Lee, J. K., Hong, J. W. & Kim, G. C. (**2013**). Low-temperature atmospheric plasma increases the expression of anti-aging genes of skin cells without causing cellular damages. *Arch. Dermatol. Res.* **305**, 133–140.

Chuangsuwanich, A., Assadamongkol, T. & Boonyawan, D. (**2016**). The Healing Effect of Low-Temperature Atmospheric-Pressure Plasma in Pressure Ulcer: A Randomized Controlled Trial. *Int. J. Low. Extrem. Wounds* **15**, 313–19.

Chung, T.-H. *et al.* (**2020**). Cell Electropermeabilisation Enhancement by Non-Thermal-Plasma-Treated PBS. *Cancers (Basel).* **12**, 219–39.

Coletti, L., Battaglia, V., De Simone, P., Turturici, L., Bartolozzi, C. & Filipponi, F. (**2017**). Safety and feasibility of electrochemotherapy in patients with unresectable colorectal liver metastases: A pilot study. *Int. J. Surg.* **44**, 26–32.

Cooper, G. M. (**2000**). The Development and Causes of Cancer. In *The Cell: A Molecular Approach*, p. 743.

Cornelis, F. H., Ben Ammar, M., Nouri-Neuville, M., Matton, L., Benderra, M. A., Gligorov, J., Fallet, V. & Mir, L. M. (**2019**). Percutaneous Image-Guided Electrochemotherapy of Spine Metastases: Initial Experience. *Cardiovasc. Intervent. Radiol.* **42**, 1806–9.

Cramariuc, R., Tudorache, A., Popa, E., Branduse, E., Nisiparu, L., Mitelut, A., Turtoi, O. & Fotescu, L. (**2008**). Corona discharge in electroporation of cell membranes. In *Journal of Physics: Conference Series*, p. 12062. Institute of Physics Publishing.

Crookes, W. (**1879**). On Radiant Matter. In *Lecture delivered before the British Association for the Advancement of Science*, p. Sheffield.

Daeschlein, G. *et al.* (**2013**). Comparison between cold plasma, electrochemotherapy and combined therapy in a melanoma mouse model. *Exp. Dermatol.* **22**, 582–6.

Daeschlein, G., Hillmann, A., Gumbel, D., Sicher, C., von Podewils, S., Stope, M. B. & Junger, M. (**2018**). Enhanced Anticancer Efficacy by Drug Chemotherapy and Cold Atmospheric Plasma Against Melanoma and Glioblastoma Cell Lines In Vitro. *IEEE Trans. Radiat. Plasma Med. Sci.* **2**, 153–9.

Danaei, G., Vander Hoorn, S., Lopez, A. D., Murray, C. J. L. & Ezzati, M. (**2005**). Causes of cancer in the world: Comparative risk assessment of nine behavioural and environmental risk factors. *Lancet* **366**, 1784–93.

Daud, A. I. *et al.* (**2008**). Phase I trial of interleukin-12 plasmid electroporation in patients with metastatic melanoma. *J. Clin. Oncol.* **26**, 5896–903.

Davalos, R. V., Mir, L. M. & Rubinsky, B. (**2005**). Tissue ablation with irreversible electroporation. *Ann. Biomed. Eng.* **33**, 223–31.

De Geyter, N. & Morent, R. (**2012**). Nonthermal Plasma Sterilization of Living and Nonliving Surfaces. *Annu. Rev. Biomed. Eng.* **14**, 255–74.

Dejeans, N., Manié, S., Hetz, C., Bard, F., Hupp, T., Agostinis, P., Samali, A. & Chevet, E. (**2014**). Addicted to secrete - novel concepts and targets in cancer therapy. *Trends Mol. Med.* **20**, 242–50.

Delemotte, L. & Tarek, M. (**2012**). Molecular dynamics simulations of lipid membrane electroporation. *J. Membr. Biol.* **245**, 531–43.

Deodhar, A., Dickfeld, T., Single, G. W., Hamilton, W. C., Thornton, R. H., Sofocleous, C. T., Maybody, M., Gónen, M., Rubinsky, B. & Solomon, S. B. (**2011**). Irreversible Electroporation Near the Heart: Ventricular Arrhythmias Can Be Prevented With ECG Synchronization. *Am. J. Roentgenol.* **196**, W330-5.

Desagher, S., Glowinski, J. & Prémont, J. (**1997**). Pyruvate Protects Neurons against Hydrogen Peroxide-Induced Toxicity. *J. Neurosci.* **17**, 9060–9067.

Domenge, C., Orlowski, S., Luboinski, B., De Baere, T., Schwaab, G., Jean Belehradek, J. & Mir, L. M. (**1996**). Antitumor Electrochernotherapy New Advances in the Clinical Protocol. *Cancer* **77**, 956–63.

dos Santos, A. F., de Almeida, D. R. Q., Terra, L. F., Baptista, M. S. & Labriola, L. (**2019**). Photodynamic therapy in cancer treatment - an update review. *J. Cancer Metastasis Treat.* **5**, 20pp.

Dubuc, A., Monsarrat, P., Virard, F., Merbahi, N., Sarrette, J.-P., Laurencin-Dalicieux, S. &

Cousty, S. (**2018**). Use of cold-atmospheric plasma in oncology: a concise systematic review. *Ther. Adv. Med. Oncol.* **10**, 1–12.

Duck, F. A. (**2014**). The origins of medical physics. *Phys. Medica* **30**, 397–402.

Dunbar, C. E., High, K. A., Joung, J. K., Kohn, D. B., Ozawa, K. & Sadelain, M. (**2018**). Gene therapy comes of age. *Science (80-.).* **359**, eaan4672.

Edhemovic, I. *et al.* (**2011**). Electrochemotherapy: A new technological approach in treatment of metastases in the liver. *Technol. Cancer Res. Treat.* **10**, 475–85.

Eisenhauer, E. A. *et al.* (**2009**). New response evaluation criteria in solid tumours: Revised RECIST guideline (version 1.1). *Eur. J. Cancer* **45**, 228–47.

Eliezer, S. & Eliezer, Y. (**2001**). *The Fourth State of Matter: An Introduction to Plasma Science, 2nd updated edition*. Bristol: Institute of Physics Publishing.

Eljack, N. D., Ma, H. Y. M., Drucker, J., Shen, C., Hambley, T. W., New, E. J., Friedrich, T. & Clarke, R. J. (**2014**). Mechanisms of cell uptake and toxicity of the anticancer drug cisplatin. *Metallomics* **6**, 2126–33.

Erinjeri, J. P. & Clark, T. W. I. (**2010**). Cryoablation: Mechanism of action and devices. *J. Vasc. Interv. Radiol.* **21**, S187.

Escoffre, J.-M. & Rols, M.-P. (**2012**). Electrochemotherapy: Progress and Prospects. *Curr. Pharm. Des.* **18**, 3406–15.

Esmaeili, N. & Friebe, M. (**2019**). Electrochemotherapy: A Review of Current Status, Alternative IGP Approaches, and Future Perspectives. *J. Healthc. Eng.* 11 pages.

Falk, H., Matthiessen, L. W., Wooler, G. & Gehl, J. (**2018**). Calcium electroporation for treatment of cutaneous metastases; a randomized double-blinded phase II study, comparing the effect of calcium electroporation with electrochemotherapy. *Acta Oncol. (Madr).* **57**, 311–9.

Faurie, C., Rebersek, M., Golzio, M., Kanduser, M., Escoffre, J.-M., Pavlin, M., Teissié, J., Miklavčič, D. & Rols, M.-P. (**2010**). Electro-mediated gene transfer and expression are controlled by the life-time of DNA/membrane complex formation. *J. Gene Med.* **12**, 117–25.

Fiedler, S. & Wirth, R. (**1988**). Transformation of bacteria with plasmid DNA by electroporation. *Anal. Biochem.* **170**, 38–44.

Fiorentzis, M., Viestenz, A., Siebolts, U., Seitz, B., Coupland, S. E. & Heinzelmann, J. (**2019**). The Potential Use of Electrochemotherapy in the Treatment of Uveal Melanoma: In Vitro Results in 3D Tumor Cultures and In Vivo Results in a Chick Embryo Model. *Cancers (Basel).* **11**, 1344.

Foest, R., Kindel, E., Ohl, A., Stieber, M. & Weltmann, K.-D. (**2005**). Non-thermal atmospheric pressure discharges for surface modification. *Plasma Phys. Control. Fusion* **47**, B525–B536.

Foster, W. K., Moy, R. L. & Fincher, E. F. (**2008**). Advances in plasma skin regeneration. *J. Cosmet. Dermatol.* **7**, 169–79.

Frandsen, S. K. & Gehl, J. (**2018**). A review on differences in effects on normal and malignant cells and tissues to electroporation-based therapies: A focus on calcium electroporation.

Technol. Cancer Res. Treat. **17**, 1–6.

Frandsen, S. K., Gissel, H., Hojman, P., Tramm, T., Eriksen, J. & Gehl, J. (**2012**). Direct therapeutic applications of calcium electroporation to effectively induce tumor necrosis. *Cancer Res.* **72**, 1336–41.

Frankenhaeuser, B. & Widén, L. (**1956**). Anode break excitation in desheathed frog nerve. *J. Physiol.* **131**, 243–7.

Freund, E., Liedtke, K. R., van der Linde, J., Metelmann, H.-R., Heidecke, C.-D., Partecke, L.-I. & Bekeschus, S. (**2019**). Physical plasma-treated saline promotes an immunogenic phenotype in CT26 colon cancer cells in vitro and in vivo. *Sci. Rep.* **9**, 634.

Fridman, G., Peddinghaus, M., Ayan, H., Fridman, A., Balasubramanian, M., Gutsol, A., Brooks, A. & Friedman, G. (**2006**). Blood coagulation and living tissue sterilization by floating-electrode dielectric barrier discharge in air. *Plasma Chem. Plasma Process.* **26**, 425–42.

Fridman, G., Shereshevsky, A., Jost, M. M., Brooks, A. D., Fridman, A., Gutsol, A., Vasilets, V. N. & Friedman, G. (**2007**). Floating electrode dielectric barrier discharge plasma in air promoting apoptotic behavior in Melanoma skin cancer cell lines. *Plasma Chem. Plasma Process.* **27**, 163–76.

Fridman, G., Friedman, G., Gutsol, A., Shekhter, A. B., Vasilets, V. N. & Fridman, A. (**2008**). Applied plasma medicine. *Plasma Process. Polym.* **5**, 503–33.

Friedman, P. C., Miller, V., Fridman, G., Lin, A. G. & Fridman, A. (**2017**). Successful treatment of actinic keratoses using nonthermal atmospheric pressure plasma: A case series. *J. Am. Acad. Dermatol.* **76**, 349–50.

Friedmann, T. & Roblin, R. (**1972**). Gene therapy for human genetic disease? *Science (80-.).* **175**, 949—955.

Fyfe, A. J. & Mckay, P. (**2010**). Toxicity associated with bleomycin. *J R Coll Physicians Edinb* **40**, 213–8.

Gabriel, B. & Teissié, J. (**1997**). Direct observation in the millisecond time range of fluorescent molecule asymmetrical interaction with the electropermeabilized cell membrane. *Biophys. J.* **73**, 2630–7.

García-Sánchez, T., Mercadal, B., Polrot, M., Muscat, A., Sarnago, H., Lucia, O. & Mir, L. M. (**2020**). Successful tumor Electrochemotherapy using Sine Waves. *IEEE Trans. Biomed. Eng.* **67**, 1040–9.

Garcia, P. A., Kos, B., Rossmeisl, J. H., Pavliha, D., Miklavčič, D. & Davalos, R. V. (**2017**). Predictive therapeutic planning for irreversible electroporation treatment of spontaneous malignant glioma. *Med. Phys.* **44**, 4968–80.

Gaylor, D. C., Prakah-Asante, K. & Lee, R. C. (**1988**). Significance of cell size and tissue structure in electrical trauma. *J. Theor. Biol.* **133**, 223–37.

Gehl, J., Skovsgaard, T. & Mir, L. M. (**1998**). Enhancement of cytotoxicity by electropermeabilization: An improved method for screening drugs. *Anticancer. Drugs* **9**, 319–25.

Gehl, J., Sørensen, T. H., Nielsen, K., Raskmark, P., Nielsen, S. L., Skovsgaard, T. & Mir, L. M. (**1999**). In vivo electroporation of skeletal muscle: Threshold, efficacy and relation to

electric field distribution. *Biochim. Biophys. Acta - Gen. Subj.* **1428**, 233–40.

Gehl, J., Skovsgaard, T. & Mir, L. M. (**2002**). Vascular reactions to in vivo electroporation: Characterization and consequences for drug and gene delivery. *Biochim. Biophys. Acta - Gen. Subj.* **1569**, 51–58.

Gehl, J., Serša, G., Garbay, J. R., Soden, D. M., Rudolf, Z., Marty, M., O'Sullivan, Geertsen, P. F. & Mir, L. M. (**2006**). Results of the ESOPE (European Standard Operating Procedures on Electrochemotherapy) study: Efficient, highly tolerable and simple palliative treatment of cutaneous and subcutaneous metastases from cancers of any histology. *J. Clin. Oncol.* **24**, 8047.

Gehl, J. *et al.* (**2018**). Updated standard operating procedures for electrochemotherapy of cutaneous tumours and skin metastases. *Acta Oncol. (Madr).* **57**, 874–82.

Gerlini, G., Sestini, S., Di Gennaro, P., Urso, C., Pimpinelli, N. & Borgognoni, L. (**2013**). Dendritic cells recruitment in melanoma metastasis treated by electrochemotherapy. *Clin. Exp. Metastasis* **30**, 37–45.

Geukes Foppen, M. H., Donia, M., Svane, I. M. & Haanen, J. B. A. G. (**2015**). Tumor-infiltrating lymphocytes for the treatment of metastatic cancer. *Mol. Oncol.* **9**, 1918–35.

Gilbert, R. A., Jaroszeski, M. J. & Heller, R. (**1997**). Novel electrode designs for electrochemotherapy. *Biochim. Biophys. Acta - Gen. Subj.* **1334**, 9–14.

Gimsa, J. & Wachner, D. (**2001**). Analytical description of the transmembrane voltage induced on arbitrarily oriented ellipsoidal and cylindrical cells. *Biophys. J.* **81**, 1888–96.

Ginsberg, G. G., Barkun, A. N., Bosco, J. J., Burdick, J. S., Isenberg, G. A., Nakao, N. L., Petersen, B. T., Silverman, W. B., Slivka, A. & Kelsey, P. B. (**2002**). *The argon plasma coagulator: February 2002.* Gastrointest Endosc.

Girard, P.-M., Arbabian, A., Fleury, M., Bauville, G., Puech, V., Dutreix, M. & Sousa, J. S. (**2016**). Synergistic Effect of H2O2 and NO2 in Cell Death Induced by Cold Atmospheric He Plasma. *Sci. Rep.* **6**, 29098.

Glover, J. L., Bendick, P. J. & Link, W. J. (**1978**). The use of thermal knives in surgery: Electrosurgery, lasers, plasma scalpel. *Curr. Probl. Surg.* **15**, 1–78.

Glover, J. L., Bendick, P. J., Link, W. J. & Plunkett, R. J. (**1982**). The plasma scalpel: A new thermal knife. *Lasers Surg. Med.* **2**, 101–106.

Gómez, B., Munekata, P. E. S., Gavahian, M., Barba, F. J., Martí-Quijal, F. J., Bolumar, T., Campagnol, P. C. B., Tomasevic, I. & Lorenzo, J. M. (**2019**). Application of pulsed electric fields in meat and fish processing industries: An overview. *Food Res. Int.* **123**, 95–105.

Gothelf, A. & Gehl, J. (**2010**). Gene Electrotransfer to Skin; Review of Existing Literature and Clinical Perspectives. *Curr. Gene Ther.* **10**, 287–99.

Gothelf, A. & Gehl, J. (**2012**). What you always needed to know about electroporation based DNA vaccines. *Hum. Vaccines Immunother.* **8**, 1694–1702.

Gothelf, A., Mir, L. M. & Gehl, J. (**2003**). Electrochemotherapy: Results of cancer treatment using enhanced delivery of bleomycin by electroporation. *Cancer Treat. Rev.* **29**, 371–87.

Graves, D. B. (**2012a**). The emerging role of reactive oxygen and nitrogen species in redox biology and some implications for plasma applications to medicine and biology. *J. Phys.*

D. Appl. Phys. **45**, 263001.

Graves, D. B. (**2012b**). The emerging role of reactive oxygen and nitrogen species in redox biology and some implications for plasma applications to medicine and biology. *J. Phys. D. Appl. Phys.* **45**, 3001.

Graves, D. B. (**2014**). Reactive species from cold atmospheric plasma: Implications for cancer therapy. *Plasma Process. Polym.* **11**, 1120–7.

Graves, D. B. (**2017**). Mechanisms of Plasma Medicine: Coupling Plasma Physics, Biochemistry, and Biology. *IEEE Trans. Radiat. Plasma Med. Sci.* **1**, 281–92.

Greaney, S. K. *et al.* (**2020**). Intratumoral Plasmid IL12 Electroporation Therapy in Patients with Advanced Melanoma Induces Systemic and Intratumoral T-cell Responses A C. *Cancer Immunol. Res.* **8**, 246–54.

Gresser, I. & Bourali, C. (**1970**). Antitumor effects of interferon preparations in mice. *J Natl Cancer Inst.* **45**, 365–76.

Griseti, E., Kolosnjaj-Tabi, J., Gibot, L., Fourquaux, I., Rols, M.-P., Yousfi, M., Merbahi, N. & Golzio, M. (**2019**). Pulsed Electric Field Treatment Enhances the Cytotoxicity of Plasma-Activated Liquids in a Three-Dimensional Human Colorectal Cancer Cell Model. *Sci. Rep.* **9**, 7583.

Griseti, E., Merbahi, N. & Golzio, M. (**2020**). Anti-Cancer Potential of Two Plasma-Activated Liquids: Implication of Long-Lived Reactive Oxygen and Nitrogen Species. *Cancers (Basel).* **12**, 721.

Groselj, A., Kranjc, S., Bosnjak, M., Krzan, M., Kosjek, T., Prevc, A., Čemažar, M. & Serša, G. (**2018**). Vascularization of the tumours affects the pharmacokinetics of bleomycin and the effectiveness of electrochemotherapy. *Basic Clin. Pharmacol. Toxicol.* **123**, 247–56.

Grund, K. E., Storek, D. & Farin, G. (**1994**). Endoscopic argon plasma coagulation (APC) first clinical experiences in flexible endoscopy. *Endosc. Surg. Allied Technol.* **2**, 42–46.

Grupp, S. A. *et al.* (**2013**). Chimeric Antigen Receptor-Modified T Cells for Acute Lymphoid Leukemia. *N Engl J Med* **368**, 1509–1527.

Guo, L., Xu, R., Zhao, Y., Liu, D., Liu, Z., Wang, X., Chen, H. & Kong, M. G. (**2018a**). Gas Plasma Pre-treatment Increases Antibiotic Sensitivity and Persister Eradication in Methicillin-Resistant Staphylococcus aureus. *Front. Microbiol.* **9**, 537.

Guo, L., Xu, R., Gou, L., Liu, Z., Zhao, Y., Liu, D., Zhang, L., Chen, H. & Kong, M. G. (**2018b**). Mechanism of virus inactivation by cold atmospheric-pressure plasma and plasma-activated water. *Appl. Environ. Microbiol.* **84**, e00726-18.

Gupta, G. P. & Massagué, J. (**2006**). Cancer Metastasis: Building a Framework. *Cell* **127**, 679–95.

Hachey, S. J. & Boiko, A. D. (**2016**). Therapeutic implications of melanoma heterogeneity. *Exp. Dermatol.* **25**, 497–500.

Haertel, B., von Woedtke, T., Weltmann, K.-D. & Lindequist, U. (**2014**). Non-thermal atmospheric-pressure plasma possible application in wound healing. *Biomol. Ther.* **22**, 477–90.

Halsted, W. S. (**1894**). The Results of Operations for the Cure of Cancer of the Breast Performed

at the Johns Hopkins Hospital from June, 1889, to January, 1894. *Ann Surg* **20**, 497–555.

Hamilton, W. A. & Sale, A. J. H. (**1967**). Effects of high electric fields on microorganisms. II. Mechanism of action of the lethal effect. *BBA - Gen. Subj.* **148**, 789–800.

Hamilton, J. G. & Soley, M. H. (**1939**). STUDIES IN IODINE METABOLISM BY THE USE OF A NEW RADIOACTIVE ISOTOPE OF IODINE. *Am. J. Physiol.* **127**, 557–72.

Hanahan, D. & Weinberg, R. A. (**2011**). Hallmarks of cancer: The next generation. *Cell* **144**, 646–74.

Hanahan, D. & Weinberg, R. A. (**2017**). Biological Hallmarks of Cancer. In *Holland-Frei Cancer Medicine* (ed. Robert C. Bast Jr., Carlo M. Croce, William N. Hait, Waun Ki Hong, Donald W. Kufe, Martine Piccart-Gebhart, Raphael E. Pollock, Ralph R. Weichselbaum, Hongyang Wang, and J. F. H.), pp. 1–10. American Cancer Society.

Hara, H., Taniguchi, M., Kobayashi, M., Kamiya, T. & Adachi, T. (**2015**). Plasma-activated medium-induced intracellular zinc liberation causes death of SH-SY5Y cells. *Arch. Biochem. Biophys.* **584**, 51–60.

Hara, H., Sueyoshi, S., Taniguchi, M., Kamiya, T. & Adachi, T. (**2017**). Differences in intracellular mobile zinc levels affect susceptibility to plasma-activated medium-induced cytotoxicity. *Free Radic. Res.* **51**, 306–15.

Harvey, W. (**1628**). *An Anatomical Disquisition on the Motion of the Heart and Blood in Animals*. London.

Hattori, N. *et al.* (**2015**). Effectiveness of plasma treatment on pancreatic cancer cells. *Int. J. Oncol.* **47**, 1655–62.

Heat and Control (**2019**). HOW ELECTROPORATION CAN REDUCE ACRYLAMIDE, LOWER OIL CONTENT AND IMPROVE YIELD IN POTATO PRODUCTION CAN WE HAVE OUR CHIP AND EAT IT TOO? *https//www.heatandcontrol.com/sites/default/files/content/resource/pdf/2019-05/Electroporation to Reduce Acrylamide%2C Low. Oil Content %26 Improv. Yield.pdf*.

Heinlin, J., Morfill, G. E., Landthaler, M., Stolz, W., Isbary, G., Zimmermann, J. L., Shimizu, T. & Karrer, S. (**2010**). Plasma medicine: possible applications in dermatology. *JDDG - J. Ger. Soc. Dermatology* **8**, 968–77.

Heller, R. (**1995**). Treatment of cutaneous nodules using electrochemotherapy. *J. Fla. Med. Assoc.* **82**, 147–50.

Heller, R. & Heller, L. C. (**2015**). Gene Electrotransfer Clinical Trials. In *Advances in Genetics*, pp. 235–62. Elsevier Ltd.

Heller, R., Cruz, Y., Heller, L. C., Gilbert, R. A. & Jaroszeski, M. J. (**2010**). Electrically mediated delivery of plasmid DNA to the skin, using a multielectrode array. *Hum. Gene Ther.* **21**, 357–62.

Hockenbery, D., Nuñez, G., Milliman, C., Schreiber, R. D. & Korsmeyer, S. J. (**1990**). Bcl-2 is an inner mitochondrial membrane protein that blocks programmed cell death. *Nature* **348**, 334–6.

Hoffmann, C., Berganza, C. & Zhang, J. (**2013**). Cold Atmospheric Plasma: Methods of production and application in dentistry and oncology. *Med. Gas Res.* **3**, 21.

Hong, K. & Georgiades, C. (**2010**). Radiofrequency ablation: Mechanism of action and devices. *J. Vasc. Interv. Radiol.* **21**, S179.

Huggins, C. & Hodges, C. V. (**1941**). Studies on Prostatic Cancer. I. The Effect of Castration, of Estrogen and of Androgen Injection on Serum Phosphatases in Metastatic Carcinoma of the Prostate. *Cancer Res.* **1**, 293–7.

Ikeda, J., Tanaka, H., Ishikawa, K., Sakakita, H., Ikehara, Y. & Hori, M. (**2018**). Plasma-activated medium (PAM) kills human cancer-initiating cells. *Pathol. Int.* **68**, 23–30.

Ingólfsson, H. I., Melo, M. N., Van Eerden, F. J., Arnarez, C., Lopez, C. A., Wassenaar, T. A., Periole, X., De Vries, A. H., Peter Tieleman, D. & Marrink, S. J. (**2014**). Lipid Organization of the Plasma Membrane. *J. Am. Chem. Soc.* **136**, 14554–9.

Isbary, G. *et al.* (**2010**). A first prospective randomized controlled trial to decrease bacterial load using cold atmospheric argon plasma on chronic wounds in patients. *Br. J. Dermatol.* **163**, 78–82.

Isbary, G., Zimmermann, J. L., Shimizu, T., Li, Y. F., Morfill, G. E., Thomas, H. M., Steffes, B., Heinlin, J., Karrer, S. & Stolz, W. (**2013a**). Non-thermal plasma-More than five years of clinical experience. *Clin. Plasma Med.* **1**, 19–23.

Isbary, G., Shimizu, T., Li, Y. F., Stolz, W., Thomas, H. M., Morfill, G. E. & Zimmermann, J. L. (**2013b**). Cold atmospheric plasma devices for medical issues. *Expert Rev. Med. Devices* **10**, 367–77.

Ivorra, A., Al-Sakere, B., Rubinsky, B. & Mir, L. M. (**2008**). Use of conductive gels for electric field homogenization increases the antitumor efficacy of electroporation therapies. *Phys. Med. Biol.* **53**, 6605–18.

IXL Netherlands B.V. and IXL e-Cooker B.V. THE SPECIAL AND UNIQUE NUTRI-PULSE® E-COOKER® FOR PULSED ELECTRIC FIELDS FOOD RESEARCH. *https://www.sevvy.nl/index.html*.

Jablonowski, H. & von Woedtke, T. (**2015**). Research on plasma medicine-relevant plasma-liquid interaction: What happened in the past five years? *Clin. Plasma Med.* **3**, 42–52.

Jagtap, J. C., Chandele, A., Chopde, B. A. & Shastry, P. (**2003**). Sodium pyruvate protects against H2O2 mediated apoptosis in human neuroblastoma cell line-SK-N-MC. *J. Chem. Neuroanat.* **26**, 109–118.

Jallabert, J. (**1749**). *Experiences sur l'électricité, avec quelques conjectures sur la cause de ses effets*. Geneva.

Jarm, T., Čemažar, M., Miklavčič, D. & Serša, G. (**2010**). Antivascular effects of electrochemotherapy: Implications in treatment of bleeding metastases. *Expert Rev. Anticancer Ther.* **10**, 729–46.

Jaroszeski, M. J., Gilbert, R. A. & Heller, R. (**1997**). Electrochemotherapy: An emerging drug delivery method for the treatment of cancer. *Adv. Drug Deliv. Rev.* **26**, 185–97.

Jaroszeski, M. J., Dang, V., Pottinger, C., Hickey, J., Gilbert, R. & Heller, R. (**2000**). Toxicity of anticancer agents mediated by electroporation in vitro. *Anticancer. Drugs* **11**, 201–8.

Jinno, M., Ikeda, Y., Motomura, H., Kido, Y. & Satoh, S. (**2016**). Investigation of plasma induced electrical and chemical factors and their contribution processes to plasma gene

transfection. *Arch. Biochem. Biophys.* **605**, 59–66.

Judée, F. & Dufour, T. (**2019**). Plasma gun for medical applications: Engineering an equivalent electrical target of the human body and deciphering relevant electrical parameters. *J. Phys. D. Appl. Phys.* **52**, 16LT02.

Judée, F., Fongia, C., Ducommun, B., Yousfi, M., Lobjois, V. & Merbahi, N. (**2016**). Short and long time effects of low temperature Plasma Activated Media on 3D multicellular tumor spheroids. *Sci. Rep.* **6**, 21421.

Judée, F., Simon, S., Bailly, C. & Dufour, T. (**2018**). Plasma-activation of tap water using DBD for agronomy applications: Identification and quantification of long lifetime chemical species and production/consumption mechanisms. *Water Res.* **133**, 47–59.

Kalghatgi, S. U., Fridman, G., Cooper, M., Nagaraj, G., Peddinghaus, M., Balasubramanian, M., Vasilets, V. N., Gutsol, A. F., Fridman, A. & Friedman, G. (**2007**). Mechanism of blood coagulation by nonthermal atmospheric pressure dielectric barrier discharge plasma. *IEEE Trans. Plasma Sci.* **35**, 1559–66.

Kaushik, N., Uddin, N., Sim, G. B., Hong, Y. J., Baik, K. Y., Kim, C. H., Lee, S. J., Kaushik, N. K. & Choi, E. H. (**2015**). Responses of solid tumor cells in DMEM to reactive oxygen species generated by non-thermal plasma and chemically induced ROS systems. *Sci. Rep.* **5**, 8587.

Ke, Z. & Huang, Q. (**2016**). Haem-assisted dityrosine-cross-linking of fibrinogen under non-thermal plasma exposure: one important mechanism of facilitated blood coagulation. *Sci. Rep.* **6**, 26982.

Keevil, S. F. (**2012**). Physics and medicine: A historical perspective. *Lancet* **379**, 1517–24.

Keidar, M., Walk, R. M., Shashurin, A., Srinivasan, P., Sandler, A. D., Dasgupta, S., Ravi, R., Guerrero-Preston, R. & Trink, B. (**2011**). Cold plasma selectivity and the possibility of a paradigm shift in cancer therapy. *Br. J. Cancer* **105**, 1295–1301.

Kim, S. J. & Chung, T. H. (**2016**). Cold atmospheric plasma jet-generated RONS and their selective effects on normal and carcinoma cells. *Sci. Rep.* **6**, 20332.

Kinosita, K. & Tsong, T. Y. (**1977a**). Formation and resealing of pores of controlled sizes in human erythrocyte membrane. *Nature* **268**, 438–41.

Kinosita, K. & Tsong, T. Y. (**1977b**). Hemolysis of human erythrocytes by a transient electric field. *Proc. Natl. Acad. Sci. U. S. A.* **74**, 1923–7.

Kinosita, K. & Tsong, T. Y. (**1977c**). Voltage-induced pore formation and hemolysis of human erythrocytes. *BBA - Biomembr.* **471**, 227–42.

Kinosita, K. & Tsong, T. Y. (**1978**). Survival of sucrose-loaded erythrocytes in the circulation. *Nature* **272**, 258–60.

Klebes, M. *et al.* (**2014**). Effects of tissue-tolerable plasma on psoriasis vulgaris treatment compared to conventional local treatment: A pilot study. *Clin. Plasma Med.* **2**, 22–27.

Kochenderfer, J. N. & Rosenberg, S. A. (**2013**). Treating B-cell cancer with T cells expressing anti-CD19 chimeric antigen receptors. *Nat. Rev. Clin. Oncol.* **10**, 267–76.

Kogelschatz, U. (**2003**). Dielectric-barrier Discharges: Their History, Discharge Physics, and Industrial Applications. *Plasma Chem. Plasma Process.* **23**, 46 pages.

Kondeti, V. S. S. K., Phan, C. Q., Wende, K., Jablonowski, H., Gangal, U., Granick, J. L., Hunter, R. C. & Bruggeman, P. J. (**2018**). Long-lived and short-lived reactive species produced by a cold atmospheric pressure plasma jet for the inactivation of Pseudomonas aeruginosa and Staphylococcus aureus. *Free Radic. Biol. Med.* **124**, 275–87.

Kotnik, T. & Miklavčič, D. (**2000**). Analytical description of transmembrane voltage induced by electric fields on spheroidal cells. *Biophys. J.* **79**, 670–9.

Kotnik, T., Rems, L., Tarek, M. & Miklavčič, D. (**2019**). Membrane Electroporation and Electropermeabilization: Mechanisms and Models. *Annu. Rev. Biophys.* **48**, 63–91.

Kruse, E., Uehlein, N. & Kaldenhoff, R. (**2006**). The aquaporins. *Genome Biol.* **7**, 206.

Kubinova, S., Zaviskova, K., Uherkova, L., Zablotskii, V., Churpitaa, O. & Lunov, O. (**2017**). Non-thermal air plasma promotes the healing of acute skin wounds in rats. *Sci. Rep.* **7**, 54183.

Kurake, N., Tanaka, H., Ishikawa, K., Kondo, T., Sekine, M., Nakamura, K., Kajiyama, H., Kikkawa, F., Mizuno, M. & Hori, M. (**2016**). Cell survival of glioblastoma grown in medium containing hydrogen peroxide and/or nitrite, or in plasma-activated medium. *Arch. Biochem. Biophys.* **605**, 102–08.

Kurake, N., Ishikawa, K., Tanaka, H., Hashizume, H., Nakamura, K., Kajiyama, H., Toyokuni, S., Kikkawa, F., Mizuno, M. & Hori, M. (**2019**). Non-thermal plasma-activated medium modified metabolomic profiles in the glycolysis of U251SP glioblastoma. *Arch. Biochem. Biophys.* **662**, 83–92.

Langmuir, I. (**1928**). Oscillations in Ionized Gases. *Proc. Natl. Acad. Sci.* **14**, 627–637.

Larkin, J. O., Collins, C. G., Aarons, S., Tangney, M., Whelan, M., O'Reily, S., Breathnach, O., Soden, D. M. & O'Sullivan, G. C. (**2007**). Electrochemotherapy: Aspects of preclinical development and early clinical experience. *Ann. Surg.* **245**, 469–79.

Laroussi, M. (**1996**). Sterilization of contaminated matter with an atmospheric pressure plasma. *IEEE Trans. Plasma Sci.* **24**, 1188–91.

Lauterbur, P. C. (**1973**). Image formation by induced local interactions: Examples employing nuclear magnetic resonance. *Nature* **242**, 190–1.

Lechardeur, D. & Lukacs, G. L. (**2006**). Nucleocytoplasmic transport of plasmid DNA: A perilous journey from the cytoplasm to the nucleus. *Hum. Gene Ther.* **17**, 882–9.

Leduc, M., Guay, D., Leask, R. L. & Coulombe, S. (**2009**). Cell permeabilization using a non-thermal plasma. *New J. Phys.* **11**, 115021.

Lee, R. C. & Kolodney, M. S. (**1987**). Electrical injury mechanisms: Electrical breakdown of cell membranes. *Plast. Reconstr. Surg.* **80**, 672–9.

Lee, R. C., Gaylor, D. C., Bhatt, D. & Israel, D. A. (**1988**). Role of cell membrane rupture in the pathogenesis of electrical trauma. *J. Surg. Res.* **44**, 709–19.

Leonard, J. P., Sherman, M. L., Fisher, G. L., Buchanan, L. J., Larsen, G., Atkins, M. B., Sosman, J. A., Dutcher, J. P., Vogelzang, N. J. & Ryan, J. L. (**1997**). Effects of single-dose interleukin-12 exposure on interleukin-12-associated toxicity and interferon-gamma production. *Blood* **90**, 2541–8.

Levine, Z. A. & Vernier, P. T. (**2010**). Life cycle of an electropore: Field-dependent and field-independent steps in pore creation and annihilation. *J. Membr. Biol.* **236**, 27–36.

Liao, X., Liu, D., Xiang, Q., Ahn, J., Chen, S., Ye, X. & Ding, T. (**2017**). Inactivation mechanisms of non-thermal plasma on microbes: A review. *Food Control* **75**,.

Lin, A. G., Truong, B., Patel, S., Kaushik, N. K., Choi, E. H., Fridman, G., Fridman, A. & Miller, V. (**2017**). Nanosecond-pulsed dbd plasma-generated reactive oxygen species trigger immunogenic cell death in a549 lung carcinoma cells through intracellular oxidative stress. *Int. J. Mol. Sci.* **18**, 966.

Lin, A. G., Xiang, B., Merlino, D. J., Baybutt, T. R., Sahu, J., Fridman, A., Snook, A. E. & Miller, V. (**2018**). Non-thermal plasma induces immunogenic cell death in vivo in murine CT26 colorectal tumors. *Oncoimmunology* **7**,.

Link, W. J., Glover, J. L., Edwards, J. L., Henderson, M. R., Yaw, P. B. & Incropera, F. P. (**1973**). Wound healing of mouse skin incised with a plasma scalpel. *J. Surg. Res.* **14**, 505–11.

Linnert, M., Iversen, H. K. & Gehl, J. (**2012**). Multiple brain metastases - Current management and perspectives for treatment with electrochemotherapy. *Radiol. Oncol.* **46**, 271–8.

Litster, J. D. (**1975**). Stability of lipid bilayers and red blood cell membranes. *Phys. Lett. A* **53**, 193–4.

Lobo, R. A. (**2017**). Hormone-replacement therapy: Current thinking. *Nat. Rev. Endocrinol.* **13**, 220–31.

Longo, F. *et al.* (**2019**). Electrochemotherapy as palliative treatment in patients with advanced head and neck tumours: Outcome analysis in 93 patients treated in a single institution. *Oral Oncol.* **92**, 77–84.

López, M., Calvo, T., Prieto, M., Múgica-Vidal, R., Muro-Fraguas, I., Alba-Elías, F. & Alvarez-Ordóñez, A. (**2019**). A review on non-thermal atmospheric plasma for food preservation: Mode of action, determinants of effectiveness, and applications. *Front. Microbiol.* **10**, 622.

Lu, X., Naidis, G. V., Laroussi, M., Reuter, S., Graves, D. B. & Ostrikov, K. (**2016**). Reactive species in non-equilibrium atmospheric-pressure plasmas: Generation, transport, and biological effects. *Phys. Rep.* **630**, 1–84.

Lubner, M. G., Brace, C. L., Hinshaw, J. L. & Lee, F. T. (**2010**). Microwave tumor ablation: Mechanism of action, clinical results, and devices. *J. Vasc. Interv. Radiol.* **21**, S192.

Lunov, O., Zablotskii, V., Churpita, O., Jäger, A., Polívka, L., Syková, E., Dejneka, A. & Kubinová, Š. (**2016**). The interplay between biological and physical scenarios of bacterial death induced by non-thermal plasma. *Biomaterials* **82**, 71–83.

Mahmood, F. & Gehl, J. (**2011**). Optimizing clinical performance and geometrical robustness of a new electrode device for intracranial tumor electroporation. *Bioelectrochemistry* **81**, 10–16.

Mahnič-Kalamiza, S., Vorobiev, E. & Miklavčič, D. (**2014**). Electroporation in Food Processing and Biorefinery. *J. Membr. Biol.* **247**, 1279–1304.

Maho, T., Damany, X., Dozias, S., Pouvesle, J.-M. & Robert, É. (**2018**). Atmospheric Pressure Multijet Plasma Sources For Cancer Treatments. *Clin. Plasma Med.* **9**, 3–4.

Maisch, T., Shimizu, T., Isbary, G., Heinlin, J., Karrer, S., Klämpfl, T. G., Li, Y. F., Morfill, G. E. & Zimmermann, J. L. (**2012**). Contact-free inactivation of Candida albicans biofilms by cold

atmospheric air plasma. *Appl. Environ. Microbiol.* **78**, 4242–7.

Mansfield, P. & Grannell, P. K. (**1973**). NMR 'diffraction' in solids? *J. Phys. C Solid State Phys.* **6**, L422–L426.

Markelc, B., Serša, G. & Čemažar, M. (**2013**). Differential Mechanisms Associated with Vascular Disrupting Action of Electrochemotherapy: Intravital Microscopy on the Level of Single Normal and Tumor Blood Vessels. *PLoS One* **8**, e59557.

Marquet, P. (**1992**). Iatrophysics to biomechanics. From Borelli (1608-1679) to Pauwels (1885-1980). *J. Bone Jt. Surg.* **74**-**B**, 335–9.

Marsden, P. K., Strul, D., Keevil, S. F., Williams, S. C. R. & Cash, D. (**2002**). Simultaneous PET and NMR. *Br. J. Radiol.* **75**, S53–S59.

Marty, M. *et al.* (**2006**). Electrochemotherapy - An easy, highly effective and safe treatment of cutaneous and subcutaneous metastases: Results of ESOPE (European Standard Operating Procedures of Electrochemotherapy) study. *Eur. J. Cancer, Suppl.* **4**, 3–13.

Matthiessen, L. W., Johannesen, H. H., Hendel, H. W., Moss, T., Kamby, C. & Gehl, J. (**2012**). Electrochemotherapy for large cutaneous recurrence of breast cancer: A phase II clinical trial. *Acta Oncol. (Madr).* **51**, 713–21.

Mauduyt (**1784**). *Mémoire sur les différentes manières d'administrer l'électricité, et observations sur les effets qu'elles ont produits*. (ed. Royale, L.) Paris: Extrait des Mémoires de la société royale de médecine.

McCrudden, C. M. & McCarthy, H. O. (**2013**). Cancer Gene Therapy – Key Biological Concepts in the Design of Multifunctional Non-Viral Delivery Systems. In *Gene Therapy - Tools and Potential Applications*, p. 36pp. InTech.

Mekid, H., Tounekti, O., Spatz, A., Čemažar, M., Kebir, E. & Mir, L. M. (**2003**). In vivo evolution of tumour cells after the generation of double-strand DNA breaks. *Br. J. Cancer* **88**, 1763–71.

Melchior, F. & Gerace, L. (**1995**). Mechanisms of nuclear protein import. *Curr. Opin. Cell Biol.* **7**, 310–8.

Metelmann, H.-R. *et al.* (**2015**). Head and neck cancer treatment and physical plasma. *Clin. Plasma Med.* **3**, 17–23.

Metelmann, H.-R. *et al.* (**2018a**). Clinical experience with cold plasma in the treatment of locally advanced head and neck cancer. *Clin. Plasma Med.* **9**, 6–13.

Metelmann, H.-R., von Woedtke, T. & Weltmann, K.-D. (**2018b**). *Comprehensive clinical plasma medicine: Cold physical plasma for medical application*. Springer International Publishing.

Meyer, F. De & Smit, B. (**2009**). Effect of cholesterol on the structure of a phospholipid bilayer. *PNAS* **10**, 3654–8.

Miklavčič, D., Beravs, K., Šemrov, D., Čemažar, M., Demšar, F. & Serša, G. (**1998**). The importance of electric field distribution for effective in vivo electroporation of tissues. *Biophys. J.* **74**, 2152–8.

Miklavčič, D., Snoj, M., Zupanic, A., Kos, B., Čemažar, M., Kropivnik, M., Bracko, M., Pecnik, T., Gadzijev, E. & Serša, G. (**2010**). Towards treatment planning and treatment of deep-

seated solid tumors by electrochemotherapy. *Biomed. Eng. Online* **9**, 10.

Miklavčič, D., Serša, G., Brecelj, E., Gehl, J., Soden, D. M., Bianchi, G., Ruggieri, P., Rossi, C. R., Campana, L. G. & Jarm, T. (**2012**). Electrochemotherapy: Technological advancements for efficient electroporation-based treatment of internal tumors. *Med. Biol. Eng. Comput.* **50**, 1213–25.

Miklavčič, D., Kos, B., Heller, R. & Serša, G. (**2014**). Electrochemotherapy : from the drawing board into medical practice. *Biomed. Eng. Online* **13**, 29.

Milevoj, N., Tozon, N., Licen, S., Lampreht Tratar, U., Serša, G. & Čemažar, M. (**2020**). Health-related quality of life in dogs treated with electrochemotherapy and/or interleukin-12 gene electrotransfer. *Vet MEd Sci.* **6**, 290–8.

Miller, J. M., Palanker, D. V, Vankov, A., Marmor, M. F. & Blumenkranz, M. S. (**2003**). Precision and Safety of the Pulsed Electron Avalanche Knife in Vitreoretinal Surgery. *Arch Ophthalmol.* **121**, 871–7.

Miller, V., Lin, A. G. & Fridman, A. (**2016**). Why Target Immune Cells for Plasma Treatment of Cancer. *Plasma Chem. Plasma Process.* **36**, 259–68.

Minchinton, A. I. & Tannock, I. F. (**2006**). Drug penetration in solid tumours. *Nat. Rev. Cancer* **6**, 583–92.

Mir, L. M. (**2006**). Bases and rationale of the electrochemotherapy. *Eur. J. Cancer, Suppl.* **4**, 38–44.

Mir, L. M. (**2009**). Nucleic acids electrotransfer-based gene therapy (electrogenetherapy): past, current, and future. *Mol. Biotechnol.* **43**, 167–76.

Mir, L. M. (**2014**). Electroporation-based gene therapy: Recent evolution in the mechanism description and technology developments. *Methods Mol. Biol.* **1121**, 3–23.

Mir, L. M., Banoun, H. & Paoletti, C. (**1988**). Introduction of definite amounts of nonpermeant molecules into living cells after electropermeabilization: Direct access to the cytosol. *Exp. Cell Res.* **175**, 15–25.

Mir, L. M., Orlowski, S., Belehradek, J. & Paoletti, C. (**1991a**). Electrochemotherapy potentiation of antitumour effect of bleomycin by local electric pulses. *Eur. J. Cancer Clin. Oncol.* **27**, 68–72.

Mir, L. M., Belehradek, M., Domenge, C., Orlowski, S., Poddevin, B., Belehradek, J., Schwaab, G., Luboinski, B. & Paoletti, C. (**1991b**). Electrochemotherapy, a new antitumor treatment: first clinical trial. *C. R. Acad. Sci. III.* **313**, 613–8.

Mir, L. M., Orlowski, S., Poddevin, B. & Belehradek, J. (**1992**). Electrochemotherapy tumor treatment is improved by interleukin-2 stimulation of the host's defenses. *Eur. Cytokine Netw.* **3**, 331–4.

Mir, L. M., Roth, C., Stéphane, O., Françoise, Q. C., Fradelizi, D., Belehradek, J. & Kourilsky, P. (**1995**). Systemic Antitumor Effects of Electrochemotherapy Combined with Histoincompatible Cells Secreting Interleukin-2. *J. Immunother.* **17**, 30–38.

Mir, L. M., Tounekti, O. & Orlowski, S. (**1996**). Bleomycin: Revival of an old drug. *Gen. Pharmacol.* **27**, 745–8.

Mir, L. M., Devauchelle, P., Quintin-Colonna, F., Delisle, F., Doliger, S., Fradelizi, D., Belehradek,

J. & Orlowski, S. (**1997**). First clinical trial of cat soft tissue sarcomas treatment by electrochemotherapy. *Br. J. Cancer* **76**, 1617–22.

Mir, L. M. *et al.* (**1998**). Effective treatment of cutaneous and subcutaneous malignant tumours by electrochemotherapy. *Br. Joumal Cancer* **77**, 2336–42.

Mir, L. M., Bureau, M. F., Gehl, J., Rangara, R., Rouy, D., Caillaud, J. M., Delaere, P., Branellec, D., Schwartz, B. & Scherman, D. (**1999**). High-efficiency gene transfer into skeletal muscle mediated by electric pulses. *Proc. Natl. Acad. Sci. U. S. A.* **96**, 4262–7.

Mir, L. M., Moller, P. H., André, F. & Gehl, J. (**2005**). Electric Pulse-Mediated Gene Delivery to Various Animal Tissues. *Adv. Genet.* **54**, 83–114.

Mir, L. M., Gehl, J., Serša, G., Collins, C. G., Garbay, J. R., Billard, V., Geertsen, P. F., Rudolf, Z., O'Sullivan, G. C. & Marty, M. (**2006**). Standard operating procedures of the electrochemotherapy: Instructions for the use of bleomycin or cisplatin administered either systemically or locally and electric pulses delivered by the CliniporatorTM by means of invasive or non-invasive electrodes. *Eur. J. Cancer, Suppl.* **4**, 14–25.

Mogul, R., Bol'shakov, A. A., Chan, S. L., Stevens, R. M., Khare, B. N., Meyyappan, M. & Trent, J. D. (**2003**). Impact of low-temperature plasmas on Deinococcus radiodurans and biomolecules. *Biotechnol. Prog.* **19**, 776–83.

Morley, J., Grocott, P., Purssell, E. & Murrells, T. (**2019**). Electrochemotherapy for the palliative management of cutaneous metastases: A systematic review and meta-analysis. *Eur. J. Surg. Oncol.* **45**, 2257–67.

Mousa, S. A. & Davis, P. J. (**2017**). Angiogenesis and Anti-Angiogenesis Strategies in Cancer. In *Anti-Angiogenesis Strategies in Cancer Therapeutics*, pp. 1–19. Elsevier.

Müller, G. J., Berlien, P. & Scholz, C. (**2006**). The medical laser. *Med. Laser Appl.* **21**, 99–108.

Nakamura, K., Peng, Y., Utsumi, F., Tanaka, H., Mizuno, M., Toyokuni, S., Hori, M., Kikkawa, F. & Kajiyama, H. (**2017**). Novel Intraperitoneal Treatment With Non-Thermal Plasma-Activated Medium Inhibits Metastatic Potential of Ovarian Cancer Cells. *Sci. Rep.* **7**, 6085.

Nakayama, Y., Aruga, A. & Harper, D. M. (**2015**). Comparison of Current Regulatory Status for Gene-Based Vaccines in the U.S., Europe and Japan. *Vaccines* **3**, 186–202.

Napotnik, T. B. & Miklavčič, D. (**2017**). In vitro electroporation detection methods - An overview. *Bioelectrochemistry* **120**, 166–82.

Neumann, E., Schaefer-Ridder, M., Wang, Y. & Hofschneider, P. H. (**1982**). Gene transfer into mouse lyoma cells by electroporation in high electric fields. *EMBO J.* **1**, 841–5.

Noah, H. M. (**1849**). *Lectures on Electricity: Comprising Glavanism, Magnetism, Electro-Magnetism, Magneto- and Thermo- Electricity, and Electro-Physiology*. 3rd ed. London: Knight.

Nollet, J.-A. (**1749**). *Recherches sur les causes particulieres des phénoménes électriques et sur les effets nuibles ou avantageux qu'on peut en attendre*. Paris.

Nysten, P.-H. (**1814**). *Dictionnaire de médecine et des sciences accessoires à la médecine: avec l'étymologie de chaque terme*. Brossan. Paris.

Orlowski, S., Belehradek, J., Paoletti, C. & Mir, L. M. (**1988**). Transient electropermeabilization of cells in culture. Increase of the cytotoxicity of anticancer drugs. *Biochem. Pharmacol.*

37, 4727–33.

Ozturk, B. & Anli, E. (**2017**). Pulsed electric fields (PEF) applications on wine production: A review. In *BIO Web of Conferences*, p. 02008. EDP Sciences.

Palucka, A. K. & Coussens, L. M. (**2016**). The Basis of Oncoimmunology. *Cell* **164**, 1233–47.

Parent, A. (**2007**). Félix Vicq d'Azyr: Anatomy, medicine and revolution. *Can. J. Neurol. Sci.* **34**, 30–37.

Pavlin, D., Cemazar, M., Sersa, G. & Tozon, N. (**2012**). *IL-12 based gene therapy in veterinary medicine*.

Peinado, H. *et al.* (**2017**). Pre-metastatic niches: Organ-specific homes for metastases. *Nat. Rev. Cancer* **17**, 302–17.

Peng, Y., Wang, H., Feng, J., Fang, S., Zhang, M., Wang, F., Chang, Y., Shi, X., Zhao, Q. & Liu, J. (**2018**). Efficacy and Safety of Argon Plasma Coagulation for Hemorrhagic Chronic Radiation Proctopathy: A Systematic Review. *Gastroenterol. Res. Pract.* **2018**, 3087603.

Pepple, P. T. & Gerber, D. A. (**2014**). Laparoscopic-Assisted Ablation of Hepatic Tumors: A Review. *Semin Interv. Radiol* **31**, 125–8.

Pichi, B., Pellini, R., de Virgilio, A. & Spriano, G. (**2018**). Electrochemotherapy: A well-accepted palliative treatment by patients with head and neck tumours. *Acta Otorhinolaryngol. Ital.* **38**, 181–7.

Poddevin, B., Orlowski, S., Belehradek Jr., J. & Mir, L. M. (**1991**). Very high cytotoxicity of bleomycin introduced into the cytosol of cells in culture. *Biochem. Pharmacol.* **42**, S67–S75.

Porter, R. (**1997**). *The Greatest Benefit to Mankind: A Medical History of Humanity*. HarperColl. London.

Postow, M. A. *et al.* (**2012**). Immunologic Correlates of the Abscopal Effect in a Patient with Melanoma. *N. Engl. J. Med.* **366**, 925–31.

Potter, H., Weir, L. & Leder, P. (**1984**). *Enhancer-dependent expression of human Kc immunoglobulin genes introduced into mouse pre-B lymphocytes by electroporation (DNA-mediated transfection/tissue-specific gene expression/B-lymphocyte development/gpt selection)*.

Pouvesle, J. & Robert, É. (**2013**). Applications thérapeutiques des plasmas froids atmosphériques. *Reflets la Phys.* 17–22.

Prausnitz, M. R., Bose, V. G., Langer, R. & Weaver, J. C. (**1993**). Electroporation of mammalian skin: A mechanism to enhance transdermal drug delivery. *Proc. Natl. Acad. Sci. U. S. A.* **90**, 10504–8.

Privat-Maldonado, A., Schmidt, A., Lin, A. G., Weltmann, K.-D., Wende, K., Bogaerts, A. & Bekeschus, S. (**2019**). ROS from Physical Plasmas: Redox Chemistry for Biomedical Therapy. *Oxid. Med. Cell. Longev.* **2019**, 29 pages.

Probst, U., Fuhrmann, I., Beyer, L. & Wiggermann, P. (**2018**). Electrochemotherapy as a new modality in interventional oncology: A review. *Technol. Cancer Res. Treat.* **17**, 1–12.

Pron, G., Mahrour, N., Orlowski, S., Tounekti, O., Poddevin, B., Belehradek, J. & Mir, L. M.

(**1999**). Internalisation of the bleomycin molecules responsible for bleomycin toxicity: A receptor-mediated endocytosis mechanism. *Biochem. Pharmacol.* **57**, 45–56.

Raffy, S. & Teissié, J. (**1999**). Control of Lipid Membrane Stability by Cholesterol Content. *Biophys. J.* **76**, 2072–80.

Rajabi, M. & Mousa, S. A. (**2017**). The role of angiogenesis in cancer treatment. *Biomedicines* **5**, 12 pages.

Ramirez', L. H., Orlowski2, S., An'*, D., Bindoula3, G., Dzodic3t, R., Ardouin4, P., Bognel5, C., Belehradek, J., Munck3, J.-N. & Mir4, L. M. (**1998**). Electrochemotherapy on liver tumours in rabbits. *Br. Joumal Cancer* **77**, 2104–11.

Rathmell, J. C. & Thompson, C. B. (**2002**). Pathways of apoptosis in lymphocyte development, homeostasis, and disease. *Cell* **109**,.

Razzokov, J., Yusupov, M., Cordeiro, R. M. & Bogaerts, A. (**2018**). Atomic scale understanding of the permeation of plasma species across native and oxidized membranes. *J. Phys. D. Appl. Phys.* **51**, 365203.

Riley, T. R., Gauthier-Lewis, M. L., Sanchez, C. K. & Douglas, J. S. (**2017**). Role of agents for reversing the effects of target-specific oral anticoagulants. *Am. J. Heal. Pharm.* **74**, 54–61.

Ringe, K. I., Lutat, C., Rieder, C., Schenk, A., Wacker, F. & Raatschen, H.-J. (**2015**). Experimental Evaluation of the Heat Sink Effect in Hepatic Microwave Ablation. *PLoS One* **10**, e0134301.

Ritts, A. C., Li, H., Yu, Q., Xu, C., Yao, X., Liang, H. & Wang, Y. (**2010**). Dentin surface treatment using a non-thermal argon plasma brush for interfacial bonding improvement in composite restoration. *Eur J Oral Sci* **118**, 510–6.

Robert, É., Darny, T., Dozias, S., Iseni, S. & Pouvesle, J.-M. (**2015**). New insights on the propagation of pulsed atmospheric plasma streams: From single jet to multi jet arrays. *Phys. Plasmas* **22**, 122007.

Rogers, S. (**1971**). Gene therapy: a potentially invaluable aid to medicine and mankind. *Res Commun Chem Pathol Pharmacol.* **2**, 587–600.

Rolong, A., Davalos, R. V. & Rubinsky, B. (**2017**). History of electroporation. In *Irreversible Electroporation in Clinical Practice*, pp. 13–37. New York: Springer International Publishing.

Rols, M.-P. & Teissié, J. (**1990**). Electropermeabilization of mammalian cells. Quantitative analysis of the phenomenon. *Biophys. J.* **58**, 1089–98.

Rols, M.-P. & Teissié, J. (**1998a**). Electropermeabilization of mammalian cells to macromolecules: Control by pulse duration. *Biophys. J.* **75**, 1415–23.

Rols, M.-P., Delteil, C., Golzio, M., Dumond, P., Gros, S. & Teissie, J. (**1998b**). In vivo electrically mediated protein and gene transfer in murine melanoma. *Nat. Biotechnol.* **16**, 168–71.

Rols, M.-P., Golzio, M., Gabriel, B. & Teissié, J. (**2002**). Factors Controlling Electropermeabilisation of Cell Membranes. *Technol. Cancer Res. Treat.* **1**, 319–27.

Rosazza, C., Escoffre, J. M., Zumbusch, A. & Rols, M.-P. (**2011**). The actin cytoskeleton has an active role in the electrotransfer of plasmid DNA in mammalian cells. *Mol. Ther.* **19**, 913–

21.

Rosazza, C., Haberl Meglic, S., Zumbusch, A., Rols, M.-P. & Miklavčič, D. (**2016**). Gene Electrotransfer: A Mechanistic Perspective. *Curr. Gene Ther.* **16**, 98–129.

Roux, S., Bernat, C., Al-Sakere, B., Ghiringhelli, F., Opolon, P., Carpentier, A. F., Zitvogel, L., Mir, L. M. & Robert, C. (**2008**). Tumor destruction using electrochemotherapy followed by CpG oligodeoxynucleotide injection induces distant tumor responses. *Cancer Immunol. Immunother.* **57**, 1291–300.

Rubinsky, B., Onik, G. & Mikus, P. (**2007**). Irreversible electroporation: A new ablation modality - Clinical implications. *Technol. Cancer Res. Treat.* **6**, 37–48.

Rudolf, Z., Stabuc, B., Čemažar, M., Miklavčič, D., Vodovnik, L. & Serša, G. (**1995**). Electrochemotherapy with bleomycin. The first clinical experience in malignant melanoma patients. *Radiol. Oncol.* **29**, 229–35.

Saadati, F., Mahdikia, H., Abbaszadeh, H.-A. & Abdollahifar, M. (**2018**). Comparison of Direct and Indirect cold atmospheric-pressure plasma methods in the B 16 F 10 melanoma cancer cells treatment. *Sci. Rep.* **8**, 7689.

Saito, K., Asai, T., Fujiwara, K., Sahara, J., Koguchi, H., Fukuda, N., Suzuki-Karasaki, M., Soma, M. & Suzuki-Karasaki, Y. (**2016**). Tumor-selective mitochondrial network collapse induced by atmospheric gas plasma-activated medium. *Oncotarget* **7**, 19910–27.

Sakudo, A., Yagyu, Y. & Onodera, T. (**2019**). Disinfection and sterilization using plasma technology: Fundamentals and future perspectives for biological applications. *Int. J. Mol. Sci.* **20**, 5216.

Sale, A. J. H. & Hamilton, W. A. (**1967**). Effects of high electric fields on microorganisms. I. Killing of bacteria and yeasts. *BBA - Gen. Subj.* **148**, 781–8.

Sasaki, S., Honda, R., Hokari, Y., Takashima, K., Kanzaki, M. & Kaneko, T. (**2016**). Characterization of plasma-induced cell membrane permeabilization: Focus on OH radical distribution. *J. Phys. D. Appl. Phys.* **49**, 334002.

Satkauskas, S., Bureau, M. F., Puc, M., Mahfoudi, A., Scherman, D., Miklavčič, D. & Mir, L. M. (**2002**). Mechanisms of in vivo DNA electrotransfer: Respective contribution of cell electropermeabilization and DNA electrophoresis. *Mol. Ther.* **5**, 133–40.

Sato, Y., Yamada, S., Takeda, S., Hattori, N., Nakamura, K., Tanaka, H., Mizuno, M., Hori, M. & Kodera, Y. (**2018**). Effect of Plasma-Activated Lactated Ringer's Solution on Pancreatic Cancer Cells In Vitro and In Vivo. *Ann. Surg. Oncol.* **25**, 299–307.

Scheffer, H. J., Nielsen, K., De Jong, M. C., Van Tilborg, A. A. J. M., Vieveen, J. M., Bouwman, A., Meijer, S., Van Kuijk, C., Van Den Tol, P. & Meijerink, M. R. (**2014**). Irreversible electroporation for nonthermal tumor ablation in the clinical setting: A systematic review of safety and efficacy. *J. Vasc. Interv. Radiol.* **25**, 997–1011.

Schoenbach, K. H., Peterkin, F. E., Alden, R. W. & Beebe, S. J. (**1997**). The effect of pulsed electric fields on biological cells: Experiments and applications. *IEEE Trans. PLASMA Sci.* **25**, 284–92.

Schulz-Von Der Gathen, V., Schaper, L., Knake, N., Reuter, S., Niemi, K., Gans, T. & Winter, J. (**2008**). Spatially resolved diagnostics on a microscale atmospheric pressure plasma jet. *J. Phys. D. Appl. Phys.* **41**, 194004.

Schuster, M. *et al.* (**2016**). Visible tumor surface response to physical plasma and apoptotic cell kill in head and neck cancer. *J. Cranio-Maxillofacial Surg.* **44**, 1445–52.

Schwan, H. P. (**1957**). Electrical properties of tissue and cell suspensions. *Adv. Biol. Med. Phys.* **5**, 147–209.

Sebti, S. M. & Lazo, J. S. (**1988**). Metabolic inactivation of bleomycin analogs by bleomycin hydrolase. *Pharmacol. Ther.* **38**, 321–9.

Semmler, M. L. *et al.* (**2020**). Molecular Mechanisms of the Efficacy of Cold Atmospheric Pressure Plasma (CAP) in Cancer Treatment. *Cancers (Basel).* **12**, 269.

Sensenig, R. *et al.* (**2011**). Non-thermal plasma induces apoptosis in melanoma cells via production of intracellular reactive oxygen species. *Ann. Biomed. Eng.* **39**, 674–87.

Seror, O. (**2015**). Ablative therapies: Advantages and disadvantages of radiofrequency, cryotherapy, microwave and electroporation methods, or how to choose the right method for an individual patient? *Diagn. Interv. Imaging* **96**, 617–624.

Serša, G. (**2006**). The state-of-the-art of electrochemotherapy before the ESOPE study; advantages and clinical uses. *Eur. J. Cancer, Suppl.* **4**, 52–59.

Serša, G., Čemažar, M. & Miklavčič, D. (**1995**). Antitumor Effectiveness of Electrochemotherapy with cis-Diamminedichloroplatinum(II) in Mice. *Cancer Res.* **55**, 3450–5.

Serša, G., Čemažar, M., Menart, V., Gaberc-Porekar, V. & Miklavčič, D. (**1997a**). Anti-tumor effectiveness of electrochemotherapy with bleomycin is increased by TNF-α on SA-1 tumors in mice. *Cancer Lett.* **116**, 85–92.

Serša, G., Miklavčič, D., Čemažar, M., Belehradek, J., Jarm, T. & Mir, L. M. (**1997b**). Electrochemotherapy with CDDP on LPB sarcoma: Comparison of the anti- tumor effectiveness in immunocompetent and immunodeficient mice. In *Bioelectrochemistry and Bioenergetics*, pp. 279–83. Elsevier Science S.A.

Serša, G., Čemažar, M., Parkins, C. S. & Chaplin, D. J. (**1999**). Tumour blood flow changes induced by application of electric pulses. *Eur. J. Cancer* **35**, 672–7.

Serša, G., Teissié, J., Čemažar, M., Signori, E., Kamensek, U., Marshall, G. & Miklavčič, D. (**2015**). Electrochemotherapy of tumors as in situ vaccination boosted by immunogene electrotransfer. *Cancer Immunol. Immunother.* **64**, 1315–27.

Sgantzos, M., Tsoucalas, G., Laios, K. & Androutsos, G. (**2014**). The physician who first applied radiotherapy, Victor Despeignes, on 1896. *Hell. J. Nucl. Med.* **17**, 45–46.

Shahryari, A., Jazi, M. S., Mohammadi, S., Nikoo, H. R., Nazari, Z., Hosseini, E. S., Burtscher, I., Mowla, S. J. & Lickert, H. (**2019**). Development and clinical translation of approved gene therapy products for genetic disorders. *Front. Genet.* **10**, 868.

Shi, L., Yu, L., Zou, F., Hu, H., Liu, K. & Lin, Z. (**2017**). Gene expression profiling and functional analysis reveals that p53 pathway-related gene expression is highly activated in cancer cells treated by cold atmospheric plasma-activated medium. *PeerJ* **2017**, e3751.

Shinitzky, M. (**1984**). Membrane fluidity in malignancy Adversative and recuperative. *BBA - Rev. Cancer* **738**, 251–61.

Siegel, R. L., Miller, K. D. & Jemal, A. (**2020**). Cancer Statistics, 2020. *CA. Cancer J. Clin.* **70**, 7–

30.

Simioni, A., Valpione, S., Granziera, E., Rossi, C. R., Cavallin, F., Spina, R., Sieni, E., Aliberti, C., Stramare, R. & Campana, L. G. (**2020**). Ablation of soft tissue tumours by long needle variable electrode-geometry electrochemotherapy: final report from a single-arm, single-centre phase-2 study. *Sci. Rep.* **10**, 2291.

Sitzmann, W., Vorobiev, E. & Lebovka, N. (**2017**). Pulsed electric fields for food industry: Historical overview. In *Handbook of Electroporation*, pp. 2335–2354. Springer International Publishing.

Škop, V., Guo, J., Liu, N., Xiao, C. & Hall, K. D. (**2020**). Mouse Thermoregulation: Introducing the Concept of the Thermoneutral Point. *CellReports* **31**, 107501.

Snoj, M., Čemažar, M., Srnovrsnik, T., Kosir, S. P. & Serša, G. (**2009**). Limb sparing treatment of bleeding melanoma recurrence by electrochemotherapy. *Tumori* **95**, 398–402.

Société royale de médecine (**1790**). *Nouveau plan de constitution pour la médecine en France: présenté à l'Assemblée Nationale par la Société Royale de Médecine*. Paris.

Spanggaard, I. *et al.* (**2013**). Gene electrotransfer of plasmid antiangiogenic metargidin peptide (AMEP) in disseminated melanoma: Safety and efficacy results of a phase i first-in-man study. *Hum. Gene Ther. Clin. Dev.* **24**, 99–107.

Spugnini, E. P. & Baldi, A. (**2019**). Electrochemotherapy in Veterinary Oncology: State-of-the-Art and Perspectives. *Vet. Clin. North Am. - Small Anim. Pract.* **49**, 967–79.

Stämpfli, R. (**1958**). Reversible electrical breakdown of the excitable membrane of a Ranvier node. *Ann. Acad. Bras. Cien.* **30**, 57–63.

Stämpfli, R. & Willi, M. (**1957**). Membrane potential of a ranvier node measured after electrical destruction of its membrane. *Experientia* **13**, 297–8.

Stancampiano, A., Forgione, D., Simoncelli, E., Laurita, R., Tonini, R., Gherardi, M. & Colombo, V. (**2019**). The Effect of Cold Atmospheric Plasma (CAP) Treatment at the Adhesive-Root Dentin Interface. *J. Adhes. Dent.* **21**, 229–37.

Stanton, A. (**1896**). On a new kind of rays. By Wilhelm Conrad Röntgen, translation of a paper read before the Würzburg Physical and Medical Society. *Nature* **53**, 274–6.

Stoffels, E., Flikweert, A. J., Stoffels, W. W. & Kroesen, G. M. W. (**2002**). Plasma needle: A non-destructive atmospheric plasma source for fine surface treatment of (bio)materials. *Plasma Sources Sci. Technol.* **11**, 383–8.

Sugár, I. P. (**1979**). A theory of the electric field-induced phase transition of phospholipid bilayers. *BBA - Biomembr.* **556**, 72–85.

Takeda, S. *et al.* (**2017**). Intraperitoneal Administration of Plasma-Activated Medium: Proposal of a Novel Treatment Option for Peritoneal Metastasis From Gastric Cancer. *Ann. Surg. Oncol.* **24**, 1188–94.

Tamzali, Y., Borde, L., Rols, M.-P., Golzio, M., Lyazrhi, F. & Teissié, J. (**2012**). Successful treatment of equine sarcoids with cisplatin electrochemotherapy: A retrospective study of 48 cases. *Equine Vet. J.* **44**, 214–20.

Tanaka, H. & Hori, M. (**2017a**). Medical applications of non-thermal atmospheric pressure plasma. *J. Clin. Biochem. Nutr.* **60**, 29–32.

Tanaka, H., Mizuno, M., Ishikawa, K., Nakamura, K., Kajiyama, H., Kano, H., Kikkawa, F. & Hori, M. (**2011**). Plasma-activated medium selectively kills glioblastoma brain tumor cells by down-regulating a survival signaling molecule, AKT kinase. *Plasma Med.* **1**, 265–77.

Tanaka, H., Mizuno, M., Ishikawa, K., Nakamura, K., Utsumi, F., Kajiyama, H., Kano, H., Maruyama, S., Kikkawa, F. & Hori, M. (**2012**). Cell survival and proliferation signaling pathways are downregulated by plasma-activated medium in glioblastoma brain tumor cells. *Plasma Med.* **2**, 207–20.

Tanaka, H., Nakamura, K., Mizuno, M., Ishikawa, K., Takeda, K., Kajiyama, H., Utsumi, F., Kikkawa, F. & Hori, M. (**2016**). Non-thermal atmospheric pressure plasma activates lactate in Ringer's solution for anti-tumor effects. *Sci. Rep.* **6**, 36282.

Tanaka, H., Ishikawa, K., Mizuno, M., Toyokuni, S., Kajiyama, H., Kikkawa, F., Metelmann, H.-R. & Hori, M. (**2017b**). State of the art in medical applications using non-thermal atmospheric pressure plasma. *Rev. Mod. Plasma Phys.* **1**, 89 pages.

Tanaka, H. *et al.* (**2019**). Oxidative stress-dependent and -independent death of glioblastoma cells induced by non-thermal plasma-exposed solutions. *Sci. Rep.* **9**, 13657.

Tarek, M. (**2005**). Membrane electroporation: A molecular dynamics simulation. *Biophys. J.* **88**, 4045–53.

Tatum, E. L. (**1966**). Molecular biology, nucleic acids, and the future of medicine. *Perspect. Biol. Med.* **10**, 19–32.

Tauffenberger, A., Fiumelli, H., Almustafa, S. & Magistretti, P. J. (**2019**). Lactate and pyruvate promote oxidative stress resistance through hormetic ROS signaling. *Cell Death Dis.* **10**, 653.

Teissié, J. & Rols, M.-P. (**1993**). An experimental evaluation of the critical potential difference inducing cell membrane electropermeabilization. *Biophys. J.* **65**, 409–13.

Teissié, J. & Tsong, T. Y. (**1981**). Electric Field Induced Transient Pores in Phospholipid Bilayer Vesicles. *Biochemistry* **20**, 1548–54.

Teissié, J., Golzio, M. & Rols, M.-P. (**2005**). Mechanisms of cell membrane electropermeabilization: A minireview of our present (lack of ?) knowledge. *Biochim. Biophys. Acta - Gen. Subj.* **1724**, 270–80.

Teleanu, R. I., Chircov, C., Grumezescu, A. M. & Teleanu, D. M. (**2019**). Tumor Angiogenesis and Anti-Angiogenic Strategies for Cancer Treatment. *J. Clin. Med.* **9**, 84.

Thomson, K. R., Cheung, W., Ellis, S. J., Federman, D., Kavnoudias, H., Loader-Oliver, D., Roberts, S., Evans, P., Ball, C. & Haydon, A. (**2011**). Investigation of the safety of irreversible electroporation in humans. *J. Vasc. Interv. Radiol.* **22**, 611–21.

Titomirov, A. V., Sukharev, S. & Kistanova, E. (**1991**). In vivo electroporation and stable transformation of skin cells of newborn mice by plasmid DNA. *BBA - Gene Struct. Expr.* **1088**, 131–4.

Toepfl, S., Heinz, V. & Knorr, D. (**2005**). Overview of pulsed electric field processing for food. *Emerg. Technol. Food Process.* 69–97.

Tornin, J., Mateu-Sanz, M., Rodríguez, A., Labay, C., Rodríguez, R. & Canal, C. (**2019**). Pyruvate Plays a Main Role in the Antitumoral Selectivity of Cold Atmospheric Plasma in

Osteosarcoma. *Sci. Rep.* **9**, 10681.

Torre, L. A., Bray, F., Siegel, R. L., Ferlay, J., Lortet-Tieulent, J. & Jemal, A. (**2015**). Global Cancer Statistics, 2012. *CA Cancer J Clin* **65**, 87–108.

Tounekti, O., Pron, G., Belehradek, J. & Mir, L. M. (**1993**). Bleomycin, an Apoptosis-mimetic Drug That Induces Two Types of Cell Death Depending on the Number of Molecules Internalized. *Cancer Res.* **53**, 5462–9.

Tounekti, O., Kenani, A., Foray, N., Orlowski, S. & Mir, L. M. (**2001**). The ratio of single-to double-strand DNA breaks and their absolute values determine cell death pathway. *Br. J. Cancer* **84**, 1272–9.

Trachootham, D., Alexandre, J. & Huang, P. (**2009**). Targeting cancer cells by ROS-mediated mechanisms: A radical therapeutic approach? *Nat. Rev. Drug Discov.* **8**, 579–91.

Turrini, E. *et al.* (**2020**). Plasma-activated medium as an innovative anticancer strategy: Insight into its cellular and molecular impact on in vitro leukemia cells. *Plasma Process. Polym.* e2000007.

Umezawa, H., Maeda, K., Takeuchi, T. & Okami, Y. (**1966**). New antibiotics, bleomycin A and B. *J. Antibiot.* **19**, 200–9.

Umezawa, H., Hori, S., Sawa, T., Yoshioka, T. & Takeuchi, T. (**1974**). A bleomycin-inactivating enzyme in mouse liver. *J. Antibiot. (Tokyo).* **27**, 419–24.

Utsumi, F., Kajiyama, H., Nakamura, K., Tanaka, H., Mizuno, M., Ishikawa, K., Kondo, H., Kano, H., Hori, M. & Kikkawa, F. (**2013**). Effect of indirect nonequilibrium atmospheric pressure plasma on anti-proliferative activity against chronic chemo-resistant ovarian cancer cells in vitro and in vivo. *PLoS One* **8**, 1–10.

Utsumi, F., Kajiyama, H., Nakamura, K., Tanaka, H., Mizuno, M., Toyokuni, S., Hori, M. & Kikkawa, F. (**2016**). Variable susceptibility of ovarian cancer cells to non- Thermal plasma-Activated medium. *Oncol. Rep.* **35**, 3169–77.

Valkenburg, K. C., De Groot, A. E. & Pienta, K. C. (**2018**). Targeting the tumour stroma to improve cancer therapy. *Nat Rev Clin Oncol* **15**, 366–81.

van Blitterswijk, W. J., de Veer, G., Krol, J. H. & Emmelot, P. (**1982**). Comparative lipid analysis of purified plasma membranes and shed extracellular membrane vesicles from normal murine thymocytes and leukemic GRSL cells. *BBA - Biomembr.* **688**, 495–504.

Van Boxem, W., Van Der Paal, J., Gorbanev, Y., Vanuytsel, S., Smits, E., Dewilde, S. & Bogaerts, A. (**2017**). Anti-cancer capacity of plasma-treated PBS: Effect of chemical composition on cancer cell cytotoxicity. *Sci. Rep.* **7**, 1–9.

Van Der Meer, F. J. M., Rosendaal, F. R., Vandenbroucke, J. P. & Briët, E. (**1993**). Bleeding Complications in Oral Anticoagulant Therapy: An Analysis of Risk Factors. *Arch. Intern. Med.* **153**, 1557–62.

Van der Paal, J., Neyts, E. C., Verlackt, C. C. W. & Bogaerts, A. (**2016**). Effect of lipid peroxidation on membrane permeability of cancer and normal cells subjected to oxidative stress. *Chem. Sci.* **7**, 489–98.

Van Der Paal, J., Verheyen, C., Neyts, E. C. & Bogaerts, A. (**2017**). Hampering Effect of Cholesterol on the Permeation of Reactive Oxygen Species through Phospholipids

Bilayer: Possible Explanation for Plasma Cancer Selectivity. *Sci. Rep.* **7**, 39526.

van Hoeve, J. C., Elferink, M. A. G., Klaase, J. M., Kouwenhoven, E. A., Schiphorst, P. P. J. B. M. & Siesling, S. (**2015**). Long-term effects of a regional care pathway for patients with rectal cancer. *Int. J. Colorectal Dis.* **30**, 787–95.

Van Loenhout, J. *et al.* (**2019**). Cold Atmospheric Plasma-Treated PBS Eliminates Immunosuppressive Pancreatic Stellate Cells and Induces Immunogenic Cell Death of Pancreatic Cancer Cells. *Cancers (Basel).* **11**, 1597.

Vandamme, M., Robert, É., Pesnel, S., Barbosa, E., Dozias, S., Sobilo, J., Lerondel, S., Pape, A. Le & Pouvesle, J.-M. (**2010**). Antitumor effect of plasma treatment on u87 glioma xenografts: Preliminary results. *Plasma Process. Polym.* **7**, 264–73.

Vandamme, M. e*t al.* (**2012**). ROS implication in a new antitumor strategy based on non-thermal plasma. *Int. J. Cancer* **130**, 2185–94.

Vargo, J. J. (**2004**). Clinical applications of the argon plasma coagulator. *Gastrointest. Endosc.* **59**, 81–88.

Vásquez, J. L., Gehl, J. & Hermann, G. G. (**2012**). Electroporation enhances mitomycin C cytotoxicity on T24 bladder cancer cell line: A potential improvement of intravesical chemotherapy in bladder cancer. *Bioelectrochemistry* **88**, 127–33.

Verkman, A. S., Hara-Chikuma, M. & Papadopoulos, M. C. (**2008**). Aquaporins - New players in cancer biology. *J. Mol. Med.* **86**, 523–529.

Vernier, P. T., Levine, Z. A., Wu, Y. H., Joubert, V., Ziegler, M. J., Mir, L. M. & Tieleman, D. P. (**2009**). Electroporating fields target oxidatively damaged areas in the cell membrane. *PLoS One* **4**, e7966.

Vijayarangan, V., Delalande, A., Dozias, S., Pouvesle, J.-M., Robert, É. & Pichon, C. (**2020**). New insights on molecular internalization and drug delivery following plasma jet exposures. *Int. J. Pharm.* **589**, 119874.

Villemejane, J. & Mir, L. M. (**2009**). Physical methods of nucleic acid transfer: General concepts and applications. *Br. J. Pharmacol.* **157**, 207–19.

Vitturi, D. A. & Patel, R. P. (**2011**). Current perspectives and challenges in understanding the role of nitrite as an integral player in nitric oxide biology and therapy. *Free Radic. Biol. Med.* **51**, 805–12.

Volotskova, O., Dubrovsky, L., Keidar, M. & Bukrinsky, M. (**2016**). Cold atmospheric plasma inhibits HIV-1 replication in macrophages by targeting both the virus and the cells. *PLoS One* **11**, e0165322.

von Woedtke, T., Weltmann, K.-D., Wolff, C. M., Kolb, J. F. & Steuer, A. (**2018**). Cell stimulation versus cell death induced by sequential treatments with pulsed electric fields and cold atmospheric pressure plasma. *PLoS One* **13**, e0204916.

Von Woedtke, T., Schmidt, A., Bekeschus, S., Wende, K. & Weltmann, K. D. (**2019**). Plasma medicine: A field of applied redox biology. *In Vivo (Brooklyn).* **33**, 1011–26.

Wada, N., Ikeda, J. ichiro, Tanaka, H., Sakakita, H., Hori, M., Ikehara, Y. & Morii, E. (**2017**). Effect of plasma-activated medium on the decrease of tumorigenic population in lymphoma. *Pathol. Res. Pract.* **213**, 773–7.

Wang, X., Perez, E., Liu, R., Yan, L.-J., Mallet, R. T. & Yang, S.-H. (**2007**). Pyruvate Protects Mitochondria from Oxidative Stress in Human Neuroblastoma SK-N-SH Cells. *Brain Res.* **1132**, 1–9.

Wang, M., Holmes, B., Cheng, X., Zhu, W., Keidar, M. & Zhang, L. G. (**2013**). Cold Atmospheric Plasma for Selectively Ablating Metastatic Breast Cancer Cells. *PLoS One* **8**, e73741.

Wang, H., Schoebel, S., Schmitz, F., Dong, H. & Hedfalk, K. (**2020**). Characterization of aquaporin-driven hydrogen peroxide transport. *Biochim. Biophys. Acta - Biomembr.* **1862**, 183065.

Weidinger, A. & Kozlov, A. V (**2015**). Biological Activities of Reactive Oxygen and Nitrogen Species: Oxidative Stress versus Signal Transduction. *Biomolecules* **5**, 472–84.

Weiner, B., Fischer, T. & Waxman, S. (**2003**). Hemostasis in the era of the chronic anticoagulated patient. *J. Invasive Cardiol.* **15**, 669–73; quiz 674.

Wells, P. N. T. (**2001**). Physics and engineering: Milestones in medicine. *Med. Eng. Phys.* **23**, 147–53.

Weltmann, K.-D., Metelmann, H.-R. & Woedtke, T. von (**2016**). Low temperature plasma applications in medicine. *Europhys. News* **47**, 39–41.

Winter, J., Brandenburg, R. & Weltmann, K.-D. (**2015**). Atmospheric pressure plasma jets: An overview of devices and new directions. *Plasma Sources Sci. Technol.* **24**, 064001.

Wohlgemuth, R., Naddeo, V., Regestein, L., Mathys, A. & Buchmann, L. (**2019**). Perspective on Pulsed Electric Field Treatment in the Bio-based Industry. *Front. Bioeng. Biotechnol* **7**, 265.

Wolff, C. M., Steuer, A., Stoffels, I., von Woedtke, T., Weltmann, K.-D., Bekeschus, S. & Kolb, J. F. (**2019**). Combination of Cold Plasma and Pulsed Electric Fields – A Rationale for Cancer Patients in Palliative Care. *Clin. Plasma Med.* **16**, 100096.

Wolff, C. M., Kolb, J. F., Weltmann, K.-D., von Woedtke, T. & Bekeschus, S. (**2020**). Combination Treatment with Cold Physical Plasma and Pulsed Electric Fields Augments ROS Production and Cytotoxicity in Lymphoma. *Cancers (Basel).* **12**, 845.

Wong, T. K. & Neumann, E. (**1982**). Electric field mediated gene transfer. *Biochem. Biophys. Res. Commun.* **107**, 584–7.

Workman, P. *et al.* (**2010**). Guidelines for the welfare and use of animals in cancer research. *Br. J. Cancer* **102**, 1555–77.

World Health Organization (**2018**). *Handbook for national quality policy and strategy: a practical approach for developing policy and strategy to improve quality of care*. Geneva: Licence: CC BY-NC-SA 3.0 IGO.

World Health Organization (**2020**). *WHO report on cancer: setting priorities, investing wisely and providing care for all*. Geneva.

Yan, D., Sherman, J. H., Cheng, X., Ratovitski, E. A., Canady, J. & Keidar, M. (**2014**). Controlling plasma stimulated media in cancer treatment application. *Appl. Phys. Lett.* **105**,.

Yan, D., Talbot, A., Nourmohammadi, N., Sherman, J. H., Cheng, X. & Keidar, M. (**2015**). Toward understanding the selective anticancer capacity of cold atmospheric plasma—A model based on aquaporins (Review). *Biointerphases* **10**, 040801.

Yan, D., Sherman, J. H. & Keidar, M. (**2017**). Cold atmospheric plasma, a novel promising anti-cancer treatment modality. *Oncotarget* **8**, 15977–95.

Yarmush, M. L., Golberg, A., Serša, G., Kotnik, T. & Miklavčič, D. (**2014**). Electroporation-Based Technologies for Medicine: Principles, Applications, and Challenges. *Annu. Rev. Biomed. Eng.* **16**, 295–320.

Yonson, S., Coulombe, S., Léveillé, V. & Leask, R. L. (**2006**). Cell treatment and surface functionalization using a miniature atmospheric pressure glow discharge plasma torch. *J. Phys. D. Appl. Phys.* **39**, 3508–13.

Yoshikawa, N. *et al.* (**2020**). Plasma-activated medium promotes autophagic cell death along with alteration of the mTOR pathway. *Sci. Rep.* **10**, 1614.

Yost, A. D. & Joshi, S. G. (**2015**). Atmospheric nonthermal plasma-treated PBS inactivates Escherichia coli by oxidative DNA damage. *PLoS One* **10**, e0139903.

Yusupov, M., Van der Paal, J., Neyts, E. C. & Bogaerts, A. (**2017**). Synergistic effect of electric field and lipid oxidation on the permeability of cell membranes. *Biochim. Biophys. Acta - Gen. Subj.* **1861**, 839–47.

Zerbib, D., Amalric, F. & Teissié, J. (**1985**). Electric field mediated transformation: Isolation and characterization of a TK+ subclone. *Biochem. Biophys. Res. Commun.* **129**, 611–8.

Zhang, Q., Zhuang, J., Von Woedtke, T., Kolb, J. F., Zhang, J., Fang, J. & Weltmann, K.-D. (**2014**). Synergistic antibacterial effects of treatments with low temperature plasma jet and pulsed electric fields. *Appl. Phys. Lett.* **105**, 104103.

Zhang, S., Rousseau, A. & Dufour, T. (**2017**). Promoting lentil germination and stem growth by plasma activated tap water, demineralized water and liquid fertilizer. *RSC Adv.* **7**, 31244.

Zimmermann, U. (**1982**). Electric field-mediated fusion and related electrical phenomena. *BBA - Rev. Biomembr.* **694**, 227–77.

Zmuc, J. *et al.* (**2019**). Large Liver Blood Vessels and Bile Ducts Are Not Damaged by Electrochemotherapy with Bleomycin in Pigs. *Sci. Rep.* **9**, 3649.

Zucker, S. N., Zirnheld, J., Bagati, A., DiSanto, T. M., Des Soye, B., Wawrzyniak, J. A., Etemadi, K., Nikiforov, M. & Berezney, R. (**2012**). Preferential induction of apoptotic cell death in melanoma cells as compared with normal keratinocytes using a non-thermal plasma torch. *Cancer Biol. Ther.* **13**, 1299–1306.

GLOSSARY & KEY TERMS

This glossary gives general definitions of terms used in this manuscript and provides an overview of cancer terms and medical terms related to oncology.

Ablation (also called **ablative therapy**): treatment that removes or destroys all or part of a body or tissue; can also be used to remove or halt the function of an organ (*e.g.,* removing the ovaries or testicles or taking medicines that cause them to stop making their hormones). Ablation may be performed by surgery, hormones, drugs, radiofrequency, extreme heat, freezing, irreversible electroporation or other methods.

Abnormal: not normal (a state, condition or behaviour that differs from what is considered normal). An abnormal lesion or growth in or on the body may be benign (not cancer), precancerous or premalignant (likely to become cancer) or malignant (cancer).

Abscess: an enclosed collection of pus in tissues, organs or confined spaces in the body. An abscess is a sign of infection and is usually swollen and inflamed.

Abscopal effect: a hypothesis in the treatment of metastatic cancer whereby the shrinking or disappearance of tumours in parts of the body that were not the direct target of local therapy, such as radiation therapy. It is thought that in the abscopal effect, the immune system is stimulated to fight cancer in the whole body as a result of local treatment. Learning more about the abscopal effect may help develop new cancer treatments, especially for metastatic cancer.

Actinic keratosis, also called **solar keratosis** (**keratoses** as *plural noun*): a rough raised area of skin that can develop after years of sun exposure. They are benign, but a few will develop into squamous cell cancer and can be removed with cold, lasers, chemicals, or creams. See also **squamous cell carcinoma**.

Acute: severe; sharp; begins quickly.

Adenocarcinoma: a benign growth starting in the glandular (secretory) cells. Glandular cells are found in tissue that lines specific internal organs and makes and releases substances in the body, such as mucus, digestive juices or other fluids. Most breast, pancreas, lung, prostate, and colon cancers are adenocarcinomas.

Adenocarcinoma *in situ* (also called **AIS**): a condition in which abnormal cells are found in the glandular tissue that lines specific internal organs, such as the uterus, cervix, lung, pancreas, and colon. Adenocarcinoma *in situ*, which occurs most often in the cervix, may become cancer and spread to nearby normal tissue.

Adenoma: a tumour that is not cancer and starts in gland-like cells of the epithelial tissue (thin layer of tissue that covers organs, glands, and other structures within the body).

Adenopathy: large or swollen lymph glands.

Adenosarcoma: A tumour that is a mixture of an adenoma (a tumour that starts in the gland-like cells of epithelial tissue) and sarcoma (a tumour that begins in bone, cartilage, fat, muscle,

blood vessels or other connective or supportive tissue). An example of an adenosarcoma is Wilms tumour.

Adenosis: a disease or abnormal change in a gland. Breast adenosis is a benign condition in which the lobules are more prominent than usual.

Adenosquamous carcinoma: a type of cancer that contains squamous cells (thin, flat cells that line specific organs) and gland-like cells.

Adjunct agent: a drug or substance used in cancer therapy in addition to the primary treatment.

Adjunct therapy (also called **adjunctive therapy**): another treatment used together with the primary treatment. Its purpose is to assist the primary treatment.

Adjuvant therapy: additional cancer treatment given after the primary treatment to lower the risk that cancer will come back. Adjuvant therapy may include chemotherapy, radiation therapy, hormone therapy, targeted therapy or biological therapy.

Advanced cancer: cancer that is unlikely to be cured or controlled with treatment. Cancer may have spread from where it first started to nearby tissue, lymph nodes, or distant body parts. Treatment may be given to help shrink the tumour, slow the growth of cancer cells or relieve symptoms.

Adverse effect (also called an **adverse event**): an unexpected medical problem during treatment with a drug or other therapy. Adverse effects may be mild, moderate or severe and may be caused by something other than the drug or treatment.

Adult-type fibrosarcoma: a type of cancer that forms in fibrous (connective) tissue. It can occur anywhere in the body. Adult-type fibrosarcoma may spread to nearby tissue or other body parts, such as the lungs or bones. It may also recur (come back) after treatment. Adult-type fibrosarcoma usually occurs in young and middle-aged adults but also children. It is a type of soft tissue sarcoma.

Agonist: a substance or drug that binds to a receptor inside a cell or on its surface and causes the same action as the substance that normally binds to the receptor.

Allograft: see Xenograft

Alopecia: hair loss.

Anaesthesia: A loss of feeling or awareness caused by drugs or other substances. Anaesthesia keeps patients from feeling pain during surgery or other procedures. Local anaesthesia is a loss of sensation in a tiny body area. Regional anaesthesia is a loss of sensation in a part of the body, such as an arm or leg. General anaesthesia is a loss of sensation and a complete loss of awareness that feels like profound sleep.

Angiogenesis: blood vessel formation. Tumour angiogenesis is the growth of new blood vessels that tumours need to develop, a process caused by the release of chemicals by the tumour and by nearby host cells.

Angiogenesis inhibitors: are used to prevent the formation of blood vessels, thereby depleting the cancer cells of oxygen and nutrients.

Apoptosis: an active process of programmed cell death, characterised by visible shrinking cells, cleavage of chromosomal DNA, chromatin condensation, and fragmentation of both the nucleus and the cell. Blebbing of the cell membrane is often seen.

Autophagy: a genetically regulated form of programmed cell death in which the cell digests itself. Being caspase and p53 independent, autophagy is characterised by double-membrane vacuoles in the cytoplasm, which sequesters organelles such as mitochondria and ribosomes.

Autoradiography: the detection of radio-isotopically labelled molecules by exposure to X-ray film.

B cell (also called **B lymphocyte**): a type of white blood cell that makes antibodies. B cells are part of the immune system and develop from stem cells in the bone marrow.

B-cell lymphoma: a type of cancer that forms in B cells and may be either indolent (slow-growing) or aggressive. Most B-cell lymphomas are non-Hodgkin lymphomas. There are many different types of B-cell non-Hodgkin lymphomas. These include Burkitt lymphoma, chronic lymphocytic leukaemia/small lymphocytic lymphoma (CLL/SLL), diffuse large B-cell lymphoma, follicular lymphoma, and mantle cell lymphoma. Prognosis and treatment depend on the type and stage of cancer.

Basal cell: a small, round cell found in the lower part (or base) of the epidermis, the outer layer of the skin.

Basal cell cancer (also called **basal cell carcinoma**): cancer that begins in the lower part of the epidermis (the outer layer of the skin). It may appear as a small white or flesh-coloured bump that grows slowly and bleeds. Basal cell cancers are usually found in areas of the body exposed to the sun. Basal cell cancers rarely metastasise (spread) to other body parts. They are the most common form of skin cancer.

Bench-to-bedside: a term used to describe how the results of research done in the laboratory are directly used to develop new ways to treat patients.

Benign (also called **non-malignant**): not cancerous.

Benign tumour: a tumour that is not cancer. It does not invade nearby tissue or spread to other parts of the body but remains confined to its site of origin.

Benign vascular tumour: a type of benign (not cancer) tumour that forms from cells that make blood vessels or lymph vessels. Benign vascular tumours may occur anywhere in the body, and a patient may have several tumours in different parts of the body. They may grow large and sometimes spread to nearby tissue. The most common type of benign vascular tumour is haemangioma, which usually occurs in infants and goes away independently.

Bilateral: affecting both the right and left sides of the body, *e.g.,* bilateral Wilms tumour is cancer in both kidneys.

Bilateral cancer: cancer that occurs in both of a pair of organs, such as both breasts, ovaries, eyes, lungs, kidneys or adrenal glands, at the same time.

Biological therapy (also called **biological response modifier therapy** (BRM therapy), **biotherapy**): a type of treatment that uses substances made from living organisms to treat diseases. These substances may occur naturally in the body or be made in the laboratory. Some biological therapies stimulate or suppress the immune system to help the body fight cancer. Other biological therapies attack specific cancer cells, which may help keep them from

growing or killing them. They may also lessen specific side effects caused by some cancer treatments. Biological therapy includes immunotherapy (such as cytokines, cancer treatment vaccines, and some antibodies) and some targeted therapies.

Biomarker (also called **molecular marker** and **signature molecule**): a biological molecule found in blood, other body fluids or tissues that signify a normal or abnormal process or a condition or disease. A biomarker may be used to see how well the body responds to a treatment for an illness or condition.

Biopsy: the removal of cells or tissues for examination by a pathologist. The pathologist may study the tissue under a microscope or perform other tests on the cells or tissue. There are many different types of biopsy procedures. The most common types include (1) incisional biopsy, in which only a sample of tissue is removed; (2) excisional biopsy, in which an entire lump or suspicious area is removed; and (3) needle biopsy, in which a sample of tissue or fluid is removed with a needle. The procedure is called a core biopsy when a wide needle is used. When a thin needle is used, the process is called a fine-needle aspiration biopsy.

Biorefinery: a facility that integrates sustainable biomass processing into a spectrum of bio-based products and bioenergy. It can also be defined as the optimised use of biomass for materials, chemicals, fuels and energy applications, where use relates to costs, economics, markets, yield, environment, impact, carbon balance and social aspects.

Blood-brain barrier (also called **BBB**): a network of blood vessels and tissue made up of closely spaced cells that help keep harmful substances from reaching the brain. The BBB lets some substances, such as water, oxygen, carbon dioxide, and general anaesthetics, pass into the brain but keeps out bacteria and other substances, such as many anticancer drugs. The BBB is formed by the tight interactions between the brain endothelium, surrounded by the basal lamina and stabilised by pericytes, glial cells and neurons.

Blood plasma: a “yellowish liquid” component of blood that makes up more than half (about 55%) of its overall content and contains nutrients, glucose, proteins, hormones, minerals, enzymes, and other substances.

Burden: the “load” carried by society expressed in terms of an observable fact — for cancer burden, this would be described in terms of cancer incidence or mortality.

Bypass: a surgical procedure in which the surgeon creates a new pathway for the flow of body fluids.

Cancer: an abnormal (continual and unregulated) proliferation of any of the different kinds of cells in the body.

Cancer cell: a cell that divides and multiplies uncontrollably and has the potential to spread throughout the body, crowding out normal cells and tissues.

Cancer cell line: cancer cells that keep dividing and growing over time, under certain conditions in a laboratory, and are used in research to study cancer biology and test cancer treatments.

Cancer continuum: a concept that describes the spectrum of cancer care from cancer biology and aetiology, prevention, early diagnosis and screening, treatment, survivorship care, palliative care and end of life care.

Cancer immunoediting: an extrinsic tumour suppressor mechanism that engages only after the cellular transformation has occurred, and intrinsic tumour suppressor mechanisms have failed.

Cancerology: a branch of basic research in medical science interested in molecular changes in cells and tissues that lead to cancer.

Carcinogen: an agent (chemical, physical or viral) that promotes carcinogenesis but does not cause cancer at all times, under all circumstances.

Carcinogenesis: the initiation of a tumour.

Carcinoma: cancer found in cells that make up epithelial - tissue that covers or lines the surfaces of internal organs, glands, and body structures. Carcinoma usually forms a solid tumour. Carcinomas include approximately 80% to 90% of human cancers.

Carcinomatosis (also called **carcinosis**): a condition in which cancer is spread extensively throughout the body or, in some cases, to a relatively large region of the body.

carcinomatous lymphangitis

Catalase (CAT, 1.11.1.6): an antioxidant enzyme present in all aerobic organisms that decompose hydrogen peroxide (H_2O_2) into water and oxygen in an energy-efficient manner in the cells exposed to environmental stress.

Cauterisation (or **cautery**): a medical practice of burning a part of the patient body (destroying some tissue) to remove or close off a part of it in an attempt to mitigate bleeding and damage, remove an undesired growth or minimise other potential medical harm, such as infections when antibiotics are unavailable.

Chemoprevention: the ability to use drugs or lifestyle modifications to prevent cancer from developing.

Chemotherapeutic agents: antineoplastic agents used to directly or indirectly inhibit the uncontrolled growth and proliferation of cancer cells and are classified according to their mechanism of action and include alkylating agents, and antimetabolites, topoisomerase inhibitors, antibiotics, mitotic inhibitors, and protein kinase inhibitors.

Chemotherapy: the use of any chemotherapeutic agent (drug) to treat any disease. For cancer treatment, chemotherapy is also called “chemo” and refers to drugs to kill cancer cells that grow and divide rapidly.

Circulating tumour cells: rare cells shed by solid tumours into the systemic circulation at an estimated frequency of 1:500.000– 1:1.000.000 circulating cells.

Clinical trial: research studies performed on people to evaluate a medical, surgical or behavioural intervention. Usually advanced through four phases, they are the primary way researchers find out if a new treatment (a new drug or diet or medical device) is safe and effective in people by evaluating their treatment, side effects, and survival.

Complementary therapy: therapies used in addition to standard treatment.

Computed tomography scan (also called a **CT** or **CAT scan**): a diagnostic imaging procedure that uses a combination of X-rays and computer technology to produce horizontal or axial images (often called slices) of the body, showing details of any part of the body, including the bones, muscles, fat, and organs. CT scans are more detailed than general X-rays.

Cytokines: cell signalling molecules that are secreted in response to external stimuli. Cytokines are peptides and cannot cross the lipid bilayer of cells to enter the cytoplasm. Cytokines include chemokines, interferons, interleukins, lymphokines, and tumour necrosis factors.

DNA vaccination: a technique for protecting an organism against disease by injecting it with a genetically engineered plasmid containing the DNA sequence encoding the antigen(s) against which an immune response is sought, so cells directly produce the antigen for an immunological response more safely than with viral vectors.

Doubling time (DT): defined as the time required to double the initial tumour volume, DT is a popular end-point of experimental tumour radiobiology (the faster a tumour grows, the smaller DT).

Drug resistance: the reduction in medication effectiveness to cure a disease or condition.

Electrochemotherapy (**ECT**): reversible electroporation that temporarily increases membrane permeability to enhance the uptake of chemotherapeutic agents in a tumour.

Electrofusion: the use of reversible electroporation to produce a fusion between cells.

Electrogenetransfer (also called **electrogenetherapy** or **EGT**): reversible electroporation to introduce plasmid DNA into living tissue cells. See Electrotransfer.

Electropermeabilisation: the generation of defects by pulsed electric fields (PEFs) or the long-term effect of electroporation.

Electrophoresis (from the Greek "ηλεκτροφόρηση" meaning "to bear electrons"): the migration and separation of charged particles (ions) under the influence of a spatially uniform electric field.

Electroporation: the generation of pores in the plasma cell membrane via pulsed electric fields (PEFs). This dynamic phenomenon is reversible or irreversible depending on the induced transmembrane voltage at the plasma membrane.

Electropulsation: exposure of cells to electric pulses, leading to their membranes' structural alteration and increased conductivity and permeability, thus allowing the transport of low- to non-permeant molecules across the membrane, bypassing the physiological limitations. **Cell electropulsation** comprises **cell electroporatio**n and **cell electropermeabilisation**.

Electrosurgery: application of an HF (radio frequency) alternating polarity, electrical current to biological tissue to cut, coagulate, desiccate or fulgurate tissue.

Electrotransfer: the movement of molecules into cells, by either passive diffusion or electrophoresis, made possible by using electric pulses. From this term, we derive DNA electrotransfer, RNA electrotransfer, PNA electrotransfer, etc.

Enhanced permeability and retention (EPR) effect: the mechanism resulting from pathophysiological processes (*e.g.,* leaky tumour vasculature, poor lymphatic drainage and tumour microenvironment interactions) that leads to the accumulation and retention of nanoparticles or macromolecules in tumours.

Oedema: swelling due to build-up of fluid.

Fibropapilloma: a condition characterised by the presence of benign proliferative neoplasms containing superficial epidermal and subjacent dermal tissue.

Fibrosis: A proliferation of fibroblasts and collagen's deposition in tissues due to a reparative process (*e.g.*, following injury, inflammation, and necrosis) or as part of a reaction to chronic irritants (*e.g.*, pneumoconiosis, chronic lymphedema).

Hodgkin disease: a type of lymphoma where the cells in the lymphatic system abnormally reproduce, eventually making the body less able to fight infection. Steady enlargement of lymph glands, spleen, and other lymphatic tissue occur.

Iatrophysics (from Greek *iatrós*, "Arzt"; *physis*, "inanimate nature"): a 17th and 18th-century theory and practice of medicine that interpreted all phenomena of health and illness as dependent on the internal physical structure of the body, its external form, and mechanical alterability. With reductionistic simplification, it attempted to apply the findings of the new experimental natural sciences to the realm of life.

IFN-γ (interferon-gamma): cytokine produced by activated T cells and natural killer cells, whose primary action is the activation of macrophages.

Immune system: the system composed of lymph fluid, lymph nodes, the lymphatic system, and white blood cells responsible for protecting the body against infection and disease.

Immunosuppression: a state in which the ability of the body's immune system to respond is decreased. This condition may be present at birth or caused by certain infections (such as human immunodeficiency virus or HIV) or cancer therapies, such as cancer cell killing (cytotoxic) drugs, radiation, and bone marrow transplant.

Immunotherapy: treatments that promote or support the body's immune system response to a disease such as cancer.

Induced transmembrane voltage (**induced TMV**): an increase in transmembrane voltage resulting from exposure to electric pulses and an increase in a transmembrane electric field.

Irreversible electroporation (**IRE**)**:** the permanent permeabilisation state of a cell exposed to an electric field that induces the loss of homeostasis and apoptotic-like cell death. IRE is a predominantly nonthermal and adjacent structure–sparring ablation modality that has been proven safe and efficient in treating liver, pancreas, and prostate cancer.

Leukaemia: a blood cancer arising from the precursors of circulating blood cells in the bone marrow, consequently keeping the marrow from making normal red and white blood cells and platelets. There are four main types of leukaemia: acute myelogenous leukaemia (AML), chronic myelogenous leukaemia (CML), acute lymphocytic leukaemia (ALL), and chronic lymphocytic leukaemia (CLL). Leukaemia and lymphomas account for approximately 8% of human malignancies.

Lipids: hydrophobic molecules that function as energy storage molecules, signalling molecules, and the major components of cell membranes.

Locally invasive: a tumour that can invade the tissues surrounding it by sending out "fingers" of cancerous cells into normal tissue. It can cause problems by pressing on nearby tissues and organs, making them unable to work the way they should.

Loco-regional (adj): in medicine, restricted to a localised region of the body.

Lymphoma: cancer that starts in lymphocytes (a type of white blood cell) part of the immune system. Lymphoma cells can build up in lymph nodes and other lymph tissues. Lymphomas

are grouped into two categories: Hodgkin lymphoma and non-Hodgkin lymphoma. Leukaemia and lymphomas account for approximately 8% of human malignancies.

Magnetic resonance imaging (**MRI**): a diagnostic procedure that uses a combination of large magnets, radiofrequencies, and a computer to produce detailed images of organs and structures within the body.

Malignancy (*adj* **malignant**) (also called **cancer**): a term for diseases in which abnormal cells divide without control and can invade nearby tissues. Malignant cells can also spread to other body parts through the blood and lymph systems. There are several main types of malignancy. Carcinoma is a malignancy that begins in the skin or tissues lining or covering internal organs. Sarcoma is a malignancy that begins in bone, cartilage, fat, muscle, blood vessels or other connective or supportive tissue. Leukaemia is a malignancy that starts in blood-forming tissue, such as the bone marrow, and causes too many abnormal blood cells. Lymphoma and multiple myeloma are malignancies that begin in the cells of the immune system. Central nervous system cancers are malignancies that form in the brain and spinal cord tissues.

Margin: the edge or border of the tissue removed in cancer surgery. The margin is described as negative or clean when the pathologist finds no cancer cells at the edge of the tissue, suggesting that all cancer has been removed. The margin is described as positive or involved when the pathologist finds cancer cells at the edge of the tissue, suggesting that all cancer has not been removed.

Mean (the **arithmetic mean**, also called the **expected value** or **average**): a statistics and probability term, the central value of a discrete set of numbers. The mean is the sum of a set of numbers divided by how many numbers are in the set.

Median: a statistics and probability term, a value separating the higher half from the lower half of a data sample, a population or a probability distribution.

Median overall survival (also called **median survival**): the length of time from either the date of diagnosis or the start of treatment for a disease, such as cancer, that half of the patients in a group of patients diagnosed with the disease are still alive. In a clinical trial, measuring the median overall survival is one way to see how well a new treatment works.

Metastasis: the spread of cancer cells through the blood or lymphatic system, causing the development of secondary tumours in a part of the body that is far from the original primary cancer.

Metastasis-initiating cells: tumour cells that can survive and proliferate in distant metastatic sites.

Metastatic niche: microenvironment in distant organs that supports the survival and outgrowth of tumour cells.

Mitochondria: cytoplasmic organelles responsible for synthesising most of the ATP in eukaryotic cells by oxidative phosphorylation.

Mitotic cell death: the type of cell death which results from failure to arrest the cell cycle before or during mitosis in response to DNA damage with hallmarks including nuclear fragmentation and multiple micronuclei.

Mortality rate: Proportion of a population who dies from a particular disease in a specified time.

Myeloma: cancer that starts in the plasma cells of bone marrow. In some cases, the myeloma cells collect in one bone and form a single tumour (a plasmacytoma). In other cases, the myeloma cells contain in many bones and form many tumours (multiple myeloma).

Non-Hodgkin lymphoma: a type of lymphoma that causes the cells in the lymphatic system to abnormally reproduce, eventually causing tumours to grow. Non-Hodgkin lymphoma cells can also spread to other organs.

Non-thermal irreversible electroporation (**NTIRE**): an electroporation-based non-thermal tissue ablation method, leading to cell death either directly through excessive damage inflicted to cells and membranes (necrosis) or via apoptosis

Oncogene: a gene capable of inducing one or more characteristics of cancer cells.

Oncogenesis: the maintenance and subsequent evolution of a tumour.

Oncology: a branch of medical science that focuses on disease, symptoms, treatment and other medical aspects of cancer.

Oxidative phosphorylation: the synthesis of ATP from ADP coupled to the energetically favourable transfer of electrons to molecular oxygen as the final acceptor in an electron transport chain.

p53: a transcription factor (encoded by the p53 tumour suppressor gene) that arrests the cell cycle in G1 in response to damaged DNA and is required for apoptosis induced by various stimuli.

Palliative care: an approach that improves the quality of life of patients and their families facing the problem associated with any life-threatening illness through the prevention and relief of suffering using early identification and impeccable assessment and treatment of pain and other issues, physical, psychosocial and spiritual. The primary purpose is to improve the patient's quality of life.

Phospholipid bilayer: the basic structure of biological membranes. The hydrophobic tails of phospholipids are buried in the interior of the membrane, and their polar head groups are exposed to the aqueous solution on either side.

Phospholipid transfer protein: a protein that transports phospholipid molecules between cell membranes.

Phospholipids: the principal components of cell membranes, consisting of two hydrocarbon chains (usually fatty acids) joined to a polar head group containing phosphate.

Plasma membrane: a phospholipid bilayer with associated proteins that surrounds the cell.

Plasmid: a small, circular DNA molecule capable of independent replication in a host cell.

Precancerous lesion: abnormal tissue changes in an early stage of cancer that could progress to invasive cancer if left untreated.

Prediction intervals: range of possible future observations that consider the random variation inherent in the past trends and the future prediction.

Prevalence: the number of people with the disease at a given time point. Cancer prevalence often refers to the number of people living with cancer who require care.

Prevention: eliminating or minimising exposure to the causes of cancer, and includes reducing individual susceptibility to the effects of such reasons.

Primary prevention: Elimination or reduction of exposure to recognised risk factors in susceptible populations to prevent disease. Primary prevention of cancer comprises a broad spectrum of strategies, from legislation and policies to minimise or eliminate exposure to carcinogens to promoting healthy behaviour and health sector programmes.

Primary tumour (also called original or primary cancer): a tumour grows at the anatomical site where tumour progression began and proceeded to yield a cancerous mass. See secondary tumour.

Programmed cell death: a standard physiological form of cell death characterised by apoptosis.

Proto-oncogene: a normal gene in the cell that can be converted into an oncogene.

Pulsed electric field (**PEF**) **treatment**: see electropulsation.

Radical: an atom or group of atoms with at least one unpaired electron, a feature that makes a radical very chemically reactive.

Reactive oxygen species (**ROS**): include oxygen ions, free radicals and peroxides, both inorganic and organic. They are generally highly reactive due to unpaired valence shell electrons. ROS form a natural by-product of normal oxygen metabolism and are essential in cell signalling. However, ROS levels can increase dramatically during environmental stress, resulting in significant damage to cell structures.

Redox status: balance of the reduced state *versus* the oxidised form of a biochemical system, influenced by the level of reactive oxygen and nitrogen species (ROS and RNS) relative to the capacity of antioxidant systems to eliminate ROS and RNS.

Reversible electroporation: the temporary permeabilisation state of a cell exposed to an electric field that disturbs the phospholipid bilayer, allowing molecules to reach the cell interior through the cell plasma membrane. After the end of the electric pulse, the transport of molecules ceases, the plasma membrane reseals, and the cells remain viable.

Sarcoma: cancer that starts in connective tissue cells, including blood and lymph vessels, cartilage, fat, muscle, tendon, and bone cells. For example, osteosarcoma is the most common type of cancer that starts in the bone; chondrosarcoma is cancer that begins in cartilage cells.

Secondary prevention: (of cancer) involves the use of examinations and tests to detect cancer as early as possible before signs and symptoms would cause a patient to seek care. It has previously been used synonymously with screening.

A **secondary tumour** (also called **secondary cancer**): cancer that has spread (metastasised) from the place where it first started (the primary tumour) to another part of the body. Secondary tumours are the same type of cancer as the original (primary) cancer. See primary tumour.

Standard deviation (**SD**): measures the amount of variability or dispersion from the individual data values to the mean.

Standard ECT: fixed electrode-geometry electrochemotherapy.

The **standard error** (**SE**) **of a statistic**: the approximate standard deviation of a statistical sample population that measures the accuracy of a sample distribution representing a population using SD. In statistics, a sample mean deviates from the actual mean of a population—this deviation is the standard error of the mean (SEM).

The **standard error of the mean** (**SEM**): the measure of how far the sample mean of the data is likely to be from the actual population mean. The SEM is always smaller than the SD.

Thermo-neutral point (**TNP**): a discrete ambient temperature below which energy expenditure increases and above which body temperature increases. Humans do not have a TNP. The mouse TNP is *ca.* 29°C in the light phase and *ca.* 33°C in the dark phase.

Thermo-neutral zone (**TNZ**): the ambient temperatures where metabolic rate is at a minimum. The TNZ is critical for understanding the thermal biology differences between individuals.

Transfection: introducing a foreign genetic material (DNA, RNA) into eukaryotic cells, done by viruses, electroporation, microinjection, liposomes, etc.

Transforming growth factor β (**TGF β**): polypeptide growth factor that generally inhibits animal cell proliferation.

Tumour: any abnormal proliferation of cells.

Tumour necrosis factor (**TNF**): a polypeptide growth factor that induces programmed cell death.

Tumour promotor: a compound that leads to tumour development by stimulating cell proliferation.

Tumour suppressor gene: a gene whose inactivation leads to tumour development.

Tumour virus: a virus capable of causing cancer in animals or humans.

Ultrasound (also called **sonography**): a diagnostic imaging technique that uses high-frequency sound waves and a computer to create images of blood vessels, tissues, and organs. Ultrasounds are used to view internal organs as they function and to assess blood flow through various vessels.

Unilateral: affecting one side of the body (*e.g.,* unilateral kidney cancer occurs in one kidney only.)

Variable-geometry ECT: long-needle variable electrode-geometry electrochemotherapy.

Vascular disruption effect of ECT: a cascade of tumour cell death surrounding obstructed tumour vessels, resulting from the drug used in the electroporation of endothelial cells and contributing to the overall effectiveness of ECT

Vascular lock: transient reduction of perfusion, at a greater extent in tumours than in normal tissues that occurs after application of electric pulses to tissues

X-ray: a type of radiation (electromagnetic energy beams) that can pass through the body and onto film, making pictures of areas inside the body. X-rays may be used in a diagnostic test (in low dose) and treatment (in high amount) of cancer and other diseases.

X-ray crystallography: a method in which the diffraction pattern of X rays is used to determine the arrangement of individual atoms within a molecule.

X-ray therapy: a type of radiation therapy that uses high-energy radiation from x-rays to destroy cancer cells and shrink tumours.

Xenobiotics: any substance (synthetic or natural) that is not naturally present in the body of an organism.

Xenograft: The transplant of an organ, tissue or cells to an individual of another species.

- Cell line xenograft models: established human tumour cell lines transplanted into immune-deficient host
- Patient-derived xenograft (**PDX**) models: Human tumour explants grown in immune-deficient host
- Syngeneic models: established mouse tumour cell lines transplanted into immune-competent hosts (**allograft**)
- Genetically engineered mouse models (GEMMs): Genetic modification that permits spontaneous or induced tumour development

Xenogram (also called **xeroradiograph**): a body picture recorded on paper rather than film.

Xerostomia: dry mouth (occurring when the body is not able to make enough saliva)

université PARIS-SACLAY

ÉCOLE DOCTORALE
Innovation thérapeutique
du fondamental à l'appliqué
(ITFA)

Titre : Amélioration de l'efficacité de l'électrochimiothérapie par association avec des liquides traités par des plasmas froids : mise au point des protocoles expérimentaux et preuve de concept

Mots clés : cancer ; électro-chimiothérapie ; plasmas froids ; amplitude du champ électrique ; mélanome ; espèces réactives de l'oxygène et de l'azote (RONS)

Résumé :

L'électrochimiothérapie (ECT) - une méthode établie pour l'éradication locale des tumeurs cutanées basée sur la technologie d'électroporation - est largement utilisée en Europe en médecine humaine et vétérinaire avec très peu d'effets secondaires systémiques. Les plasmas froids (NTP) ont récemment pris de l'ampleur pour leur application en cancérologie grâce à leur riche source en espèces réactives à courte durée de vie ainsi qu'en espèces réactives de l'oxygène et de l'azote à longue durée de vie (RONS) qui peuvent être transférées aux liquides traités par du NTP. Nous cherchions à combiner ces technologies afin d'améliorer les capacités de l'ECT et de mieux comprendre la contribution des RONS dans ces stratégies anticancéreuses.

En tant qu'étude multidisciplinaire utilisant à la fois de la physique, de la chimie, des biotechnologies et de la médecine, cette thèse visait à mettre en évidence les effets bénéfiques de la combinaison de l'ECT et du plasma froid. Une nouvelle source de plasma d'hélium multi-jet (PMJ) a été utilisée pour des études *in vitro* sur trois lignées cellulaires différentes (les cellules DC-3F, B16-F10 et LPB), et pour des études *in vivo* sur les souris nude et C57Bl/6 porteuses de tumeurs sous-cutanées. Nous avons démontré que le pH et la température de stockage du PBS traité par le PMJ (pPBS), ayant une influence importante sur la stabilité des trois principaux RONS (H_2O_2, NO_2^- et NO_3^-), étaient cruciaux pour conserver la capacité anticancéreuse du pPBS. Le traitement combinant du pPBS et une ECT à une amplitude de champs électrique plus faible que celle utilisée habituellement a permis de restaurer l'efficacité de l'ECT, ralentissant la croissance des tumeurs chez la souris et, en conséquence, améliorant le taux de survie des animaux traités.

Title: Enhancement of electrochemotherapy by non-thermal plasma-treated liquids: protocol design and proof of concept

Keywords: cancer; electrochemotherapy; non-thermal atmospheric pressure plasmas (NTP); pulsed electric field amplitude; malignant melanoma; reactive oxygen and nitrogen species (RONS)

Abstract:

Electrochemotherapy (ECT) – an established method for the local eradication of cutaneous tumours based on electroporation technology – is widely used in Europe in human and veterinary medicine with very few systemic side effects. Non-thermal plasmas (NTP) are recently gaining momentum for application in oncology based on their rich content of short-lived reactive species as well as long-lived reactive oxygen and nitrogen species (RONS) which can be transferred to liquids being treated with NTP. We sought to combine those technologies to enhance the ECT capabilities and to better understand the contribution of RONS in those anticancer strategies.

As a multidisciplinary study at the crossroads of physics, chemistry, biotechnologies and medicine, this thesis aimed at emphasising the potent beneficial outcome of the combination of ECT and NTP medicine. A novel, stable source of helium plasma multi-jet (PMJ) has been utilised for *in vitro* investigations on three different cell lines (the DC-3F, B16-F10 and LPB cells), and for *in vivo* studies on nude and C57Bl/6 mice bearing sub-cutaneous tumours. We demonstrated that the pH of the plasma-treated PBS (pPBS) and the stability of the three main RONS (H_2O_2, NO_2^- and NO_3^-) under various storage conditions were crucial for the storage of plasma-treated liquids while maintaining their anti-cancer capabilities. In combination with ECT at an electric field amplitude lower than the one usually applied, those stable pPBS partially restored the ECT efficacy, delaying tumour growth and hence prolonging mice survival.

Université Paris-Saclay
Espace Technologique / Immeuble Discovery
Route de l'Orme aux Merisiers RD 128 / 91190 Saint-Aubin, France